Decadal rainfall variability over Southern Africa

David John Preece

Department of Geography, UCL

Thesis submitted in fulfilment of the requirements

of the Doctor of Philosophy degree

I, David John Preece, confirm that the work presented in this thesis is my own. Where information has been derived from other sources, I confirm that this has been indicated in the thesis.

…….. dated ……..

Abstract:

Southern Africa is a region of vulnerability, with high seasonal and interannual rainfall variability combined with rain-dependent agriculture. This variability is underpinned by influences from ENSO and other oceanic forcing, and known to exhibit quasi-decadal variability at 16-20 years (Tyson, 1975). This study uses a combination of proxy, observed and climate model data to explore the nature, mechanisms and anthropogenic forcing of rainfall variability at decadal scales.

The spatial nature of decadal rainfall variability, demonstrated through EOF analysis and composite decadal events, is similar to that at interannual scales. Spectral analysis of observed data confirms the presence of variability at ENSO-related timescales, combined with influences in the 10-12 year and 16-20 year band. Model simulated rainfall agrees broadly with this analysis, although there are variations in spectral peaks in different simulations.

The mechanisms of quasi-decadal variability are also shown to be similar to interannual forcing patterns: showing links to ENSO, the tropical and South Atlantic oceans, and the South West Indian Ocean. Rainfall correlation at decadal scales is dominated by the SW Indian Ocean, but the "dipole" like forcing observed at interannual timescales is notably less coherent at quasi-decadal scales. Model-specific differences are explored, and thought to be the result of the interaction between a weak (strong) decadal ENSO signal and a strong (weak) Southern Annular Mode influence at multi-decadal timescales. The quasi-decadal rainfall is thought to be the result of the integration of seasonal, annual, and multi-annual variability (Vimont, 2007), and not a separate mechanism.

Using state of the art model simulations (Gonzalez-Rouco et al., 2003; Tett et al., 2007) that incorporate anthropogenic forcings, the study also explores the impact of climate change on the quasi-decadal signals over the region. Results show that quasi-decadal variability is spectrally damped under anthropogenic forcing, despite similar spatial structures and teleconnections. A key change occurs in the tropical Indian Ocean, which substantially alters in relationship with the southern African rainfall. Implications for decadal predictability over the region are discussed and evaluated.

Table of Contents:

Table of Figures:

Acknowledgements

This study could not exist without the help and support of a great many people. This section records my thanks to them; for their patience, understanding and advice throughout my study period.

First, to UCL's Department of Geography, without whom I would not have been able to undertake this work, and my colleagues within the Department who have offered valuable help and useful discussions. Dr. Jonathan Holmes was helpful in understanding the potential contribution of proxy datasets, and Dr. Philip Lewis, Dr. Tristan Quaife and Mr Chris Knell have made substantial contributions to the UNIX and IDL programming elements of the work. Thanks must also be extended to Dr. Richard Chandler (UCL Department of Statistics) for help with spectral analysis techniques.

Second, to the individuals who have provided data and contributed valuable discussion. Professor Julia Cole (U. Arizona) provided coral reef data, Dr. Tim Osborn (CRU) helped extensively with climate model data via the SO&P project, Dr. Philip Brohan (UK Met Office) helped with observed data and in elements of the HadCM3 experimental data, and Dr Jesus-Fidel Gonzalez-Rouco (U. Madrid) provided ERIK SST data and help.

Substantial thanks to Professor Simon Tett (U. Edinburgh, formerly UK Met Office), who allowed me to use the state of the art HadCM3 simulation experiments described in Tett et al. (2007). Without them, this study would have been significantly weaker, and far less interesting to work on!

Finally, I am indebted to Dr. Martin Todd for his supervision – the study would simply not have worked without his practical advice, encouragement and guidance over the years. His substantial input has been most valuable for my learning, and in the production of this thesis.

All of us could take a lesson from the weather: it pays no attention to criticism

Anon.

Climate is what we expect; weather is what we get

Mark Twain

(1) Introduction and Study Background

Decadal variability is a critical – yet understudied – component of modern climate science. In the recent past, and our imminent future, decadal variance will be produced by both natural and anthropogenic signals (Vimont, 2007), and it is likely that the changes to our climate will operate at decadal scales (Santer et al., 1996; Delworth & Mann, 2000). In addition, improving our knowledge of underlying natural variability is critical for reducing uncertainty in seasonal forecasting efforts (Mason, 1998; Goddard et al., 2001; Gissila et al., 2004; Bharwani et al., 2005), and increasingly important in underpinning detection and attribution of anthropogenic climate change (Douville, 2006; Zhang et al., 2007).

Southern Africa – broadly defined as Africa south of the equator – is known for established decadal variability in rainfall (Tyson, 1971; Tyson & Preston-Whyte, 2000; Tyson et al., 2002), making it an ideal location to develop our understanding of this aspect of climate variability. The region is prone to pronounced flood and drought events, associated with substantial climate variability on a range of timescales (Reason et al., 2004; Boko et al., 2007). It is one of the few regions of the world to have become poorer in the last generation (Ravallion & Chen, 2004) and the difficulty of coping with climate variability is thought to be one of the key factors contributing to the continent's economic position (Desanker & Magadza, 2001; World-Bank, 2001; Clay et al., 2003; Fischer et al., 2005; Washington et al., 2006; Giles, 2007; Osbahr & Roberts, 2007) as well as the increased frequency of conflict in the region (Hendrix & Glaser, 2007).

Southern African agriculture needs steady inputs of precipitation, rather than intense high frequency wet/dry cycles (Usman & Reason, 2004; Mapande & Reason, 2005), and as a

consequence, seasonal forecasting efforts (Cane et al., 1994; Landman et al., 2001) and the changes to precipitation intensity under anthropogenic forcing scenarios have received particular attention (Boko et al., 2007; Rocha et al., 2007).

Yet, despite the close links between human activity and rainfall variability (Jury, 2002; Tadross et al., 2005), the established decadal variability is poorly understood (Handorf et al., 1999; Reason et al., 2006a). This study presents the first coherent analysis of decadal rainfall variability over southern Africa using a range of proxy, observed and state of the art climate model simulations (Zorita et al., 2005; Gonzalez-Rouco et al., 2006; Tett et al., 2007). The study aims to improve our understanding of the behaviour of decadal rainfall variability, and how it responds to natural and anthropogenic forcing scenarios.

This chapter introduces the key themes of this study, and explores our current knowledge of decadal variability. The challenges of studying decadal variability are considered, and we review the existing understanding of the decadal rainfall variability in southern Africa. This is followed by a critical examination of the work on detection and attribution of anthropogenic climate change, and we show how improved understanding of decadal variability may be utilised in this field.

We then explore the climate of southern Africa in greater detail, and consider the key components of climate variability in the region, together with an examination of the main areas which force the climate. Having identified the existing understanding, we then define and present the principal research questions of this study.

1.1 Decadal Variability

Decadal variability – despite having influence over particularly vulnerable regions – is poorly understood and typically understudied. This section examines why this may be the case. Some of the intrinsic difficulties with studying decadal variability in general, and the decadal variability of rainfall in particular, are investigated. Potential ways of overcoming the challenges posed are discussed, and it is shown that the scientific issue of decadal variability is critical to understanding the changing climate we face.

1. 1. 1 Decadal Trends in Rainfall

Perhaps the best known example of decadal variability is the drought conditions in the Sahel (West Africa) since the early 1970s, which have been well documented by analyses of rainfall (Hulme, 1992; Lamb & Peppler, 1992; Nicholson et al., 2000), vegetation cover (Tucker et al., 1991), dust transport (Prospero & Lamb, 2003), and other agricultural and societal data. The decreasing rainfall and widespread droughts in the Sahel region during the last three decades of the 20th century are among the most undisputed and largest recent climate changes recognized by the climate research community, and substantial field-based research has been conducted into the impacts and coping strategies deployed by Sahelian pastoralist communities in response to their deteriorating natural resource base (e.g. Tarhule & Lamb, 2003).

Several possible causes or mechanisms have been identified and investigated (Moron et al., 2003), including local land–atmosphere interactions (Nicholson et al., 2000; Grist & Nicholson, 2001; Thiaw & Mo, 2005), tropospheric influence (Enfield & Mestas-Nunez, 1999), and the relationship with ENSO (Janicot et al., 1996; Janicot et al., 2001).

Like the interannual variability described in the previous chapter, the majority of work (following on from Folland et al., 1986) has concentrated on the interaction with sea surface temperatures. Studies have shown influences from the Mediterranean (Rowell, 2003), tropical Atlantic (Lamb & Peppler, 1992; Rowell et al., 1992; Ward, 1998) and the Indian Ocean (Bader & Latif, 2003; Bader et al., 2003; Chung & Ramanathan, 2006) in driving what was considered to be multi-decadal variability (Grist & Nicholson, 2001; Diedhiou et al., 2003; Dai et al., 2004; Wang et al., 2004; Hickler et al., 2005).

Recent studies, however, have investigated the role of warming SSTs (Giannini et al., 2003; Kerr, 2003; Jenkins et al., 2005; Lu & Delworth, 2005; Herceg et al., 2007) in driving the drought conditions, and suggest that Indian Ocean warming, in particular, may be the primary cause of the late twentieth century drought conditions. This is a result of concentrating on a longer time scale, and allowing the influence of secular trends to alter potential sources and mechanisms of variability.

The lack of agreement – despite concerted observation and modelling studies – in explaining the cause of variability in these regions exemplify the problems faced when studying (or attributing) decadal trends and variability in rainfall.

1. 1. 2 Decadal Variability in Rainfall

The Sahel showed how decadal variability could result in large trends in rainfall data, but variability of rainfall at decadal scales is typically noisier and less clearly defined. Examination of decadal rainfall in South Australia, for example, reveals underlying variability and trends (Power et al., 1999b; Li et al., 2005) linked to oceanic variability in a variety of locations (Ansell et al., 1998; Drosdowsky & Chambers, 2001; Murphy & Timbal, 2007). The rainfall has shown links to the Indian Ocean (Ansell et al., 2000; England et al., 2006), Indian Ocean Dipole (Ashok et al., 2003a) and role of ENSO (Power et al., 1999a), and seasonal forecasting efforts rely heavily on these predictors to estimate likely rainfall (Nelson et al., 2002). Detection and attribution studies on temperature (Karoly & Braganza, 2005a, 2005b) and rainfall (Timbal et al., 2006) has allowed some estimates to be made of the likely impact of anthropogenic forcing on the region (Christensen et al., 2007; Hennessy et al., 2007).

By comparison, the rainfall variability in southern Africa poses a different challenge – the region's decadal rainfall variability has long been thought to be dominated by an 18 year oscillation, first presented by Tyson (1971) using observed data from a variety of rainfall gauge stations across South Africa. The analysis used only 60 years of data (1910-1969) for most stations, although some sites had records extending back to 1880 available (Tyson, 1971). Both three- and seven-year running means were applied to smooth the data set, resulting in the notable absence of any power in the lower-frequency ENSO timescales, for example. Basic spectral analysis techniques were employed to show that the 18 year signal dominates the rainfall variability. A 9-10 year cycle 'tends to be filtered

out by seven year running means', and 'rainfall oscillations with periods between nine and five years do not appear to contribute to total precipitation variance in South Africa' (Tyson, 1971: 716).

Despite initial criticism (Curry, 1972) addressed in the subsequent papers (Tyson, 1980; Tyson & Dyer, 1980; Cockcroft et al., 1987), the 18 year oscillation has formed the consensual basis of southern African observed rainfall decadal studies since publication (Mason & Jury, 1997; Tyson & Preston-Whyte, 2000), and has also been observed in proxy data beyond the twentieth century period (Tyson & Lindesay, 1992; Tyson et al., 2002; Holmgren et al., 2003).

Several studies have examined southern African decadal variability without making any clear conclusions about the mechanism or forcing involved – though it is thought to pre-date an anthropogenic signal in proxy records. Possible links with SST variability were suggested, but no mechanistic explanations offered (Mason & Tyson, 1992; Mason & Lindesay, 1993), and no evidence of the oscillation was found in analysis of the principal components of SST (Mason, 1995, 2001).

The lack of progress in understanding the mechanics of this decadal variability in southern African rainfall is typical of many low frequency oscillations. Part of the inherent difficulty results from the interaction of forcing factors, in a chaotic and unpredictable manner (Landman & Mason, 2001a), but there are also fundamental challenges posed by the intrinsic nature of decadal variability as a study topic. These are explored in the next section.

1. 1. 3 Challenges Posed by Decadal Variability

There are two major challenges to studying decadal variability. First, the theoretical challenges of decadal variability, and the paradigmatic issues facing our understanding of low-frequency oscillations are explored. This section then considers the practical issues posed by the nature of observed and proxy records, coupled with the inherent difficulties faced by climate models in simulating rainfall.

Understanding the internal, unforced variability of the climate system on decadal and longer timescales is of substantial importance (Delworth & Mann, 2000). In an editorial paper describing the outcome of a recent CLIVAR summit, Vimont (2007) outlined some of the challenges facing decadal predictability. It was suggested that the integration of interannual forcing by the oceans could generate red-noise which possesses substantial 'variance on decadal scales', even in the absence of physical mechanisms which act on decadal timescales. This variance could be enhanced by the incorporation of interannual variability (e.g. ENSO forcing) in to the integration, and generating a more 'robust' decadal signal (Vimont, 2007). Other studies suggest that decadal 'modulations' of variance (i.e. clustering of interannual events, rather than true variability) may be observed in climate phenomena (Tozuka et al., 2007). Vimont (2007)'s report from the CLIVAR summit suggests that one of the key challenges of future decadal predictability studies was to identify the nature of the variability accurately.

Not only does a proper understanding of such variability have significant implications for long range climate forecasting and societal decision making, but it is precisely these timescales on which anthropogenic impacts on climate are likely to be expressed (Santer

et al., 1996). It is likely that climate change can be manifested by changes in the nature and amplitude of natural variability, but distinguishing between natural and anthropogenic origins of decadal variability is not an easy task. Furthermore, models are not yet able to consistently reproduce the spatial and temporal structures of decadal variability in the observed record, making it difficult to distinguish between various definitions of – or mechanisms responsible for – decadal variability in nature. It is not clear whether the decadal variability and prediction problem can be addressed with the phenomenon/mechanism approach, yet a better approach is not immediately obvious (Vimont, 2007).

The observed and proxy data sources are often of limited applicability for decadal predictability. The inherent 'contamination' with the anthropogenic signal, and relatively short observed record (Parker et al., 1995a; Brohan et al., 2006) are also associated with problems of incomplete records and poor data availability in certain land regions and over the oceans (Folland et al., 2001; Kruger, 2006). Suitable proxy replacements may often be of limited resolution (Burger & Cubasch, 2005; Cane et al., 2006), and have inherent problems in their extraction or spatial coverage (Stocker & Mysak, 1992; Bradley, 1999; Alverson et al., 2001)

The use of long climate model integrations provides an apparent solution to the challenges posed by the observed and proxy datasets (Carleton, 1999; Raisanen, 2007). Considerable success has been achieved in simulating the climate change and response to natural Holocene-era forcing (Blunier et al., 1995; Crucifix et al., 2002; Moy et al., 2002; Oppo et al., 2003; Von-Storch, 2004; Renssen et al., 2005; Zhao et al., 2005; Renssen et al., 2006),

warming or projected greenhouse gas scenarios (Huck et al., 2001; Collins & Sinha, 2003; Stouffer & Manabe, 2003). Additionally, the extensive integrations can provide useful insight in to variability of climate phenomena, e.g. interdecadal Pacific SST variability (Latif & Barnett, 1994; Frankignoul et al., 1997; Latif, 1998; Liu, 1999) or global THC variability (Delworth et al., 1993; Shriver & Hurlburt, 1997; Manabe & Stouffer, 1999; Delworth & Greatbatch, 2000; Huck et al., 2001; Johnson & Marshall, 2002; Dong & Sutton, 2005; Wang, 2005), but this approach has met with more limited success in the simulation of rainfall.

Rainfall is an inherently noisy variable at decadal scales (Meinke et al., 2005; Hoerling et al., 2006; Small & Islam, 2007). In the CSIRO GCM (band pass filtered between 8-200 years), for example, decadal variability was shown to explain up to 80% of variability in temperature, but only 20-40% of precipitation variability (Walland et al., 2000).

Comparison studies agree that precipitation is more difficult for climate models to simulate than other meteorological variables (McAvaney et al., 2001), and the spatial patterns of annual precipitation change are very model dependent (Yonetani & Gordon, 2001; Groisman et al., 2005). Hewitson & Crane (2006), for example, present analysis of GCM precipitation downscaling models over southern Africa, and suggest that much of discrepancy between GCM projections of precipitation may be due to differences in parameterisation schemes rather than inherent differences in the GCM simulations of regional dynamics as a result of 'fixed' forcing issues (e.g. topography, land-water boundaries; Hewitson & Crane, 2006; Singleton & Reason, 2006). This leads to the conclusion that although models capture the large scale forcing reasonably well, most of

the difference at a regional scale is likely due to variation in the way models derive their precipitation values (Hellstrom et al., 2001; Hewitson & Crane, 2006; Washington & Preston, 2006).

The simulation of variability at longer timescales is critical for a range of studies, especially those which aim to identify how the "natural" climate may respond to anthropogenic forcing scenarios. The role of decadal variability in detection and attribution of climate change is explored in the next section.

1.2 Detection & Attribution of Anthropogenic Climate Change

Distinguishing between the effects of external influences and internal climate variability requires careful comparison between observed changes and those that are expected to result from external forcing. This work is at the heart of the Intergovernmental Panel on Climate Change (IPCC)'s contribution to climate science, and the interested reader is referred to the Fourth Assessment Report (AR4; IPCC, 2007) for further detail. This section explores the importance of understanding decadal variability as a contribution to detection and attribution of climate change, and draws heavily on the IPCC reports (particularly Hegerl et al., 2007) to do so.

The concepts of climate change 'detection' and 'attribution' remain as they were defined in the IPCC's Third Assessment Report (TAR, IPCC, 2001). 'Detection' is 'the process of demonstrating that climate has changed in some defined statistical sense', without providing a reason for that change. The methods used to identify change in observations are based on the expected responses to external forcing, either from physical understanding or as simulated by climate models (Hegerl et al., 2006; Hegerl et al., 2007). Physical understanding can also be used to develop conceptual models of the anticipated pattern of response to external forcing and the consistency between responses in different variables and different parts of the climate system.

'Attribution' of causes of climate change is the process of establishing the most likely causes for the detected change with some defined level of confidence. As noted in several IPCC reports (1996; 2001; 2007), unequivocal attribution would require controlled experimentation with the climate system. Since that is not possible, in practice attribution

of anthropogenic climate change is understood to mean demonstration that a detected change is 'consistent with the estimated responses to the given combination of anthropogenic and natural forcing' and 'not consistent with alternative, physically plausible explanations of recent climate change that exclude important elements of the given combination of forcings' (IPCC, 2001).

Many studies use climate models to predict the expected responses to external forcing, and these predictions are usually represented as patterns of variation in space, time or both (Stone et al., 2001). Such patterns, or 'fingerprints', are usually derived from changes simulated by a climate model in response to forcing (Hasselman, 1993; Santer et al., 1993; Hegerl et al., 1996; Santer et al., 1996; Hasselman, 1997; Hegerl et al., 1997).

Attribution studies additionally assess whether the response to a key forcing, such as greenhouse gas increases, is distinguishable from that due to other forcings (Lee et al., 2005; Schnur & Hasselman, 2005). These questions are typically investigated using a multiple regression of observations onto several 'fingerprints' representing climate responses to different forcings that are clearly distinct from each other as distinct spatial patterns or distinct evolutions over time (Barnett et al., 1999; Wigley et al., 2000; Ziegler et al., 2003). If the response to this key forcing can be distinguished, then the evidence for a causal connection is substantially increased (Allen & Tett, 1999; Allen & Stott, 2003). This is an area of research with considerable challenges because different forcing factors may lead to similar large-scale spatial patterns of response, including decadal scale variability. It is important to understand how the decadal spatial patterns of climate are constructed, and create a 'finger print' for their modes of variability.

Both detection and attribution require knowledge of the internal climate variability on the time scales considered, usually decades or longer (Lee et al., 2005). The residual variability that remains in instrumental observations after the estimated effects of external forcing have been removed is sometimes used to estimate internal variability (Hegerl et al., 2003; Barnett et al., 2005). However, these estimates are uncertain because the instrumental record is too short to give a well-constrained estimate of internal variability, and because of uncertainties in the forcings and the estimated responses.

Model and forcing uncertainties are important considerations in attribution research. Ideally, the assessment of model uncertainty should include uncertainties in model parameters (e.g., as explored by multi-model ensembles), and in the representation of physical processes in models (structural uncertainty). Such a complete assessment is not yet available, although model intercomparison studies (Lambert & Boer, 2001; Achuta-Rao & Sperber, 2002; Guilyardi et al., 2004; Achuta-Rao & Sperber, 2006; Friedlingstein et al., 2006; Joseph & Nigam, 2006) improve the understanding of these uncertainties.

The effects of forcing uncertainties, which can be considerable for some forcing agents such as solar (Stott et al., 2003) and aerosol forcing (Graf et al., 1993; Gillett et al., 2004; Lambert et al., 2004; Lambert et al., 2005), also remain difficult to evaluate despite advances in research. Simulations of global mean 20th-century temperature change that accounted for anthropogenic greenhouse gases and sulphate aerosols as well as solar and volcanic forcing were found to be generally consistent with observations (Boer et al., 2000; Tett et al., 2002; Zorita et al., 2004; Zorita et al., 2005; Johns et al., 2006; Stott et al., 2006; Tett et al., 2007).

Detection and attribution results based on several models or several forcing histories also provide information on the effects of model and forcing uncertainty, and such studies suggest that while model uncertainty is important, key results – such as attribution of anthropogenic influence on temperature change – are robust.

Internal climate variability is therefore usually estimated from long control simulations from coupled climate models (e.g. Pope et al., 2000; Zorita et al., 2005; Min et al., 2005a, 2005b; Stott et al., 2006). Confidence is further increased by systematic intercomparison of the ability of models to simulate the various modes of observed variability (van-Oldenborgh & Burgers, 2005; Achuta-Rao & Sperber, 2006; Philip & van-Oldenborgh, 2006), by comparisons between variability in observations and climate model data (Hegerl & Allen, 2002) and by comparisons between proxy reconstructions and climate simulations of the last millennium (Boer et al., 2000; Tett et al., 2002; Tyson et al., 2002; Gladstone et al., 2005). This generates a framework under which variability can be examined, and provides guidance for methods available for use to increase confidence in the results of this study.

The most easily obtainable evidence of externally forced change has come from the global scale analyses of the combined instrumental SAT and SST records – well suited because of its high quality and broad spatial coverage (Jones & Briffa, 1992; Jones et al., 1997; Jones et al., 1999b; Jones & Moberg, 2003).

Recent studies have begun to assess whether the climate response is detectable on regional scales (e.g. Stott & Tett, 1998; Stott, 2003; Hegerl et al., 2006), since it is generally recognised that the impact of climate change will probably be felt most strongly through

changes in precipitation and short term climate extremes. This is particularly important to this study, since it is likely that at the management scale, the impacts of multi-decadal climate variability may be greater than the impacts of climate change (Hulme et al., 1999).

Initially, few studies were done at regional scales because the noise at local scales is greater than at a larger scale (Hulme et al., 1999; Karoly & Wu, 2005). Regional climates are typically characterised by pronounced interdecadal variability due to a number of factors: the intrinsic nonlinear and chaotic nature of the climate system, the occurrence of non linear modes and regimes of the general circulation, the presence of feedback and threshold processes (Zwiers & Zhang, 2003; Zhang et al., 2006). This internal variability of the climate system sets a level of background noise to attempts to estimate or predict an external or anthropogenic signal (Manabe & Stouffer, 1996; Stouffer et al., 2000)

Additionally, regional climate variability often manifests itself in geographically anchored spatial patterns with changing amplitude which determine the local climatic conditions (Schwierz et al., 2006; Rocha et al., 2007). The effects of these factors become increasingly important at the regional scale for variables such as precipitation, whose statistics can be altered substantially by relatively minor changes in general circulation features (Karoly & Braganza, 2005a). Although temperature trends can be scaled, precipitation trends cannot: the interdecadal variability of the precipitation change signal contains stochastic and chaotic elements which do not scale well (Giorgi & Francisco, 2000; Giorgi, 2005). It is therefore important that the interdecadal variability of regional climate change is fully recognised and characterised when developing climate change scenarios (Abarca-del-Rio & Mestre, 2006).

Downscaling techniques are often applied – particularly in regions of complex topography, like southern Africa – but they are often embedded in climate models and only utilise short records for analysis (for reviews see Hewitson & Crane, 2006). For longer timescales, the complexity of models makes this solution computationally impractical, leading to formulation of reduced complexity models (Raisanen et al., 2004). The parameterisation and presence of non-linear and inter-scale interactions can render this approach questionable, unless specific comparisons with higher complexity models are undertaken. A prediction by a single climate simulation that uses observational records as a constraint is subject to the uncertainties of internal and stochastic variability (Murphy et al., 2004) which is expected to increase at regional scales.

At the regional scale, the signal to noise ratio is weaker than global scale evolution, making the detection and attribution of surface warming more difficult (Spagnoli et al., 2002). In modelling climate at decadal scale, for example, the synoptic scale weather is often regarded as a noise component. Similarly, compared to a secular anthropogenic trend, the decadal scale variability could be dismissed as "noise". Coupled with the known issues relating to rainfall simulation, the detection of anthropogenic changes in mean precipitation presented a difficult challenge (Hegerl et al., 2003).

Over recent decades, precipitation trends are small or mixed in most areas, and the natural variability of precipitation can be very strong at regional scales. This seems to be a major obstacle for the detection of climate change, since modelled and observed precipitation signals respond to natural forcing, especially stratospheric aerosols resulting from volcanic activity (Lambert et al., 2004; Lambert et al., 2005). By contrast, land temperature

anomalies are thought to be dominated by anthropogenic responses (Dery & Wood, 2005), though given the potential impact on the surface energy budget, precipitation is likely to have influenced temperature trends at the regional scale (Trenberth & Shea, 2005). If the precipitation variability is not caused by anthropogenic forcing, or well captured in the climate change scenarios, then detection of temperature change at the regional scale is likely to be jeopardised.

However, Douville (2006) shows that an understanding of rainfall variability at natural time scales effectively reduces the uncertainty in our knowledge of simulated surface warming, and increases consistency with observations. If the rainfall variability is used as a constraint, the surface warming is better simulated, and the temporal evolution of the SAT trends over the past 60 years is better aligned with the greenhouse forcing signature (Douville, 2006).

Improved understanding of rainfall variability, particularly the underlying decadal variability, has now enabled studies to attribute anthropogenic signals in precipitation itself at the global scale (Zhang et al., 2007). This recent work uses a spread of natural and anthropogenic model scenarios (including contributions from HadCM3 and ECHO-G) to identify and attribute anthropogenic change in latitudinal bands of rainfall. The estimated contribution of natural variability is small relative to the anthropogenic contribution, but there is still underestimated residual variability which is unexplained and potentially under-simulated.

Other studies have now attributed changes in regional precipitation in the Sahel (Jenkins et al., 2005) or South West Australia (Karoly & Braganza, 2005a, 2005b; Timbal et al., 2006), and the subsequent effect on river runoff (Gedney et al., 2006) to the anthropogenic-driven climate change signal. The multimodel estimates are thought to be less susceptible to model error than individual contributions, and the structure of the multimodel fingerprint is shown to be consistent with observed understanding of precipitation response to anthropogenic forcing.

1.3 The Climate of Southern Africa

In order to understand decadal variability, we must first understand key elements of interannual variability over southern Africa, and identify the important factors and locations that are likely to play a role at lower frequencies. The interannual (2-7 year period) climate of southern Africa has been extensively described elsewhere (e.g. Mason & Jury, 1997; Tyson & Preston-Whyte, 2000), and this section provides a brief overview of this work. The reader is referred to these references for further detail.

First, it is important to understand the key physical features of the region. South Africa is characterised by a high interior plateau of 1-2 km and steep topography at (or near) the coast, leading to strong topographic gradients and a variety of topographically forced weather systems (Singleton & Reason, 2006). There are also strong sea surface temperature (SST) gradients (Figure 1.1) which result from coastal upwelling along the west and south coast, and the presence of the warm Agulhas Current in the east (Lutjeharms & de-Ruijter, 1996; de-Ruijter et al., 1999; Vigaud, 2007) and local oceanographic features (Matano & Beier, 2003) which may play a role in modulating local climate and atmospheric features (Figure 1.2 and Jury et al., 1993a; Reason, 2001a).

These gradients lead to zonal and meridional divisions of rainfall. The equatorial regions receive the highest rainfall totals (e.g. 2000mm/yr over the Gulf of Guinea; 1800mm/yr over the Congo basin; Vigaud, 2007), driven by seasonal migration of the Intertropical Convergence Zone (ITCZ; Tyson & Preston-Whyte, 2000). The tropical east-west gradient shows marked differences between the Bie plateau (1200mm/yr) and the Great Rift Valley (2000mm/yr over Lake Tanganyika, for example).

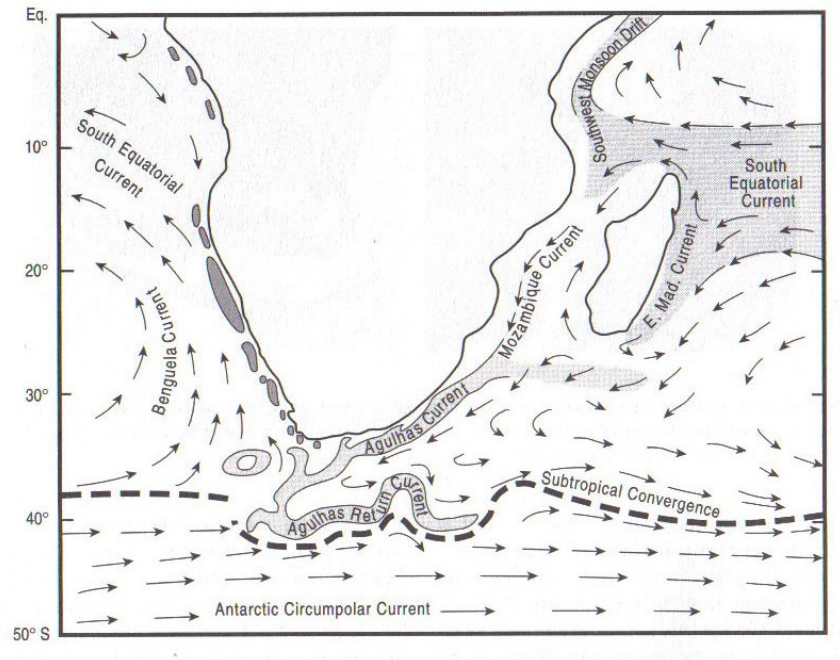

Figure 1.1: Ocean currents around southern Africa (after Niler, 1992; cf. Tyson & Preston-Whyte, 2000). The shaded areas off the west coast represent cells of upwelling cold water in the Benguela system.

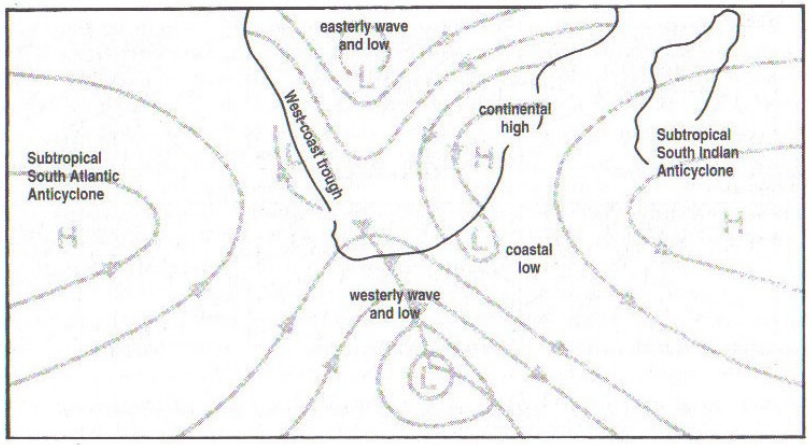

Figure 1.2: Important features of the synoptic scale circulation of southern Africa (after Tyson & Preston-Whyte, 2000).

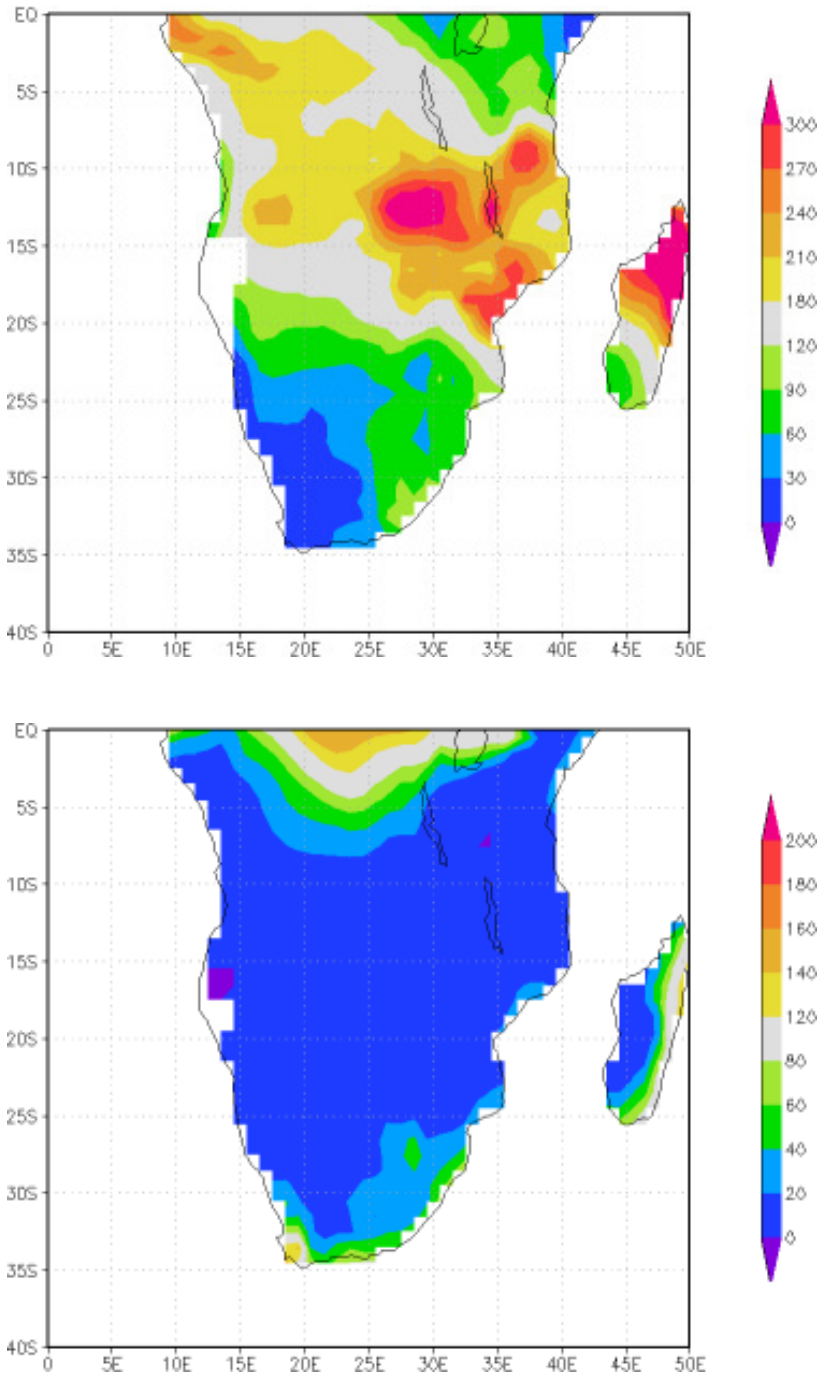

Figure 1.3: Mean rainfall distribution (mm/month) over southern Africa for the wet season (JFM, top) and dry season (JAS, bottom), using CRU TS 2.1 (0.5° resolution) precipitation data (New et al., 1999; Mitchell & Jones, 2005) generated with KNMI Climate Explorer. Note the different scale bars in wet and dry seasons.

In the subtropics, a similar east-west gradient displays differences between the wetter east coast and the drier west coast (Figure 1.3). Most subtropical regions have one rainy season, with maximum rainfall in the austral summer (November-April; Allan et al., 1995; Allan et al., 2003; Reason et al., 2005), although the Western Cape is known for the more Mediterranean climate type, with austral winter rainfall dominating the annual totals (Reason et al., 2001; Reason et al., 2002; Reason & Rouault, 2005). Rainfall variability in the region is driven by changes in the frequency, duration or intensity of large-scale weather systems responsible for days with significant rainfall (Harrison, 1984), rather than variations in the number of rain days or the length of the rainfall season (Mason & Jury, 1997). For this study, the decadal focus necessitates an annual average of rainfall, and the JFM monthly average is therefore employed throughout as a suitable proxy for this dominant summer rainfall signal (Reason & Jagadheesha, 2005; Washington & Preston, 2006).

In this section, the main influences on interannual variability are explored. Key rainfall-bearing circulation features are examined, and linked to the behaviour of regional interaction with atmospheric and oceanic variability. The role of global teleconnections and their links with southern African rainfall are also discussed. This review emphasises the importance of understanding the contribution and interaction of rainfall variability components.

1. 3. 1 What drives interannual variability?

For much of southern Africa, the most important summer rainfall generating system is the tropical-temperate trough, which links a surface heat low that forms in the tropical easterlies over the landmass with a mid-latitude disturbance south of Africa, generally forming a band of cloud and associated convection oriented northwest-southeast (Todd & Washington, 1999). These systems are responsible for much of the summer rainfall over large regions of southern Africa (Washington & Todd, 1999). When the surface heat low is over Namibia/Angola, the cloud band and associated rains tend to occur over southern Africa (Tyson & Preston-Whyte, 2000), describing a NW-SE orientation found in much of southern African climate analysis.

Heavy rainfall events over southern Africa may also be associated with the infrequent passage of tropical cyclone across the coastal margins (Jury & Levey, 1993), which provide a negligible percentage of rainfall totals, but can cause localised flooding (Diab et al., 1991). Tropical cyclones are more typically linked to dry conditions over southern Africa, when the cyclone remains in the Mozambique Channel and generates anomalous offshore flow (Jury et al., 1993b). Other synoptic scale systems do contribute to southern African rainfall, but contribute a lower proportion of annual rainfall (Mason & Tyson, 1992). Interannual rainfall variability over southern Africa can be related to changes in the incidence, persistence and strength of these important synoptic conditions, and this is confirmed by the observed similarity between the atmospheric conditions associated with wet/dry conditions at a range of different temporal scales (Tyson, 1980; Tyson & Preston-Whyte, 2000).

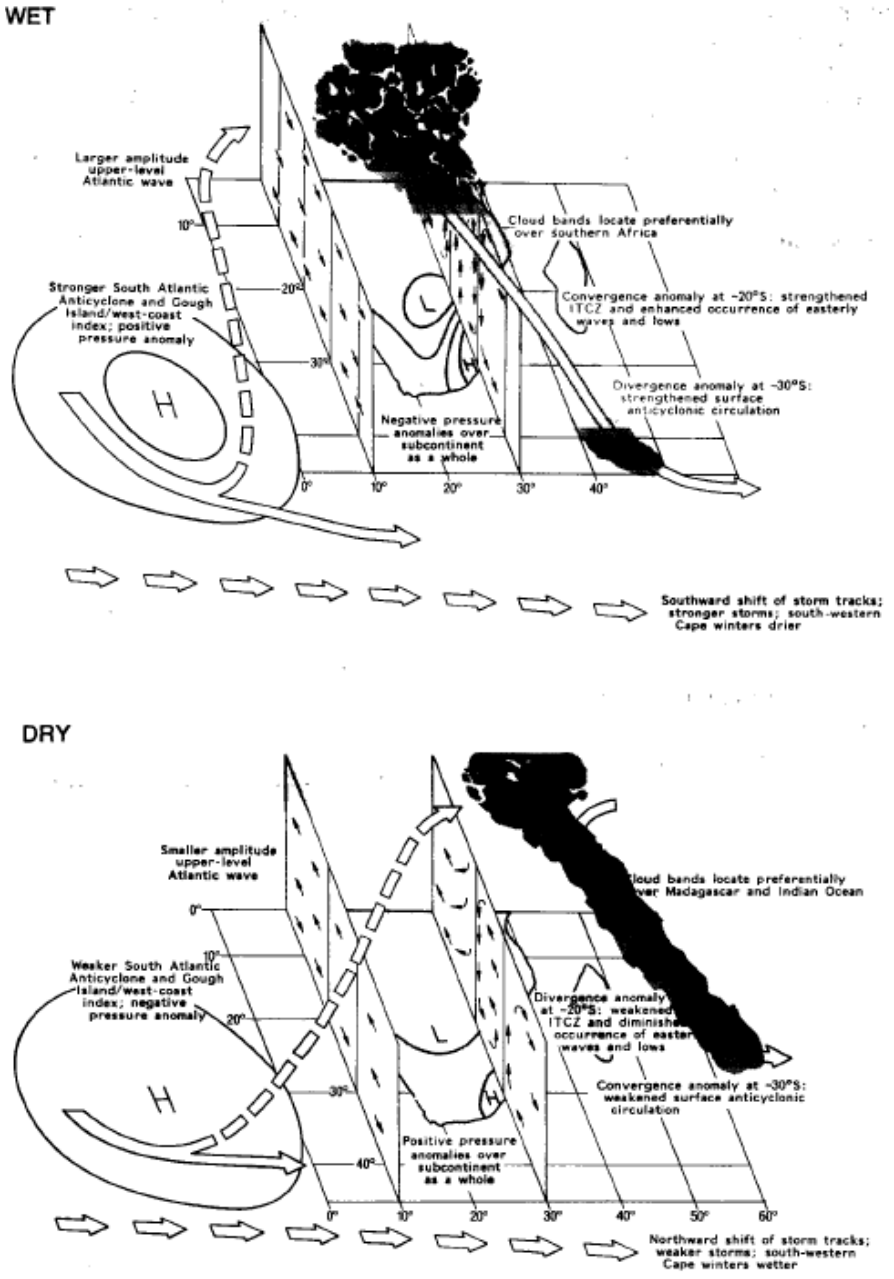

Figure 1.4: Conceptual models of the anomalous meridional circulations over southern Africa during spells of predominantly wet (top) and dry (bottom) conditions. After Tyson (1986) cf. Mason & Jury (1997).

Conceptual models of the atmospheric circulation during wet and dry conditions have been proposed by Tyson (1986, cf. Mason & Jury, 1997), and are illustrated in Figure 1.4. Dry summers are dominated by tropospheric winds which reduce the potential for convection over southern Africa, and typically accompany increased tropical disturbances in the south west Indian Ocean. This is represented by an eastward shift in the preferred location for summer convection (Hastenrath et al., 1995), and is supported by analysis of outgoing long-wave radiation and geopotential height. These changes are consistent with a weakened divergence of moisture from the equatorial Indian Ocean (D'Abreton & Lindesay, 1993), suggesting that decreased rainfall over southern Africa is often offset by increased east African rainfall (Hastenrath, 2000). The longitudinal shifts in convection have substantial impact on the Hadley circulation, which strengthens over southern Africa and is associated with enhanced westerlies south of the sub-continent.

Wet summers are typically more closely linked to the south-west Indian Ocean than the Atlantic basin; with enhanced atmospheric variability and warm oceans leading to a larger moisture flux. The alignment of the NW-SE trough over the subcontinent generates the sustained rainfall needed by agriculture (Usman & Reason, 2004; Mapande & Reason, 2005), whereas an east coast-displaced trough is associated with weaker and more patchy rainfall (Jury & Levey, 1993). As well as the primary rainfall effects, increased atmospheric water vapour over southern Africa during wet years also encourages atmospheric instability and stronger convection (Harrison, 1984).

This circulation pattern is thought to be influenced by a range of variables in the generation of interannual variability. First, there is thought to be a response to atmospheric

forcing. The stratospheric Quasi-Biennial Oscillation (QBO) was previously thought to play a significant role in modulating the behaviour of El Nino-Southern Oscillation (ENSO) over southern Africa. Links were proposed between the phase of the QBO (Jury, 1997), and the Walker circulation over the western Indian Ocean, suggesting that lower stratospheric easterly zonal winds may provide upper-tropospheric wind stress which enhances Walker cell overturning with a descending limb over southern Africa (Mason & Lindesay, 1993; Jury & Engert, 1999; Jury et al., 2002). During westerly phase years, the reversal of the Walker cell could generate a rising limb over southern Africa and enhance convection and rainfall over the subcontinent (Mason & Tyson, 1992). With the mechanism and links to southern Africa poorly understood, the influence of the QBO has declined in importance as a theoretical component of the regional climate system.

Some studies have suggested that the climate may also respond to solar forcing. Although widely recognised as having a role in millennial scale variability (Shindell et al., 1999; Shindell et al., 2001; Shindell et al., 2003; Gray et al., 2005; Cubasch et al., 2006), the influence of solar variability on shorter time scales is debated. A range of studies have linked solar cycles (the 11 or 18 year luni-solar cycles in particular; Currie, 1993, 1993; van-Loon & Labitzke, 2000; Coughlin & Tung, 2004; Crooks & Gray, 2005; Weng, 2005) to climatic variability, with mechanisms providing a link to stratospheric climate (Mason & Tyson, 1992; Coughlin & Tung, 2004; Cubasch et al., 2005), but showing fairly limited potential influence on the troposphere (Balachandran et al., 1999; van-Loon & Labitzke, 2000; Dima et al., 2005; Weng, 2005) and solar variability is not thought to be of substantial influence.

Most studies agree that the oceanic influences dominate the known components of rainfall variability over southern Africa. As well as the highly local influences exerted by the Agulhas Current (Jury et al., 1993a; Crimp et al., 1998; Kruger, 1999; Reason, 2001a; Rouault et al., 2002; Schouten et al., 2002; Schouten et al., 2003) and Benguela regions (Nicholson & Entekhabi, 1987; Walker, 1990; Rautenbach & Smith, 2001; Florenchie et al., 2003) on immediate coastal rainfall, there is also substantial evidence for wider oceanic forcing of southern African rainfall (Mason, 1995; Mason & Jury, 1997; Jury et al., 2004). Principal component-based weighting of ocean basins shows links to the Indian Ocean (containing intrinsic and ENSO-led modes of variability), the tropical south east Atlantic, the North Atlantic and the Agulhas region (Jury et al., 1999).

With warmer waters, the Indian Ocean is typically considered as the main source of moisture for southern Africa. Evidence for a close association between summer rainfall and SST anomalies in the South West Indian Ocean (SWIO) has been suggested by a range of observed, reanalysis and model studies. There is substantial evidence of decadal to multidecadal variability in SST over the South Indian Ocean (Allan et al., 1995; Ansell et al., 1998; Reason, 2002), which involves broad warming/cooling and strengthening/weakening of the winds across the sub-tropics/mid-latitudes of this basin, and it is thought that on decadal to multidecadal scales, modulations here may be linked to southern African rainfall variability. Observations suggest that when SST is warm to the south of Madagascar, increased summer rains occur over large areas of south eastern Africa. Behera & Yamagata (2001) described the existence of a coupled air-sea pattern of variability within the southern subtropical IO during winter. Reason (2002) forced an

atmospheric GCM with positive SST anomalies in the SW Indian Ocean and negative SST anomalies in the SE Indian Ocean. The results show increased rainfall over south eastern Africa, a result consistent with previous modelling and observational studies (Goddard & Graham, 1999; Reason & Mulenga, 1999; Behera & Yamagata, 2001; Reason, 2001b; Terray et al., 2003; Reason et al., 2006a). Fauchereau et al. (2003) have linked this southern Indian Ocean SST dipole with a similar mode of variability in the Southern Atlantic Ocean (Fauchereau et al., 2003b; Hermes & Reason, 2005), and Terray et al (2003) have provided evidence of a link between this SST dipole in the south Indian Ocean and Indian summer monsoon variability.

This "SST dipole" pattern in the SW Indian Ocean leads to increased rainfall via enhanced convergence of moister than average air over the region by enhanced surface fluxes and mid-latitude baroclinicity (Walker, 1990; Walker & Shillington, 1990). Increased evaporation occurs over the warm pole in the South West Indian Ocean and this moist air is advected towards Mozambique and eastern South Africa as a result of the low pressure anomaly generated over this pole which strengthens the onshore flow (Reason, 2001b). The large scale velocity potential field suggests that there is relative enhancement of the local Walker circulation over the western Indian Ocean/southern African region and relative weakening of this cell over northern Australia. Particular attention is paid to the model sensitivity to the location of the warm pole in the SWIO and to the presence of the cold pole, suggesting that the response over south eastern Africa is stronger if the warm pole is located closer to the subcontinent (Behera & Yamagata, 2001; Reason, 2002; Hansingo & Reason, 2006).

The South Atlantic has typically been regarded as a secondary moisture source for the summer rainfall over southern Africa (D'Abreton & Lindesay, 1993; Tyson & Preston-Whyte, 2000,) and linked primarily to SW Cape rainfall (Reason, 1998; Reason et al., 2001; Reason et al., 2002; Rouault et al., 2003) and modification of the winter storm track (Venegas et al., 1997; Sterl & Hazeleger, 2003; O'Mahony et al., 2005). Recent studies (Hermes & Reason, 2005; Reason & Jagadheesha, 2005) have suggested that connected atmospheric circulations may also affect southern African climate, and modify rainfall during austral summer (Tennant & Reason, 2005). Observed and model studies have shown anomalous South Atlantic SST patterns with links to quasi-decadal spectral power (Venegas et al., 1996, 1997; Sterl, 2001; Sterl & Hazeleger, 2003; Colberg et al., 2004; Colberg & Reason, 2007), and suggested that these modes could influence rainfall at these timescales (Vigaud, 2007).

The main difficulty in splitting oceanic influence by component analysis-style techniques derives from their inherent interaction in the real world. A series of studies (Hermes & Reason, 2005; Reason et al., 2006a) have suggested potential links between the South Atlantic and South West Indian Oceans, for example, and this is typical of a range of studies which demonstrate that forcing of southern African rainfall does not happen in isolation (Reason et al., 2006a). In the next section, the link between southern African rainfall and ENSO variability is explored further, and the viability of intrinsic Indian Ocean variability discussed in greater detail.

1. 3. 2 The role of El Nino-Southern Oscillation (ENSO)

Much of the seasonal forecasting and interannual rainfall variability in the southern African region has been linked strongly to the behaviour of El Nino-Southern Oscillation (ENSO), with up to 20% of rainfall estimated to be ENSO driven (Lindesay, 1988). Local links have been observed in Zimbabwe (Cane et al., 1994; Waylen & Henworth, 1996; Makarau & Jury, 1997), Namibia (Jury & Engert, 1999), Lesotho (Hyden & Sekoli, 2000) and Tanzania (Kijazi & Reason, 2005; Mapande & Reason, 2005), as well as in wider regional analysis. At the sub-continental scale, ENSO's influence is particularly related to austral summer rainfall (Landman & Goddard, 2002; Reason et al., 2005). Analysis shows that although much of southern Africa displays significant correlation with the ENSO signal in JFM (Nicholson, 1997; Nicholson & Kim, 1997), the southern African response is weaker by AMJ, and is confined to Namibia and western South Africa (Allan et al., 1995; Allan et al., 2003). The previously identified JFM average is therefore thought to be appropriate to capture ENSO's variability in the region (Guilyardi et al., 2004; Collins et al., 2005; Guilyardi, 2006; Leloup et al., 2007).

Echoing the circulation model shown previously, Figure 1.5 shows a schematic representation of the anomalous Walker circulation driven by ENSO (after Harrison, 1986). During the low phase of ENSO (Pacific warm events), the warming of the surface ocean changes the stream function and alters the (anti) cyclonicity of the flow. This changes the velocity potential, and shifts the zone of cloud-band convergence offshore, taking with it the highest rainfall levels. During the high phase of ENSO (Pacific cold events), the cloud bands locate preferentially over southern Africa, and enhance rainfall.

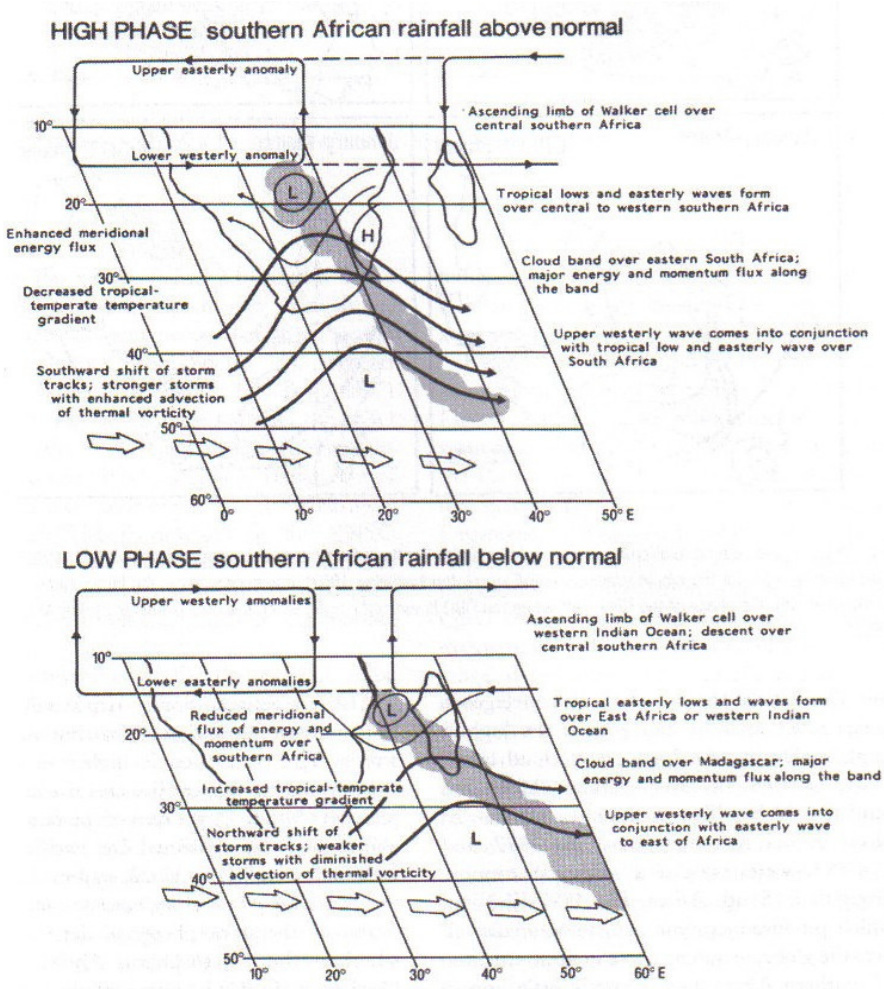

Figure 1.5: Schematic representation of the anomalous Walker Circulation over southern Africa, after Harrison (1986) cf. Tyson & Preston-Whyte (2000: Fig. 13.21). Top: during the high (La Nina) phase of the Southern Oscillation, when above-normal rainfall may occur over southern Africa. Bottom: during the low (El Nino) phase of the Southern Oscillation, when droughts may be expected. Light lines indicate surface flow, heavy lines denote upper tropospheric conditions.

A range of studies have confirmed the relationship between ENSO and southern African rainfall in model and observed data (Nicholson & Kim, 1997; Rocha & Simmonds, 1997, 1997b; Goddard & Graham, 1999; Hyden & Sekoli, 2000; Fauchereau et al., 2003a; Reason & Jagadheesha, 2005; Shongwe et al., 2006; Lyon & Mason, 2007). Increasingly, ENSO phase is used as one of the primary contributors to seasonal forecasts over southern Africa (Landman et al., 2001; Landman & Goddard, 2002; Murphy et al., 2002; Mulenga et al., 2003; Tippett & Giannini, 2006) and other rainfall dependent regions (Nelson et al., 2002; Podesta et al., 2002; Hansen et al., 2006).

The interaction of ENSO and decadal ENSO-like oscillations is potentially vital to this study, particularly given ENSO's known influence over southern African rainfall at interannual timescales, and the potential for change in ENSO forcing at decadal-centennial scales (Gershunov & Barnett, 1998; Power et al., 1999a; Kleeman & Power, 2000; Richard et al., 2000; Goddard et al., 2001; Fauchereau et al., 2003a).

On interannual timescales, ENSO provides a very well defined phenomenon that may be understood as the result of a defined mechanism (e.g. delayed oscillator theory, recharge-discharge) that has shaped interannual prediction methods (Kirtman & Schopf, 1998). In contrast, the decadal "phenomenon" does not appear to be so clearly defined. Large scale patterns, such as the Pacific Decadal Oscillation (strictly defined by Mantua et al., 1997, and more loosely interpreted by Zhang et al., 1997; Wang & Neelin, 1998), are not thought to dominate decadal variability to the same degree as ENSO dominates interannual variability (Latif & Barnett, 1994, 1996; Bratcher & Giese, 2002; Auad, 2003; Latif, 2006), and moreover may represent the superposition and/or convolution of several

mechanisms (e.g. Schneider & Cornuelle, 2005; Newman, 2007) rather than the result of one identifiable physical process (Vimont, 2007).

Tropical Pacific decadal variability bears a strong resemblance to interannual variations, suggesting that the two phenomena are related (Tourre et al., 1999; Gedalof & Smith, 2001; Wang et al., 2003a, 2003b; Chelliah & Bell, 2004; Mokhov et al., 2004). This relationship is made clear by attempts to reconstruct tropical Pacific decadal variability using spatial structures associated with interannual variability (Kleeman & Power, 2000; Newman et al., 2003; Vimont, 2005; Yeh & Kirtman, 2005). This exercise reveals that the spatial structure of "ENSO-like" decadal variability is reproduced by averaging over precursor, peak and antecedent variability associated with the interannual ENSO cycle (Luo et al., 2003; Newman et al., 2003; Rodgers et al., 2004; Yeh & Kirtman, 2004, 2005; Hasegawa & Hanawa, 2006; An et al., 2007). This includes an influence of mid-latitude atmospheric variability on ENSO through subtropical ocean-atmosphere interactions (Barnett et al., 1999; Timmerman & Jin, 2002; Qiu, 2003; Lohmann & Latif, 2005).

This relationship between Pacific interannual and decadal variability provides a null hypothesis for tropical Pacific decadal variability, and a metric for testing model simulations of decadal variability, but it is not yet clear whether the "phenomenon/mechanism" paradigm for ENSO prediction will be applicable at decadal timescales (Vimont, 2007).

The challenge for southern African rainfall variability is that the ENSO influence at classic and decadal timescales is subtle and there a number of potential factors of importance (Hagos & Cook, 2005; Tennant & Reason, 2005), as well as potential

evidence that the correlation between ENSO and southern Africa is not constant. Although it has been suggested that any inconsistent ENSO relationships are fundamentally statistical sampling-driven (van-Oldenborgh & Burgers, 2005; Sterl et al., 2007), analysis of the long term variability of the relationship shows that there are periods of weak ENSO influence over southern Africa (Allan, 2000; Kleeman & Power, 2000; Richard et al., 2000). This variability may be driven at centennial scales (Gershunov & Barnett, 1998; Tudhope et al., 2001; D'Arrigo et al., 2005; Zhang & Busalacchi, 2005) and have underlying implications for the behaviour of decadal variability (Zinke et al., 2004; Damassa et al., 2006; Yu & Zwiers, 2007).

It is also clear that ENSO is not the only cause of SST-led rainfall variability over southern Africa, and its changing relationship may have close links to intrinsic variability in the Indian Ocean itself. This hypothesis is explored in the next section.

1. 3. 3 The role of ENSO-independent forcing

As well as ENSO-related forcing, the Indian Ocean is thought to have an important intrinsic driving factor in low-frequency variations of the tropical climate. Unusually, the basin is bounded in the north, and therefore dominated by westerlies driven by the Indonesian low (Jochum & Murtugudde, 2004, 2005) rather than the gyre circulation mechanisms thought to dominate the North Pacific at decadal scales (e.g. Latif & Barnett, 1994; Latif, 2006). Significant long term changes in the distribution of Indo-Pacific SST and tropical teleconnection patterns, dating from the 1976-77 shift (Nitta & Yamada, 1989; Kumar et al., 1999; Clark et al., 2000; Wang & An, 2001), or links to the global

thermohaline circulation (Reason et al., 1996a, 1996b) may also contribute to variability in the region.

The 'classic' view of the Indian Ocean is as a passive element in the tropical system, essentially controlled by El Nino through an 'atmospheric bridge' (Lau & Nath, 1994, 1996; Klein et al., 1999; Alexander et al., 2002; Lau & Nath, 2003; Aldrian et al., 2007) and by the Asian summer monsoon via air-sea fluxes (Webster et al., 1999). However, the capability of the Indian Ocean to generate stochastic internal variability has been suggested in a range of different mechanisms. The Indian Ocean Dipole Mode (IODM; Saji et al., 1999; Vinayachandran et al., 2002; Yamagata et al., 2002; Saji & Yamagata, 2003; Saji et al., 2006) is perhaps the most well studied intrinsic variability, and has been linked to a range of potential teleconnections (Ashok et al., 2003a; Kripalani & Kumar, 2004; Ashok et al., 2004a; Ashok et al., 2004b; Annamalai et al., 2006; Yadav et al., 2007). However, the timing (and location) of the IODM peak variability does not influence southern African rainfall.

Less is known about the intrinsic interannual variability in the southern Indian Ocean which is known to have associations with southern African rainfall variability. Some studies have suggested that the subtropical Indian Ocean plays an important role in modulating local climate dynamics (Goddard & Graham, 1999; Behera & Yamagata, 2001; Collins et al., 2004; Kay, 2005; Washington & Preston, 2006), and this has been suggested as an area of particular importance in ENSO dynamics among others (Tyson & Preston-Whyte, 2000).

Washington & Preston (2006), for example, showed that the indices of ENSO and anomalous years of extreme rainfall in southern Africa did not always match, and suggested that ENSO controlled less than half the interannual variance of JFM SSTs in the Indian Ocean. Linear regression to remove the ENSO signal tested the response of the atmosphere to SWIO SST anomalies, although the multi-decadal impact of ENSO and potential implications on the Indian Ocean were not considered (Washington & Preston, 2003). JFM composite SST anomalies derived from the GISST data (Rayner et al., 2003) showed enhanced (reduced) poleward gradient off Madagascar for dry (wet) conditions. This analysis then formed the basis for idealised SST anomalies which were used to force HadAM3's atmospheric response. Despite acknowledging problems with model convective parameterisation, Washington & Preston (2006) showed that local SST anomalies in the SWIO could generate ENSO-independent rainfall variability over southern Africa, with up to 40% of the significant circulation response (700hPa moisture flux) due to the anomalous SST forcing.

The intrinsic variability of the SWIO must therefore be taken in to consideration, as a key location for southern African rainfall variability, and a region of considerable internal and external variability.

1. 3. 4 Summary of interannual variability

Derived from the synoptic-scale variability associated with tropical-temperate troughs and their rainfall, southern African interannual rainfall variability has been linked to atmospheric and oceanic links which control the formation of troughs. A coherent mechanism has been proposed which effectively explains both 'wet' and 'dry' conditions

over southern Africa (Harrison, 1984; Tyson & Preston-Whyte, 2000), and has been supported by a range of observed, reanalysis and model data-based studies. The similarity between synoptic and interannual patterns of variability shows evidence of being linked to ENSO-type forcing, together with intrinsic variability of the SW Indian Ocean region to generate oscillations at lower frequencies.

Regions of the globe that are impacted by 'classical' ENSO events are often those showing most prominent (multi) decadal variations in climate (Allan, 2000). Enhanced (quiescent) signal strength tends to be aligned with epochs of robust (weak) low frequency ENSO powers – reinforcing the notion that ENSO modulations must be viewed in conjunction with decadal variability (Kruger, 1999). Similarly, understanding the underlying decadal variability is thought to be key to understanding the interannual variability in the IO and Pacific (Terray & Dominiak, 2005).

This review has identified the principal regions of influence over southern African rainfall. Knowledge of the interannual variability helps to define the areas of particular interest for the study of decadal variability, and it has been shown that there are areas where additional work is required to improve our understanding. A series of study aims have been developed in order to address these gaps in the existing knowledge.

1.4 Study Aims

The review of current knowledge in decadal variability demonstrates considerable advances made in the last twenty five years. The development of new models and data sets has enabled an increased understanding of natural and anthropogenic variability at quasi-decadal scales, and these approaches can now be applied to southern African variability. This study aims to build on the knowledge of interannual variability and forcing mechanisms outlined here, and explore how observed, proxy and climate model sources demonstrate decadal variability in southern African rainfall under control and forced scenarios.

In order to focus the study, four specific research questions are posed, which are then investigated through the thesis.

(1) To what extent do General Circulation Models reproduce the southern African decadal variability?

Given the short observed record, climate models are often regarded as the most suitable method of studying variability at decadal scales. This research question addresses the key issue underpinning the study of decadal variability in southern Africa, and explores how the models simulate the region's climate. Evaluation of the model's ability to simulate the climatological mean will be made with reference to observed and palaeoclimatic data for selected key variables, to test this research question and provide an assessment of the model data for use in the rest of the study. This does not intend to provide an in-depth evaluation of model-specific problems, but aims instead to give an overview of the attributes and principal limitations of this data source in studying decadal variability.

(2) What is the nature of decadal variability in southern African rainfall?

The 18-20 year rainfall oscillation has long been considered the dominant decadal signal over the summer rainfall region of southern Africa (Tyson, 1971). However, since this oscillation is not of significance in all palaeoclimate studies, varies with regional analysis of observed data, and has no coherent mechanistic explanation, it is left unclear whether this is a "manifestation of the present resolution of the record[s], or a real result which needs to be tested" (Holmgren et al., 1999). This study will investigate the decadal variability in observed, palaeoclimate and model data, and present a clearer understanding of the temporal and spatial nature of decadal rainfall variability over the region.

(3) What ocean-atmosphere variability is associated with decadal rainfall variability over southern Africa?

Ocean-atmosphere interaction has been identified as a key driver of interannual variability over southern Africa, with several regions identified as sources of forcing. This interaction is thought to be both intrinsic and linked to global teleconnections like ENSO. This research question explores whether these associations remain consistent at decadal scales, and investigates how any changes may influence rainfall variability over southern Africa.

(4) Is decadal variability altered by anthropogenic forcing?

Having established the nature of decadal variability under "control" and "natural" conditions, this research question explores how the decadal rainfall variability of southern Africa may be altered under anthropogenic forcing. Potential changes to the spatial and spectral nature of the variability are considered, together with the implications of any changes in associated ocean-atmosphere variability. This section will employ further proxy analysis to assist in understanding the behaviour of the real world.

These research questions are designed to build upon the issues identified in this chapter, and consolidate and develop the existing knowledge. In order to do this effectively, a coherent and appropriate methodology must be employed. This is outlined in Chapter (2), which outlines the principal data sources and climate model simulations employed in the study, and identifies the appropriate research method design to address the study aims.

The four research questions are answered in separate chapters. Hence, Chapter (3) presents the evaluation of the model simulations of southern African climate, and describes their limitations and subsequent steps taken to generate robust results. Chapter (4) describes the spatial and temporal nature of the rainfall variability over the region, and presents the variability identified in proxy, observed and climate model data. The variability associated with decadal rainfall variability over southern Africa is explored in Chapter (5), and comparisons made between observed and modelled climate simulations. This comparison is continued in Chapter (6), which investigates the role of anthropogenic forcing using state of the art climate simulations, and draws upon proxy data to establish whether the nature and mechanisms of decadal rainfall variability over southern Africa are affected by warming trends. Finally, Chapter (7) provides a discussion of the results and implications of this study, and avenues of further work are explored.

(2) Data & Research Methods

This chapter describes the data and research techniques employed throughout the study. The choice of data and method is shown to be a direct response to the study aims, and to generate a robust analysis of the decadal rainfall variability over southern Africa.

2.1 Data Sources:

In presenting one of the first evaluations of southern African rainfall variability at decadal scales, a comprehensive range of data sources are employed to understand the region fully. This section identifies the principal datasets used through this study, and explains how they contribute to our understanding of decadal variability. A multi-method analysis is presented to reduce the uncertainty associated with individual data limitations, and to ensure a more robust result. Full details of the technical elements of each dataset can be obtained from the relevant papers, and further detail of how the data have been acquired can be found in Appendix 1.

2. 1. 1 Palaeoclimatic Data

The instrumental record in southern Africa is relatively short, but valuable insight in to the longer-term behaviour of the climate system can be gained by examining proxy climate records (Goosse et al., 2006; Therrell et al., 2006). Unlike the northern hemisphere (Stocker & Mysak, 1992; Stocker, 2000), continuous high resolution late-Holocene palaeoclimate data sources are still rare in the southern hemisphere, and southern Africa in particular (Tyson & Lindesay, 1992; Tyson, 1999; Tyson et al., 2002), and many palaeoenvironmental investigations have been hampered by 'issues of access, the paucity

of closed sites, and geochronological difficulties associated with establishing the timing of development of key geomorphic features' (Thomas & Shaw, 2002). At the millennial to century scale, a range of work has been carried out using speleothem methods (Holmgren et al., 1999; Holmgren et al., 2003), geomorphic and luminescence techniques (Bullard et al., 1997; Partridge et al., 1997; O'Connor & Thomas, 1999; Jones et al., 1999a; Thomas & Shaw, 2002; Powers et al., 2005; Vuille et al., 2005) and oceanic core measurements (Cohen & Tyson, 1995; Kirst et al., 1999; Holland et al., 2006). These techniques have typically concentrated on the understanding of long-term climatic shifts in the region – typically between glacial/interglacial or the timing of pluvial epochs – but have not identified decadal-century scale oscillations or variability.

The immediate focus of this study, however, is on dendrochronology. Many palaeoclimate studies at the decadal scale use dendrochronology as their basis (Helama et al., 2005), with significant advantages for use in this study, showing established links to summer rainfall variability with appropriate spatial resolution and extent.

Nonetheless, this work is not without detractions: southern Africa presents particular problems in the application of dendrochronological techniques because of difficulties associated with poorly defined, locally absent and converging rings (February & Stock, 1998). Initial work using *W. cedarbergensis* and *Podocarpus* species (e.g. Dunwiddie & Lamarche, 1980 *inter alia*) were shown to have insignificant relationships with rainfall variability (February & Stock, 1998).

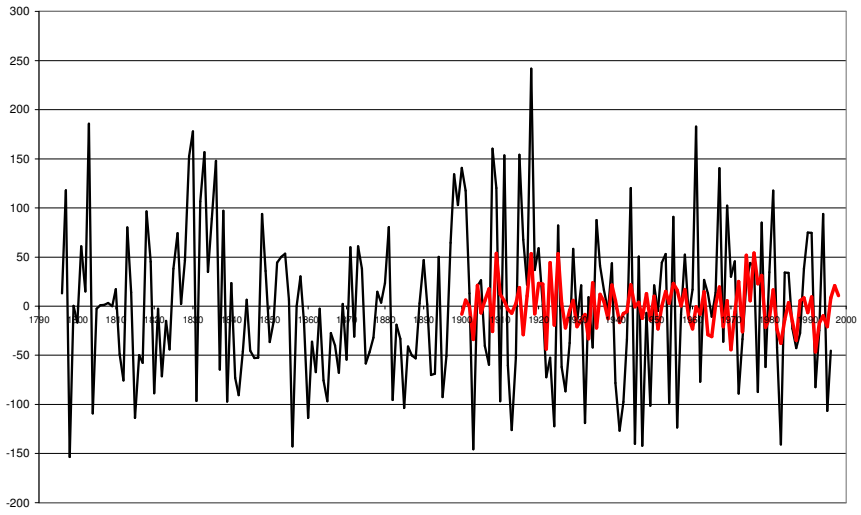

Figure 2.1: Time series of mean JFM rainfall plotted over the extent of the available record as anomalies with respect to the long term mean. This figure shows the dendrochronology-based proxy rainfall reconstruction (black line, Therrell et al., 2006) and CRU JFM rainfall over 15-35ºS, 15-35ºE (red line, Hulme et al, 1992; 1998).

However, a range of studies have shown that growth ring patterns in *Pterocarpus angolensis DC* are significantly correlated to wet season regional precipitation (Stahle et al., 1999; Fichtler et al., 2004), and moreover, showed no correlation with relative humidity or temperature data for the same period (Trouet et al., 2006).

This study therefore examines a *P. angolensis*-based rainfall reconstruction from Zimbabwe by Therrell et al., 2006, who used standard dendrochronological techniques in the deconstruction of growth rings (detailed methodology in Bradley, 1999; Stahle et al., 1999 and references therein) to generate a tree ring chronology. This was then regressed with regional mean precipitation based on four grid boxes from the CRU global gridded dataset (Hulme, 1992; Hulme et al., 1998) to establish an estimate of precipitation based on ring width. Tested using a split-period calibration and verification procedure, the reconstruction is thought to explain 46% of the summer rainfall variance with no significant trend in the regression residuals (Therrell et al., 2006). The proxy reconstruction covers a 200 year time period (1796-1996) and was initially made available in monthly resolution. In common with the analysis presented throughout the remainder of this study, a Jan-Feb-Mar (JFM) seasonal mean was taken for each year.

Figure 2.1 compares the observed rainfall over the sub-continental region (CRU JFM mean rainfall, over a grid encompassing 15-35ºS, 15-35ºE, chosen to incorporate the major land area of southern Africa) to the rainfall reconstructed using the dendrochronology proxy methods (JFM mean). Both rainfall time series are plotted as anomalies with respect to their long term means, and are presented as annual rainfall totals with no digital filtering methods applied. The wider spatial coverage of the observed index

may explain the substantially muted variance in rainfall over the region compared to the more variable proxy reconstruction. Further examination shows that there are elements of in-phase relationships in the timing of some major peaks (for example, in 1919, or 1939) and that the variability of the proxy record broadly matches the observed record for periods of overlapping record.

Therrell et al. (2006) show relatively low correlation and weak verification statistics between the observed and reconstructed rainfall, and suggest that despite their techniques, dendrochronological methods are still limited in their representation of southern African rainfall variability. Some limitations are linked to suggestions regarding the sensitivity of growth to rainfall, and the stability of the regional rainfall average (Stahle et al., 1999; Fichtler et al., 2004). The interpretation of 'complex poorly defined anatomy of annual growth rings in this species' (Therrell et al., 2006: 683) may explain the difference between CRU data and proxy reconstruction described here. The difference between the observed and reconstructed data suggests that the proxy is unreliable as a method of establishing annual precipitation totals with any precision. However, analysis of the spectrum of the proxy record (Therrell et al., 2006) agrees with other proxy methods (e.g. Tyson et al., 2002) and suggests that the proxy reconstruction may be suitable for further analysis at decadal scale.

In addition, this study analyses proxy methods which reconstructs variables known to be associated with southern African climate variability, to aid in understanding the evolution of the decadal scale changes in rainfall. These records are intended to help answer the fourth study aim, and contribute to our understanding of the nature of decadal variability

under anthropogenic forcing. By utilising records which give an overview of the nature of the southern African circulation in pre-anthropogenic conditions, comparisons can be made to observed and more recent proxy methods to investigate the role of climate change on decadal variability.

In order to fulfil this aim, oxygen isotope records derived from coral reef growth records are sampled from a range of studies in the Western Indian Ocean (Grottoli & Eakin, 2007). The nature of the isotopic reconstruction gives indicators of the general climate variability, rather than specific rainfall reconstruction (Zinke et al., 2004), and typically will be used as proxy records for SST and circulation indices (Bradley, 1999). Data from the Seychelles (Charles et al., 1997), La Reunion (Pfeiffer et al., 2004), Kenya (Cole et al., 2000), Tanzania (Damassa et al., 2006) and Madagascar (Zinke et al., 2004) are examined to provide an indication of the behaviour of the SW Indian Ocean and the circulation over southern Africa at high temporal resolution. This work is presented in Chapter (6).

2. 1. 2 Observed Data Sources

A range of instrumental and observed data is used as the foundation of this study. Despite recent advances in space-based measurement of precipitation (Geerts & Dejene, 2005; Layberry et al., 2006), these sources of data represent only a very small portion of the instrumental record, and do not therefore contribute significantly to understanding decadal variability. Reliance on more traditional methods of rainfall measurement, and observations of land and marine surface level temperature and pressure comes with associated errors and limitations, but remains the most widely used and established record of observed trends and variability.

This section aims to provide only a short introduction to each dataset and overview of the key details. Full technical details of individual dataset construction, validation and more specialised data evaluation can be found in the relevant description papers (Hulme et al., 1998; Hulme, 1999; Allan & Ansell, 2006; Brohan et al., 2006; Rayner et al., 2006).

Precipitation

This study makes use of the CRU global gridded terrestrial precipitation dataset (Hulme, 1992, 1994; Hulme et al., 1998; Hulme, 1999). The dataset consists of monthly estimates from 1900-1998 for land grid boxes at a 2.5° latitude x 3.75° longitude, the same resolution as the Hadley Centre model grid. The global data derives from 12,000 land gauge records subject to previously described homogeneity procedures (Eischeid et al., 1991; Hulme, 1992).

In the original decadal rainfall analysis paper (Tyson, 1971), identifying the 18-20 year rainfall oscillation, the spatial variability of the spectral trends was discussed at length. Using individual station data, Tyson (1971 et seq.) showed that the multi-annual and decadal rainfall oscillations exhibited geographical coherence and preferred particular areas over South Africa. The spatial coverage of the CRU is notably weak in this aspect. It is not clear which stations are used in assembling the blended rainfall data set, and the propensity of the records towards e.g. coastal rainfall bias, and the subsequent implications for this on decadal analysis are not fully understood. It is thought that the analytical focus on large "box grid" analysis techniques over the blended data will smooth out the potential bias here, but the precise composition of the rainfall stations is not

available for analysis, and consequently, the observed rainfall data must be treated with some caution.

It is also worth considering the temporal limitations of this dataset for use in this study. The twentieth-century coverage, in particular, poses two limitations with regard to the study of decadal variability. First, a relatively short record limits the ability to interpret meaningful low-frequency (decadal) variability and establish significance with respect to the signal to noise ratio (Meinke et al., 2005). Second, the continental focus for the dataset limits the ability to accurately render oceanic features of precipitation (e.g. the Atlantic ITCZ) which influence southern Africa. These issues may limit the usefulness of this data in fully examining decadal rainfall variability in the region.

The dataset has been widely used in a range of studies, including the intended comparison with model data (Hulme et al., 1998) and is therefore the most suitable choice for use as the observed precipitation dataset.

Temperature

Surface and marine temperatures are obtained by use of the HadCRUT3 (Brohan et al., 2006) and HadSST2 (Rayner et al., 2006) datasets, covering grid boxes at 5° resolution. Although the data sets extend to 1846, the spatial coverage through the nineteenth century is poor. In order to provide consistency with the CRU dataset, and to improve the reliability of the results, the data are therefore considered for the twentieth century period only.

The historical surface temperature dataset HadCRUT (Jones, 1994; Jones & Moberg, 2003) has been extensively used as a source of information on surface temperature trends and variability (e.g. IPCC, 2001). Since the last update (Jones et al., 2001; Jones & Moberg, 2003), advances have been made in the marine component of the data (Rayner et al., 2006) and these have been incorporated in to a new dataset, HadCRUT3. Additional quality control work has also been undertaken, using the ERA-40 analysis dataset identify potentially anomalous stations and identify monthly outliers (Simmons et al., 2004) The new SST analysis is based on the collection of measurements within ICOADS version 2.0 (Worley et al., 2005) and contains blended archives with improved data coverage relative to Met Office Historical Sea Surface Temperature (MOHSST) dataset (Parker et al., 1995a). The new climatology was created by iterative refinement of the Global Sea Ice and Sea Surface Temperature dataset (GISST 2.0) 1961-1990 climatology (Parker et al., 1995b) used for both MOHSST and the first version of the HadSST (Parker et al., 1995a; Jones et al., 2001).

The net result is to produce a coherent global gridded dataset that integrates land and marine data in a new weighting. This dataset – like the global precipitation data – can be used to reasonably constrain and inform the model output, and may be split in to separate global fields where required for more cohesive spatial analysis. The uncertainty estimations (Brohan et al., 2006; Rayner et al., 2006) are designed to assist the quantification of detection and attribution studies, rather than the underlying "natural" variability, and they are not extensively considered here.

Pressure

HadSLP2 is the most recent version of the Hadley Centre's historical globally complete gridded MSLP data products: GMSLP1 and HadSLP1 (Basnett & Parker, 1997). As in the temperature data sets described previously, the 5° resolution is considered over the twentieth century period. The validation was performed using a combination of several existing datasets, including ADVICE, the Smith & Reynolds (2004) dataset, the Kaplan et al. (2000) dataset, the 40 yr ECMWF Re-Analysis (ERA40) and HadSLP1, although not all of these products have complete spatial or temporal overlap with HadSLP2 (Basnett & Parker, 1997; Jones et al., 1999c; Kaplan et al., 2000; Smith & Reynolds, 2004; Uppala et al., 2005). A comparison of the monthly climatologies have shown some improvements in HadSLP2 when compared with HadSLP1, with notably stronger anticyclones in the subtropical high pressure belt and deeper lows to the south of Greenland and in the Norwegian Sea. During the austral winter, however, it appears that the pressures in the southern Atlantic and Indian Ocean mid-latitude regions are too high in comparison to both ERA-40 and HadSLP1 and will be addressed in future revisions (Allan & Ansell, 2006).

Measurement and sampling errors are particularly large in the high southern latitudes, where the number of observations is very low. At times, these errors are as large as the pressure signal itself. Correlations between HadSLP2 and other products are weakest pre-1950 in the southern hemisphere, consistent with locally poor sampling and lower number of observations (Allan & Ansell, 2006). Based on their analysis, Allan & Ansell (2006) urge caution when using HadSLP2 in southern high-latitude regions and some concern

regarding the importance of the Southern Annular Mode in spatial studies has been expressed.

Summary

These observed datasets represent the state of the art understanding of the climate of the last 150 years. Recent improvements in archive techniques and interpolation make these a good estimate of global climate, but it should be noted that there are still limitations of resolution, spatial and temporal coverage, together with aspects of collection and data processing that are more fully explored in their respective papers. The twentieth century has been identified as possessing the optimum spatial and temporal coverage in the record, and all observed data is limited to this period only in order to facilitate comparison between observed data sets.

2. 1. 3 Climate Model Data Sources

It has been previously established that climate models offer a useful tool to examine the gaps between the temporal extent provided by palaeoclimate data and the gridded suite of observations at high resolution of time and space provided by modern observed and instrumental data. In addressing the study aims outlined previously, climate models offer substantial advantages over the observed and proxy methods.

The second study aim explores the nature of the decadal variability in rainfall. Unlike the observed and proxy records, climate models offer the ability to examine a high resolution data set which extends substantially further than the observed record. This is particularly important for investigations of decadal variability, which can be hampered by an

abbreviated record. The long records available through climate models increase the confidence in the results of spectral analysis.

The third study aim investigates the variability which is associated with decadal rainfall variability over southern Africa. The evaluation of interannual variability and the associated mechanisms presented in Chapter (1) suggests that a range of ocean-atmosphere interactions are likely to substantially influence rainfall variability. The wide range of output fields of climate models act as a diagnostic tool to understand the associated variability, and potentially look for mechanisms which are driving the variability at decadal timescales.

Finally, the fourth study aim asks whether this decadal variability is likely to be changed under anthropogenically driven forcing conditions. Climate models offer the ability to design experimental runs, which can isolate forcing factors and explore their influence in a detailed manner. Naturally forced and anthropogenic simulations enable us to probe the likely responses of the climate system to defined conditions, and identify particular areas of interest.

We are, of course, limited by the ability of the climate models to represent the climate accurately. The confidence in the results obtained in the study will be heavily dependent on the outcome of the first study aim, and the evaluation of the capability of the models to simulate variability over southern Africa presented in Chapter (3). Consequently, appropriate model choice is critical to the success of the study, and the selection of multiple models allows the comparison of model specific results. A series of key factors were identified as important to choosing a model that could address the study aims:

(i) Availability: the model needs to be available beyond any particular climate modelling community, and have a range of variables available in order to help understand the rainfall variability and to diagnose the associated variability.

(ii) Resolution: sufficient length to enable examination of decadal scale variability is critical to choice of model and experiment. Comparing models with similar spatial resolution also reduces the likelihood of results being model resolution-specific.

(iii) Forcing simulation: the response of the low frequency variability to anthropogenic forcing and the climate change record can only be established relative to naturally forced experiment runs or control run data. For inclusion, a model should have more than one simulation available, preferably across the range of control, natural and anthropogenic simulation experiments.

The choice of models is greatly limited by the requirement to have a realistic simulation of the recent Holocene, and the open availability requirement. Two models were identified as fulfilling these criteria: the third generation Hadley Centre Global Climate Model (HadCM3), and the German Climate Centre (DKSS) Hamburg model ECHO-G (ECHAM-4), and are described here.

Hamburg Coupled Climate Model (ECHO-G):

The Hamburg Climate Centre model version used in this study is an older variant. The new generation of ECHAM-5 coupled with the MPI-OPM ocean model has been released (Giorgetta et al., 2006; Hagemann et al., 2006; Jungclaus et al., 2006; Roeckner et al., 2006; Wild & Roeckner, 2006), but has not been made available beyond the immediate Hamburg/GKSS community. Problems with acquisition of data also means that only the ERIK and ENAT runs are used in this study.

Model Details:

The ECHO-G climate model consists of the ECHAM-4 atmospheric GCM (Roeckner et al., 1996) coupled to the HOPE-G ocean GCM (Wolff et al., 1997; Legutke & Maier-Reimer, 1999; Legutke & Voss, 1999), both developed at the Max-Planck Institute in Hamburg (Gonzalez-Rouco et al., 2003; von-Storch et al., 2004; Aldrian et al., 2007). The atmospheric data is at T30 resolution (3.75 deg), with 20 vertical levels, and the ocean is at T42 resolution (2.8 degrees) with 19 vertical levels.

Control Run Details:

A 1000 year control simulation (Zorita et al., 2003) was generated using external forcings set to present day values (solar constant = 1365 W m^{-2}, CO_2 = 353 ppm, CH_4 = 1720 ppb, N_2O = 310 ppb). To enable the model to sustain a simulated climate approximating the present day climate, with minimal drift, the heat and freshwater fluxes between atmosphere and ocean are modified by constant (in time) adjustment terms. The flux adjustments were successful in preventing a long term drift in the global mean 2m air temperature, though regional evaluations show a warming in the southern hemisphere and a relative cooling in the northern hemisphere by approximately 0.2K over the 1000 yr run. This model run is not available for use in this study, unfortunately limiting our understanding of the model's intrinsic simulated variability.

Natural Forcings Experiment (ENAT):

The natural forcing experiment (ENAT) is therefore required to act as both "control" and "natural forcing" element for the ECHAM suite. Using pre-industrial climate levels as a starting point, the only time-varying natural forcings used in the ECHO-G simulations are

solar irradiance changes and short-wave forcing related to known volcanic eruptions and their effects.

The volcanic forcing is implemented by reducing the effective solar irradiance to achieve the desired atmospheric effect (Ammann et al., 2003; Boer et al., 2007). This may underestimate the absorption of short-wave and long-wave radiation by volcanic aerosols that can lead to stratospheric warming (Dufresne et al., 2005).

The natural variations in solar irradiance are extrapolated from data generated by Crowley (2000) from a combination of the Lean et al. (1995) sunspot-based estimates and an ice core record of cosmogenic 10Be (scaled by Gonzalez-Rouco et al. (2003) to match its variance to the Lean et al. (1995) time series during the 20th century).

Natural and Anthropogenic Forcing Experiment (ERIK):

The ERIK simulation is an attempt to model climate variations from 1000 to 1990 as a response to natural and anthropogenic forcings (Gonzalez-Rouco et al., 2003; von-Storch et al., 2004). In addition to ENAT's natural forcing, combined anthropogenic and natural fluctuations in the concentrations of the CO_2, CH_4, N_2O well mixed greenhouse gases, including pre-industrial fluctuations in CO_2 and CH_4 (Blunier et al., 1995; Etheridge et al., 1996) were added. It is argued that a number of potentially important forcings were not included in the ERIK experiment, most notably the negative forcing due to anthropogenic tropospheric sulphate aerosols during the 20th century, but also variations in some other greenhouse gases (halocarbons and ozone) and the effect of land use change (Osborn et al., 2006). The impact of this omission is discussed later.

The initial conditions of the ERIK simulation were taken from year 100 of the control run, but are representative of the present-day rather than pre-industrial climate. The experiment design therefore included a 30 year adjustment period where the control run forcing was linearly reduced to appropriate levels for 1000 AD, followed by a 50 year period with fixed forcing that allowed the model climate to equilibrate with the new reduced forcing (solar constant=1,364.92 W m^{-2}; CO_2=283 ppm; CH_4=691ppb; N_2O=277ppb). The ERIK simulation then proceeded from the conditions after this 50 year period.

Hadley Centre Climate Model, Version 3 (HadCM3):

Although initial experiments and validation studies for the Hadley Centre's next generation "Global Environmental Model" have been recently published (Johns et al., 2006; Martin et al., 2006; Ringer et al., 2006), and the first impact evaluation studies completed (Davies et al., 2006; James, 2006; Stott et al., 2006), the model has not been widely disseminated outside the immediate Met Office community. Therefore, this study uses the third generation of the Hadley Centre Climate Model series, HadCM3.

Model Details:

The atmospheric component of HadCM3 is a version of the UK Met Office Unified Model (Cullen, 1993). The model dynamics and physics are solved on a 3.75° x 2.5° grid with 19 hybrid vertical levels. Significant changes with respect to the previous version (HadCM2; Johns et al., 1997) include the introduction of a new radiation scheme (Edwards & Slingo, 1996; Cusack et al., 1998), the representation of convective momentum transport (Gregory et al., 1997), the introduction of a new surface scheme (Cox et al., 1999), better representation of the effects of sub-grid scale orography (Milton & Wilson, 1996; Gregory et al., 1998), a reformulation of the treatment of clouds in the model (see Gordon et al., 2000 for more details) and a revision of the boundary layer scheme (Smith, 1990). More details of the formulation and climate of the atmospheric component of the model can be found in a review by Pope et al., 2000.

The oceanic component is also an updated version of the Cox (1984) model used in HadCM2. The horizontal resolution is increased to 1.25° x 1.25° with 20 vertical levels. The vertical levels are distributed to provide enhanced surface and mid-layer resolution, with topography modified from the ETOPO5 (1988) dataset to better emulate observed

flow on the Greenland-Iceland-Scotland ridge. HadCM3 employs the Gent and McWilliams (1990) scheme for adiabatic diffusion of tracers with variable coefficients (Gent & McWilliams, 1990; Visbeck et al., 1997; Wright, 1997), vertical mixing is parameterised using Kraus-Turner scheme and salinity conservation is achieved using a representation of river runoff and by assuming a balance between iceberg calving and accumulation of snow on the ice sheets.

CONTROL run:

The CONTROL run is an important part of this study – enabling examination of variability and teleconnections resulting from intrinsic atmospheric processes and atmosphere-ocean coupling. Control runs demonstrate the skill of state of the art AOGCMs to reproduce reliably the large scale aspects of climate (Renssen et al., 2004). In order to evaluate the modelled climate variability under natural and anthropogenic forcing factors, two experimental runs designed by Simon Tett et al. (2007) are used.

The model was initialised in September using a previously derived model atmospheric state and September ocean observations (Levitus et al., 1994) with zero ocean currents. The atmosphere and ocean are coupled once a day. After an initial spin up phase, the CONTROL run continues to couple and resolve physical processes according to the natural variability of the model. One thousand years of data are available for examination, with nominal years 2280 to 3289.

Natural Forcing Experiment (NAT500):

NAT500 was started using initial conditions from year 1000 of CONTROL, giving a start date of 1/12/1491. In addition to the natural internal variability of the model climate,

external forcings are applied. A summary of the key forcing changes is provided briefly here, with more detail available in descriptions of the experiments (Tett et al., 2007). Volume mixing ratios of greenhouse gases were set to pre-industrial levels (CO_2 = 277.5 ppmv, CH_4 = 790 ppbv and N_2O = 270 ppbv) and sulphate aerosol loading was varied according to the scale and time of known volcanic eruptions. Changes in orbital parameters (after Berger, 1978) and solar forcing (using the Lean et al., 1995 reconstruction of irradiance) were spliced with a reconstruction of irradiance changes using ^{10}Be (Crowley, 2000). Vegetation fields were set at 1750 levels, and remained constant throughout the simulation.

Natural and Anthropogenic Forcing Experiment (ALL250):

ALL250 was initialised in model year 1749 using NAT500 conditions, as part of the experiment suite by Tett et al. (2007). In addition to the forcings of NAT500, the ALL250 simulation also incorporated time-evolving greenhouse gas alterations in line with the HadCM3 experiments (Johns et al., 2003) which closely modelled the real world changes in greenhouse gases. The experimental emission and ozone fields (Johns et al., 2003) were used from 1860 onwards, translating the real world changes in to model specific variables. By including natural and key anthropogenic forcing changes defined by the observed record, this experiment is thought to represent the best simulation of the 'real world' climate between 1750 and 2000 that is currently available.

Climate Model Summary:

The models and experiment runs chosen for use in this study represent the best available options for the study of decadal variability at timescales which extend beyond the capability of the observed records. They employ a range of forcing scenarios and reconstructions to best simulate the recent Holocene period.

A summary of the simulations is provided here for reference:

	ECHO-G 3.75º x 3.75º resolution	**HadCM3** 3.75º x 2.5º resolution
Control simulation	Not available for use in this study	CONTROL 1000 years of data (nominal years)
Natural forcing simulation	ENAT Time varying natural changes in solar irradiance and short wave forcing. 220 years of data.	NAT500 Time varying natural changes in solar irradiance, short wave forcing. Pre-industrial greenhouse gas and vegetation levels 500 years of data, simulated from 1490AD
Anthropogenic forcing simulation	ERIK Natural forcings, plus changes in greenhouse gas concentrations. 990 years of data, initialised in 1000AD (see text for limits to this)	ALL250 Natural forcings, plus changes in greenhouse gas concentrations. 250 years of data, initialised in 1750AD

2.2 Research Methods

A series of statistical techniques form the basis of this study, with the majority of these being familiar and well documented methods for use in climate studies (e.g. Carleton, 1999; Zwiers & von-Storch, 2004). This study does not aim to introduce and develop new methods of investigation in climatology but relies extensively on proven and validated analytical techniques to generate robust results and to develop the analysis of this region at decadal scales.

This brief outline of the principal techniques employed in this study shows that although limitations exist, their combination in multi-method analysis increases the confidence in the results obtained, and reduces the uncertainty associated with individual methods (Carleton, 1999). Statistical techniques are often subject to interpretation and questions over their validity (e.g. Nicholls, 2000; Dommenget & Latif, 2002; Domingues et al., 2005; Dommenget, 2006). Although statistical technique validation is beyond the scope of this work, reference will be made to ongoing debates, and the steps taken to improve the reliability of the results will be demonstrated. This section is not intended as a complete guide to the techniques, but merely to address their principal advantages and limitations for use within this study. The interested reader is referred to the original papers and texts (e.g. von-Storch & Zwiers, 1999) for further details. The research methods are introduced here thematically, in order to show how they address specific study aims.

2. 2. 1 Study Aim 1: To what extent do General Circulation Models reproduce the southern African decadal rainfall variability?

Chapter (3) describes the model evaluation, and examines how reliably the climate models simulate aspects of the southern African climate. With extensive references to the existing literature on analysing climate model performance, and utilising a previous investigation of HadCM3's simulation of southern African rainfall as a guide (Hudson & Jones, 2002a, 2002b), the chapter focuses principally on the simulation of the mean state of the climate. Comparisons are made to the observed data described in the previous part of this chapter, together with other observed data sets as appropriate.

For this study, two key decisions are made to appropriately parameterize the rainfall data to a focus suitable for decadal variability. First, previous analysis has identified the JFM seasonal mean as a suitable measure of southern African rainfall (Mason & Jury, 1997; Nicholson, 1997; Tyson & Preston-Whyte, 2000). Chapter (3) therefore concentrates on this seasonal average and this focus is retained throughout the study.

Second, the need to examine variability at a broad spatial scale that is easily referenced and directly comparable leads to the requirement for a "box grid" over the southern African sub-continent. Preliminary work with EOF analysis and iterative experimentation tested a wide range of potential box sizes and locations, and established a grid over 15-35ºS, 15-35ºE as the most suitable. This domain was shown to capture the main spatial patterns of variability, as well as fulfilling the requirement of comparison between data sources. This sub-continental scale focus is employed frequently throughout the study.

2. 2. 2 Study Aim 2: What is the nature of decadal variability in southern African rainfall?

In order to address the nature of decadal rainfall variability, this study needs to employ three separate methodological themes. First, the decadal variability needs to be examined in isolation, which is accomplished through digital filtering techniques. Second, the spectral nature of the variability should be examined. Multiple spectral techniques are employed to ensure robust results, and these are described here. Finally, the decadal variability is explored in space using Empirical Orthogonal Function techniques that identify the dominant structures.

Digital Filtering Techniques

With decadal variability identified in the observed and modelled data, isolating the signal is a critical element of this study's approach (Handorf et al., 1999; Hannachi & Allen, 2001; Katz, 2002). The aim is to remove centennial (to millennial) scale variability (e.g. warming trends, solar variability), as well as the higher-frequency variability. Linear regression may be employed to remove particular signals (e.g. Washington & Preston (2006)'s detrending to remove the classic ENSO signal), but requires *a priori* knowledge of the signal characteristics (Moron, 1997). Without knowing the decadal bands in advance, digital filtering appears to be the best method (Allen & Smith, 1997; Meehl et al., 1998).

For this study, a single filter is employed throughout, reducing the possibility of method-based results. A "Kaiser" filter was chosen: designed to minimise spectral leakage, reduce the possibility of artefact introduction, and to ensure that the patterns reflect the dominant

spatial structure of decadal variability (Kaiser, 1974; Kaiser & Reed, 1977; Kaiser & Schafer, 1980). In this study, a 7-50 "band pass" configuration is employed. By isolating this portion of variability, this method removes interannual and high frequency (e.g. 2-3 yr Quasi-Biennial Oscillation) signals, together with centennial scale variability and trends which may contaminate a decadal variability signal.

Spectral Analysis

In order to understand the nature of variability in time, this research utilises methods developed to identify quasi-periodic time evolutions of a given climate structure, including a variety of spectral analysis techniques (Mason & Mimmack, 1992; Mann & Park, 1994; Mann et al., 1995; Mann & Park, 1999; Hannachi & Allen, 2001; von-Storch et al., 2004) and wavelet functions (Daubechies, 1990, 1992; Farge, 1992; Torrence & Compo, 1998; Torrence & Webster, 1999). This approach gives an insight in to the dominant frequencies of variability, how they vary through the records and time series data available, and how reliable they are. Multiple methods are used to reduce the possibility of results being technique-dependent.

Spectral techniques are designed to extract information from noisy time series and thus provide insight in to the unknown dynamics of the system (Gilman et al., 1963; Ghil et al., 2002). A variety of methods to derive the time domain analysis and spectral patterns can be utilised, and several of these are usefully combined in the SSA-MTM "toolkit" used in this study (full details can be found in Ghil et al., 2002 and references therein).

The Multi-Taper method (MTM) provides this study with a basic means for spectral estimation and signal reconstruction of a time series which is believed to exhibit a

spectrum containing both continuous and singular components. The MTM aims to reduce the variance of spectral estimates by the use of three tapers, rather than a unique spectral window used by the classical methods. Data are pre-multiplied by orthogonal tapers constructed to minimize the spectral leakage due to the finite length of the time series, and a set of independent estimates of the power spectrum is then computed (Ghil et al., 2002). The MTM describes structures that are modulated in frequency and amplitude, with an optimal trade-off between spectral resolution and variance (Joly et al., 2007). The confidence levels are obtained relative to a red noise background (Mann & Lees, 1996).

This method has been widely applied to problems in geophysical signal analysis, including analyses of atmospheric and oceanic data (e.g., Mann et al., 1995; Mann & Park, 1996, 1999; Knopf et al., 2005; Meinke et al., 2005; Min et al., 2005). As well as MTM, peaks in the observed spectral power are confirmed with reference to other methods in the "tool kit" (e.g. Blackman-Tukey windowed correlogram, maximum entropy method) and wavelet analysis in order to provide a multi-technique validation.

Wavelet Analysis

Wavelet transform techniques have become increasingly widespread in recent climate research (Lau & Weng, 1995; Handorf et al., 1999; Hannachi & Allen, 2001; Gu & Adler, 2003; Luo et al., 2003; Mwale et al., 2004; Terray & Dominiak, 2005; Terray et al., 2005), providing a valuable perspective on the stability of a quasi-periodic pattern as it devolves through time-frequency space. This study makes extensive use of wavelets, both as an analytical tool in their own right, and as a verification of spatial and spectral analysis techniques.

Wavelet transform methods stemmed from signal processing research (Daubechies, 1990, 1992; Farge, 1992) as a tool for analysing localised variations of power within a timeseries (Foufoula-Georgiou & Kumar, 1995; Jevrejeva et al., 2005). By application of wavelet transform, a time series is decomposed in to time-frequency space, showing the dominant modes of variability and how these modes vary with time (Torrence & Compo, 1998; Torrence & Webster, 1999; Jevrejeva et al., 2005).

For climate analysis, a Morlet wavelet – consisting of a complex exponential modulated by a Gaussian transform – is used for the transform function, since it is well localised in time and frequency space (Torrence & Compo, 1998). To test for non-stationary changes in variance, a background Fourier spectrum must be chosen; with the global wavelet spectrum generally suited for this purpose (Torrence & Webster, 1999). The global wavelet spectrum – given by the time average of the wavelet power spectrum (Kestin et al., 1998) – is equivalent to the Fourier power spectrum smoothed by the Morlet wavelet function in Fourier space (Farge, 1992). The wavelet power spectrum is then distributed as chi-squared (2 d.f.) about the global wavelet spectrum (Torrence & Compo, 1998). An optional significance relative to red noise background is set to ensure compatibility with the MTM technique outlined previously.

Empirical Orthogonal Function (EOF) Techniques

Next, to identify dominant spatial structures and ascertain potential areas of forcing and teleconnective links, established methods are used to produce patterns in the phase space where the probability density function is very high. A variety of such methods exist (canonical correlation analysis (CCA) and principal oscillation patterns (POPs;

Hasselman, 1988), for example), but this study employs Empirical Orthogonal Function (EOF) techniques (Hannachi et al., 2006; Hannachi et al., 2007) as one of the most reliably used in climate research (Carleton, 1999; Dima et al., 2005). These mathematical methods are supported by correlation and composite analysis, to ensure that the results have some spatial coherence and to reduce the uncertainty associated with individual technique choice.

Empirical Orthogonal Function analysis is one of a series of eigenvector based approaches to statistical spatial analysis introduced to climate science by Lorenz (1956; details of which can be found in von-Storch & Zwiers, 1999). Use of EOF techniques has several advantages: first, it produces an explicitly characteristic pattern using an objective algorithm (Zwiers & von-Storch, 2004); second, low order EOFs can represent natural modes of variation of the climate system; and third, it is thought that the time coefficients obtained by projecting the data field on to EOFs are uncorrelated and represent the variability of the field effectively (von-Storch & Zwiers, 1999; von-Storch et al., 2004).

Despite critiques (Dommenget & Latif, 2002; Behera et al., 2003; Dommenget & Latif, 2003; Jolliffe, 2003) and a range of proposed modifications to their application (Allen & Robertson, 1996; Allen & Smith, 1997; Dommenget, 2006) EOFs remain a commonly used tool in climate studies. In this study, low-frequency filtering techniques and correlation and ratification of results against other methods (e.g. composite, correlation mapping) will be employed to avoid over reliance on the orthogonality of the EOF outputs.

2. 2. 3 Study Aim 3: What ocean-atmosphere variability is associated with decadal rainfall variability over southern Africa?

The third study aim explores the variability of the ocean and atmospheric fields associated with decadal rainfall variability over southern Africa. The sub-continent scale index is used to identify regions of correlation in the observed and model data fields, filtered using the digital techniques described earlier. Areas of particular coherence or strength are then examined further.

Typically, a correlation analysis of this sort would demarcate levels of significant correlation (von-Storch & Zwiers, 1999). However, this relies on the identification of a number of degrees of freedom to calculate the correlation required for a particular significance level. The use of the digital filter in this study – essential to isolating the quasi-decadal band – proves to be unhelpful in this case, since it does not allow the degrees of freedom to be calculated (Chandler, 2007). It has also been suggested that hypothesis-testing based significance levels are only of use in specific scenarios in climate research (Nicholls, 2000), and that the identification of associated variability without *a priori* knowledge of the relationship is not an appropriate use of significance tests. They are therefore not employed in this study.

For some variables, correlation is not appropriate. In wind vector analysis, for example, a linear regression with separate u- and v- wind components is then combined to generate a vector. This is typically plotted as the vector outcome of wind regression based on 2σ variable anomaly (i.e. what wind anomaly is generated by a 2σ precipitation anomaly?), and linked to SLP-based circulation correlation.

The exploration of individual areas of interest also employs regression techniques to assess the phase relationship of variability associated with decadal rainfall over southern Africa. As for the correlation analysis, the absence of degrees of freedom under filtered conditions does not warrant significance testing as an appropriate method. The predictive nature of the regression technique is therefore employed with appropriate caution.

2. 2. 4 Study Aim 4: Is decadal variability altered by anthropogenic forcing?

The final study aim integrates the methods employed in the three previous chapters to assess the contribution of anthropogenic forcing to the decadal variability of rainfall over southern Africa.

The final results chapter presents analysis of proxy-based and anthropogenic climate model experiment data, and examines whether there is a detectable influence on the spectral nature of variability. Unfiltered spectral analysis is typically presented to explore the impact of anthropogenic forcing on all timescales, including interannual/classic ENSO variability, which helps to understand the larger picture of forcing-induced change. The anthropogenic model runs are then examined using the EOF techniques described to explore whether there are any discernable changes in the spatial structure of rainfall variability under the anthropogenic forcing experiments compared to the control and natural simulations. Using the correlation and regression techniques described for the third study aim, changes in the associated variability are then investigated.

2.3 Summary

This chapter has developed the aims identified in the first chapter, and explored the benefits and limitations of the data sources and methods used to explore the questions posed. This study does not aim to develop new methods, but rather to consolidate our knowledge of decadal variability over southern Africa using established and proven techniques.

Where possible, the limitations to their accuracy have been identified, and are minimised by the use of multiple techniques to ensure a corroborated and more robust result. This gives a solid platform from which to examine the nature and associations of decadal variability in southern African rainfall, beginning with the evaluation of the models' capability to simulate this region. This is presented in the next chapter.

(3) To what extent do General Circulation Models reproduce the southern African decadal rainfall variability?

This chapter addresses the first study aim, and evaluates the climate model data to understand to what extent the complex regional climate of southern African can be simulated. Some of the major elements of southern African climate simulation have already been established through intercomparison studies, and this section will draw heavily on previous assessments of climate model performance. For each climate model, the focus in this chapter is on understanding the climatological mean, and establishing how the major patterns of circulation can be simulated. The exploration of the nature of decadal variability in rainfall is presented in the next chapter.

The validation assessment covers the JFM seasonal mean for the twentieth century, as this provides the most comprehensive information from the observed datasets, and covers the wet season in southern Africa which is the focus of this study. Nominal years are chosen for the HadCTR data, since that has no time-specific forcing included. It is expected that the HadCTR data will show no significant trends, but will provide valuable commentary on the spatial patterns and variance driven by purely internal model variability. Additionally, this evaluation tests the approach chosen in this study, and aims to establish how effectively the models can be integrated with the observed and palaeoclimatic data to make comments on the potential variability of the region. Although some obvious limitations will be proposed and clearly demonstrated, this chapter will conclude that the use of integrated observations, palaeoclimatic and multi-model data – while far from perfect – is the best method of investigating variability.

3.1 How are climate models evaluated?

Although it is possible to use objective measurement techniques (e.g. root-mean-square error, spatio-temporal correlations) to characterise the agreement between models and observations for particular variables, there is no generally accepted method for measuring model performance as a whole (Raisanen, 2007). Climate model evaluation is complicated by an incomplete and error-based observation record. As illustrated by McAvaney et al. (2001) for time-mean SAT, precipitation and SLP, differences between observational data sets can be as large as the differences between the best models and observations. In addition, the role of internal variability means that there will never be precise agreement with observations (Schwierz et al., 2006; Raisanen, 2007).

Both the agreement between climate change simulations and the importance of internal variability depend on the horizontal scale considered. With increased geographical averaging, internal variability decreases. Conversely, agreement between model simulations tend to increase with larger scale; Raisanen (2001) found this particularly pronounced for precipitation, with much more inter-model agreement on the large scale features than on local details. Many comparison and detection/attribution studies therefore focus on the changes in global mean temperature and other large-scale aspects of climate (Giorgi & Francisco, 2000; Raisanen, 2001), although there is recent work incorporating the detection and attribution of anthropogenic climate change based on precipitation records (Zhang et al., 2007).

This problem arises because climate models do not – primarily for reasons of computational expense – simulate the full complexity of the real world. Processes like

rainfall (that act on scales smaller than the grid spacing) cannot be resolved explicitly and therefore need to be 'parameterised' – that is to say, estimated indirectly from grid-scale conditions simulated by the model. Typically, parametrisation schemes are based on a combination of physical theory, observational evidence and, in some cases, simulation by higher-resolution models (e.g. Noh et al., 2003). These sources give constraints for the parameters, and therefore different models have parametrisation schemes that are different in both their basic structure and the numerical values used in their equations (Phillips et al., 2004). Rainfall and cloud parametrisation, and how the parameters interact with the model therefore play a key role in the explanations of model evaluation studies.

At the global scale, poor data coverage over the oceans before the satellite era largely limits precipitation comparison between observed and model simulations to land areas. Raisanen (2007) suggests that simulated variations in global land area mean precipitation on interannual to interdecadal scales agree qualitatively with observations (Gillett et al., 2004; Lambert et al., 2004; Lambert et al., 2005), although models appear to underestimate the magnitude of variability. Both the observed and simulated variations appear to be affected more strongly by volcanic aerosols than anthropogenic forcing, but observation estimates of trends in the 20th century bear similarity to the responses of models to increasing greenhouse gas concentrations (Folland et al., 2001). Observed increases in heavy precipitation in many parts of the world (e.g. Groisman et al., 2005) also appear consistent with increases that are expected to occur with warming, although it is unclear whether these changes are distinguishable from natural variability (Kiktev et al., 2003).

At the regional scale, coarse resolution affects both the simulation of time-mean climate changes (Giorgi & Francisco, 2000) and extreme simulations. A prominent example is precipitation change in areas of complex topography. Raisanen (2007) discusses examples from Norway and the Scandinavian mountains which show up to a 70% localised increase in precipitation in a high-resolution Regional Climate Model (Raisanen et al., 2004) driven by the global model (Roeckner et al., 1999). Statistical downscaling techniques suggest this might be even more variable on smaller spatial scales than those used in RCM simulations (Hellstrom et al., 2001; Hansen-Bauer et al., 2003).

Hewitson & Crane (2006) suggest that the use of differences between model precipitation outputs could provide a measure of uncertainty – to provide high and low bounds for a climate scenario – but suggest that this is a problematic approach. Rather than estimating the magnitude of change, slight phase shift, or offset in the location of some controlling feature (e.g. storm tracks, etc.), different outcomes represent equally possible responses to the same forcing, and the differences could be regarded as a measure of uncertainty in the climate system.

However, if the differences are due to the differences in precipitation parameterisation schemes and their interaction with the model dynamics (or model topography, land surface climatology) then the spatial representations are more likely to measure uncertainty in the ability to effectively simulate the climate system over this region (Hewitson & Crane, 2006).

True uncertainty on small spatial scales is likely to be larger than indicated by global model variation, particularly for precipitation (Hansen-Bauer et al., 2003). For a precise

simulation of climate changes in geographically complex areas, such as mountain ranges and coastal regions, both a high resolution and realistic simulation of large-scale atmospheric circulation are important. This provides an important benchmark for southern African climate simulations, given the steep topography of the area.

3.2 Evaluating the basic state of the climate models

In this section, the basic simulation state of the climate models is compared to observed data, to demonstrate the capability of the models to understand and simulate the climate physics of the southern African region. A comprehensive review of HadCM3's performance over this region, together with a nested regional climate model, is extensively utilised in this section (Hudson & Jones, 2002a, 2002b).

This section presents the JFM mean data from the observed datasets, the control simulation of HadCM3, and the ENAT experiment from ECHO-G as described previously. All mean data represents the long term mean of the entire simulation period. Strictly speaking, this is not a fair comparison – evaluating the difference between a control, naturally forced and anthropogenically forced climate – but these choices are considered the "basic" states of each dataset respectively. It was not considered valid to compare the anthropogenic experiments of the climate models without first evaluating their unforced counterparts, but the significance of this comparison method should be considered throughout.

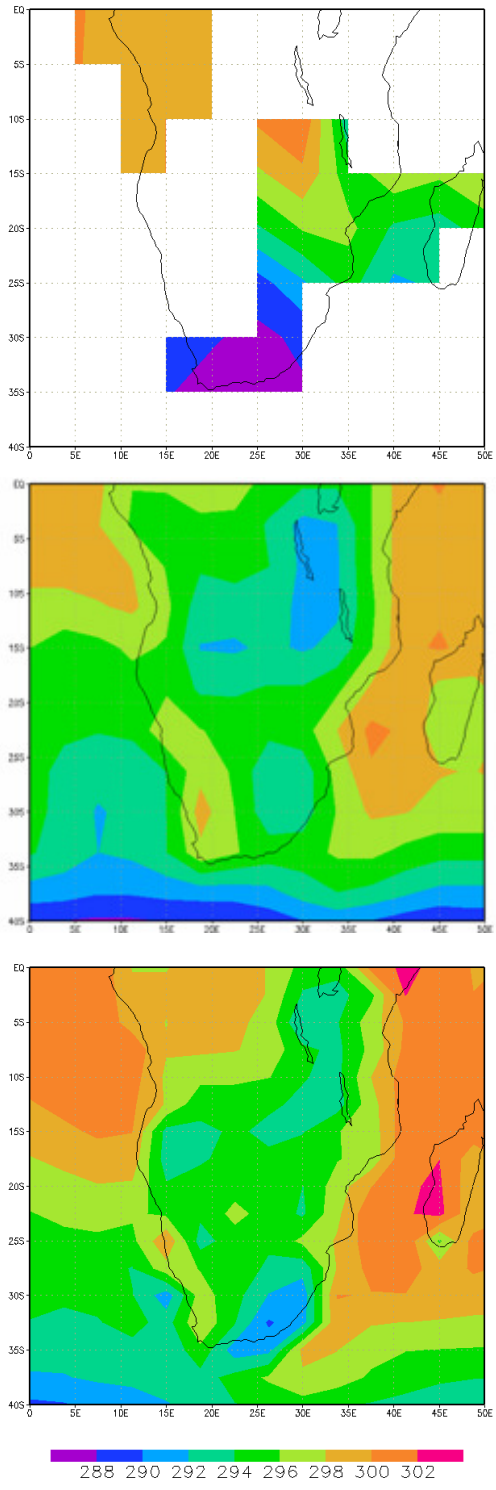

Figure 3.1: Climatological (JFM) mean surface air temperature. Top: observed data (1900-1998), middle: as simulated by ECHO-G ENAT (220 years), bottom: as simulated by HadCM3 CTR (1000 years). Units are in Kelvin.

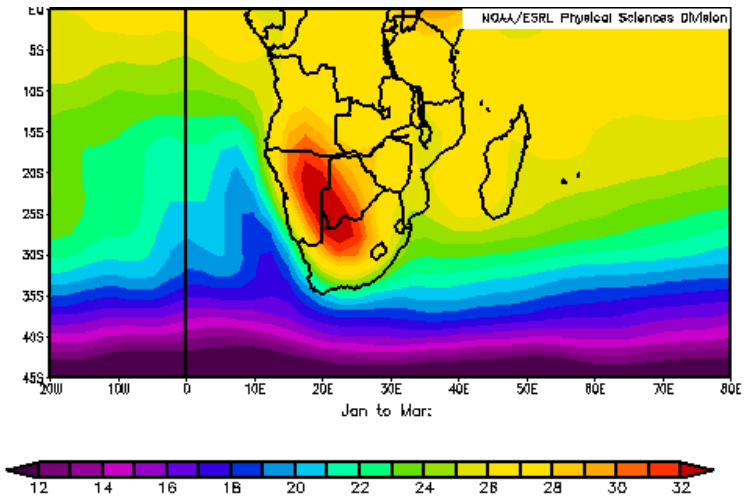

Figure 3.2: Climatological (JFM) mean surface air temperature for the NCEP/NCAR Reanalysis (1948-2007), as generated by the KNMI Climate Explorer. Note the different scale to the previous figure, and the use of Celsius rather than Kelvin.

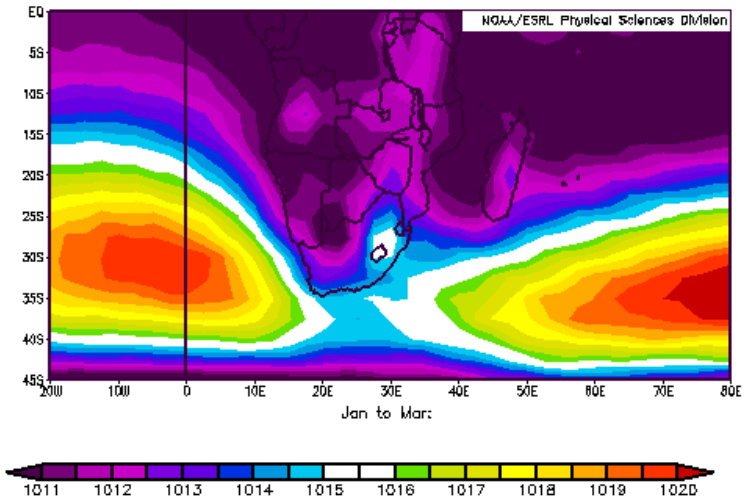

Figure 3.3: Climatological (JFM) mean sea level pressure for the NCEP/NCAR Reanalysis (1948-2007), as generated by the KNMI Climate Explorer. Note that the scale differs compared to the next figure.

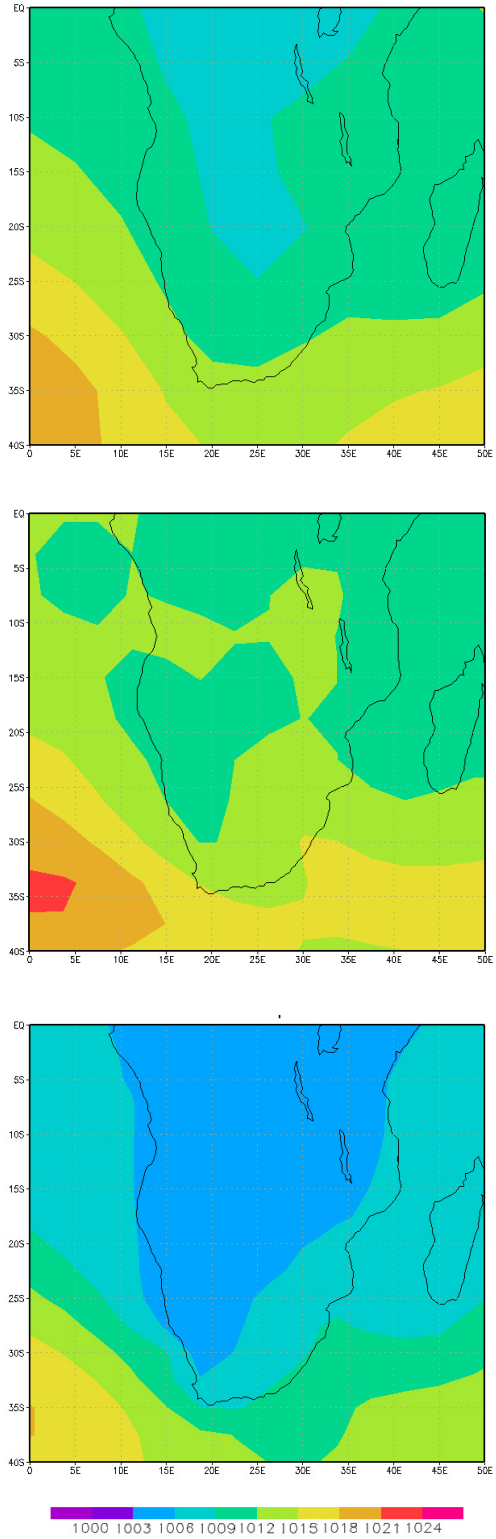

Figure 3.4: Climatological (JFM) mean sea level pressure. Top: observed data (1900-1998), middle: as simulated by ECHO-G ENAT (220 years), bottom: as simulated by HadCM3 CTR (1000 years).

Figure 3.1 shows the comparison between representations of mean surface air temperature. The observed data shows substantial spatial gaps in the record, which represent fields with non-continuous data, but is generally suggestive of an east-west gradient in temperature. The model simulations – which extend over the ocean – show a gradient between land and ocean temperatures, but a more homogenous continental temperature gradient than the observed.

Further comparison with observed data shows the model weaknesses more clearly. Figure 3.2 shows the JFM mean temperature of the NCEP/NCAR Reanalysis data (Kalnay et al., 1996; Kistler et al., 2001) over a more extended spatial domain, and captures the model's deficiencies in simulating the area of peak temperature over Angola, Namibia and Botswana associated with the "Angola heat low". The Angola low is of importance, since it generally acts as the tropical source region for the tropical-extratropical cloud bands that extend NW-SE across southern Africa south of about 15-20°S and bring much of the region's summer rainfall (Harrison, 1984; Todd & Washington, 1999). The reanalysis data shows a JFM Angola low intensifying with an area of low-level convergence extending along the ITCZ across southern Africa.

Both climate models struggle to capture this intensification during JFM, and instead show an area of low level divergence separating the Angola low region from the ITCZ over the Mozambique Channel (Reason & Jagadheesha, 2005). The modelled deficiencies in capturing the Angola low are thought to have important implications for modelling the ENSO impacts over the region. The Angola low does not weaken significantly for the 1997/8 ENSO event, and Reason & Jagadheesha (2005) suggest this is largely why the

impact of this El Nino on southern African rainfall south of 15-20°S was less than in other cases.

Figure 3.4 shows the mean SLP patterns for each dataset. The observed data agrees with the reanalysis data well, and shows a split between the continental low pressure, and the subtropical oceanic highs (shown more clearly in the extended spatial domain of the reanalysis data in Figure 3.3. Note the different scale bar to the other maps). The models, however, show some differences in this field.

As has been found with other Hadley Centre models (Stratton, 1999; Pope et al., 2000) there is a general low pressure bias in the tropics in JFM, and this is also the case over southern Africa in HadCM3. Negative geopotential height anomalies (not shown) appear to be a result of enhanced convergence in the ITCZ and are associated with increased ascent around 15°S and enhanced convergence in the Hadley and Walker circulations compared to the observed (Hudson & Jones, 2002a, 2002b).

In addition, upper tropospheric divergence in the model extends southwards in a NW-SE axis over South Africa, where the observed data shows weak convergence fields over the country. This divergence anomaly is associated with the positioning and strength of the upper level Atlantic westerly wave and upper level ridge over Southern Africa. The modelled upper level circulation is more meridional, such that South Africa is influenced by stronger divergence ahead of the trough axis (Hudson & Jones, 2002a).

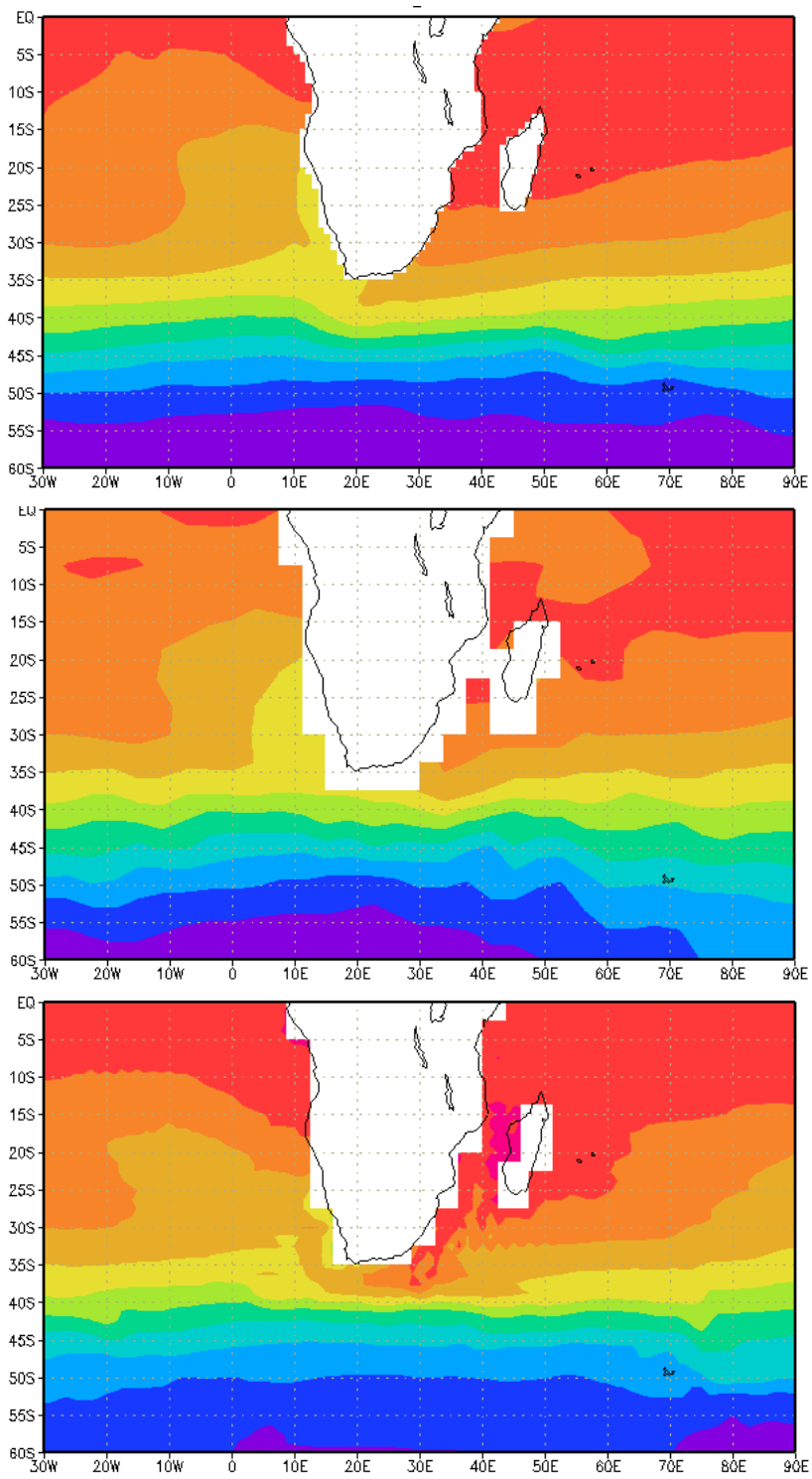

Figure 3.5: Climatological (JFM) mean sea surface temperature in the southern African region, showing local influences. Top: observed data (1900-1998), middle: as simulated by ECHO-G ENAT (220 years), bottom: as simulated by HadCM3 CTR (1000 years). The units are given in degrees Celsius.

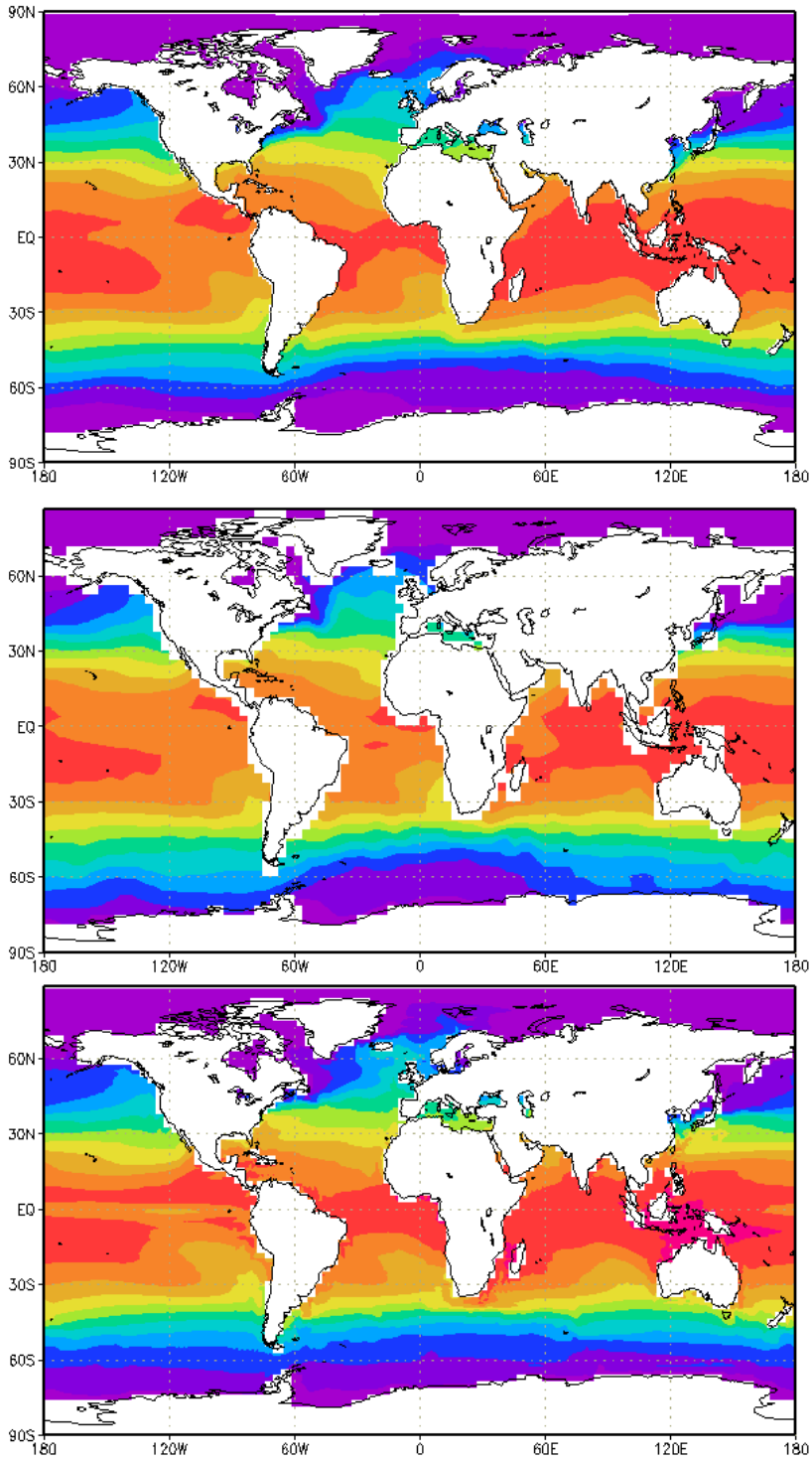

Figure 3.6: Climatological (JFM) mean sea surface temperature at the global scale, showing the influence of large scale teleconnections. Top: observed data (1900-1998), middle: as simulated by ECHO-G ENAT (220 years), bottom: as simulated by HadCM3 CTR (1000 years). The units are given in degrees Celsius.

By comparison, ECHO-G appears to simulate slightly higher pressure over the sub-continental region. A more fragmented spatial pattern over the landmass shows a more consistent link to the NCEP reanalysis dataset, and shows similarity to the distribution of pressure over the zonal gradient out to Madagascar. Variability in the temperature and pressure patterns is likely to have close links to the simulated ocean temperatures. Figure 3.5 shows the comparison plots of SSTs local to southern Africa (0-60°S, 30°W-60°E). HadCM3 and the observed data show general agreement; the warmer SW Indian Ocean regions extend around Madagascar, with a meridional gradient stretching southwards to the cooler Southern Oceans. The control simulation shows slightly warmer temperatures at higher latitudes (~60°S) than both ENAT and observed data.

ENAT shows a qualitatively similar SST distribution to the observed and HadCM3 data, but has some differences in the temperature of sub-tropical to tropical regions in particular. Evident in the regional SST analysis, it is more clearly shown in global scale SST patterns (Figure 3.6). The general agreement in distribution between HadCM3 and the observed data serves to highlight the cooler tropical oceans in ENAT, and particularly the lack of spatial coherence in the Pacific Ocean.

This agrees broadly with the result of intercomparison studies aimed at identifying the nature of ENSO simulation in different coupled climate models (Achuta-Rao & Sperber, 2002, 2006). In one review, using interchangeable atmospheres and oceans, ECHO-G and HadCM3 components are shown to substantially differ in their ENSO reproduction (Guilyardi et al., 2004).

There is clear separation in El Nino periodicity between HadAM3 and ECHAM4 suites, with HadAM3 preferring a 3-yr and ECHAM preferring a 2-yr ENSO cycle, regardless of which ocean components are used. Additionally, the ECHAM suite shows that the amplitude of El Nino tends to be weaker than in HadAM3, particularly in direct comparison using the same OPA ocean model (Guilyardi, 2006). However, it should be remembered that the forcing of ECHO-G is naturally driven (Gonzalez-Rouco et al., 2003), compared to the control simulation of HadCM3, and this may have implications for the starting conditions and the magnitude of variability of the model simulated ocean temperature (Collins, 2002; Osborn et al., 2006).

The influence and simulation of the regional topography is a potential explanation for the differences observed between models, and in the model-observations comparison. Figure 3.7 shows the regional precipitation under observed and model simulated conditions. It is interesting to note that no topographic weighting has been applied to the interpolation scheme of the CRU gridded dataset (Hulme, 1992; 1994; Hulme et al., 1998), for example. A number of different methods exist for incorporating the effects of topography (e.g. the PRISM and AURELHY methods and the spline algorithms of Hutchinson, 1995) on precipitation, but their exclusion is argued to be reasonable on the grounds of interpolation of precipitation anomalies rather than absolute values (Hulme, 1999).

The observed data suggests qualitative agreement with the model simulated rainfall, and shows a broad NW-SE spatial distribution alignment. Greater agreement is found when a more spatially complete observed data set is used (Global Precipitation Climatology Project version 2; Xie & Arkin, 1997; Adler et al., 2003; Xie et al., 2003) in Figure 3.8.

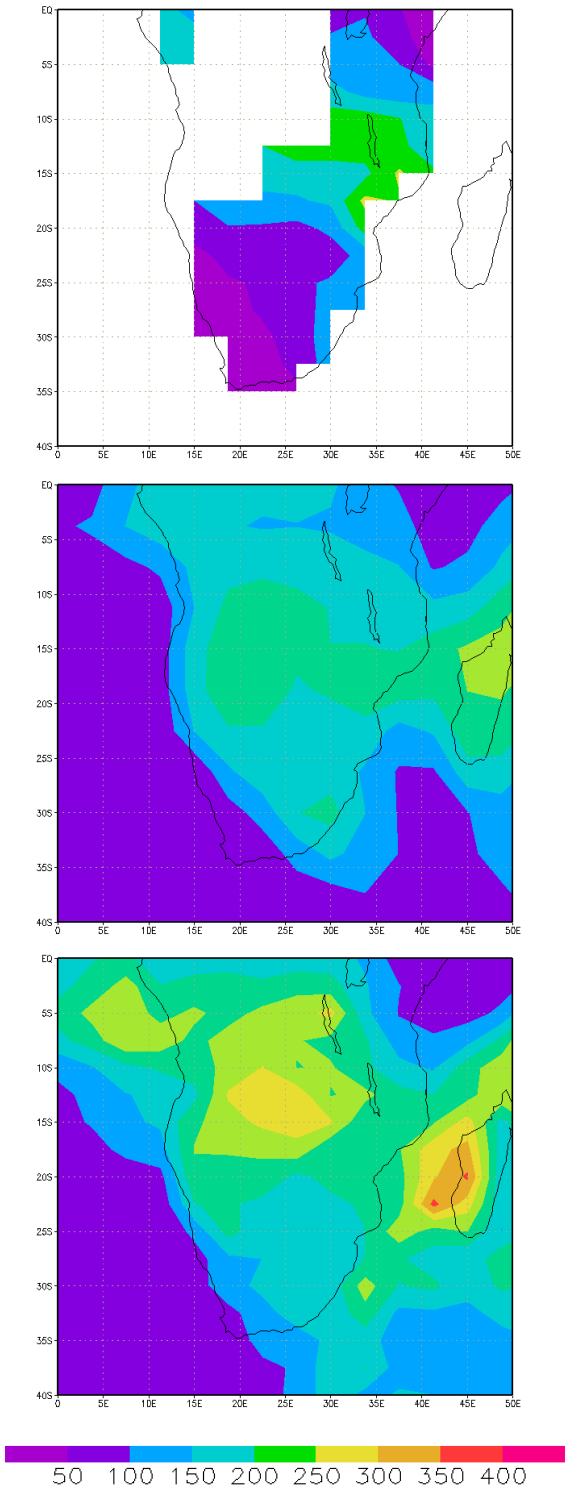

Figure 3.7: Climatological (JFM) mean rainfall in the southern African region. Top: observed data (1900-1998), middle: as simulated by ECHO-G ENAT (220 years), bottom: as simulated by HadCM3 CTR (1000 years). All units have been converted to mm/month.

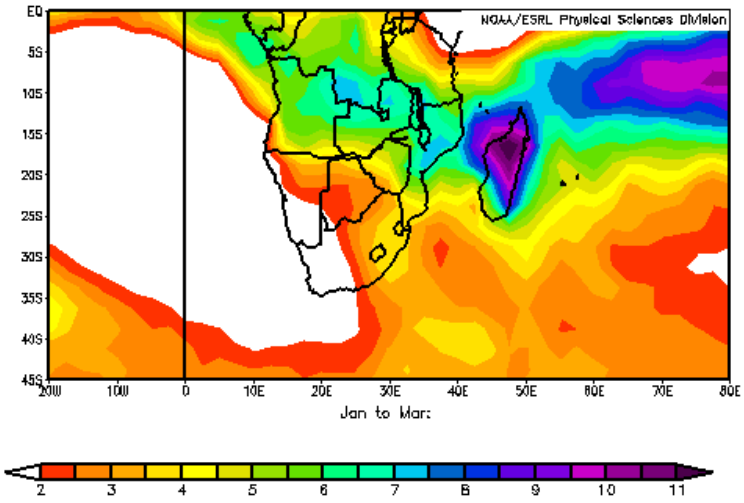

Figure 3.8: Climatological (JFM) mean rainfall in the southern African region, from the Global Precipitation Climatology Project version 2 (1979-2007; Xie & Arkin, 1997; Adler et al., 2003; Xie et al., 2003). Note the different units to those displayed in the previous figure.

Interannual variability of seasonal mean precipitation has been analysed over southern Africa, and the models are shown to capture the general pattern in summer quite well. Variation between HadCM3 and ECHO-G is likely to be related to the horizontal resolution of the model and links to insufficient topographical forcing and dynamical uplift associated with the steep escarpment near the coast (Hudson & Jones, 2002a).

It is likely that the models are deficient in their simulation of the tight east-west gradient of rainfall that is observed over South Africa, with too much rainfall being simulated over the arid western areas. HadCM3, in particular, shows evidence of more rainfall than the observed and ECHO-G simulated isohyets. Pope et al. (2000) found a tendency for the seasonal shifts in tropical rainfall over Africa to occur earlier in HadAM3 and to be more marked than observed, leading to errors in transition seasons. Consequently, although the model captures the general pattern of rainfall over the subcontinent, the magnitude of rainfall is typically overestimated, especially south of 10°S (Hudson & Jones, 2002a; Hewitson, 2007, personal communication). However, HadCM3 is also thought to be too dry in regions near significant orography (e.g. eastern Madagascar, south eastern Africa and southern Angola), at least in part, because it does not develop significant troughing downstream of the Madagascan mountains, the Drakensberg and Chimanimani mountains in south eastern Africa or the Bie plateau in Angola (Reason & Jagadheesha, 2005).

Consistent with the view that it is the model deficiencies in capturing regional circulation features that are the main problem over southern Africa, Hudson & Jones (2002b) compare global 850 and 200 hPa velocity potential anomaly fields (not shown) for the various ENSO events, and suggest the model modulations of the Walker circulation over

the Pacific region are similar to NCEP fields. Thus, it appears that the model can do a good job on the large scale re-organisation of the atmospheric circulation, but is less successful at capturing the impacts on locally important southern African regional circulation features such as the Angola low (Reason & Jagadheesha, 2005).

This analysis suggests that most of the large scale spatial features of the seasonal circulation over southern Africa are reasonably represented by the model, and that the broad distribution of rainfall agrees with the observed data. Although local orographic resolution prevents some finer details being resolved, with potential implications for synoptic scale variability (e.g. the resolution of the Angola low and its' influence on the formation of tropical-temperate troughs), the JFM mean sub-continental scale rainfall appears to be adequately simulated by the climate models. This has positive implications for the reproduction of variability at decadal timescales, but remains reliant on model-specific interpretations.

Analysis of rainfall variability at quasi-decadal scales should therefore start at this spatial scale, and the reviews presented here indicate that with due care, both HadCM3 and ECHO-G can be used to study the physical processes underlying the general circulation over the region.

3.3 Review of model forcing scenarios

In this section, the model forcing experiments are reviewed with reference to the existing literature. Although certain areas of concern are noted, the experimental runs still represent the best simulation of the recent Holocene that we possess at present.

Work using a simplified intermediary 3D climate model (ECBILT-CLIO-VECODE, Renssen et al., 2005; Goosse et al., 2005b) to examine the construction of model response to forcing scenarios has identified four potential causes of intra-model variation (Goosse et al., 2005a).

First, the experiments may have been performed with different reconstructions of the past radiative forcing. Second, the difference in model formulation may impact on their response to external forcing, often measured by equilibrium climate sensitivity or transient climate response (Gregory et al., 2004b; Hoerling et al., 2006). Third, because of the lack of palaeoclimate data, it is not possible to accurately specify the initial conditions for the model, and different start up procedures for the experiments and initial value problems could alter the results (Collins, 2002; Renssen et al., 2006). Finally, these complex climate models include representations of the internal variability of the climate system at many timescales. As a consequence, two simulations performed with the same model and using the same external forcing may differ because of random internal climate variability.

Comparison of ECBILT-CLIO-VECODE with GCMs strongly suggests that the differences between simulations lie in the differences between model transient sensitivities, and Goosse et al. (2005a) suggest that using different forcings is probably not

the dominant cause of differences since they are associated with changes well within the range of the internal variability of the model at a decadal scale.

The uncertainties in past radiative forcing and reconstructions render it difficult to interpret any difference between model and observations (Goosse et al., 2005a). It is therefore more productive to analyse the nature and variability of model results, rather than attempting to identify the simulation that best agrees with palaeoclimatic reconstructions (Goosse et al., 2005b).

The relatively recent HadCM3-based NAT500 and ALL250 experiments of Tett et al. (2007) have not been fully evaluated in intercomparison methods. Tett et al. (2007)'s initial paper contains a validation exercise, which suggests that the NATURAL500 and ALL250 experiments perform well against comparable observations and benchmark assessments at both global and regional scales. There is some evidence of reduced variability in the model, but Tett et al. (2007) do not explore this in great detail. Further work remains to be done with this state of the art simulation, and future tests will explore more about the driving factors of the anthropogenically forced climate.

By contrast, ERIK has been explored more critically in the literature. Osborn et al. (2006), for example, evaluate the performance of the ERIK simulation against other coupled GCMs and find that it exhibits atypical behaviour to the ensemble mean, with a stronger cooling trend in the first seven centuries, and a stronger warming trend during the final two centuries of the millennium. Using the MAGICC climate model (details in Osborn et al., 2006 and references therein), it has been shown that the absence of the anthropogenic tropospheric sulphate aerosol is the most significant factor in ERIK's overestimation of

temperature variability. Though the magnitude of this forcing factor is uncertain, it is argued that the range of forcing change from 1750 to present is negative (Ramaswamy et al., 2001) and this might reduce northern hemisphere warming by approximately 0.5K.

Further investigations of the differences between ECHO-G ERIK simulation and the NCAR CSM model, suggest that the spin up procedure may have influenced climate sensitivity in ECHO-G and lead to a warming trend (Goosse et al., 2005a; Goosse et al., 2005b). Although acknowledging this factor, Osborn et al. (2006) suggest that the absence of tropospheric cooling is more important to explain the ERIK trends found. In recognition of these problems, a second simulation (ERIK-2) has been carried out by the Max Planck Institute, using cooler initial conditions to avoid the model drift (Gonzalez-Rouco et al., 2006). These external evaluations are consistent with the simulation patterns found in the global scale analysis shown here, but since the ERIK-2 data is not available beyond the ECHAM community, the ERIK-1 run is utilised with caution concerning warming trends and model drift.

3.4 Summary

Model evaluation showed that observed and climate model datasets display some similarities and large differences (Jones & Mann, 2004; Tett et al., 2007). Models tend to be better at simulating large-scale changes linked to rainfall variability than they are at simulating the rainfall variability itself (Timbal et al., 2006). Regional rainfall is a notoriously difficult quantity to simulate (Gillett et al., 2004) and therefore is often be used as a benchmark to test model performance (DeMott et al., 2007). In accordance with the expected results, the analysis presented in this chapter suggest that HadCM3 and ECHAM-4 differ in their simulation of this complex region (Hewitson & Crane, 2006).

The model evaluation presented here is a basic examination of the long term mean simulation of basic state climate at the regional scale. The variability of the simulated climate has not been explored – in part because the interannual (Lambert & Boer, 2001) and ENSO-scale variability is relatively well evaluated (Achuta-Rao & Sperber, 2002; Guilyardi, 2006), and in part because to extend this further would reproduce the findings presented in Chapter (4). In order to overcome this limitation, the pertinent intercomparison project results will be discussed as they occur in the subsequent chapters, and further evaluation of the model's ability to reproduce variability presented at the appropriate stage.

The evaluation of the mean climate simulation has not, however, been entirely without merit. Analysis has shown that locally important features can often be poorly simulated by climate models, as a result of topographic and spatial resolution issues. Reason & Jagadheesha (2005), for example, showed that the Angola low – particularly important to

the formation of synoptic scale tropical-temperate troughs – was not well simulated by climate models, and the results presented here agreed broadly with this finding. It was therefore suggested that the synoptic scale variability may suffer from these problems.

However, the broad scale circulation features and mean JFM rainfall distribution were reasonably well simulated. As a consequence, it was suggested that analysis of quasi-decadal variability utilising the sub-continental scale rainfall would be adequately representative of the observed climate and would provide a solid platform for analysis in the remainder of this study. A review of model comparison studies suggests that there are model-specific differences in the simulation of variability beyond interannual timescales, including the question of ENSO simulation.

HadCM3 and ECHO-G are shown to differ considerably in their ENSO simulation capability, and this will undoubtedly play a role in how the models simulate southern African rainfall variability at all timescales, including decadal. Without prejudging the investigation of decadal variability presented in the next chapter, it seems likely from the response to ENSO that models will also differ in their simulation of decadal variability. Decadal ENSO, for example, is thought to be heavily influenced by the 3-7 year variability of the 'classic' ENSO pattern, and it is not unreasonable to suggest that climate model variability at decadal scales is less well understood and (potentially) simulated than the ENSO paradigm/mechanism (Vimont, 2007).

However, the role of this study is to investigate how that variability appears in the model, and to establish what the likely associations with decadal rainfall variability over southern Africa may be. Model and experiment-specific results cannot be ignored, but by

comparing the evidence across observed data and different climate models, it is suggested that anomalous results will be identified, and the broader trends and implications for the real world can be demonstrated.

Even the brief evaluation presented here, taken in conjunction with the more extensive model intercomparison project literature, demonstrates that the present models have some way to go in their simulation of basic state climate, let alone variability at all timescales. It is not yet clear whether significant progress has been made with the fourth generation models (HadGEM1, ECHAM5 et al.), and future comparisons will explore the advances made. The models used here represent the contemporary state of the art in simulations of the recent Holocene (Tett et al., 2002; Gonzalez-Rouco et al., 2003; Gonzalez-Rouco et al., 2006; Tett et al., 2007), and developing an increased understanding of how they operate and simulate significant features of regional climates is not an inconsequential task. Exploring the nature, and associations, of decadal variability over southern Africa gives us a better knowledge of the model development, as well as offering insight in to how the real world may operate at decadal scales. The examination of the nature of this variability is covered in the next chapter.

(4) What is the nature of decadal variability in southern African rainfall?

Despite the limitations of climate model data presented in the previous chapter, they remain useful tools with which to examine decadal variability, and possess several advantages over observed and proxy data sets. This chapter therefore aims address the second study aim, and identify the nature of southern African rainfall variability using a range of techniques. First, the spectral power of variability in the observed and proxy record will be considered at a range of spatial scales. Next, the model simulations will be discussed at the sub-continental scale – defined as a region encompassing 15-35°E, 15-35°S – in order to provide an overview of dominant spectral power and to evaluate how they relate to observed data. Finally, the data will be spatially examined using EOF analysis to demonstrate the regional influences that shape southern African rainfall variability.

4.1 Analysis of Observed and Proxy Data

Figure 4.1 shows the observed (CRU) rainfall over the sub-continental region (black line), with the band pass filter (7-50 year Kaiser band pass, described previously, and used throughout this section unless otherwise specified) applied (red line). Decadal variability is visually evident in the observed data. Regions of strong decadal power are identified using the wavelet analysis shown in Figure 4.4, and sample "high" and "low" filtered rainfall periods shown in Figure 4.2. Although poorly spatially resolved, a NW-SE orientation is suggested for both high and low rainfall samples. Despite zonal and meridional gradients, the sub-continental scale response validates the use of this method.

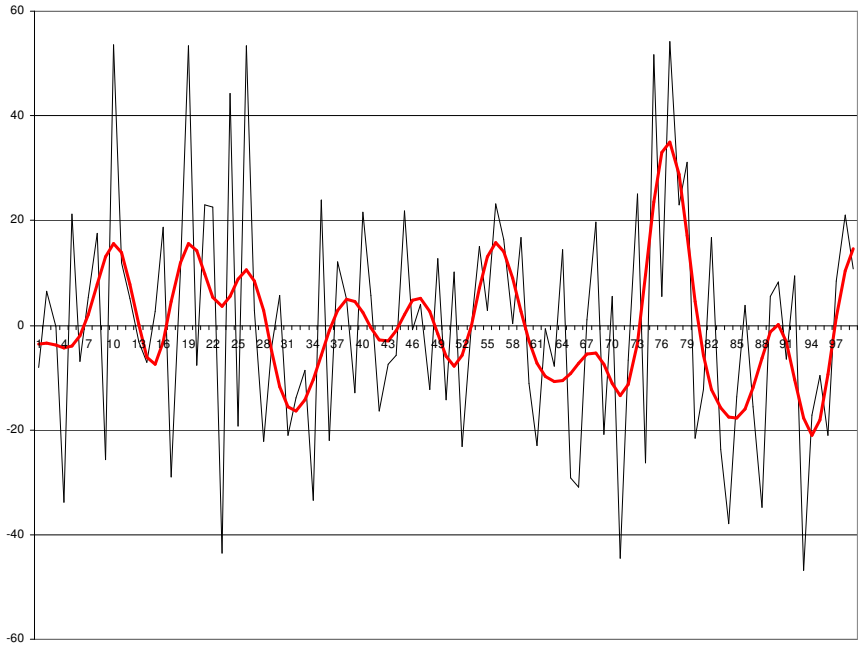

Figure 4.1: Plot of the timeseries of JFM mean precipitation from CRU observed data (1900-1998) over the sub-continental region (15-35ºS, 15-35ºE). The black line shows the unfiltered data, and the red line results from the application of a 7-50 year band pass filter.

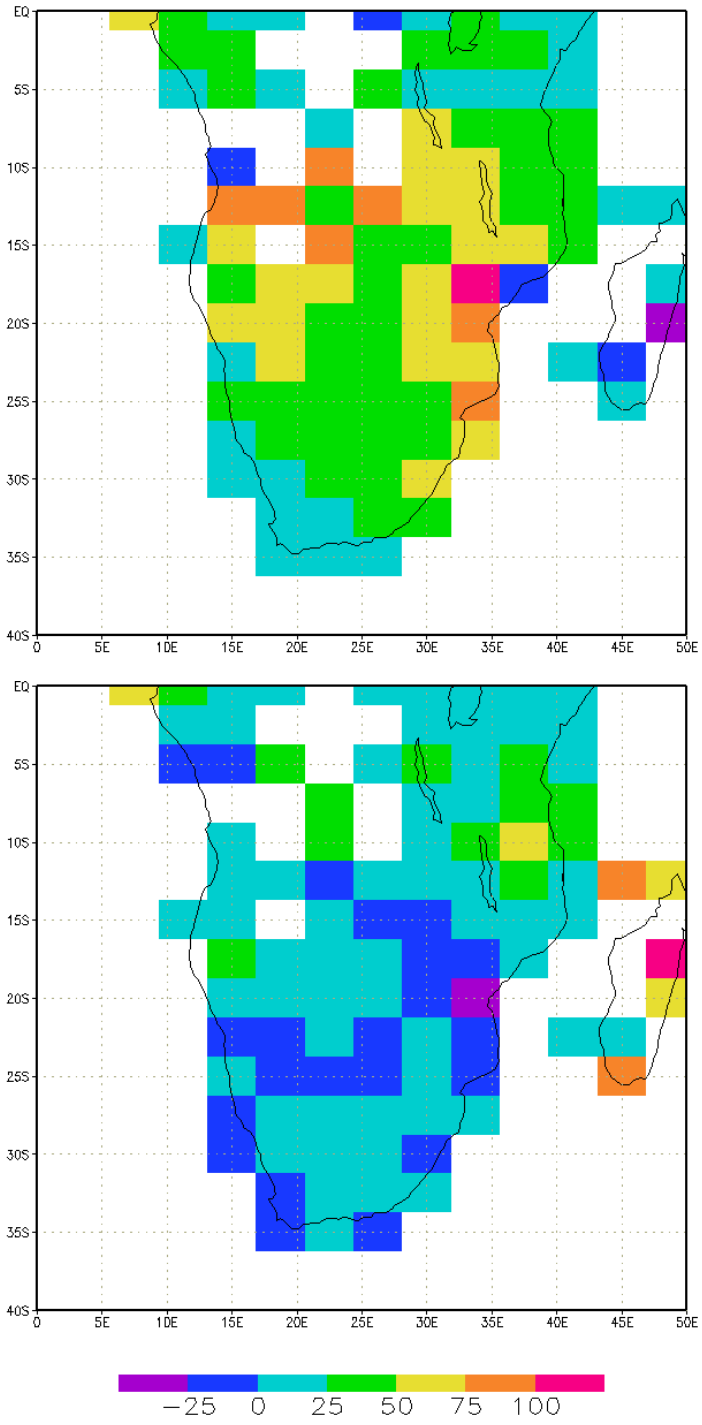

Figure 4.2: Sample quasi-decadal rainfall anomaly "events" from the observed (CRU) dataset, filtered with a 7-50 year band pass filter. Top: high (above average) rainfall event (average of year 77 ± 5 years). Bottom: low (below average) rainfall event (average of year 71 ± 5 years).

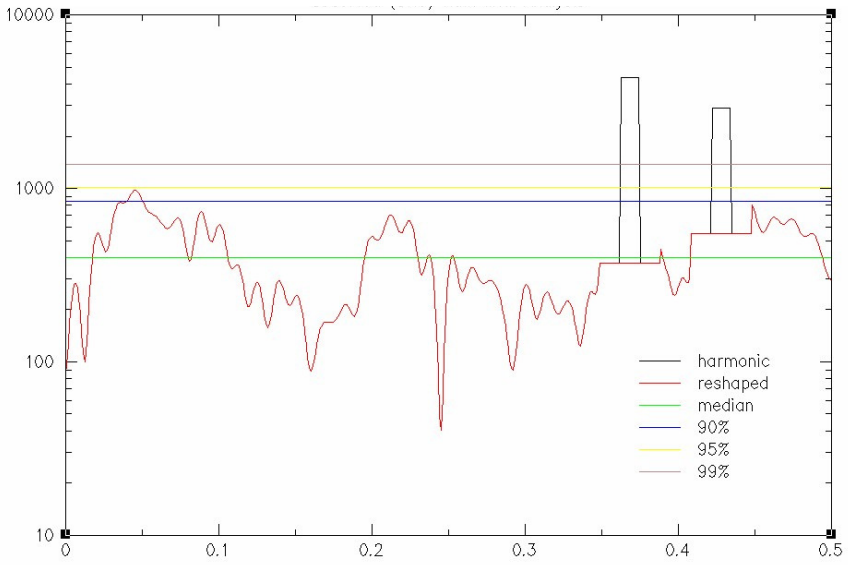

Figure 4.3: Spectral analysis (MTM, unfiltered) of observed (CRU) sub-continental (15-35ºS, 15-35ºE) rainfall. The x axis represents frequency, and the y axis indicates the spectral power.

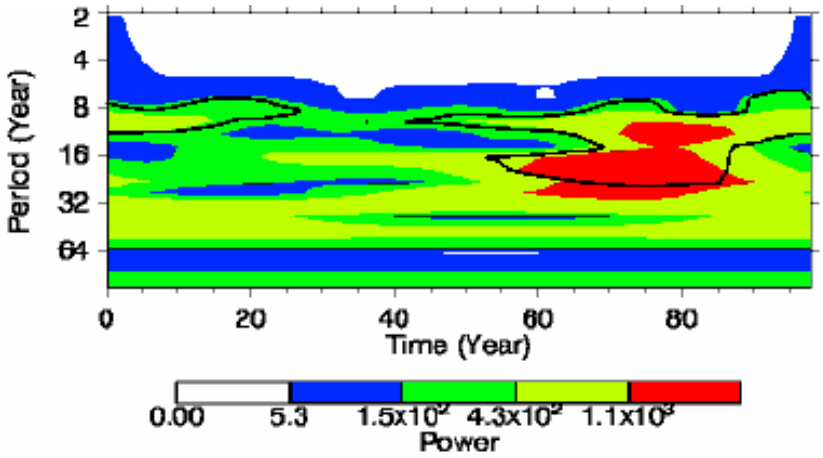

Figure 4.4: Spectral analysis (wavelet, filtered) of observed (CRU) sub-continental (15-35ºS, 15-35ºE) rainfall. The black line shows significance (95%) against a red-noise background.

Spectral analysis of the observed (CRU) data over the sub-continental region shows a range of power at different frequencies. Figure 4.3 shows harmonic peaks confirmed at the 99% confidence level in high-frequency spectral ranges at 2.3 yrs and 2.6-2.75 yrs, and a significant peak at 22 yrs (95% confidence). These peaks are also confirmed with other methods (basic periodogram, Blackman-Tukey correlogram; plots not shown) as robust signals (Allen & Robertson, 1996; Zwiers & von-Storch, 2004; Chandler, 2007). Singular spectrum analysis techniques (not shown) suggest that the spectral peaks are not truly cyclical oscillations, but instead represent a broader range of spectral power (Allen & Smith, 1996, 1997; Ghil et al., 2002; Chandler, 2007). The evolution of this spectral power through the record is described in the wavelet analysis depicted in Figure 4.4. The quasi-decadal variability observed in the MTM analysis is confined to the period 1960-1985, but although it reaches significance in the MTM spectrum, it does not have local significance against the red-noise background test applied by the wavelet method at the lower frequencies of this band.

There is some evidence of variability in a broad range between 8-12 years, both in the wavelet and MTM techniques. It does not reach the 90% level of significance in either method, but does appear across the range of spectral analyses as a defined frequency of enhanced power. The abbreviated record length (99 yrs) is the most likely explanation for the absence of variability at periods longer than 25 yrs. The proxy reconstruction of Therrell et al. (2006) provides some support for the spectral analysis of the observed precipitation. The spectral analysis (Figure 4.5) is dominated by a 9-10 yr band of power (99% confidence) which Therrell et al. demonstrate to account for 8.2% of the variance.

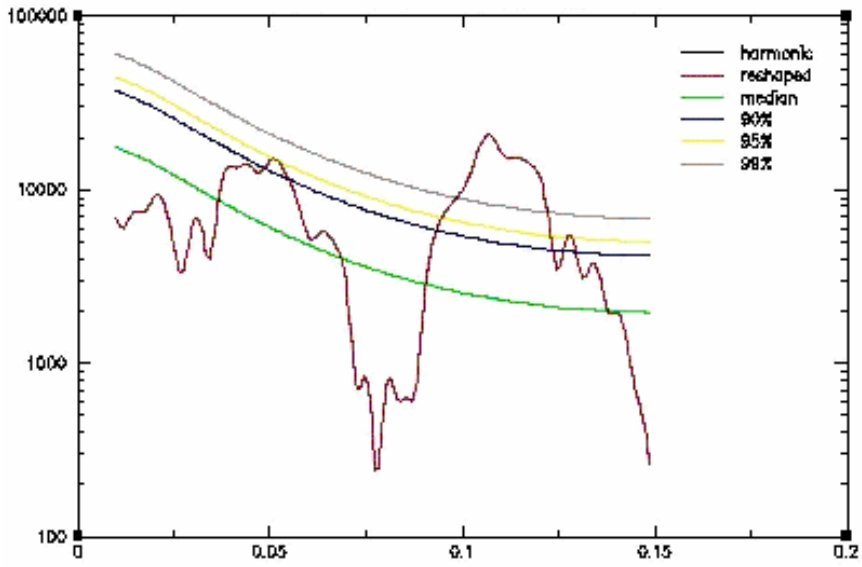

Figure 4.5: Spectral analysis (MTM, filtered) of reconstructed rainfall, based on proxy data (1796-1996) identified by Therrell et al. (2006). The x axis represents frequency, and the y axis indicates the spectral power.

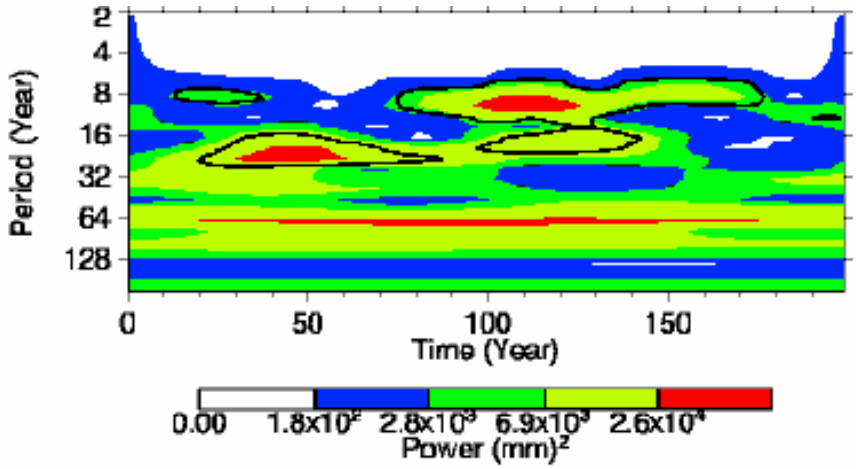

Figure 4.6: Spectral analysis (wavelet, filtered) of reconstructed rainfall, based on proxy data (1796-1996) identified by Therrell et al. (2006). The black line shows significance (95%) against a red-noise background.

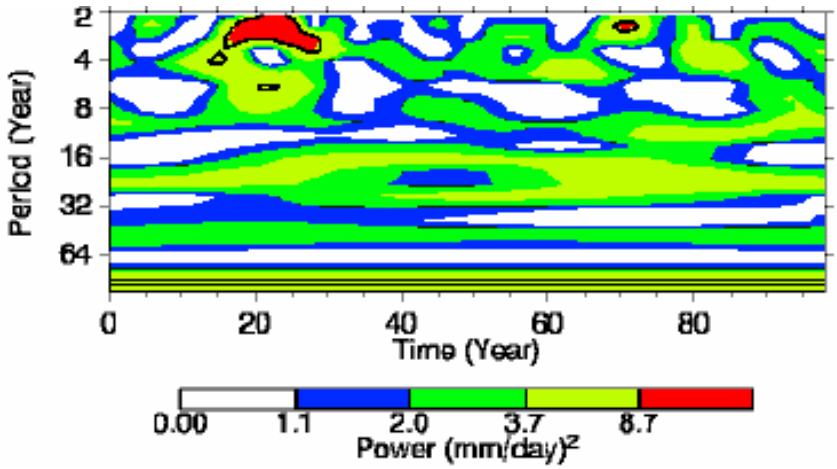

Figure 4.7: Spectral analysis (wavelet, unfiltered) of observed (CRU) rainfall extracted over the location of the proxy reconstruction (Therrell et al., 2006). The black line shows significance (95%) against a red-noise background.

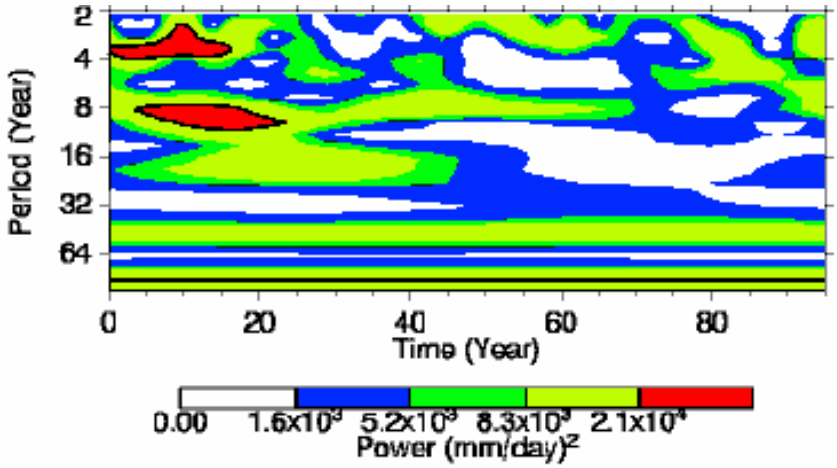

Figure 4.8: Spectral analysis (wavelet, unfiltered) of reconstructed rainfall, based on proxy data (1900-1996) identified by Therrell et al. (2006), in comparison with the observed rainfall. The black line shows significance (95%) against a red-noise background.

There are other peaks at ~20 yrs (19.4 yrs, 95% confidence) and a peak argued to relate to ENSO at 3.5 yrs (95% confidence). The increased length of the record also allows lower frequency variability at 46.75 yrs to emerge with 95% confidence. Wavelet analysis (Figure 4.6) reveals a period of ~20 yr variability between 1815-1880, and then a period of 8-10 yr variability dominates the record between 1880-1930. There are elements of the ENSO scale variability throughout the record, but they do not take a dominant role at any stage.

The wavelet analysis also highlights apparent inconsistency between the observed and proxy data, with differences in the timing of the periods of preferred power. This is perhaps best exemplified by the ~20 yr variability shown between 1960-85 in the observed (CRU) data, which is absent from a proxy record that has weak quasi-decadal variability after 1900. Further comparison can be made in Figure 4.7, which shows observed CRU rainfall extracted over the four grid cells of CRU data approximately equivalent to the proxy region, compared to the proxy record for 1900-1996 in Figure 4.8. The smaller region of observed data shows little quasi-decadal influence through the length of the record in the twentieth century, despite a period of ~20 year variability at the sub-continental scale. A similar analysis of the proxy data for the twentieth century period only shows further inconsistency. Although there is evidence of quasi-decadal variability, there is a marked difference between the spectra of the observed and CRU data, most notably in the 8-10 yr variance band.

What does this analysis of the observed and proxy data tell us about the nature of rainfall variability over southern Africa? First, there is strong evidence of variability at ENSO

timescales, a 10-12 year signal and a quasi-decadal signal in the variability of two independent records that have been confirmed by multiple spectral analysis techniques. This suggests that the recorded 10-12 year and 16-20 year oscillations are likely to be real and present in observed and proxy data to differing degrees, as well as providing a valuable reference point for examination of different model runs, and investigation of potential mechanisms.

Second, the interpretation of the wavelet analysis shows uncertainty over the timing of these periods of variability in different records. This reflects: the uncertainty associated with the proxy data reconstruction method employed by Therrell et al. (2006), the general limitations of proxy data, and the spatial variability of signals within the sub-continental scale. The wavelet analysis of the observed data over the proxy region showed substantial differences compared to the wider sub-continental wavelet, demonstrating the need to carefully examine the natural spatial patterns of variability at different time scales.

Finally, the inconsistency between observed and proxy data reaffirms the difficulty of examining decadal signals with short records – even the 200 years of proxy data does not provide a fully reliable platform from which decadal variability at 20yr or longer periods can be investigated. The proxy captures ENSO-scale variability well, but does not replicate decadal variability consistently. Model simulations over the same region, however, provide comparable estimates of precipitation to test the observed and proxy spectral results presented in this section with extended record length and the ability to examine regional and spatial variability closely.

4.2 Model Simulation at the Sub-Continental Scale

First, we examine the rainfall indices over the sub-continent in their raw form. Next, the spectral power of precipitation over the defined sub-continental region simulated by both HadCM3 and ECHO-G is examined relative to that of the observed and proxy data sets discussed in the previous section.

4. 2. 1 Rainfall Simulation in ECHO-G:

Figure 4.9 shows the JFM mean simulated precipitation for ECHO-G ENAT over the full 220 year record. A range of decadal variability is visually evident, and the filtered rainfall index (7-50) appears to closely match the unfiltered index, suggesting a large portion of variance may be explained by quasi-decadal variability. As before, periods of enhanced and reduced rainfall are identified from regions of substantial decadal power in the wavelet analysis. Figure 4.10 shows the aggregation of these events, and is characterised by a strong zonal gradient in rainfall across the sub-continent. There is less evidence of the NW-SE orientation described previously, but this appears to be consistent with the behaviour of ENAT described by the model evaluation in the previous chapter.

Figure 4.11 shows the MTM analysis for ENAT. The spectral power is dominated by a low-frequency peak at 24.82 yrs (99% confidence), spectral power at 10-12 years (99% confidence), and some variability at high frequency (2.5 yrs). There is a range of spectral power at 6.11 – 6.54 years, with confidence levels of just under 99%, and broad peaks of power at ENSO-scale in the 95% confidence range.

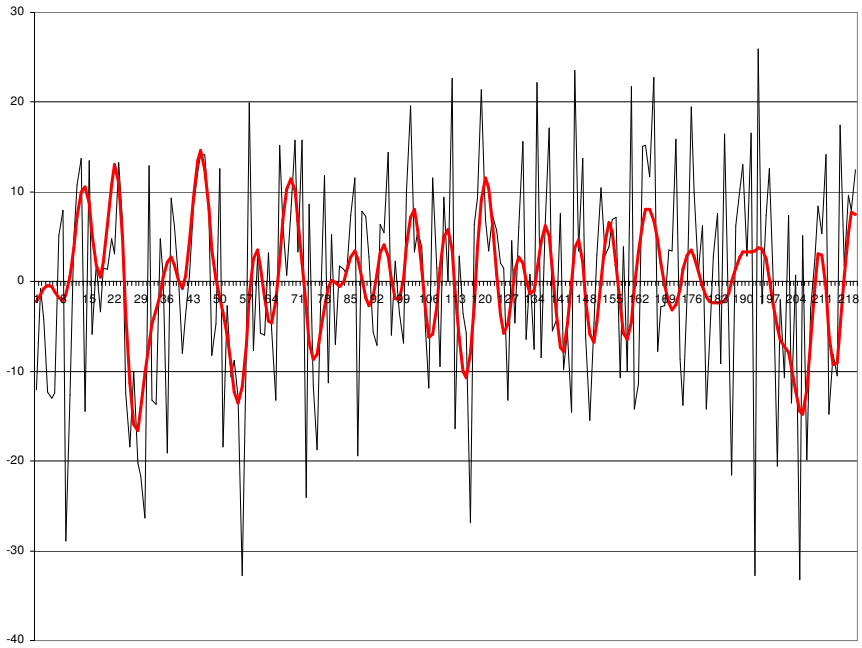

Figure 4.9: Plot of the timeseries of JFM mean precipitation from ECHO-G ENAT simulated data (1900-1998) over the sub-continental region (15-35ºS, 15-35ºE). The black line shows the unfiltered data, and the red line results from the application of a 7-50 year band pass filter.

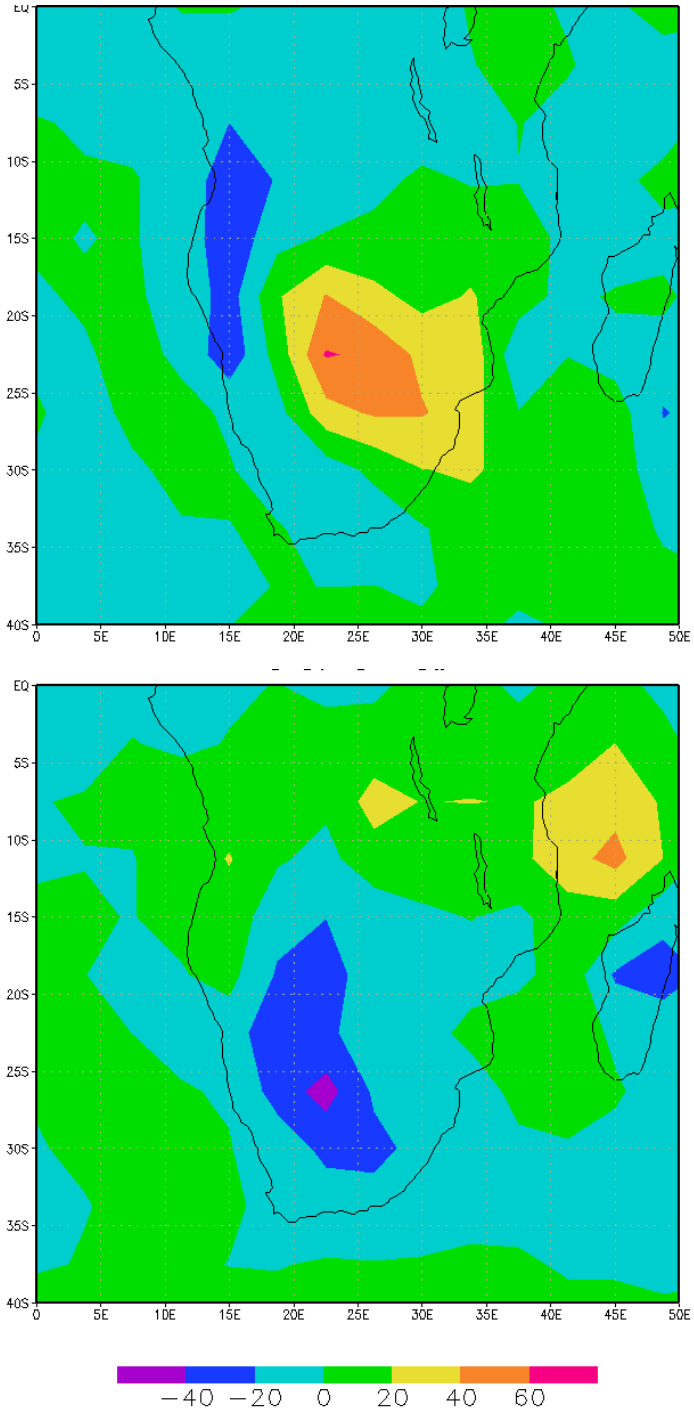

Figure 4.10: Sample quasi-decadal rainfall anomaly "events" from the ECHO-G ENAT dataset, filtered with a 7-50 year band pass filter. Top: high (above average) rainfall event (average of year 45 ± 5 years). Bottom: low (below average) rainfall event (average of year 28 ± 5 years).

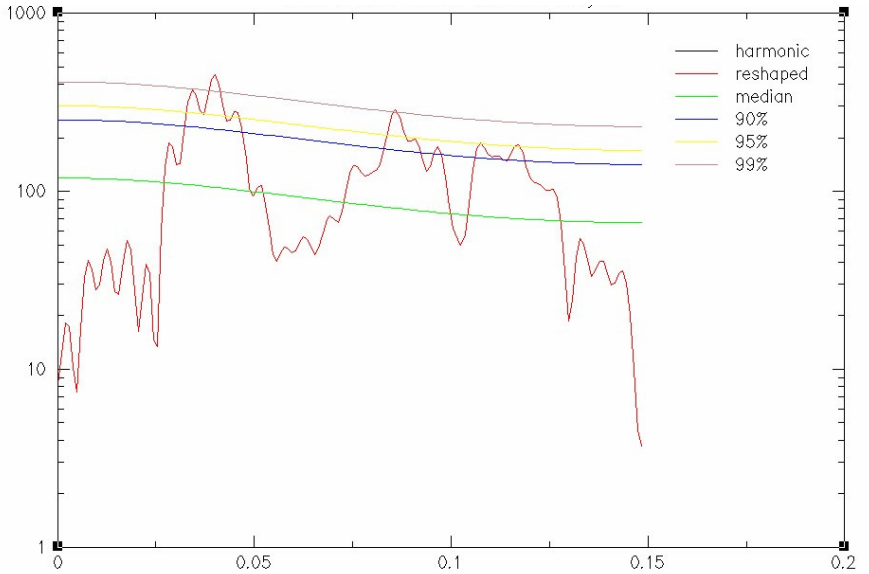

Figure 4.11: Spectral analysis (MTM, unfiltered) of ECHO-G ENAT sub-continental (15-35ºS, 15-35ºE) rainfall. The x axis represents frequency, and the y axis indicates the spectral power.

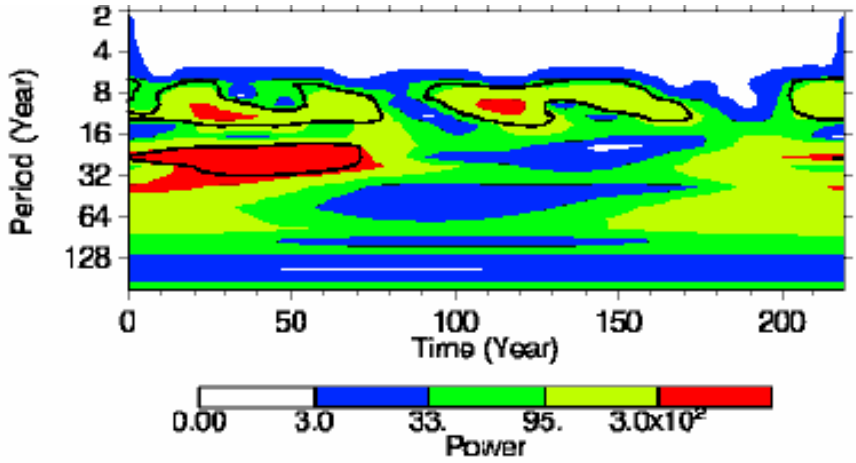

Figure 4.12: Spectral analysis (wavelet, filtered) of ECHO-G ENAT sub-continental (15-35ºS, 15-35ºE) rainfall. The black line shows significance (95%) against a red-noise background.

None of these peaks are oscillatory (SSA plot not shown), with wavelet analysis (Figure 4.12) demonstrating that although the ~25 yr variability dominates for the first 75 years of the simulation, there is then little decadal variability simulated until the last ten years. The ENSO-scale variability is intermittent and highly localised, with very few extended periods of significance.

4. 2. 2 Rainfall Simulation in HadCM3

Figure 4.13 shows the full simulation of precipitation variability under the control simulation of HadCM3, with Figure 4.14 extracting a 100 year sample to better visualise the nature of the variability. The high/low rainfall periods (Figure 4.15) are indicative of a meridional gradient, with elements of the JFM mean structure identified in the model evaluation. HadCM3's wet events tend to be wetter than those of ECHO-G, substantiating the evidence of the model evaluation which suggested over-simulation of precipitation in this model.

Figure 4.16 shows the spectral analysis of the CTR simulated rainfall for the sub-continental region. The filtered rainfall spectrum dominated by a low-frequency peak at 18.89 yrs (99% confidence level). There is also some spectral power with 95% confidence at 13.79 years. These signals are confirmed by other techniques (plots not shown) and shown by Singular Spectrum Analysis to be non-oscillatory in nature (plot not shown).

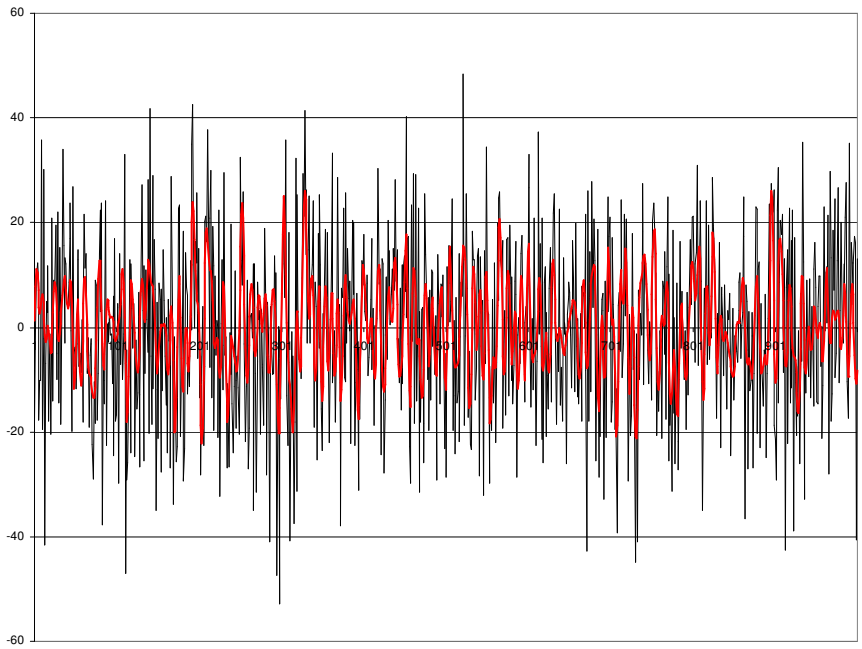

Figure 4.13: Plot of the timeseries of JFM mean precipitation from HadCM3 CTR simulated data (2240-3239) over the sub-continental region (15-35ºS, 15-35ºE). The black line shows the unfiltered data, and the red line results from the application of a 7-50 year band pass filter.

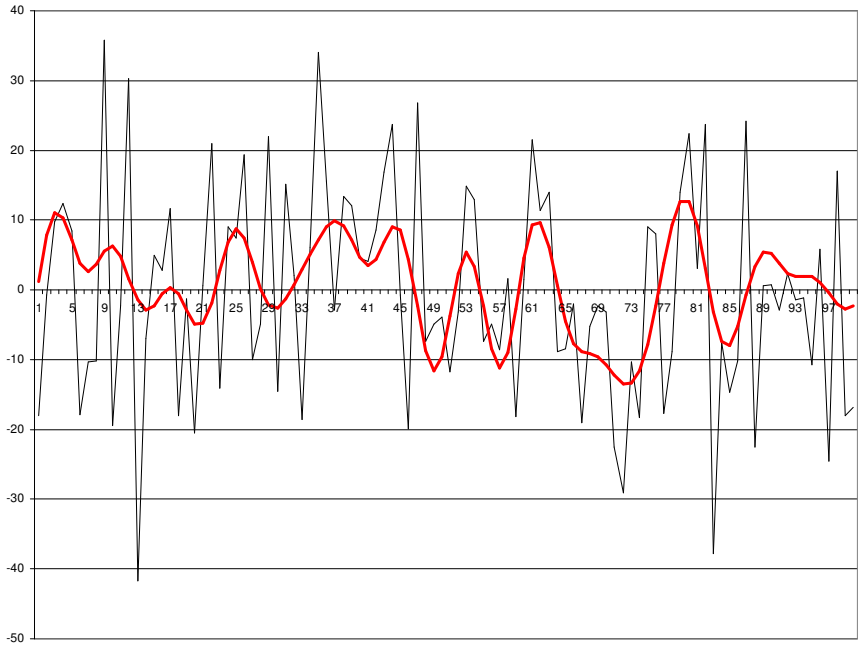

Figure 4.14: Plot of the timeseries of JFM mean precipitation from HadCM3 CTR simulated data (100 year sample plot) over the sub-continental region (15-35ºS, 15-35ºE), chosen to show the variability and filtering process in greater detail. The black line shows the unfiltered data, and the red line results from the application of a 7-50 year band pass filter.

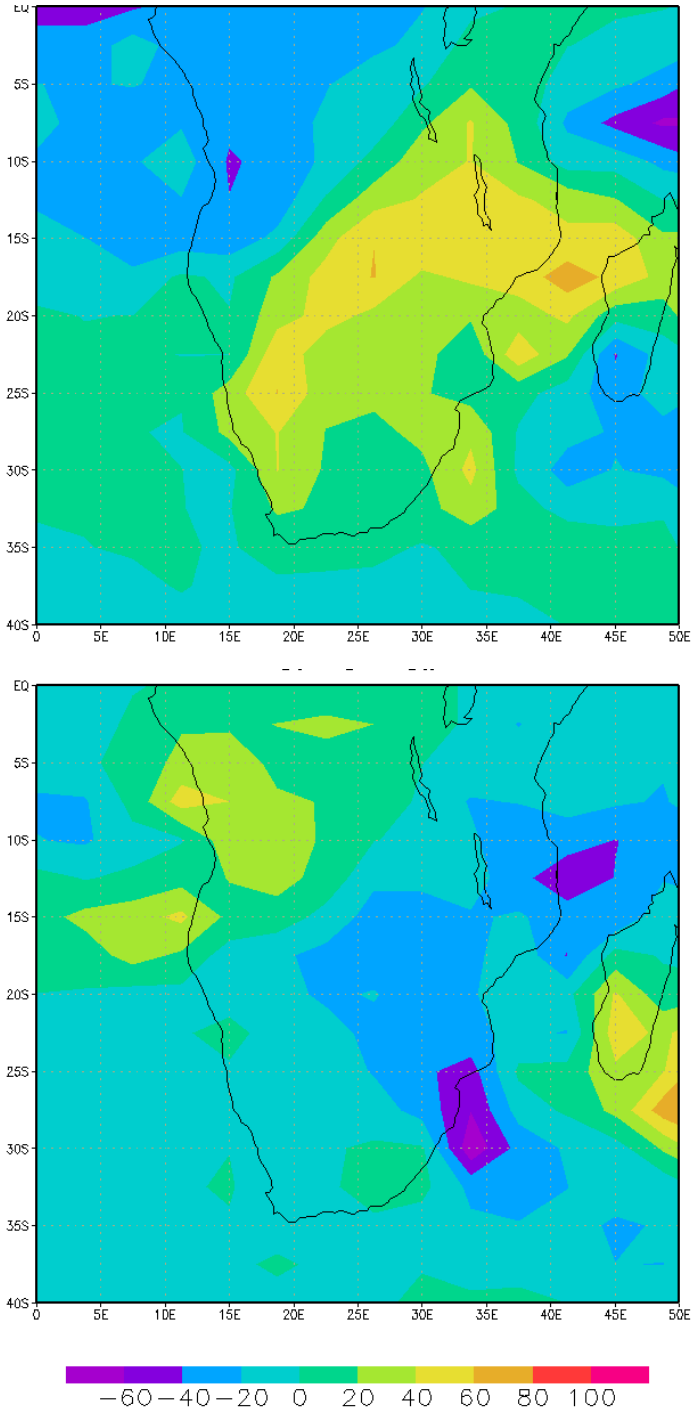

Figure 4.15: Sample quasi-decadal rainfall anomaly "events" from the ECHO-G ENAT dataset, filtered with a 7-50 year band pass filter. Top: high (above average) rainfall event (average of year 304 ± 5 years). Bottom: low (below average) rainfall event (average of year 315 ± 5 years).

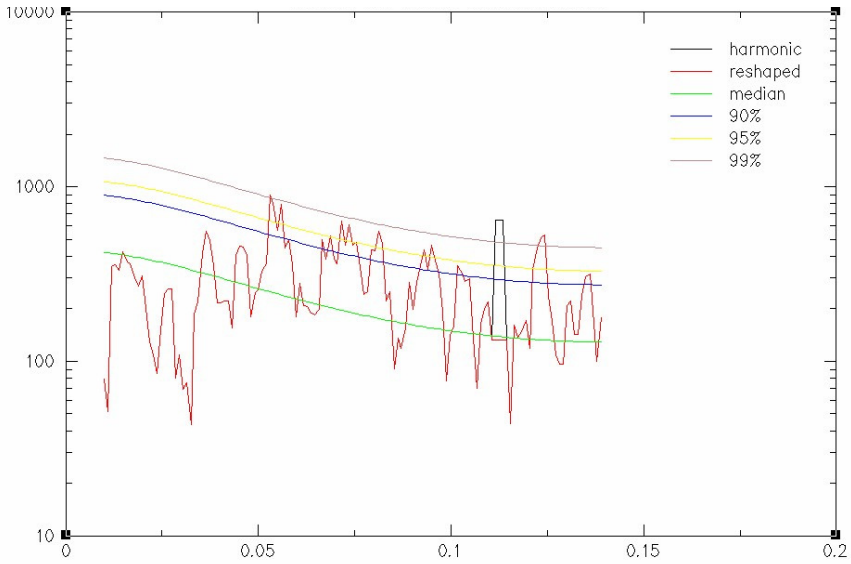

Figure 4.16: Spectral analysis (MTM, unfiltered) of HadCM3 CTR sub-continental (15-35ºS, 15-35ºE) rainfall. The x axis represents frequency, and the y axis indicates the spectral power.

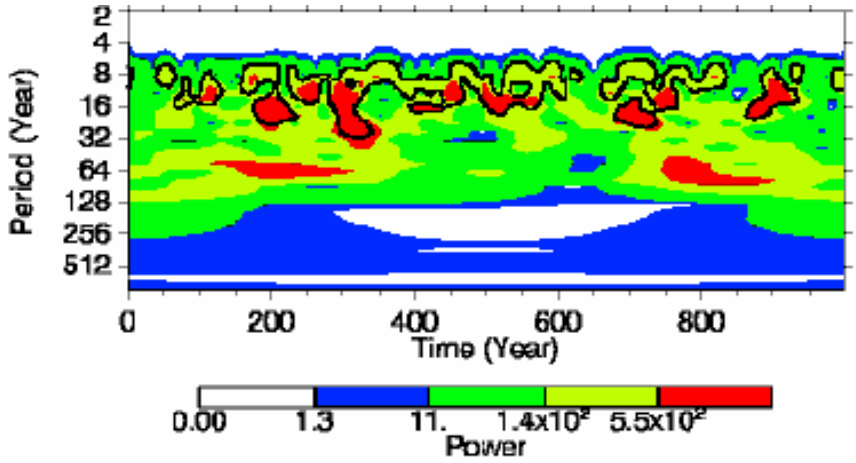

Figure 4.17: Spectral analysis (wavelet, filtered) of HadCM3 CTR sub-continental (15-35ºS, 15-35ºE) rainfall. The black line shows significance (95%) against a red-noise background.

Wavelet analysis (Figure 4.17) confirms this spectral power is intermittent through the record. There are shown to be periods of strong activity at quasi-decadal timescales, and some periods of the record where the 16-18 year cycle dominates the spectral responses. There are also periods of locally significant low-frequency variability (~120-200 yrs), but this does not appear with more than 90% confidence in the MTM analysis.

Further investigation of the behaviour of the NAT and ALL simulations are required, as they have important implications for assessing: (i) the reliability of the simulations in HadCM3 and; (ii) the impact of greenhouse forcing on quasi-decadal rainfall signals over the southern African sub-continent. This examination of the influence of forcing scenarios is detailed in Chapter (6).

4. 2. 3 Discussion

Spectral power has been observed at ENSO timescales, 10-12 yrs and 16-20 yr scales in observed and proxy data. There is reasonable agreement between the records with respect to their spectral power distribution, but further investigation using wavelet techniques revealed some uncertainty in timing the periods of variability at various timescales. The specific limitations of the proxy data and reconstruction technique have been evaluated, and may help to explain some of the disparity between Therrell et al. (2006)'s reconstruction and the CRU data set.

The analysis agrees with the wider literature (Tyson, 1971; Mason & Jury, 1997; Tyson & Preston-Whyte, 2000; Reason & Rouault, 2002; Tyson et al., 2002) in stating that there is real spectral power to be found at these timescales over the southern African sub-

continent, and that it can be found in both observed and proxy data from the region. Similar spectral distribution patterns are found in model rainfall from HadCM3's CTR simulation. The spectra of these simulations correspond broadly with the observed and proxy distribution. There is also evidence from ECHO-G simulations to show ENSO-scale and quasi-decadal oscillations in rainfall over the sub-continent, although there is less agreement between ECHO-G and observed spectral power patterns.

The precise 18 year oscillation period initially identified by Tyson (1971; 1980) that has been the focus of previous decadal rainfall studies over southern Africa is not found in any of the data presented here. First, the spectral techniques employed are biased towards identifying broad spectral power, rather than precise oscillatory frequencies (Chandler, 2007). However, although suitable techniques exist (e.g. Singular Spectrum Analysis, Ghil et al., 2002), the study is concerned with what variability there is at a wider scale. This change in scale is likely to contribute to the lack of 18 year oscillation in the results – drawing on wider resolution datasets than Tyson's station data (Tyson, 1971, 1980; Tyson & Preston-Whyte, 2000) or point source proxy techniques (Tyson et al., 2002) is thought to broaden the resulting power spectrum. Although the sub-continental region is a useful indicator of broad power, further examination is required to fully understand the nature of variability as a regionally varying. A method of spatially deconstructing the observed and simulated rainfall is presented in Section 4.3.

4.3 Spatial Variability of Model Simulated Rainfall

In order to examine the decadal nature of rainfall further, EOF techniques are used to deconstruct the variability of the rainfall in time and space. The observed rainfall data is not presented in this analysis, as prior evaluation shows two key limitations for use. First, the land-based precipitation substantially restricts the scope of the EOF domain, which has a significant and fundamental impact on the structures of variability found (von-Storch & Zwiers, 1999). Second, the relatively short record compared with the domain size renders the eigenvectors employed in EOF analysis potentially unstable (Jolliffe, 2003; Dommenget, 2006; Hannachi et al., 2006) and has implications for their ability to represent modes of variability.

For a similar reason, the gridded datasets are pre-treated with a 7–100 year band pass Kaiser filter, previously described in Section 2.2. Samples examined with a shorter filter (e.g. the 7-50 year band pass) did not retain enough time steps to generate a stable EOF. The decision was therefore taken to extend the filter towards the centennial timescale, rather than incorporating structures associated with interannual and ENSO-like variability.

It is also important to note that the filtered EOF analysis presented here concentrates on the model simulations forced by internal and natural variability only. The impact of anthropogenic greenhouse gas forcing on the spatial variability of simulated rainfall over southern Africa is discussed as a key element of Chapter (6).

4. 3. 1 Spatial variability of ECHO-G simulated rainfall

The ENAT EOF analyses show a range of spectral power across the filtered frequency domain. The leading ENAT EOF explains 13.2% of the variance, and exhibits harmonic and real power at 15-20 years (Figure 4.19) with a secondary peak at 8-9 years with 95% confidence. Describing an NW-SE structure in the south of the sub-continent, the EOF also loads over a dipole in the SW Indian Ocean east and south of Madagascar respectively (Figure 4.18).

ENAT EOF 2 shows principal loading centred on 25°E, 22°S, and secondary loading towards the tropical Atlantic and Benguela regions. There is some evidence of a NW-SE preferred mode, with a loading tail towards the SW Indian Ocean. The second EOF explains 10.3% of the variance, and spectral analysis reveals links to a ~32 yr periodicity and a range of power at approximately ENSO-timescales.

The third EOF shows a spectral peak at 20 years (not shown), and loads in a SW Indian Ocean pattern which appears visually similar to that described by ENAT EOF 1. However, the loading concentrates on the perimeter of the domain, and this potential instability is confirmed by the failure on the North test (North et al., 1982) for ENAT EOF 3. As for the HadCM3 simulations, ENAT EOFs 4 and 5 reflect a spatially incoherent pattern, with limited spectral influences, and they are effectively discarded for analysis.

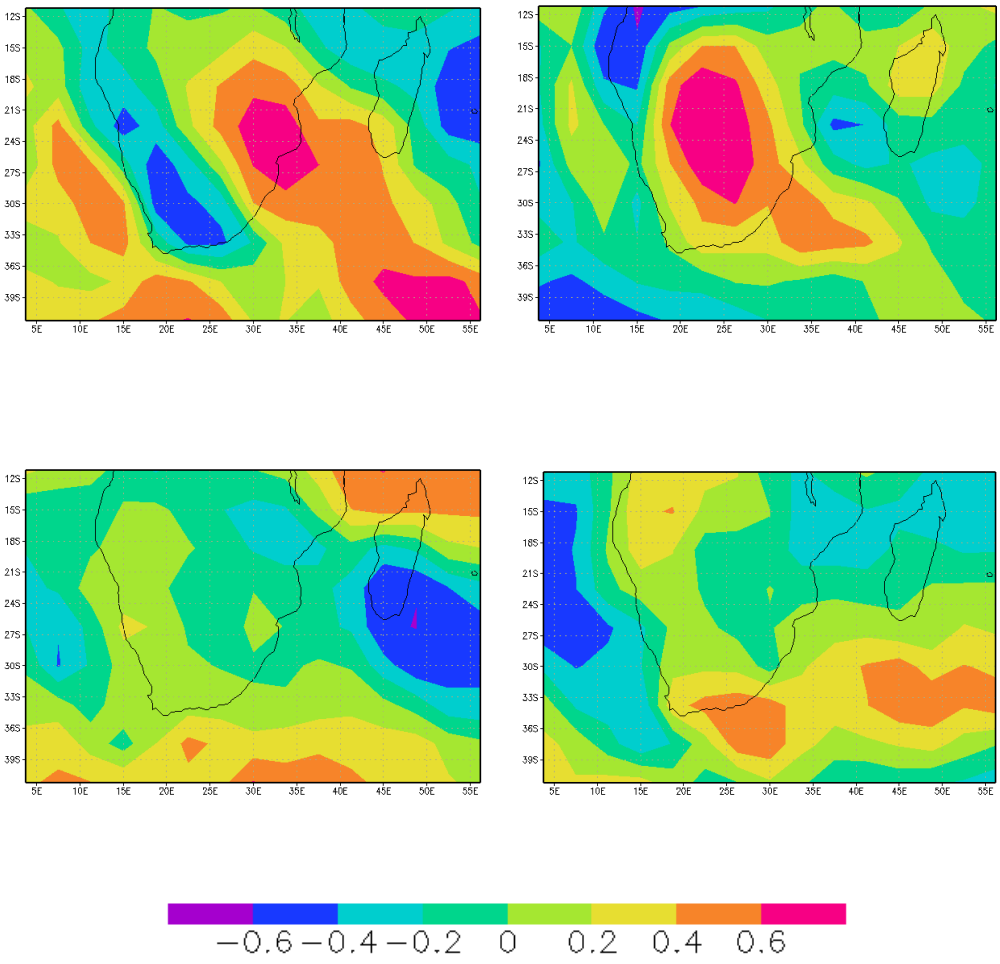

Figure 4.18: EOF analysis of filtered (7-100 year band pass) ECHO-G ENAT rainfall over the sub-continental domain. Shown here: EOF 1 (top left), EOF 2 (top right), EOF 3 (bottom left), and EOF 4 (bottom right).

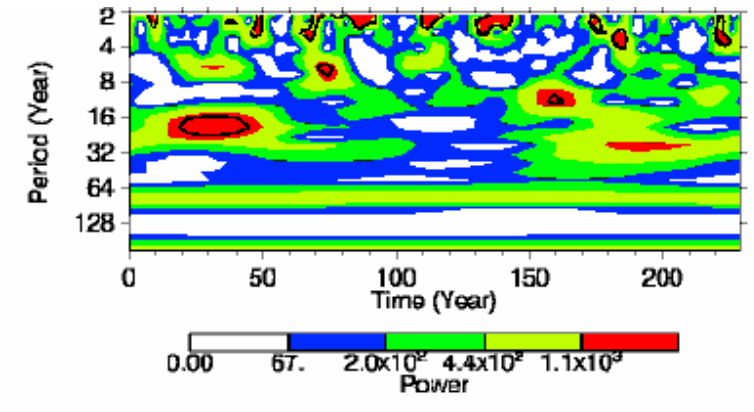

Figure 4.19: Spectral analysis (wavelet, filtered) of ECHO-G ENAT EOF 1 (top) and EOF 2 (bottom) time coefficients. The black line shows significance (95%) against a red-noise background.

The ENAT EOF analysis is consistent with the previously described spectral response at sub-continental scale, confirming the nature of the response under different spatial structures. The leading mode of variability is physically consistent with observed variability (Mason & Jury, 1997), and the second EOF is also compatible with ENSO-related variability as simulated by ECHO-G. The majority of the EOFs possess some quasi-decadal variability, with no single spatial "fingerprint" associated with the decadal structures.

4. 3. 2 Spatial variability of HadCM3 simulated rainfall

The EOF analysis of HadCM3 shows remarkable consistency between the different simulations in spatial structure and percentage of variance explained. For much of this section, the similarity between CTR and NAT simulations is apparent in spatial pattern and explanation of variability. Therefore, in order to avoid replication, only the CTR simulation is presented in this section.

For both CTR (Figure 4.20) and NAT (not shown) simulations, EOF 1 loads in a NW-SE pattern, with alternative loading poles in the SW Indian Ocean off Madagascar. The leading EOF explains approximately 15% of the variance (CTR – 14.9%; NAT 15.8%) over the region and has a broad range of spectral influences. For the CTR simulation, although the spectral power observed in EOF 1 and 2 (wavelet analysis shown in Figure 4.21) incorporates the major peaks of the sub-continental analysis, it does not reach statistically significant levels. The next EOFs show consistency between simulations, with all EOFs demonstrating elements of the NW-SE structure described by EOF 1.

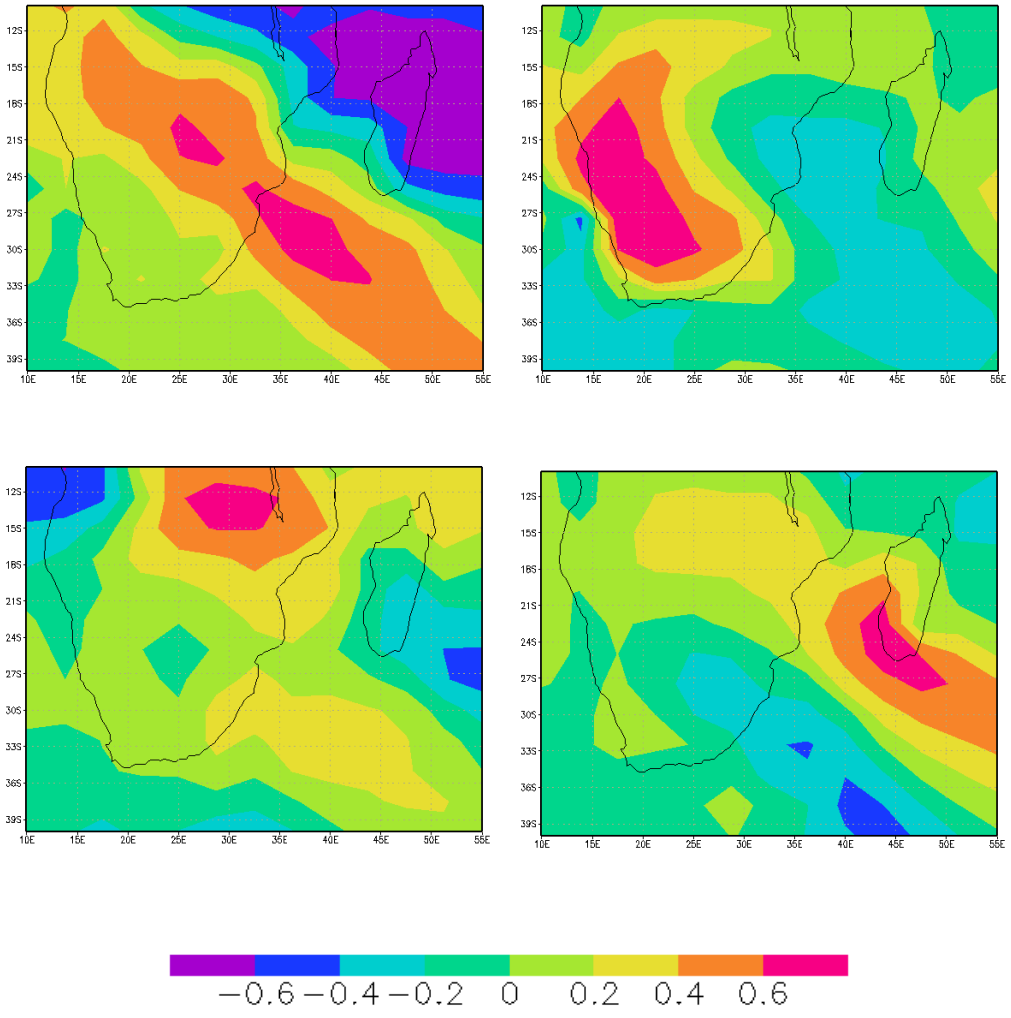

Figure 4.20: EOF analysis of filtered (7-100 year band pass) HadCM3 CTR rainfall over the sub-continental domain. Shown here: EOF 1 (top left), EOF 2 (top right), EOF 3 (bottom left), and EOF 4 (bottom right).

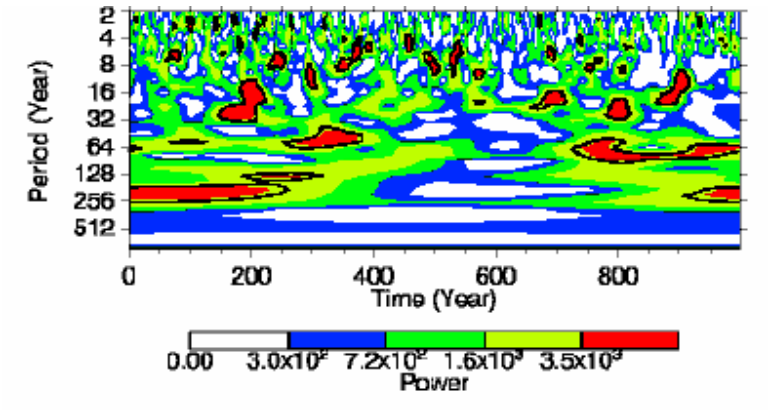

Figure 4.21: Spectral analysis (wavelet, filtered) of HadCM3 CTR EOF 1 (top) and EOF 2 (bottom) rainfall structures. The black line shows significance (95%) against a red-noise background.

CTR EOF 2 explains 7.6% of the variance at decadal scales, and has significant power in the spectrum at 10-12 and 16-20 yrs (99% confidence level). Spatially, the EOF loads over the south west of the sub-continent, with alternate loading in the Atlantic Benguela region. There is still evidence of the NW-SE orientation, and some minor variation in secondary loading strength and location can be observed between CTR and NAT simulations.

The model consistency continues with CTR EOF 3, which loads over the north of the sub-continent with alternate loading over the tropical Atlantic Ocean. There remain elements of the NW-SE pattern observed in previous EOFs. The spectral analysis (not shown) confirms power at quasi-decadal timescales. Spectral analysis of CTR EOF 3 shows spectral power between 10-15 years with 95% confidence, as well as lower frequency (~35 years) variability. For both simulations, EOFs 4 and 5 provide little additional information. The spectral analysis supports the frequency distribution described under EOF 1-3, and the spatial patterns retain elements of orthogonality while simultaneously loading towards the edges of the EOF domain and further displaying tendencies towards instability. The loading patterns link the southern continent to the Benguela and SW Indian Ocean regions, echoing the locations described elsewhere in EOF 1-3.

The analysis shows consistent spatial patterns between the leading three EOF modes of HadCM3 CTR-simulated rainfall at decadal scales. The spectral power identified in the separate EOFs conforms to the broad peaks of power identified in the sub-continental results described earlier. The NW-SE alignment described here has been found in EOF analysis of rainfall at daily (Todd & Washington, 1999), high frequency and interannual timescales in observed and model climate data over southern Africa. Tyson & Preston-

Whyte (2000) have also linked this orientation to a mechanism of ENSO influence, and it has now been shown to appear at decadal timescales in HadCM3 climate simulations across the range of radiative forcing experiments. It is not thought to be a model-specific rainfall distribution.

The spectral analysis demonstrates a range of power distribution, incorporating the key elements described at sub-continental scale in to different spatial regions described by the EOF analysis. MTM analysis shows that there is no dominant forcing frequency for any particular EOF. Although there are variations in the strength and confidence of the spectral peaks, they are part of a continuous power distribution across the simulated EOFs, and exist to some degree in all spectral analysis. This agrees with the spatial distribution, and suggests that forcing mechanisms and their resultant spectral powers do not work in regional isolation in HadCM3 simulations.

4. 3. 3 Discussion

EOF analysis has been carried out on model-simulated rainfall variability to identify preferred spatial modes of variability. Spectral analysis of these modes shows a range of power at different frequencies, many of which agree with the sub-continental scale spectral analysis shown previously. The EOF analysis of the decadally filtered rainfall simulations has consistent elements of NW-SE orientated structures in both models. Although more clearly defined in HadCM3 experiments than their ECHAM counterparts, the presence in both models suggests that it cannot be a model-specific rainfall response.

At synoptic and daily scales, this orientation has links to tropical temperate trough formation (Todd & Washington, 1999; Washington & Todd, 1999), with potential links to ENSO described by Tyson & Preston-Whyte (2000) at longer timescales. It is not clear why this pattern emerges at all timescales, including the decadal variability shown here. It is possible that this could be a function of the EOF technique as applied to this region, but this hypothesis remains to be tested.

Differences between the modelled structures of variability identified through EOF analysis are thought to represent the underlying simulation of southern African rainfall by the different models. It is not thought that the different model resolutions (3.75º x 2.5º in HadCM3 compared to 3.75º x 3.75º in ECHO-G) are responsible for the disparity in EOF results, although it cannot be fully ruled out without detailed analysis of the EOF technique which is beyond the scope of this study. The simulation of rainfall is explored though associated variability in the next chapter, which will carefully examine the way in which rainfall is generated at decadal scales in both models.

The EOF analysis does not highlight particular areas that are dominated by the 18-year rainfall oscillation described by Tyson (1971). This confirms that the quasi-decadal signals are not unique to a small segment of the subcontinent, and cannot be spatially defined by EOF techniques.

4.4 Discussion of the Nature of Variability

As described in the first chapter, previous work in southern Africa has identified quasi-decadal signals in rainfall variability. Evidence is presented here for spectral power at ENSO-related timescales (3-8 yrs), as well as broad decadal timescales of 10-12 yrs, and 16-20 yr periods from observed and proxy data examined through a range of spectral techniques.

Climate models have shown similar quasi-decadal variability at the sub-continental scale across a range of forcing scenarios. HadCM3 appears to replicate the observed spectral power more accurately than ECHO-G, which shows considerable difference in the periodicity of the main quasi-decadal spectral peak. The presence of this decadal variability in model simulations without forcing (natural or anthropogenic) suggests that ocean-atmosphere interaction or internal atmospheric variability is a likely cause of the spectral power. There is some evidence to suggest that the anthropogenic forcing may impact on the nature and scope of quasi-decadal variability in southern Africa, which will be examined more carefully in Chapter 6.

The results presented in this chapter are consistent with interpretations from the observed interannual data presented in the literature, and suggest that the models simulate the regional rainfall of southern Africa adequately. The apparent links between interannual structures of variability and those found at decadal timescales suggest that the methods chosen are appropriate to identify structures of variability associated with southern African rainfall variability.

EOF analysis confirms that the spectral distribution shown at the sub-continental scale is not an artefact of regional averaging techniques, but does not identify clear climate regions or leading patterns of variability inextricably linked to a particular oscillatory mode at decadal timescales. The model simulations qualitatively resemble known areas of influence over rainfall in the region, with both models displaying the NW-SE orientation found at all timescales in spatial analysis of southern African rainfall variability.

The absence of the 18 year rainfall oscillation identified by Tyson (1971, *et seq.*) is thought to be a result of the spatial scale (i.e. the focus on sub-continent) and resolution (i.e. grid box data, compared to point source station observations or proxy techniques) and spectral techniques employed in this study. Although this study could have concentrated on the verification of the 18 year oscillation, and employed relevant techniques to identify the regions associated with it, a deliberate choice was made to broaden the focus and examine the nature and relationships of decadal variability at all scales. This aids a greater understanding of how decadal variability operates, and integrates with the mechanisms at interannual scales and wider teleconnections, rather than attempting to isolate a spectral peak which has previously proved rather elusive (Mason, 1995; Tyson & Preston-Whyte, 2000; Mason, 2001).

The presence of decadal variability in HadCM3 and ECHO-G "control" and "natural" simulation suggests the variability is unlikely to be driven by anthropogenic climate change. The additional evidence of strong decadal variability in HadCM3 CTR suggests that it may not be strongly influenced by solar or volcanic forcing. A more extensive

discussion of associated variability follows in the next chapter, and the influence of anthropogenic forcing is discussed later in this study.

The results presented here have wider implications for the nature of variability at decadal scales, as suggested in the initial literature review. The link between interannual structures and those identified here supports the hypothesis that decadal variability is linked to the long integration of interannual variability (Vimont, 2007). It is not clear whether the decadal oscillations may operate by modulating the strength of interannual response (Tozuka et al., 2007) with underlying spectral power, or whether there are 'decadal' structures which operate independently of the interannual variability.

The complexity of forcing requires a careful approach to investigating the potential mechanisms and associated variability, if implications are to be drawn about the real-world forcing of the rainfall oscillations in the region. This investigation is presented in the next chapter.

(5) What ocean-atmosphere variability is associated with decadal rainfall variability over southern Africa?

It has been shown that quasi-decadal variability in southern African rainfall is found in observed and proxy data, and simulated by climate models under different radiative forcing scenarios. This chapter aims to address the third research question, and to examine what is associated with the variability of rainfall on decadal timescales. The rainfall variability is examined first in the observed data, and then ECHAM and HadCM3 models separately.

It is important to note that this is not a model-intercomparison study, and it is not the aim of this chapter to assess which model 'best simulates' the observed rainfall and associated ocean-atmosphere variability. Understanding the way in which individual models generate southern African climate helps to build our knowledge of the way the real world climate may operate, and the relative strengths of each model contributes to reducing the uncertainty linked to simulating this complex region.

To assist in this aim, the EOF analysis presented in the previous chapter is not utilised here; with the sub-continental scale rainfall index used to investigate the mechanisms. There were no EOFs dominated by decadal power in spectral analysis, and the majority of the leading EOFs showed some spectral power at decadal scales. In addition, there is concern about the EOF technique as a reliable interpretation of underlying structures, particularly with domain choice influencing the results. These results therefore err on the

side of caution, and are based on the sub-continental average rainfall. Where appropriate, references are made to EOF structures and how they may relate to this large scale index.

In this chapter, the regions are initially identified via correlation analysis. These regions are then examined in greater detail in order to investigate the potential teleconnections at decadal scale. This analysis begins with regions which are least likely to influence southern African rainfall at decadal scales, identified through regression and correlation, and linked to our knowledge of the interannual variability. This method helps to establish a hierarchy of associations, and to understand which regions are more important to southern African rainfall variability at decadal scales.

The chapter will conclude by summarising the important associations, drawn from a combined assessment of observed and model data, and attempting to understand which the model-specific results are. It is suggested that the coupled ocean-atmosphere associations identified at interannual scales may remain important at quasi-decadal time scales also.

5.1 Observed Variability

The investigation of the regions associated with decadal rainfall variability over southern Africa begins with the observed rainfall, SST and SLP datasets described earlier in Section 2. 1. 2. These data sets are examined only for the period 1900-1998, ensuring that they overlap with the observed precipitation record (Hulme, 1992, 1999). The fields are band-passed using a 7-50 year Kaiser filter, with an abbreviated low-frequency range employed in recognition of the short record length and to avoid spurious trend-based spectral artefacts (Chandler, 2007). All data presented in this section should be considered filtered with this 7-50 year band pass unless otherwise indicated.

Previous work has shown that the oceans around southern Africa have considerable influence over the climate and rainfall of the region (e.g. Jury et al., 2004), so correlation with SST and SLP fields forms the starting point of the analysis. The correlation on unfiltered data (Figure 5.1) agrees with previous observed work, with strong links to a dipole-like pattern in the South West Indian Ocean (SWIO), a response in the South Atlantic, and a Pacific Ocean basin response likely to relate to the influence of ENSO. The correlation on filtered data (Figure 5.2) shows a weaker and less spatially coherent response in the SWIO. The Pacific Ocean (ENSO) pattern remains a strong influence at decadal timescales, as suggested by the tropical correlation observed in the SLP field. As proposed in Chapter (2), the significance level is not displayed on these correlation maps.

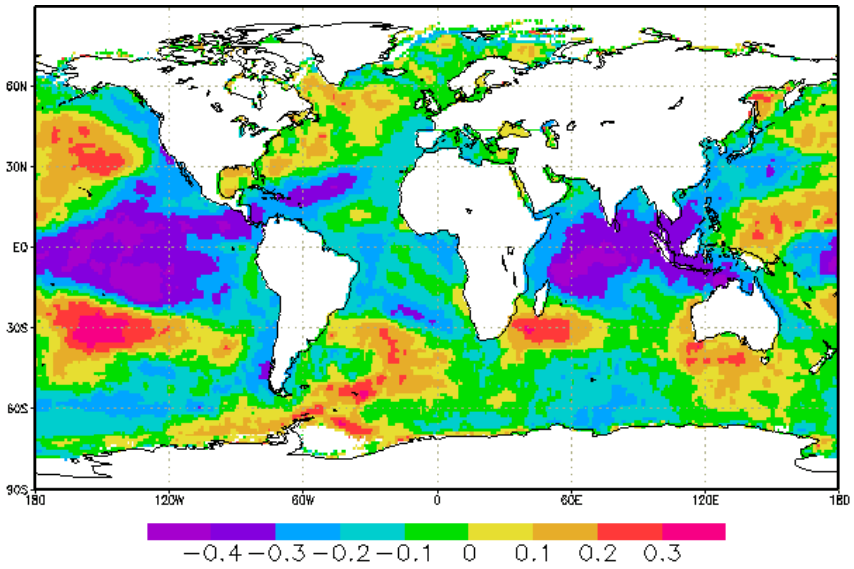

Figure 5.1: Correlation between the timeseries of observed (CRU) rainfall and observed (HadISST) global SST (unfiltered).

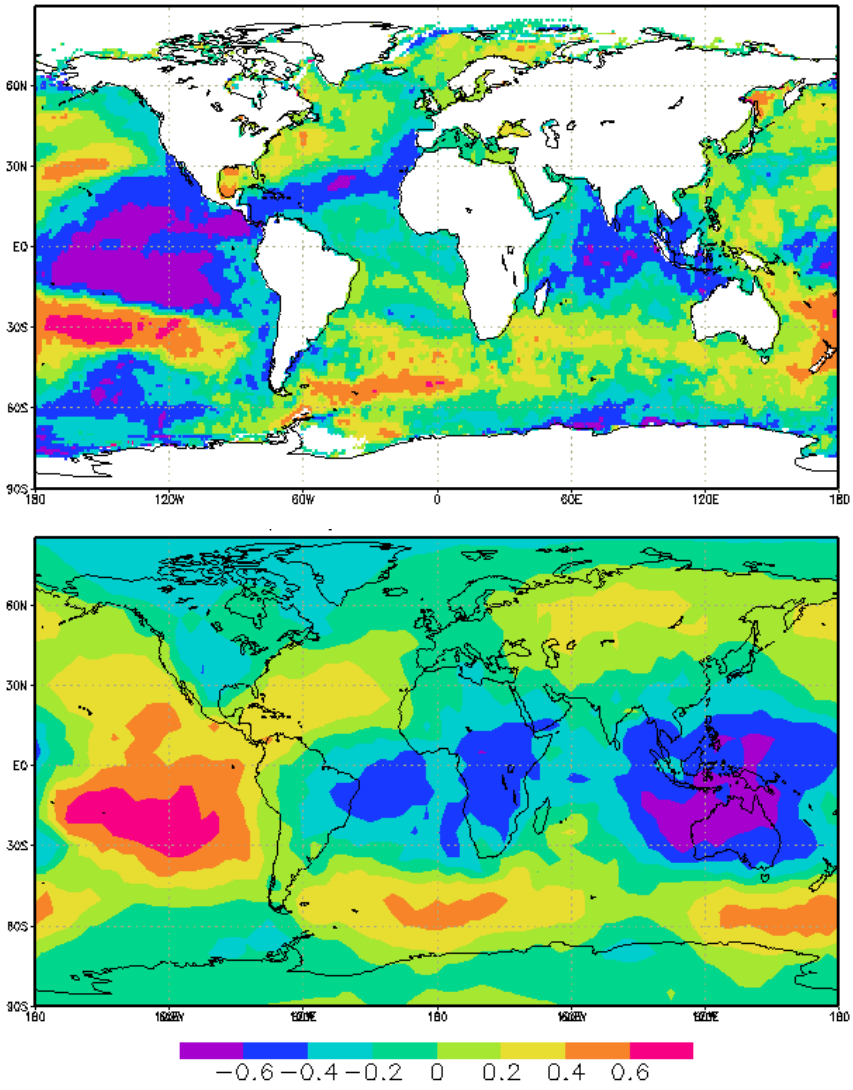

Figure 5.2: Correlation between the filtered timeseries of observed (CRU) rainfall and filtered global SST (HadISST; top) and SLP (HadSLP2; bottom).

The most notable difference in the application of the filter is in the location and strength of the correlation in the SWIO (5-40ºS, 30-75ºE). Washington & Preston (2006)'s discussion of intrinsic (i.e. non-ENSO) variability in this region suggested that the two nodes of the dipole exhibited different characteristics in their relationship with southern African rainfall. Consequently, these regions are examined separately, as a tropical (north-east) node, which exhibits negative correlation with the SAFR region, and a subtropical (south) node which is positively correlated. Questions are raised here about the coherence of the "dipole" at decadal timescales, and although the two correlation nodes are shown to correlate (r=-0.4) at interannual timescales, the correlation at decadal timescales is substantially weaker (r=-0.01179)

This creates four potential regions of influence for southern African rainfall: the South Atlantic (45-60ºS, 30-60ºW), the subtropical SW Indian Ocean node (30-35ºS, 40-60ºE) and tropical SW Indian Ocean node (5-10ºS, 60-80ºE), as well as the decadal ENSO-like behaviour (represented by the NINO 3.4 SST index, 5ºN-5ºS, 120-170ºW). These areas are therefore investigated, beginning with the South Atlantic, and moving through the South West Indian Ocean indices to ENSO. The paucity of the observed data sets may become apparent, as the potential for diagnosing mechanisms is limited.

5. 1. 1 South Atlantic Ocean

Most of the previous work in the South Atlantic has identified links to winter rainfall, and the modification of synoptic-scale conditions. There are particularly strong links to the SW Cape during austral winter, thought to be a result of large scale shifts in the jet and westerly storm tracks over the mid-latitude South Atlantic (Reason & Rouault, 2002). The South Atlantic has not been explored as a major contributor to the 'high' (JFM) summer rainfall variability, and it is not clear by what mechanism this may occur (Reason et al., 2004). Some late summer (April, May) rainfall variability is linked to the appearance of 'Benguela Nino' events in the tropical SE Atlantic along the coast of Namibia and Angola (Florenchie et al., 2003; Rouault et al., 2003; Florenchie et al., 2004, but their predictability is limited (Landman et al., 2001) and they are unlikely to operate at the quasi-decadal time scales obtained through the filtering process here. Nonetheless, the Benguela Ninos suggest that the main region of influence of the South Atlantic ocean over southern Africa is likely to be on the west coast.

To begin, the South Atlantic Ocean is explored using EOF analysis (domain: 60-0°W, 15-45°S) of filtered SST. The domain deliberately avoids including the Atlantic north of 10°S, to explicitly remove the potential influence of a tropical Atlantic mode (Chiang & Vimont, 2004). Only the leading EOF of Atlantic SSTs (Figure 5.3) exhibits a coherent structure, with others displaying spatial patterns loading towards the limits of the domain. The leading EOF is a dipole structure, loading north (negative) and south (positive) of approximately 27°S.

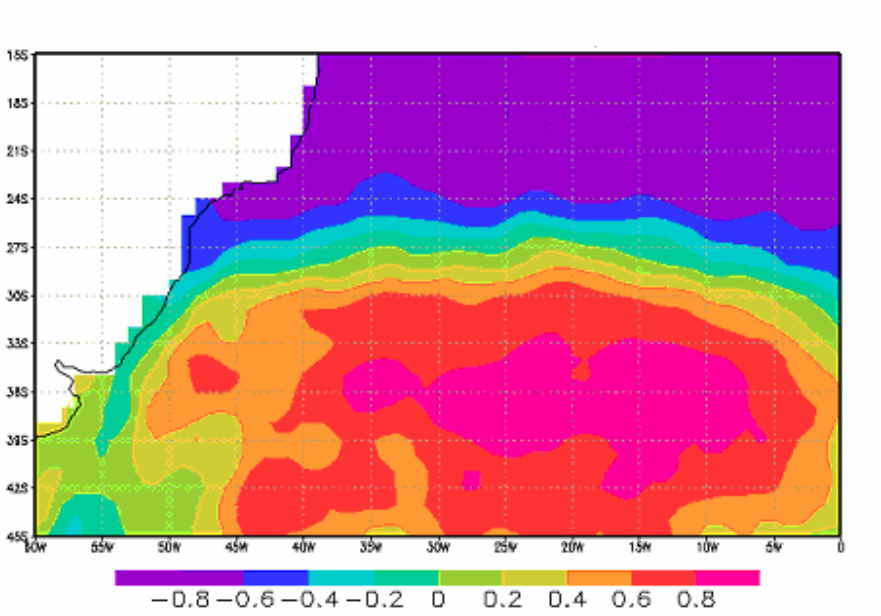

Figure 5.3: EOF 1 from EOF analysis conducted on observed (HadISST) filtered (7-50 yr band pass) SST data over the South Atlantic domain (15-55°S, 40-0°W).

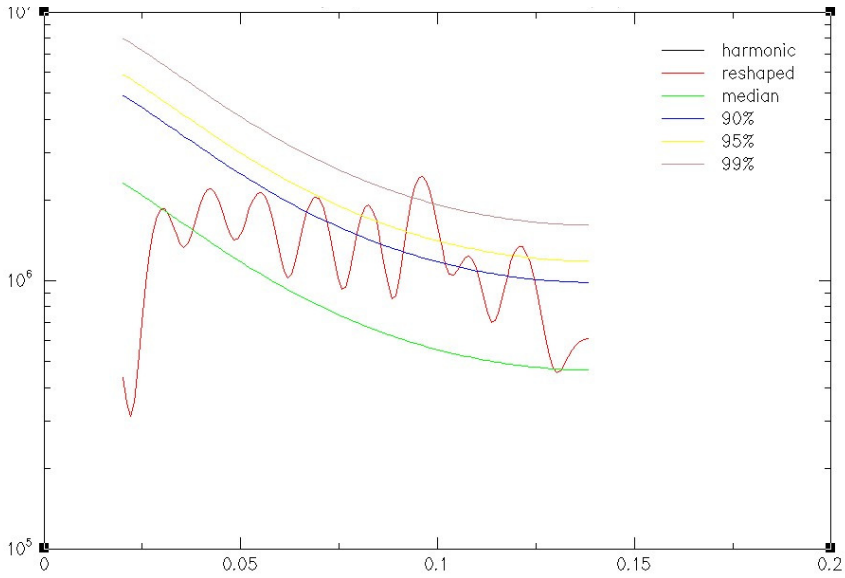

Figure 5.4: Spectral analysis (MTM, filtered), time series of the leading EOF of observed (HadISST) SST over the South Atlantic domain (15-55°S, 40-0°W).

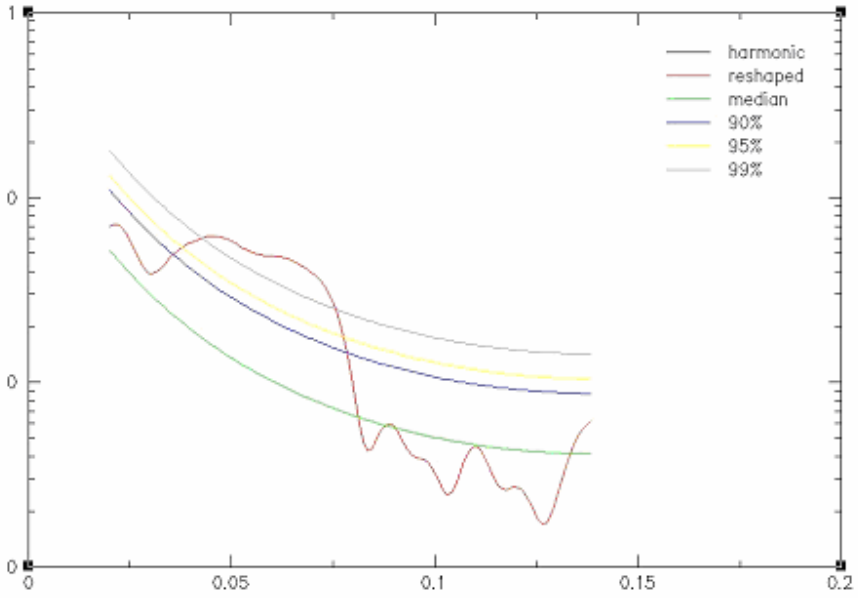

Figure 5.5: Spectral analysis (MTM, filtered), time series of South Atlantic SST index.

The leading EOF bears qualitatively strong resemblance to the second mode of variability identified in the South Atlantic by Venegas et al. (1997), and explains a similar proportion of variance (~25%). Venegas et al. (1997) used coupled SST/SLP SVD analysis to show this mode links to a change in strength of the subtropical anticyclone, and show that this mode of variability is 'dominated by interdecadal timescales' of 14-16 yr period, and strongest during the austral summer. Spectral analysis of the leading EOF (Figure 5.4) shows some decadal and interdecadal power (peaks at 10-12 and 14-16 yrs) which supports the analysis of Venegas et al. (1997).

Figure 5.4 also bears strong resemblance to the second mode of variability identified by Colberg & Reason (2007) in both reanalysis (NCEP-NCAR Reynolds-reconstructed SST) and ocean model (ORCA2 mid-layer temperature) data. This mode of variability is thought to be linked to the subtropical region, but unlike Venegas et al. (1997)'s analysis, is dominated by a 5 yr spectral power. Colberg & Reason (2007) suggest that although the mode is most pronounced in austral summer, it is significantly correlated to ENSO and agrees with previous subtropical analysis (Colberg et al., 2004; Sterl & Hazeleger, 2003). An interdecadal mode (EOF 3) is identified by Colberg & Reason (2007) which shows some resemblance to the leading EOF, but is centred further south, and further east (20°W-5°E) than the observed SST presented here.

This uncertainty in EOF analysis is addressed in Colberg & Reason (2007)'s analysis of the South Atlantic region. Unlike the EOF presented here, and the range of EOFs identified by Venegas et al. (1997) and Sterl & Hazeleger (2003), Colberg & Reason apply rotation to their EOFs. They show that this technique generates more localized

structures of variability, compared to the monopole favoured by non-rotated methods. They also consider the impacts of using detrended SST fields and different resolutions on the outcome of the EOF analysis, and show that these also exhibit technique-dependent results. They suggest that there are four principal modes of variability within the South Atlantic region: (i) a tropical mode; (ii) a NW-SE oriented mode which has spectral power between interannual and interdecadal timescales; (iii) a mid-latitude mode which forms an east-west dipole at interannual and interdecadal timescales, and; (iv) a south-western subtropical/mid-latitude mode. Colberg and Reason (2007) suggest that EOF analysis of this region will identify a mixture of these modes, and that the precise structure and ranking will rely heavily on the choice of dataset, domain and EOF method parameters.

Therefore, in recognition of the potentially technique-dependent results of EOF analysis, an index of mid-latitude South Atlantic SST is taken over the region of strongest correlation between rainfall and SST at decadal timescales (50-55°S, 40-0°W), and used as the basis for investigating this region. Spectral analysis (Figure 5.5) shows quasi-decadal power (99% confidence) in the index region, and this correlates positively (r=0.453) with the southern African rainfall. The index agrees broadly with the spectral power of the leading EOF over the region (spectral analysis not shown), and the spatial correlation with the fields presented here (results not shown), vindicating the choice of regional analysis techniques.

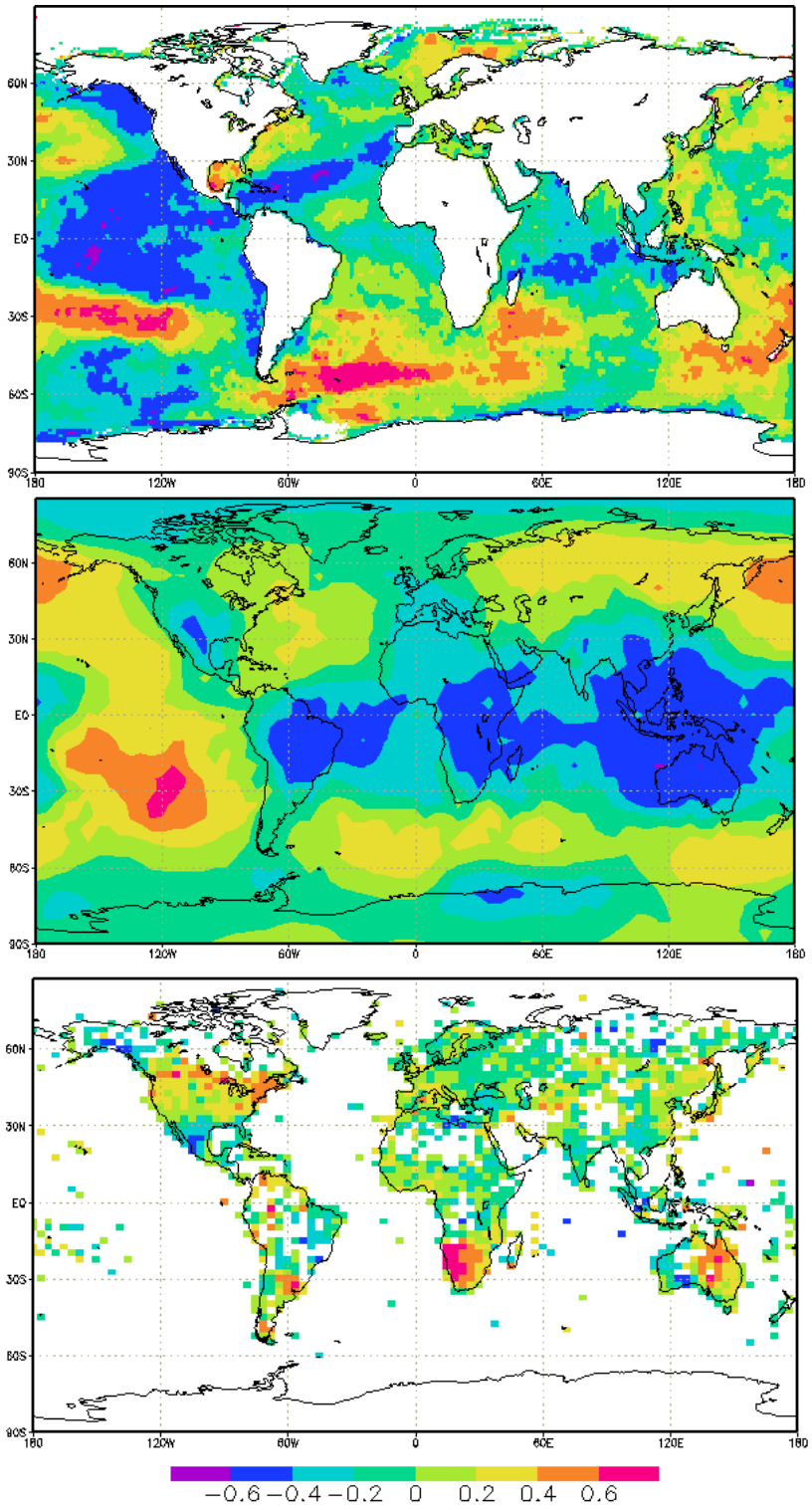

Figure 5.6: Correlation between the timeseries of observed (HadISST) South ATL SST index and global SST (top), SLP (middle), and rainfall (bottom). All correlations are based on data filtered using a 7-50 yr band pass.

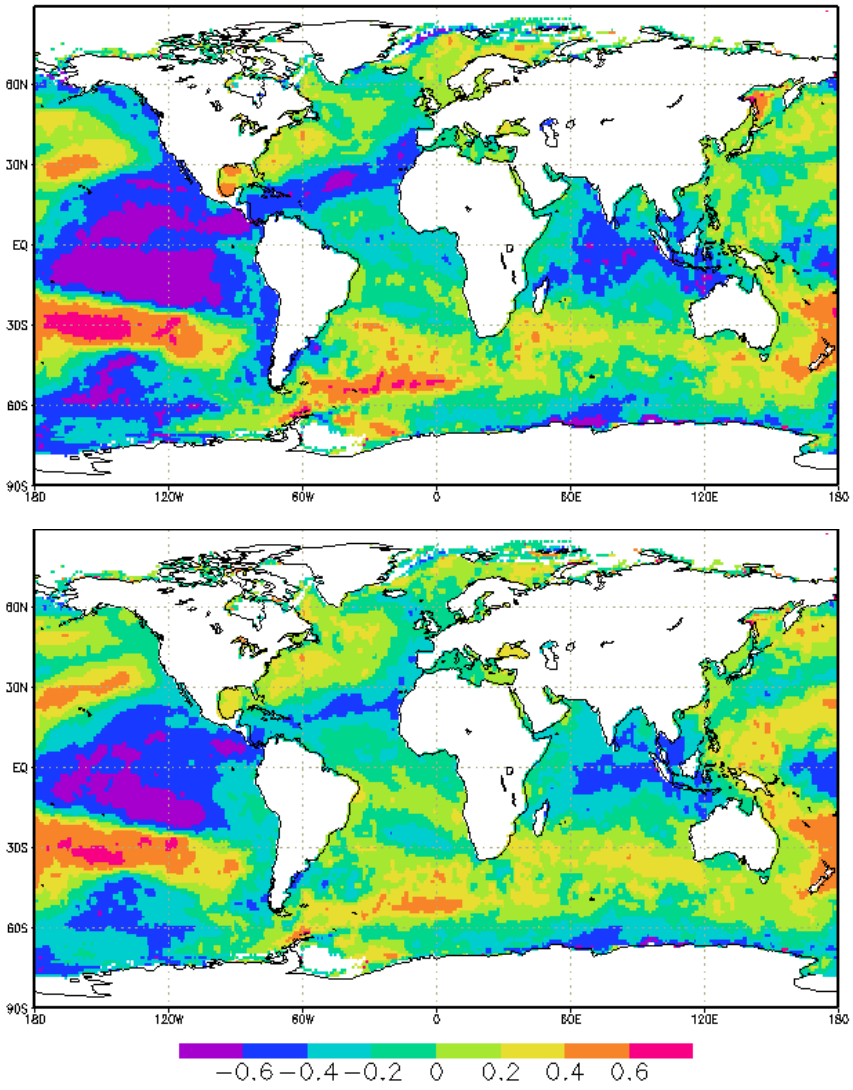

Figure 5.7: Correlation between the timeseries of regional rainfall extracted from the observed (CRU) rainfall data and observed global SST, filtered with a 7-50 year band pass. Top: west coast of southern Africa (15-25°E), bottom: east coast of southern Africa (25-35°E).

Correlation of the South Atlantic SST index with global SST (Figure 5.6) suggests that the ocean variability is linked to ENSO in the Pacific basin, and to the southern hemisphere oceans. This is supported by a meridionally banded response in SLP correlation, with distinct tropical/extra tropical correlations stretching across the Atlantic and Indian Oceans, linked to the Pacific Ocean variability over the maritime subcontinent. The South Atlantic SST index correlation with southern African rainfall shows a strong east-west gradient over the sub-continent, Like the winter rainfall (Reason & Rouault, 2002; Reason et al., 2002), the west coast shows a stronger response to South Atlantic forcing. This is tested further by constructing rainfall indexes over the east (25-35°E, 15-35°S) and west (15-25°E, 15-35°S) of the sub-continent, and correlating them with global SST fields.

The western rainfall zone (Figure 5.7) confirms the stronger response in the South Atlantic as expected. Spectral analysis of the unfiltered rainfall regions (not shown) confirms that the western zone has a stronger quasi-decadal signal, whereas the eastern zone appears to have more power in the 2-4 yr spectral band, and it is likely that the east-west distribution of South Atlantic SST-rainfall correlation simply reflects the dominance of local SST forcing. All correlation fields show a strong and coherent link between the Pacific Ocean (ENSO) and the South Atlantic at decadal timescales. These links to ENSO at decadal scales will be explored later in this section.

This analysis has examined the role of the South Atlantic Ocean in influencing summer rainfall over southern Africa. Although the weakest term in the regression analysis, the South Atlantic is shown through EOF analysis to possess structures of variability which operate at quasi-decadal scales, and which appear to correlate with rainfall on the sub-

continent. The dependency on choice of EOF technique and parameters identified by Colberg & Reason (2007) means that the exploration of the South Atlantic region using an SST index may be more useful. The timeseries of this index was shown to have quasi decadal spectral power. Correlation between this SST index and southern African rainfall resulted in an east-west gradient, and this was investigated by splitting the sub-continent in to separate east and west regions. An increased influence of the South Atlantic on the western side of southern Africa compared to the eastern side was suggested, highlighting the importance of local SST variability to coastal rainfall.

Elucidation of mechanisms in a similar manner to previous work (Venegas et al., 1997; 1998; Sterl & Hazeleger, 2003; Colberg & Reason, 2007) is limited by the paucity of observed records, but it appears unlikely that the South Atlantic has a direct influence on rainfall variability. Instead, two possible explanations for the correlation with rainfall identified in Figure 5.2 are proposed.

First, Hermes & Reason (2005) have suggested that coevolving patterns in the South Atlantic and South West Indian Oceans (driven by common atmospheric forcing) are found at a range of timescales. The South Atlantic may simply coincide with variability linked to the established relationship between SW Indian Ocean SST and southern African rainfall, and give the *appearance* of a correlation region as identified.

In a similar approach, it is also possible that the association with tropical Pacific ENSO-like variability in the decadal SST correlation could generate an apparent correlation. Although Colberg & Reason (2007) proposed an "ENSO-like" influence in their analysis of the South Atlantic, this was based upon the existence of a ~5 yr peak in spectral

analysis, and is thought only to reflect "classic" ENSO timescales. The role of the tropical Pacific and the relationship with the decadal variability of ENSO is explored further in a later section. Like the SW Indian Ocean covariance, the known relationship between ENSO and southern African rainfall (Mason & Jury, 1997) provides another plausible explanation for the *apparent correlation* with the South Atlantic SST region. This does not, however, account for the intrinsic variability of either ocean region (e.g. that demonstrated by Washington & Preston, 2006 for the SW Indian Ocean) as a potential teleconnection.

It is difficult to establish which of these possibilities (or combination thereof) are the most likely to explain the observed relationship between southern African rainfall and South Atlantic SST at decadal timescales. It seems plausible that some interaction between the proposed hypotheses takes place, and this would present a reasonable explanation for the apparent correlation patterns. Since two of the regions involve teleconnections with known SAFR rainfall variability associated with the SW Indian Ocean (directly, and via common ENSO-like forcing), this is the logical next step in exploring the observed variability at decadal scales.

5. 1. 2 South West Indian Ocean

It has been shown that one of the key regions of influence for southern African rainfall is the South West Indian Ocean (SWIO). Although analysis of interannual rainfall timeseries-based correlation (Figure 5.1) and composite analysis, together with SST-based EOF analysis (Kay, 2007, pers. comm.) suggest that the SWIO region is dominated by a "dipole"-like structure, this does not necessarily hold true for decadal time scales. Non-rotated EOF analysis to test this hypothesis is carried out for filtered (7-50 yr) SST fields over the SWIO domain (20-80°E, 0-40°S). A monopole structure in the leading EOF may be linked to the absence of EOF rotation described previously (Colberg & Reason, 2007), while the second EOF (Figure 5.8) isolates a structure which qualitatively resembles the "SWIO dipole" described. The EOF explains 22.4% of the variance, and loads in a dipole structure centred on 60-80°E, 10-15°S and 40-60°E, 30-35°S. Spectral analysis (Figure 5.9) shows evidence of ~8 and ~10 year variability at 95% confidence, with a notable absence of power at quasi decadal (16-20 yr) periods.

The timeseries of the 'dipole' EOF structure was correlated against global SST and SLP, and shows a coherent response in the southern hemisphere mid-latitudes, and echoes the links between South Atlantic and SWIO shown in the previous section (Figure 5.10). Both SST and SLP correlations with this EOF structure display decadal ENSO-like features, although the possibility of intrinsic variability (particularly in the SWIO, as identified by Washington & Preston, 2006) cannot be ruled out. The rainfall correlation shows an east-west gradient, with the possible NW-SE orientation that seems to characterise rainfall structures over the sub-continent at all timescales.

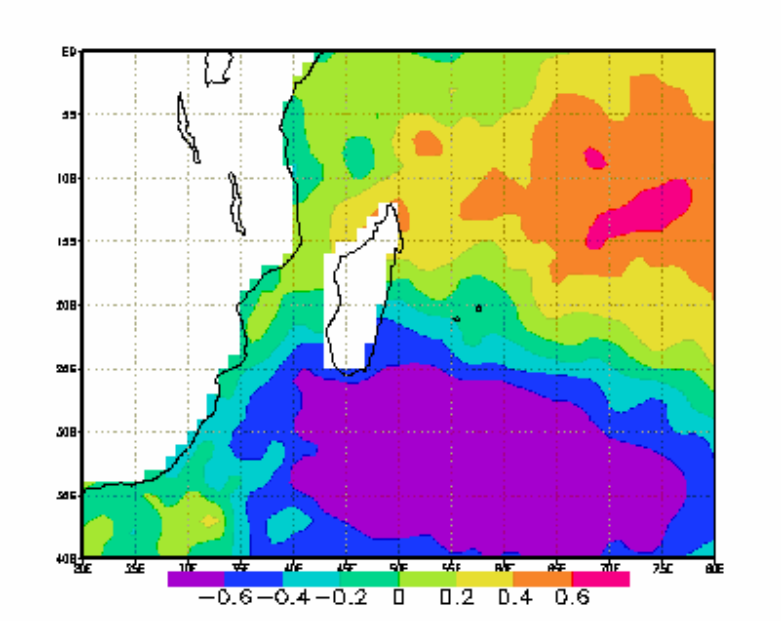

Figure 5.8: Second EOF mode from EOF analysis conducted on observed (HadISST) SST over the SWIO region (0-40°S, 20-80°E,), filtered using a 7-50 yr band pass.

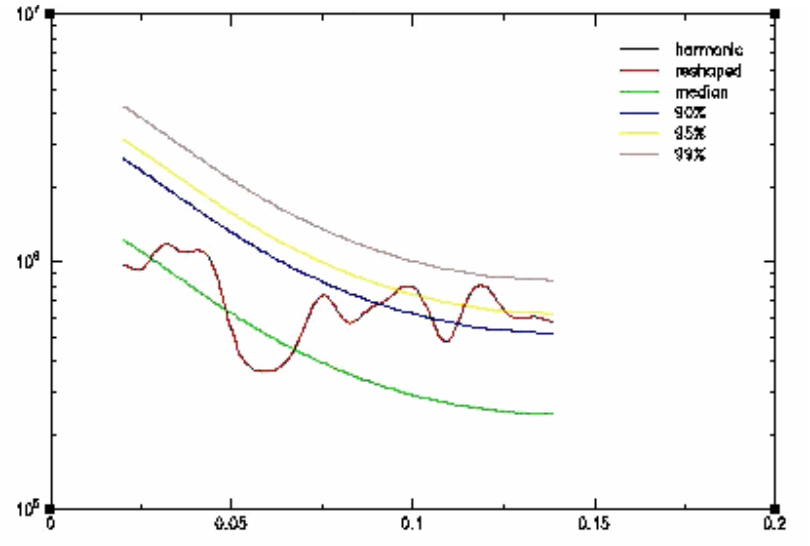

Figure 5.9: Spectral analysis (MTM, filtered) of the timeseries of the second EOF (SWIO dipole structure) of observed (HadISST) SST.

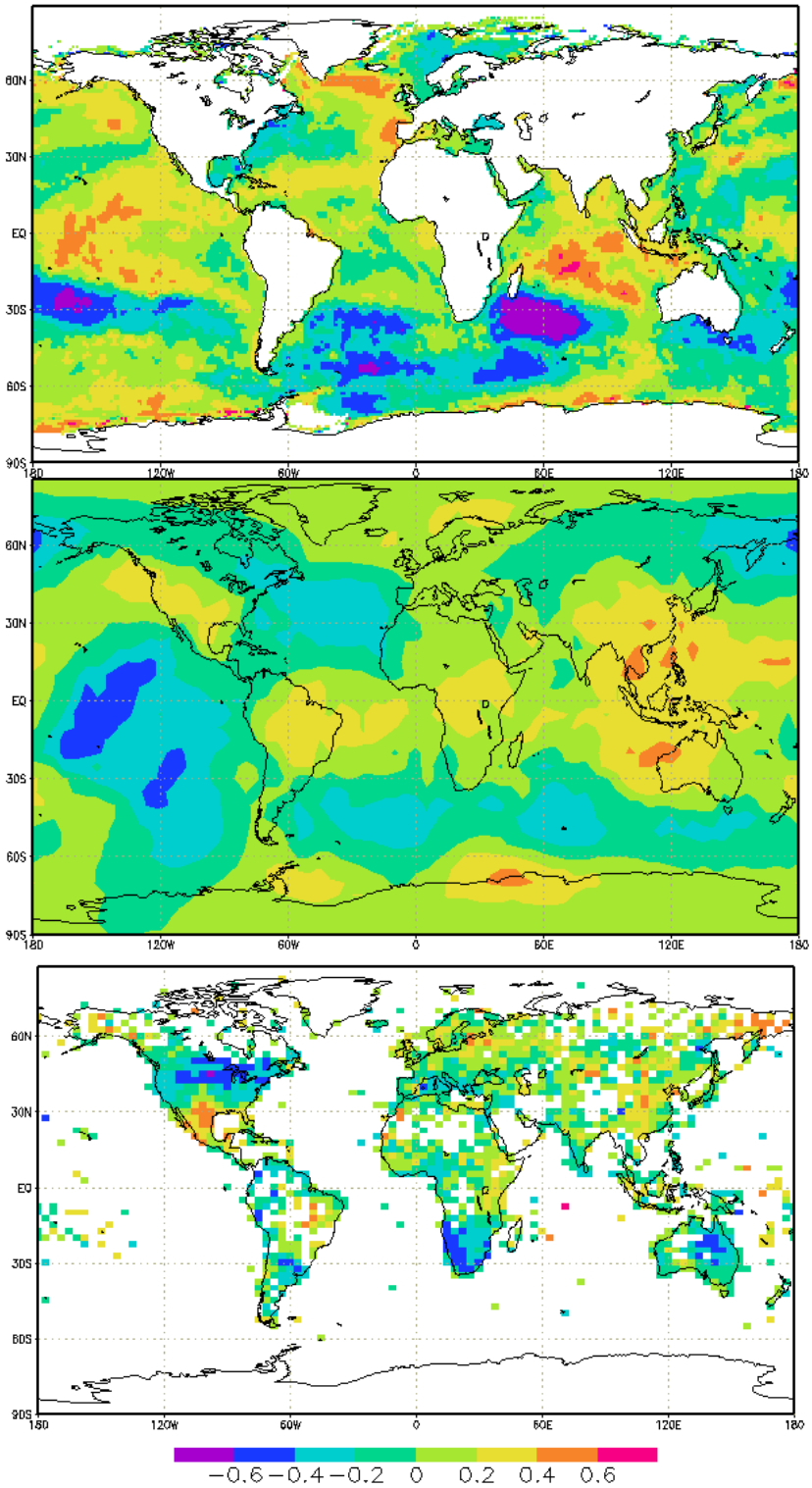

Figure 5.10: Correlation between the timeseries of the second EOF of observed (HadISST) SST over the SW Indian Ocean region filtered using a 7-50 year band pass, and global fields (similarly filtered). Top: global SST; middle: global SLP; and bottom: global rainfall.

This analysis suggests that the SWIO dipole remains a key region that is associated with southern African rainfall variability at decadal timescales. The dipole appears to link to rainfall variability in a similar mechanism to that observed at interannual scales (Tyson & Preston-Whyte, 2000, and described in the earlier review of literature).

However, there are differences in spatial structure observed at the decadal scale. In unfiltered timeseries analysis, the correlation between the tropical and subtropical 'nodes' of the SWIO "dipole" structure is approximately -0.6, but this falls substantially in the observed SST when the filter is applied (r=-0.01179). The absence of quasi-decadal spectral power in the timeseries of each SST node (Figure 5.11) is not though to be significant in explaining this change, with both nodes displaying an 8-10 year peak with 95% confidence.

Separate indices are therefore taken over the regions of strong correlation, which correspond well to the dipole-like structure identified by the EOF at decadal timescales. The subtropical (40-60°E, 30-35°S) and tropical (60-80°E, 5-10°S) nodes are correlated with southern African rainfall and show the expected difference in sign. Perhaps more significantly, the two index regions differ in correlation strength, with a weaker correlation (r=0.245) to the subtropical node than the tropical region (r=-0.555). This agrees with work by Washington & Preston (2006) on the influence of the SWIO "dipole" under ENSO and non-ENSO conditions.

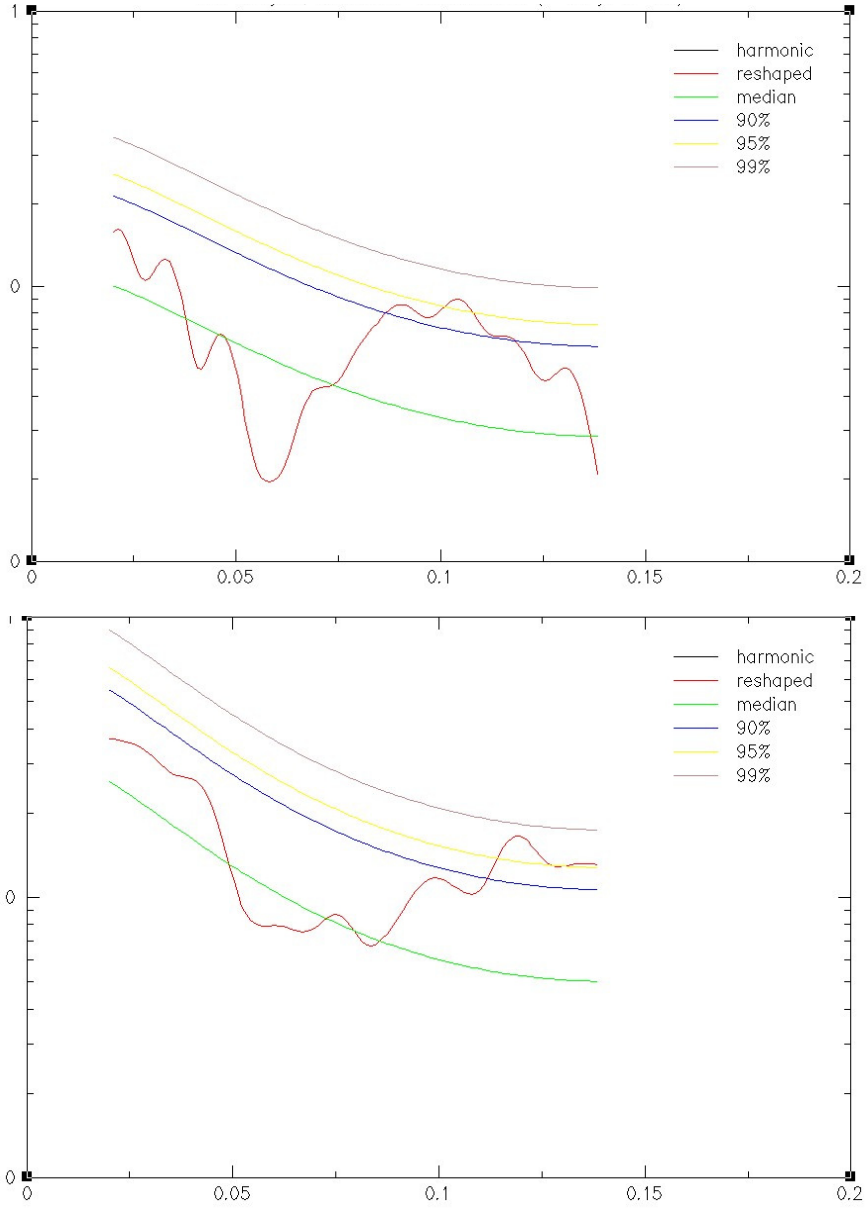

Figure 5.11: Spectral analysis (MTM, filtered) of observed (HadISST) SST index averaged over the 'tropical node' of the SW Indian Ocean (5-10°S, 60-80°E), top; and the 'subtropical node' (30-35°S, 40-60°E), bottom.

Correlation analysis extends the evidence for a different response from the two SWIO nodes. The subtropical SWIO SST index shows a coherent relationship with the South Atlantic and southern Indian Ocean SST fields (Figure 5.12), and correlation with SLP is consistent with a mid-latitude hemisphere-scale response. The relationship with rainfall is positive, but not strong nor spatially coherent over the sub-continent. The weak response to the SST correlation in the subtropical node is a good example of the "dipole-like" pattern not functioning coherently at decadal timescales.

By contrast, the tropical SWIO SST index correlation shows a stronger correlation with rainfall, and both SST and SLP fields (Figure 5.13) are consistent with a tropical ocean response allied to ENSO variability in the Pacific. This does not imply an absence of any other variability – there is a South Atlantic response in both SST and SLP fields – but the correlation is dominated by the tropical response. There is some evidence of a NW-SE alignment in the SLP correlation over the sub-continent, perhaps indicating a more cohesive link to the rainfall variability than previously shown. The evidence of a response in the subtropical high confirms the similarity to the interannual mechanisms described in Chapter (1).

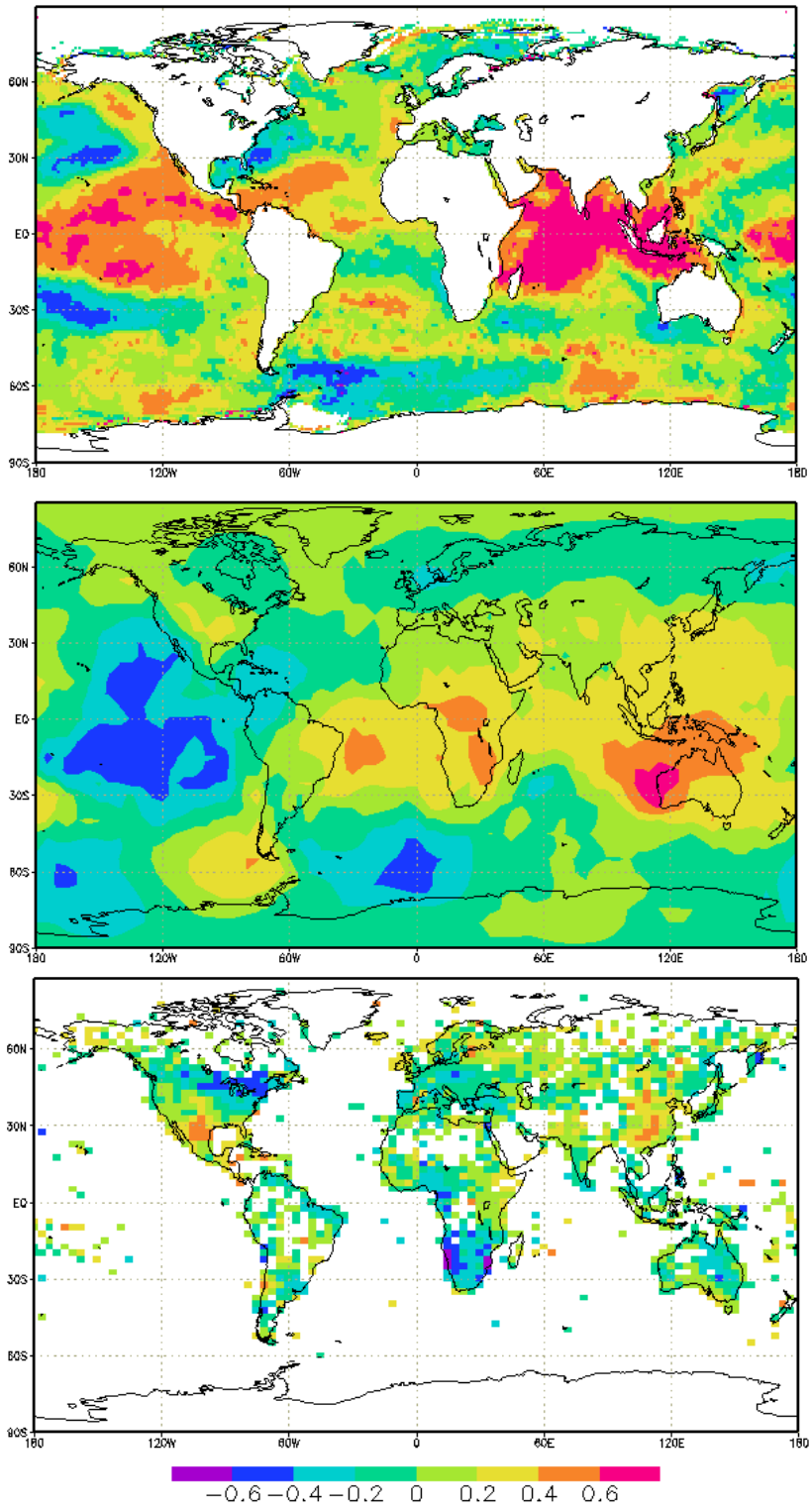

Figure 5.12: Correlation between the filtered (7-50 year band pass) timeseries of observed subtropical SWIO region SST (5-10°S, 60-80°E) and similarly filtered global fields. Top: global SST; middle: global SLP, and bottom: global rainfall.

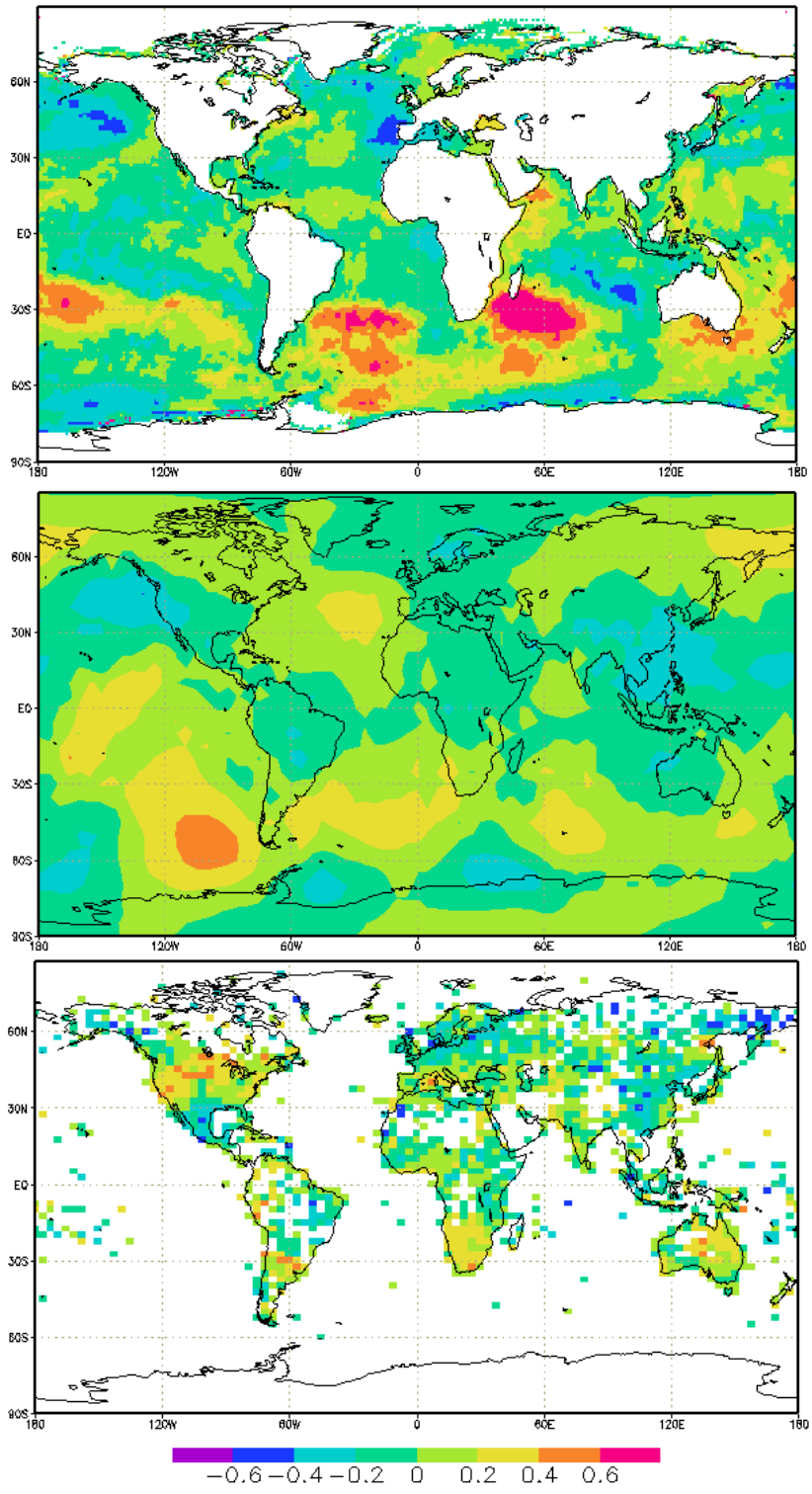

Figure 5.13: Correlation between the filtered (7-50 year band pass) timeseries of observed tropical SWIO region SST (30-35°S, 40-60°E) and similarly filtered global fields. Top: global SST; middle: global SLP, and bottom: global rainfall.

The South West Indian Ocean is identified as an important region for forcing southern African rainfall variability. At interannual timescales, the rainfall is related to a dipole like structure in SST off the coast of Madagascar, which is thought to relate to changes in the strength of the Mascarene high and alter the local Walker circulation to generate an increased moisture flux in to the sub-continent. This dipole is also found in EOF analysis of the SW Indian Ocean itself, and would appear to be an established feature of the circulation.

In analysis of observed data from the Indian Ocean basin, it is shown that SST variability over the Indian Ocean strongly correlates with Pacific ENSO (Xie et al., 2002), particularly in austral summer. During the positive ENSO events, wind stress curl associated with anomalous equatorial easterlies forces a downwelling Rossby wave. A positive SST anomaly has been shown to co-propagate with this Rossby wave, and experiments show this is likely to indicate a sub-surface to surface feedback mechanism with implications for precipitation anomalies in Africa and cyclonic surface circulation behaviour in the SW Indian Ocean region (Xie et al., 2002). It is thought that this propagation mechanism may explain part of the ENSO link to the SW Indian Ocean, and appears to coherently describe the observed variability in this region.

However, the reduced spatial coherence at decadal timescales suggests that the dipole like structure does not operate at all timescales, and a different response is observed when the "dipole" and the two separate regions are considered separately. Weak correlation leads to analysis of *two* regions of SWIO influence, and it is shown that the tropical region (negatively correlated with rainfall) plays a more significant role in modifying southern

African rainfall than the subtropical region. The subtropical node is thought to be linked with South Atlantic SSTs in a hemispheric-scale mid-latitude response (Hermes & Reason, 2005), whereas the tropical ocean responds in a manner consistent with ENSO teleconnections in the global ocean. The strong links to ENSO and the potential role of decadal ENSO-like behaviour in explaining this variability is explored more directly in the next section.

However, the work of Washington & Preston (2006) at interannual timescales showed intrinsic (non ENSO) variability in this SWIO region, and it remains possible that there is intrinsic behaviour operating at decadal timescales also. Work remains to be done in extending Washington & Preston (2006)'s analysis to decadal timescales, and establishing the longer term intrinsic variability of the SW Indian Ocean.

5. 1. 3 El Nino Southern Oscillation (ENSO)

ENSO has long been thought to have significant influence on interannual rainfall over southern Africa (for reviews see Mason & Jury, 1997; Tyson & Preston-Whyte, 2000). The role of ENSO at decadal timescales is less clearly defined, with some debate over the decadal nature of ENSO itself shaping the potential influence that it may have over global teleconnections (Nakamura et al., 1997; Moy et al., 2002; Newman et al., 2003; Mokhov et al., 2004). In addition, a series of studies have shown that the ENSO influence on southern Africa (Allan, 2000; Richard et al., 2000; Allan et al., 2003) and the wider Indian Ocean (Zhang et al., 1997; Yu & Lau, 2004; Zinke et al., 2004) is not consistent through time, and may be associated with regions which possess intrinsic variability that may influence rainfall variability at all timescales (Mulenga et al., 2003; Washington & Preston, 2003; Yu & Lau, 2004; Washington & Preston, 2006). It should be clear from the outset that this is a complex relationship, with variation in strength and teleconnection throughout the record, and that this section will only provide a brief analysis of elements of the decadal ENSO relationship.

Given the complexity of identifying and defining "decadal ENSO" described in Chapter (1), this study chooses to employ the NINO 3.4 index region as a measure of Pacific variability at decadal timescales. Simple correlation shows that the NINO 3.4 SST index (defined as 5°N-5°S, 170-120°W) has the strongest relationship with SAFR rainfall at decadal scales (r=-0.680), which enhances the confidence in this region related to southern African rainfall variability.

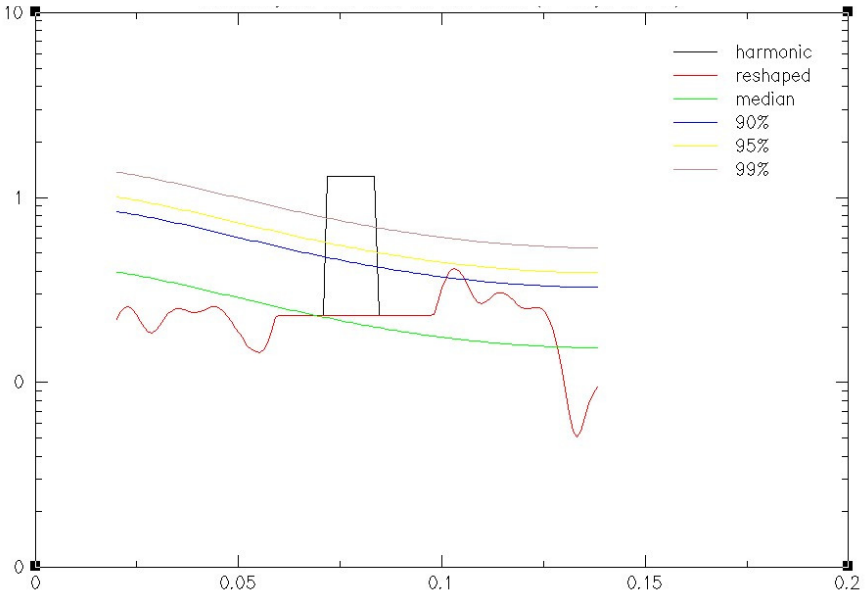

Figure 5.14: Spectral analysis (MTM, filtered), of the observed (HadISST) NINO 3.4 SST index.

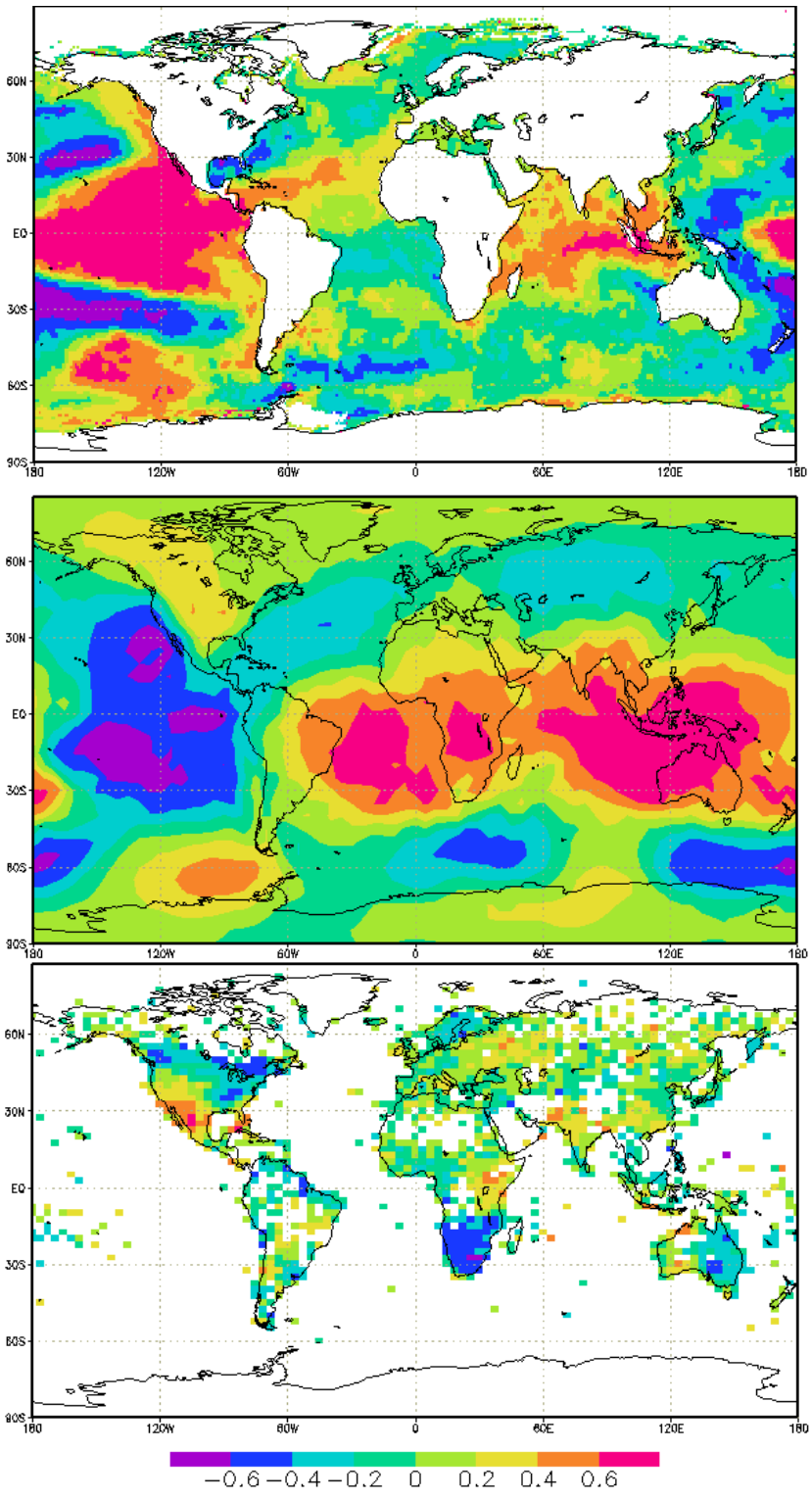

Figure 5.15: Correlation between the filtered (7-50 year) timeseries of observed (HadISST) NINO 3.4 SST index and similarly filtered global fields. Top: global SST; middle: global SLP; bottom: global rainfall.

The filtered NINO 3.4 timeseries exhibits harmonic quasi-decadal spectral power at ~12 yrs, and further variability at ~10 yrs (95% confidence). There is little evidence to suggest that there is any spectral power at lower frequencies (Figure 5.14). This partially agrees with the previous analysis of ENSO (e.g. Allan, 2000) which suggested that there was an interdecadal component to ENSO in the observed data.

Correlation analysis shows that the decadally filtered ENSO patterns are not substantially different from the interannual teleconnections (Figure 5.15). Both SLP and SST correlations are dominated by the Pacific basin, with further evidence of links to the southern hemisphere particularly noted in the SLP field. This correlation looks more like a decadally filtered version of the ENSO spatial pattern, rather than the North Pacific-focused Pacific Decadal Oscillation structure identified by Mantua et al. (1997). The positive SLP correlation to the tropical Indian and Atlantic Oceans supports the relationship with the tropical SWIO node described earlier, and the SST correlation in the Indian Ocean strongly resembles that allied to the tropical SWIO node.

Interestingly, there is no ENSO-based correlation with the South Atlantic, despite the strong response in the tropical Pacific to the South Atlantic SST index. This raises doubts about the role of ENSO in forcing South Atlantic SST variability, and perhaps strengthens the alternative hypotheses relating to the co-variability with SW Indian Ocean SST or cross-spectral relationship with SAFR rainfall. The rainfall response to the NINO index exhibits the east-west gradient that has characterised the observed rainfall at decadal scales, and shows a tendency for drying over southern Africa in common with the interannual ENSO variability (Nicholson & Kim, 1997).

This correlation and apparent relationship could be interpreted as the passive transmission of the ENSO signal via the tropical Indian Ocean (and Atlantic, to a lesser extent) to the African continent at decadal timescales. However, there are elements of SWIO variability not explained by the ENSO signal. This extends the work on the SW Indian Ocean (Washington & Preston, 2006) at interannual scales, and suggests that there is intrinsic non-ENSO variability in this region at decadal timescales, as well as the modulated ENSO signal.

The ENSO influence is difficult to untangle at interannual and decadal scales, and is complicated by the role of intrinsic variability in regions which display relationships with ENSO (especially the SW Indian Ocean). Correlation analysis with NINO 3.4 SST index shows evidence of a strong relationship with southern African rainfall at decadal timescales, and this influence appears to be exerted in a similar way to the interannual ENSO relationship (Tyson & Preston-Whyte, 2000).

It is not clear, however, how stable the ENSO teleconnection strength is (Richard et al., 2000; Mulenga et al., 2003), nor precisely to what extent ENSO is responsible for variability in locally important regions (e.g. tropical SWIO node, South Atlantic Ocean) when compared to the natural and localised variability of these areas. The role of decadal ENSO-like behaviour, in particular, is poorly understood. These areas remain of interest for prediction and understanding the decadal variability of the region, and are explored further in the model simulated climates which follow.

5. 1. 4 Summary

Acknowledging the limitations of the EOF technique in describing real world structures, analysis was conducted on the sub-continental scale to assess what variability is associated with decadal changes in southern African rainfall. The South Atlantic and South West Indian Oceans, together with the ENSO (NINO 3.4) SST variability were identified as likely candidates to drive rainfall variability.

Examination of the South Atlantic highlighted a range of potential issues related to technique-dependent results. A regional SST index isolated quasi-decadal variability with links to southern hemisphere-scale SST and SLP patterns, and associations with an east-west gradient in southern African rainfall. Comparison with EOF analysis showed this to be a reliable result, and was shown to be linked to local SST influences on the eastern (western) side of the sub-continent. Although the South Atlantic showed a relatively weak relationship, it is important to note that a South Atlantic influence on summer rainfall is not a common finding, and that most studies show the South Atlantic's dominance extends to the winter time shifts of the jet and mid-latitude storm track (Reason & Rouault, 2002) only.

Two potential explanations for the perceived influence of the South Atlantic during austral summer were proposed. One suggests that the South Atlantic has links to ENSO-like forcing at decadal timescales, evident in the SST correlation, and this relationship has coincident links to the southern African rainfall. The lack of reciprocal correlation in the ENSO-based analysis renders this explanation relatively unlikely. The second lies within the covariance of Atlantic and Indian Ocean basins, and a quasi-decadal teleconnection in

the SSTs linked to variability in Indian Ocean-led rainfall inspired by Hermes & Reason (2005)'s interannual studies. This is considered a far more likely explanation of the observed South Atlantic SST variability, and relationship with southern African rainfall.

Next, analysis of the South West Indian Ocean (SWIO) was performed. Identified as one of the key locations at interannual timescales, the SWIO is typically characterised by a dipole-like pattern in SSTs off the coast of Madagascar. Decadal filtering suggested that this was a less coherent spatial mode than at interannual scales. Although this dipole-like structure was obtained under non-rotated EOF analysis at decadal timescales, substantially reduced correlation at decadal timescales between the nodes of the dipole supported the conclusions of Washington & Preston (2006). Accordingly, the tropical and subtropical nodes of SWIO variability were examined separately. The isolated nodes showed a different response in rainfall and global teleconnection, with the tropical node linked to 10-12 yr variability associated with ENSO and a stronger link in regression and correlation to southern African rainfall, and the subtropical node showing evidence of southern hemisphere links described by the South Atlantic analysis.

The ENSO teleconnection was explored further using the NINO 3.4 SST index. Although not well understood, decadal ENSO-like variability was shown to retain a strong influence over southern Africa at quasi-decadal timescales, displaying significant harmonic spectral power at 10-12 yr periods. Links were shown between the NINO 3.4 SST and the tropical SWIO node, but it is not clear how decadal ENSO operates, and uncertainty remains in this area. Intrinsic stochastic variability and fluctuations in the strength of the NINO

teleconnection suggest that the SWIO region retains ENSO-independent features important to southern African rainfall at quasi-decadal timescales.

It is therefore suggested that a combination of forcing mechanisms from the oceanic regions influence southern African rainfall variability at decadal scale, most notably decadal ENSO-like teleconnections. It is likely that their relative importance changes over time and longer records may draw this variability out further than the twentieth century observations presented here. Coupled atmosphere ocean variability is thought to be the main driving force behind the rainfall changes, linked to SST variability in the nearby oceans.

The mechanisms do not appear to be qualitatively different from those which operate at interannual timescales, suggesting that it may be the integration and assimilation of interannual variability which generates decadal-scale variability, rather than any single underlying mechanism operating over a decadal time period (Vimont, 2007). This finding is a strong potential explanation of the decadal variability observed over southern Africa, and will be considered carefully in the model investigations which follow. This interaction and detailed examination of forcing structure and mechanisms cannot be completed under a limited array of observed data. The lack of diagnostic fields and the sparse record combine to provide an overview of potential mechanisms which may be revealed by investigation of the model runs in the next sections.

5.2 Simulated Variability in ECHO-G

To investigate potential associations of southern African rainfall variability at decadal scales further, analysis was conducted using climate models. ECHO-G offers distinct advantages compared to the observed data, with an extended spatial and temporal resolution (220 yrs) linked to full simulation of land and ocean fields giving the opportunity to diagnose some of the mechanisms of association more clearly. It is worth noting the different spectral characteristics of ENAT-simulated rainfall described in the previous chapter.

Correlation analysis is carried out between the timeseries of model-simulated southern African sub-continental rainfall (15-35ºS, 15-35ºE) and coupled atmosphere-ocean variables (global SST, global SLP) using filtered data (7-50 yr Kaiser band-pass filter, described previously). All data presented in this section is filtered using this method, unless specifically stated to the contrary. It is worth stating at the outset that despite the increased temporal coverage compared to the 1900-1998 CRU dataset, the correlations obtained in this analysis are generally weaker than those in the observed data. Figure 5.16 shows the correlation of the rainfall with the SST at decadal timescales. Regions of correlation are identified in the tropical Atlantic Ocean, together with the dipole pattern of the SW Indian Ocean described previously. The evidence presented by literature and analysis in the observed data section for the separation of SWIO 'nodes' is similarly employed in this section. Although the relationship between southern African rainfall and decadal ENSO-like variability is very weak, the spatial structures are similar to those identified in the observed data (Figure 5.2), particularly in the simulated SLP field.

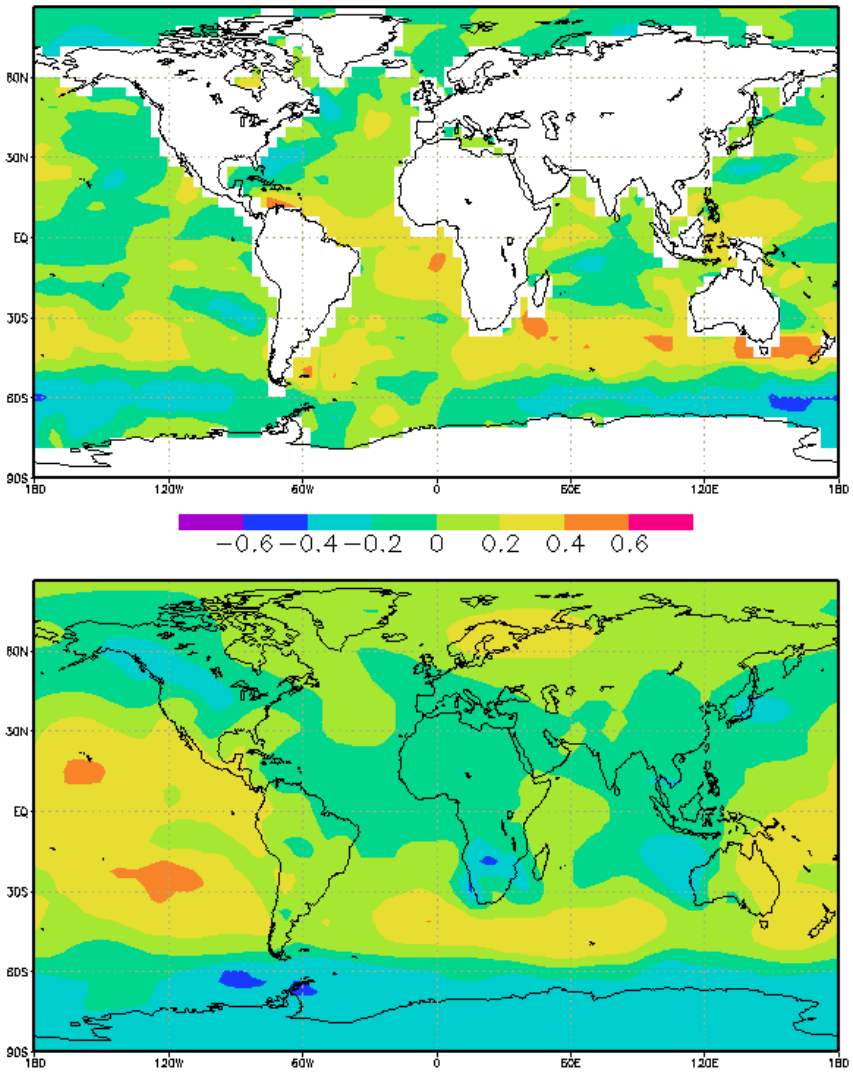

Figure 5.16: Correlation between the timeseries of filtered (7-50 year band pass) ECHO-G ENAT-simulated sub-continental rainfall (15-35ºS, 15-35ºE) and similarly filtered global fields. Top: SST, bottom: SLP

Correlation analysis shows the range of associated regions. Positive correlation with the sub-tropical SWIO (r=0.450) is stronger than the relationship with the tropical Atlantic (r=0.3496) and South Atlantic (r=0.3246) basins. A weak negative relationship with the tropical SWIO (r=-0.04857) supports the regression analysis. The stability and interaction of these relationships is explored further in analysis of each section, starting with the tropical Atlantic, before considering the South West Indian Ocean nodes. Finally, the role of large scale global teleconnections is evaluated, and summarises the proposed mechanisms simulated by ECHO-G.

5. 2. 1 Tropical Atlantic

The tropical Atlantic Ocean shows one of the strongest correlations with southern African rainfall (r=0.3496), and the index of the tropical Atlantic region (10°S-10°N, 60-0°W) also shows evidence of a relationship with ENSO-like circulation (defined using the NINO 3.4 SST index), with similar correlation strength (r=0.362). Spectral analysis of the regional index shows no quasi-decadal power (MTM analysis not shown), although the unfiltered spectrum (not shown) shows evidence of 2-4 year spectral power.

Spatial correlation analysis based on the regional index supports these correlations. Dominated by the auto-correlation with the tropical Atlantic region, the SST field also shows evidence of correlation with tropical Pacific and Indian Ocean SSTs (Figure 5.17). Local SLP correlation shows no clear link to circulation features associated with southern African rainfall variability, despite a positive correlation mapped in rainfall correlation. There is little evidence of ENSO-like structures in either SLP or SST correlation, despite

the correlation with the tropical Pacific. It is interesting to note the decadal correlation link with aspects of Australian rainfall, previously identified in the literature as an area of decadal variability (Power et al., 1999a; Power et al., 1999b).

Running correlation (constructed with a 50 yr window) between southern African rainfall and the tropical Atlantic region index exhibits considerable variability in magnitude and sign of correlation (Figure 5.18). The strong positive (r=0.6-0.8) in the early part of the record transitions through a weak correlation period before altering sign to a strong negative relationship (r=-0.6). The period of highest correlation (first 60 years) is coincident with the period of strongest decadal variability identified in Figure 4.12. The tropical Atlantic remains something of an enigma in regard to southern African rainfall. The region was not identified as important in the observed data, and it is possible that the relationship of the region with tropical Pacific variability in the model has resulted in a correlation with southern Africa despite ECHO-G's known poor ENSO simulation. This will be investigated further in analysis of the NINO 3.4 region.

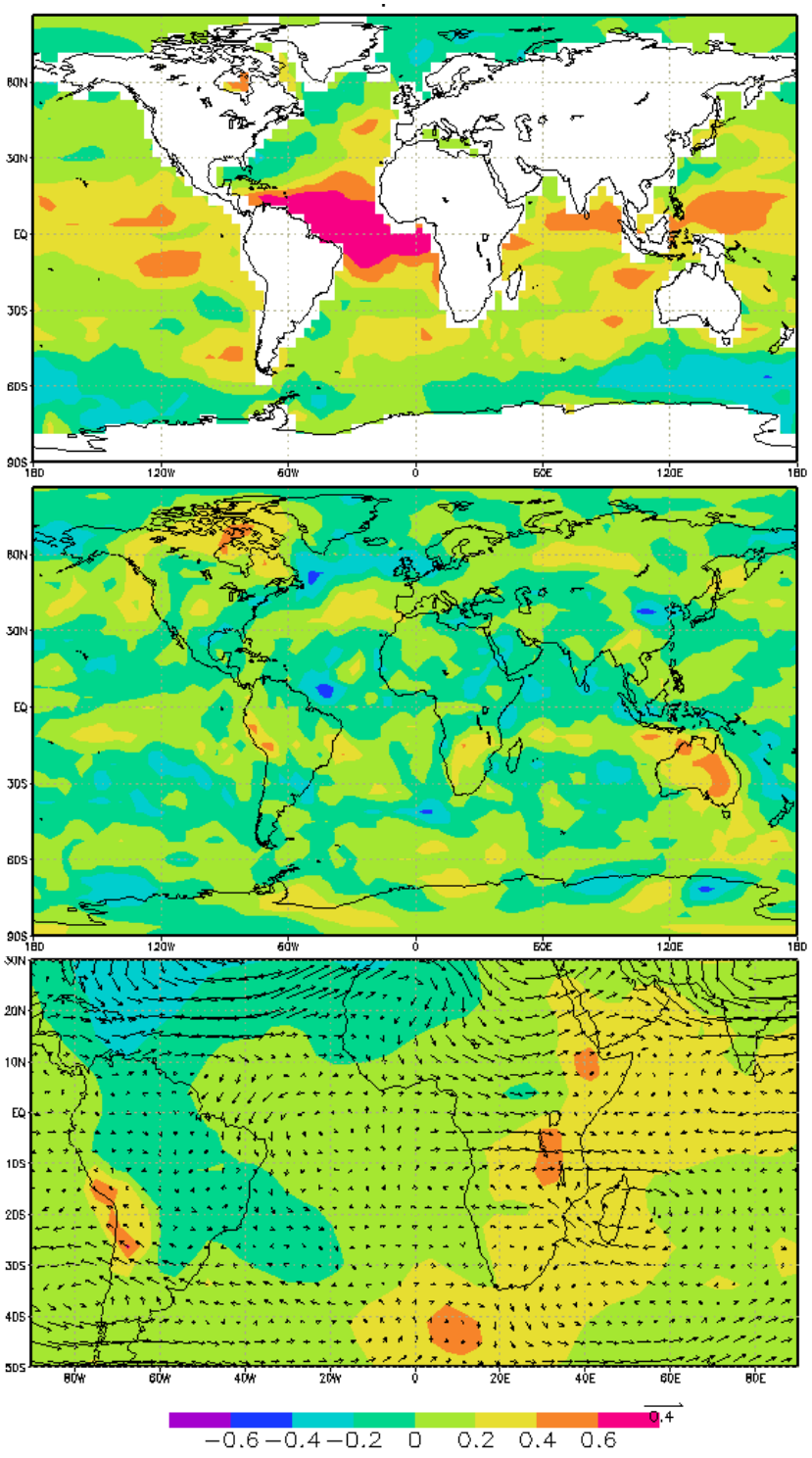

Figure 5.17: Correlation between the timeseries of ECHO-G ENAT-simulated tropical Atlantic SST index and global fields, filtered with a 7-50 year band pass. Top: global SST; middle: global rainfall; bottom: local SLP, with an overlay of 500hPa wind anomalies generated by regression on a 2σ rainfall anomaly. The wind vector scale is equivalent to 0.4 m/s

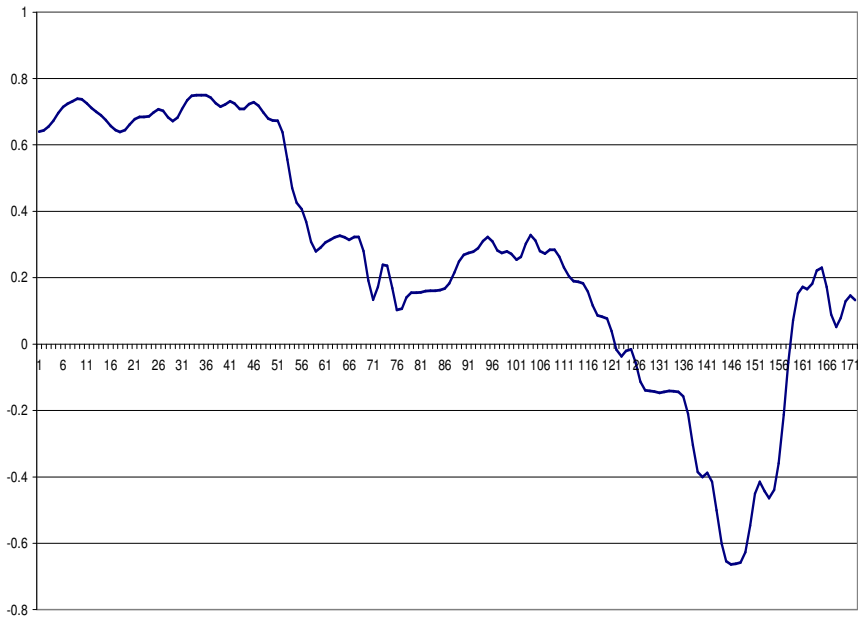

Figure 5.18: Running correlations (constructed using a 50 year correlation window) between ECHO-G ENAT-simulated southern African rainfall and the index of tropical Atlantic SST. The rainfall data and SST index are filtered using a 7-50 yr band pass filter.

5. 2. 2 South West Indian Ocean

In both interannual data (Washington & Preston, 2006) and quasi-decadal observed data, the SW Indian Ocean 'dipole' tropical and subtropical nodes behave differently with respect to southern African rainfall. In ECHO-G, at decadally filtered timescales, the nodes have minimal correlation (r=-0.0646) despite their stronger relationship at unfiltered timescales (r=-0.224). This lack of cohesion is a likely explanation for their disparity in correlation with SAFR rainfall (tropical node: r=-0.068; subtropical node: r=0.45). This section will investigate the relationships associated with these nodes in order to assess their relative influence on southern African rainfall at quasi-decadal timescales.

Tropical SWIO

Unlike the observed data, the tropical SWIO node appears through correlation and regression analysis to be the weaker of the two SWIO terms. Spectral analysis of the SST index over the region (5-10°S, 60-80°E, as defined by Washington & Preston, 2006) shows an absence of quasi-decadal spectral power (Figure 5.20), although the centennial scale peak is shown with some confidence in agreement with other unfiltered ECHO-G spectral analyses. Correlation analysis using the tropical SWIO SST index (Figure 5.19) shows a coherent response across the tropical Indian and Pacific Oceans, and a suggested anti-correlation south of 10°S in the tropical Atlantic. This seems to be linked to ENSO-like variability, but shows minimal influence over southern African rainfall.

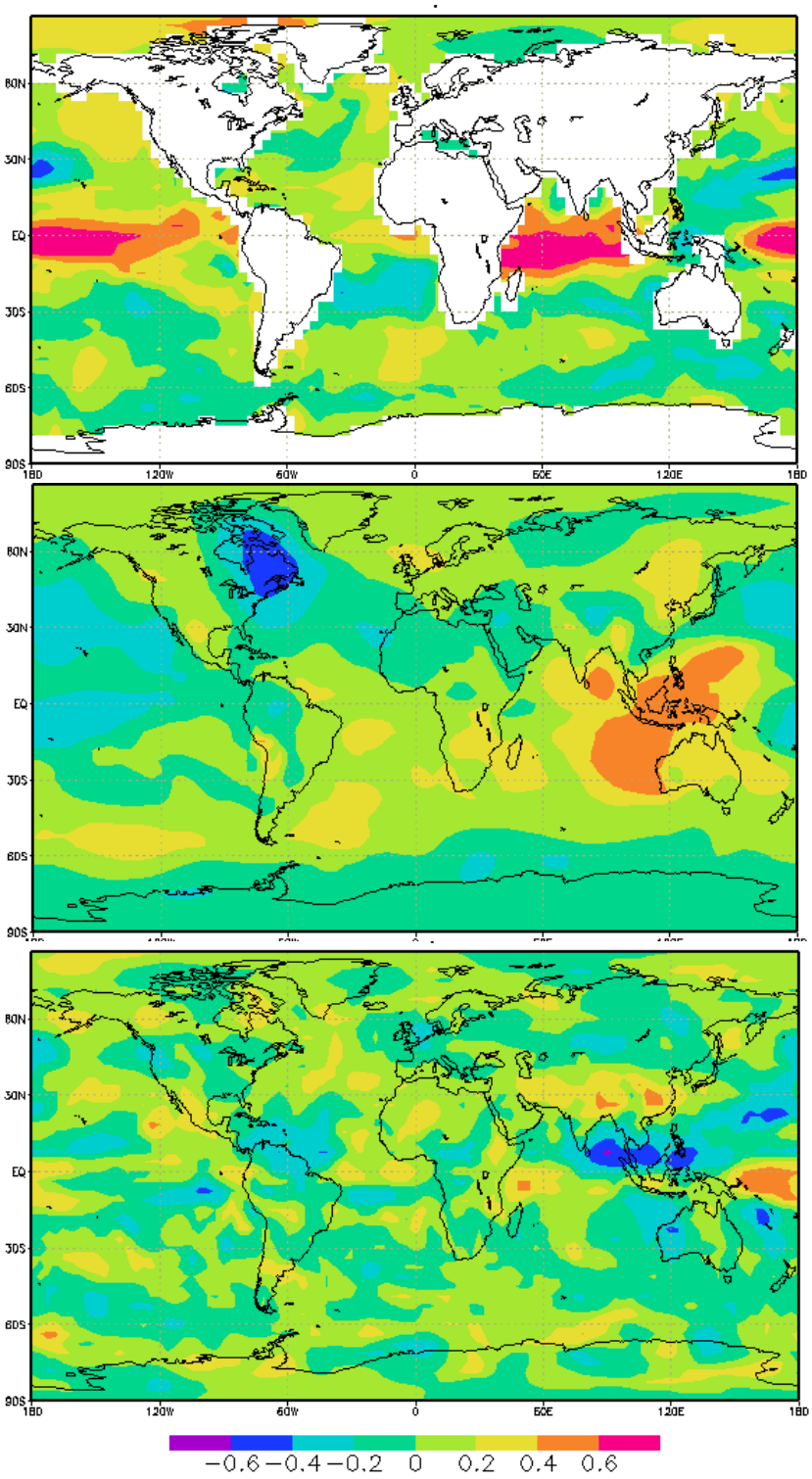

Figure 5.19: Correlation between the timeseries of ECHO-G ENAT-simulated tropical SW Indian Ocean SST index and global fields, filtered using a 7-50 year band pass. Top: global SST, middle: global SLP, bottom: global rainfall.

Correlation with global SLP suggests a link to Pacific ENSO-type variability, displaying a coherent region of positive correlation over the maritime continent ("atmospheric bridge") region, extending in to the subtropical east Indian Ocean. Global rainfall correlation is strongest in the same region, lending further support to the hypothesis proposed for the tropical SWIO in the observed data relating the tropical Indian Ocean to ENSO teleconnections. The direct rainfall response over southern Africa is minimal, but shows symptoms of a NW-SE alignment, unlike the tropical and South Atlantic correlations.

Running correlation (constructed with a 50 yr window) suggests that the long term correlation may not be stable. Large (centennial) scale variability is observed in the record, ranging from r=-0.4 (first 6 yrs) through to r=0.685 (105 yrs) before returning to more muted negative correlation towards the end of the record. The correlation links between the tropical SWIO SST and ENSO-like variability are explored further. Demonstrating the highest correlation (r=0.695) of all variables, NINO 3.4 variability explains 48.1% of the tropical SWIO SST variance. The relationship between these variables is also shown to be coherent in exerting influence over southern African rainfall variability. Figure 5.21 shows the running correlation between rainfall and NINO 3.4 and tropical SWIO SST indexes. The change in sign, and the reversed relationship it represents, is not clearly understood at this stage.

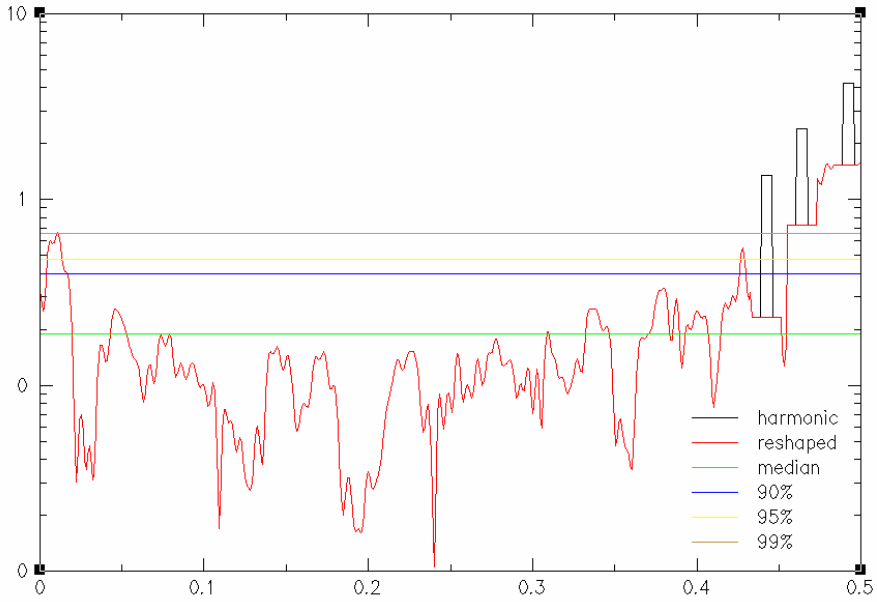

Figure 5.20: Spectral analysis (MTM, unfiltered) of ECHO-G ENAT-simulated tropical SW Indian Ocean SST (5-10ºS, 60-80ºE).

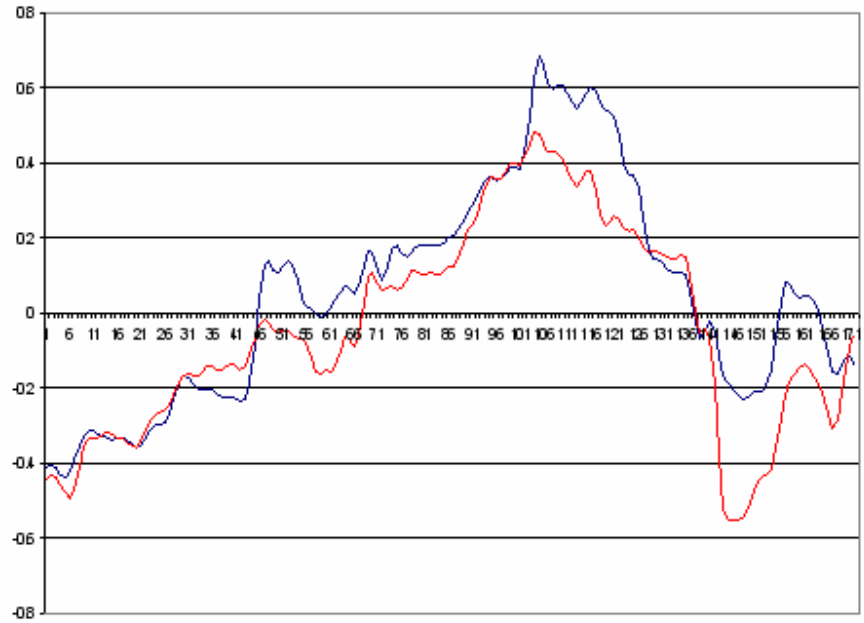

Figure 5.21: Running correlation between ECHO-G ENAT rainfall over southern Africa (15-35ºS, 15-35ºE) and (i) tropical SW Indian Ocean SST index (blue line) and (ii) NINO 3.4 SST index (red line). All indexes are filtered (7-50 yr BP) and examined through a 50 yr correlation window.

The relationship between the tropical SWIO and decadal ENSO-like behaviour has been identified at quasi-decadal timescales in both observed and modelled data, suggesting that it is not a data-specific result. Although there is clearly evidence for independent Indian Ocean variability in aspects of climate (e.g. Saji et al., 1999), the evidence here suggests that the behaviour of ENSO is important in determining the impact of the tropical SWIO on southern African rainfall, and the role of ENSO is examined separately.

Sub-tropical SWIO

By comparison, the subtropical region of the SWIO (defined as 30-35°S, 40-60°E) explains more of the variability in southern African rainfall at decadally filtered timescales, with up to 20% of the variance explained. Spectral analysis (Figure 5.23) shows power at quasi-decadal scales, with peaks at ~25 yrs (95% confidence) and between 7-9 years (95% confidence). The ~25 year peak in this region is the closest link to the spectral power identified in the sub-continental rainfall in Section 4. 2. 1.

As in the observed data, the correlation analysis shows a relationship between SWIO subtropical SST and South Atlantic SST (r=0.636), as well as a mid-latitude band in the South Pacific (Figure 5.22). Global SLP correlation (figure not shown) qualitatively resembles a southern hemisphere-wide pattern, not unlike the SAM. This is locally evident – as in the South Atlantic SST analysis – as anomalous pressure centres in the South Atlantic and SW Indian Ocean, with a negative pressure trough over southern Africa in a moisture-bearing circulation pattern. The rainfall appears to respond over the sub-continent, as well as in a band centred on 45°S and across the East Indian Ocean in to continental Australia.

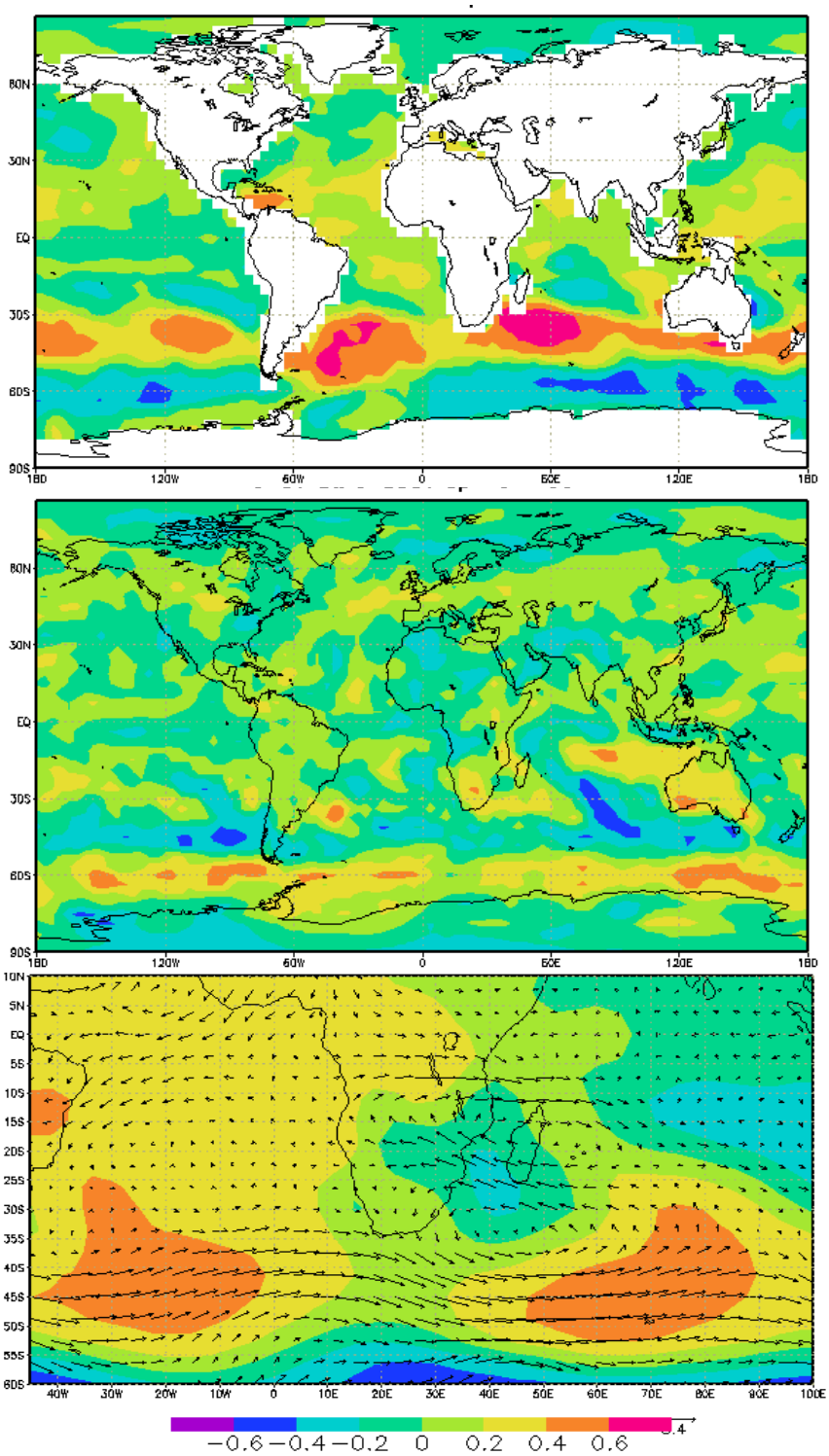

Figure 5.22: Correlation between the timeseries of ECHO-G ENAT-simulated subtropical SW Indian Ocean SST index and global fields, filtered using a 7-50 year band pass filter. Top: global SST; middle: rainfall; bottom: local SLP with an overlay of 500hPa wind anomalies generated by regression on a 2σ rainfall anomaly. The scale of the wind vector is 0.4 m/s

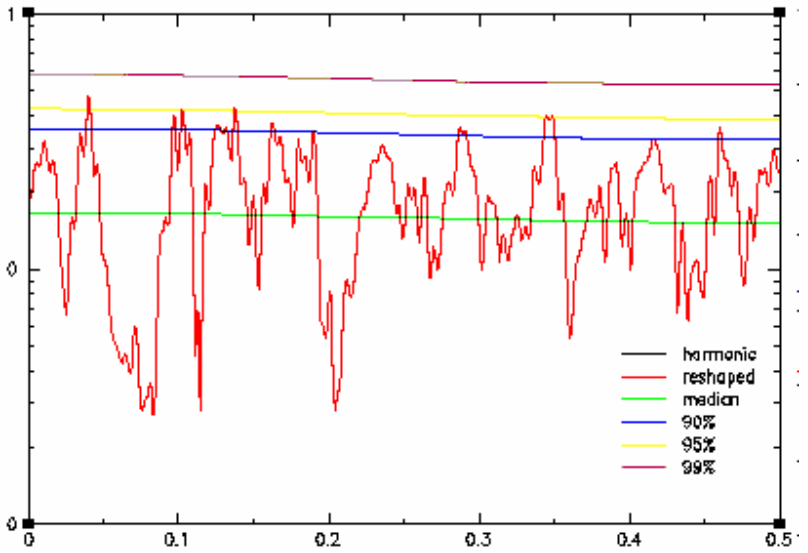

Figure 5.23: Spectral analysis (MTM, unfiltered) of ECHO-G ENAT-simulated sub-tropical SW Indian Ocean SST (30-35ºS, 40-60ºE).

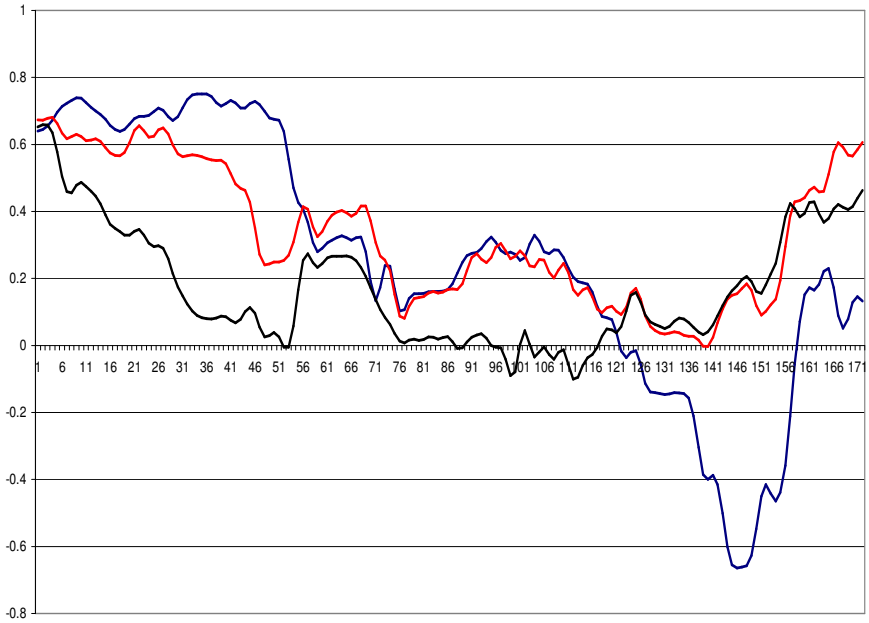

Figure 5.24: Running correlation between the timeseries of ECHO-G ENAT southern African rainfall (15-35ºS, 15-35ºE) and: (i) tropical Atlantic SST index (blue line); (ii) South Atlantic SST index (black line), and (iii) subtropical SW Indian Ocean SST index (red line). All indexes are filtered at 7-50 yr band pass, and examined through a 50 yr correlation window.

The cross-spectral links at ~25 years, together with the rainfall response in correlation analysis suggests that the subtropical SWIO is the most significant teleconnection for southern African rainfall at decadal scales. It is thought likely that the mechanism of rainfall variability operates in a similar mechanism outlined in Chapter (1), and modifies the basic circulation state in a manner consistent with Figure 1.4.

Further investigation supports the hypothesis linking the SWIO subtropical mode to the south Atlantic basin. Figure 5.24 shows the running correlation (constructed with a 50 yr window) between decadal SAFR rainfall and key SST index regions. The covariance of these regions exhibits distinct 'phases' – the general weakening trend in the first 56 yrs is marked by some spread in the correlation with rainfall. Between 56-76 yrs, the range of all three correlations is reduced, before different interactions are demonstrated. First, there is coherent variability in tropical Atlantic and SWIO subtropical rainfall correlation (76-120 yrs; r=0.9185) while the south Atlantic is weakly correlated with rainfall. Next, the south Atlantic and SWIO subtropical undergo a period of coherence (120-180 yrs, r=0.954) while the tropical Atlantic is anti-correlated.

This lends further support to the hypothesis of a shared atmospheric driving mechanism between Atlantic and subtropical Indian Oceans (Hermes & Reason, 2005). The spatial correlation patterns related to both tropical Atlantic and subtropical SWIO qualitatively resemble the Southern Annular mode, and this is explored in the next section on global teleconnections.

5. 2. 3 Global Teleconnections

Two large-scale patterns have been identified as potentially playing a role in regional variability in ECHO-G ENAT simulated southern African quasi-decadal rainfall variability. ENSO-like behaviour has been found in the observed data at quasi-decadal scales, and forms the first part of this section's investigation in to the global scale teleconnections. Second, the role of the Southern Annular Mode is examined at decadal scales in relation to the apparent influence it exerts over the mid-latitude southern hemisphere circulation. Detailed mechanistic explanations of what drives these phenomena at quasi-decadal timescales are beyond the scope of this thesis – this section aims to understand their role in modulating the surrounding oceans in order to establish their relevance to decadal scale rainfall variability in southern Africa, and draw together the principal evidence outlined previously in this section.

El Nino-Southern Oscillation (ENSO)

The NINO 3.4 SST index region (defined as 5°N-5°S, 170-120°W) is extracted and filtered in the same method as the observed data. Spectral analysis of the full (unfiltered) index shows very little evidence of any low-frequency spectral power (Figure 5.25). The only peaks of any significance lie within the 2-2.3 year spectral range, consistent with the spectrum of the tropical SWIO SST index. This is consistent with the reportedly poor simulation of ENSO by ECHO-G (Guilyardi et al., 2004).

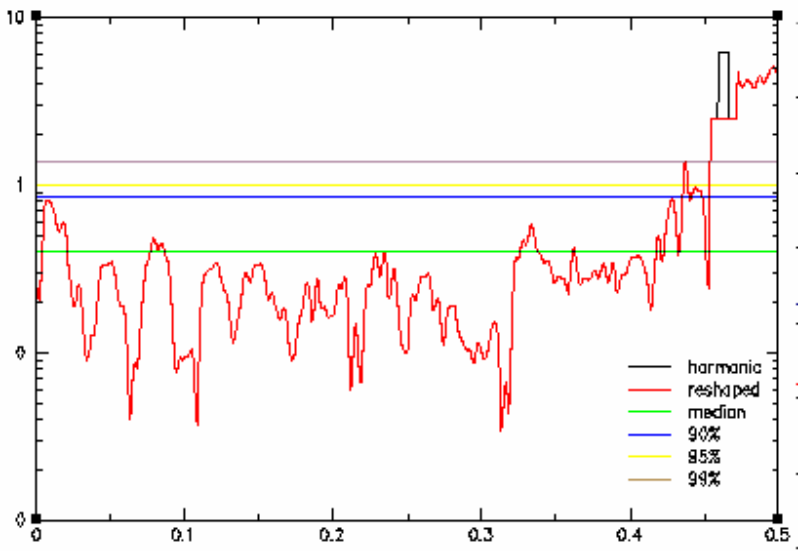

Figure 5.25: Spectral analysis (MTM, unfiltered) of ECHO-G ENAT-simulated NINO 3.4 SST index.

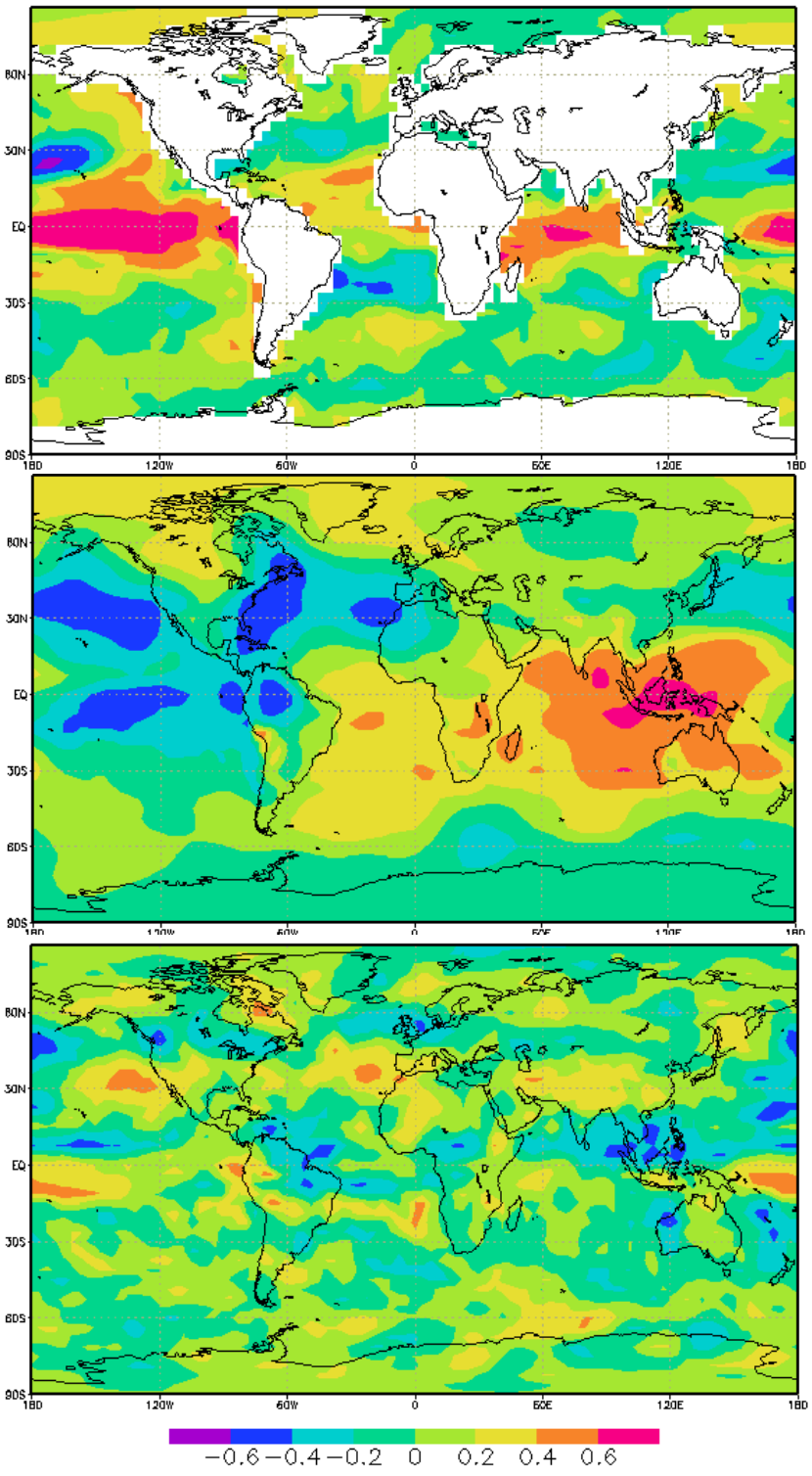

Figure 5.26: Correlation between the timeseries of ECHO-G ENAT-simulated NINO 3.4 SST index and global fields, filtered using a 7-50 year band pass filter. Top: global SST, middle, global SLP, bottom: global rainfall.

Direct correlation analysis based on the filtered NINO index shows spatial patterns in global SST and SLP in line with the expected behaviour of ENSO at interannual timescales (Figure 5.26). A dipole pattern in the tropical Pacific SST links coherently with the east-west Pacific SLP gradient.

The positive correlation in SLP over the maritime continent (centred on 120°E) is likely to invoke the atmospheric bridge mechanism (Lau & Nath, 1996; Alexander et al., 2002; Liu & Alexander, 2007) to explain the tropical Indian Ocean response. A similar mechanism may be proposed to explain the negative correlation in the Caribbean and eastern coast of the North American continent and the links to the tropical Atlantic. There is little response in either SLP or SST correlation in the southern hemisphere mid-high latitudes, leaving scope for exploration of the Southern Annular Mode's influence in this region.

The rainfall correlation is noisy, and the southern African region is weakly correlated in an east-west gradient. This is a less coherent response than the previous observed data at decadal timescales. This minimal influence is echoed in the weak correlation (SAFR rainfall-NINO3.4 SST, r=-0.04857), but needed to be explored given the correlation to Pacific Ocean structures.

Unlike the observed interannual relationship with ENSO, southern African rainfall appears to have little relationship with the NINO 3.4 index in the decadal simulation of ECHO-G. It is probable that the negligible low-frequency spectral power in the NINO 3.4 index contributes significantly to the absence of ENSO's influence at quasi-decadal time scales, and the observed data suggests that this could be a model-specific result. This hypothesis can be tested with the simulations of HadCM3, although an ensemble of models should

ideally be employed to better understand the spectral nature of ENSO-like simulations at decadal timescales. Intercomparison studies at interannual (and 2-7 year) timescales have previously demonstrated that ENSO is not well simulated by ECHO-G, and this result suggests that there is very little evidence of decadal ENSO-like variability either. The contrast with observed results presented previously raises the need to test this as a model-specific result, and this will be addressed more clearly in the simulations of HadCM3.

Southern Annular Mode (SAM)

The muted role of ENSO in modulating more than the tropical Indian Ocean contrasts with the observed quasi-decadal results, and appears linked to the augmented role of the Southern Annular Mode in ECHO-G. This section investigates the role of the SAM in more detail, and explores the potential links to southern African rainfall.

The SAM (also known as Antarctic Oscillation) is characterised by pressure anomalies of one sign centred in the Antarctic, and anomalies of the opposite sign centred between 40-50°S. Typically defined as the leading principal component of 850hPa geopotential height anomaly south of 20°S (Thompson & Wallace, 2000), the study is limited by lack of access to this simulated field. Therefore, an earlier definition – the difference of zonal mean pressure between 45° and 65°S is employed (Gong & Wang, 1999) to extract an index of SAM for the ECHO-G simulation.

Positive correlation (r=0.325) suggests that there is some influence from the SAM in explaining SAFR rainfall from this region. As described in the previous ENSO section, it seems probable that the influence is exerted through the modulation of the mid-latitude circulation.

First, the direct influence of the SAM is examined. Individual regression analysis shows that only 10% of SAFR rainfall variance is explained directly. Spectral analysis of the SAM index, however, shows decadal and quasi-decadal power (Figure 5.27). Peaks at 8.06 yrs (95% confidence) and 24.8 yrs (90% confidence) support the potential for the region to operate at low-frequency timescales. This spectral power corresponds to similar power identified in the South Atlantic (not shown) and SW Indian Ocean (Figure 5.23) indexes, as well as power identified in the sub-continental rainfall in the previous chapter.

Examination of the spatial correlation (Figure 5.28) presents a coherent mid-latitude response in all fields. The SLP correlation is dominated by latitudinal banding, with particularly strong correlation over the southern oceans and the subtropical Atlantic. This is echoed in the SST correlation, which mirrors key features of the previous subtropical SWIO analysis, including the location and strength of the South Atlantic SST anomaly and SWIO "dipole". The more extensive SST response south of Australia is likely to explain the relationship observed over the Australasian continent in the rainfall analysis and banding centred on 60°S. There is an interesting NW-SE aligned response in rainfall over southern Africa itself, with positive and negative correlation regions potentially explaining the net weaker correlation displayed by the long-term sub-continental indexes.

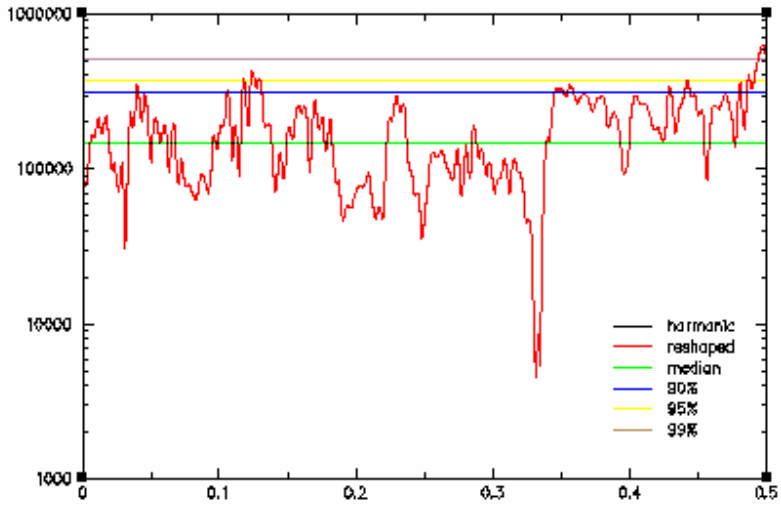

Figure 5.27: Spectral analysis (MTM, unfiltered) of ECHO-G ENAT-simulated Southern Annular Mode index.

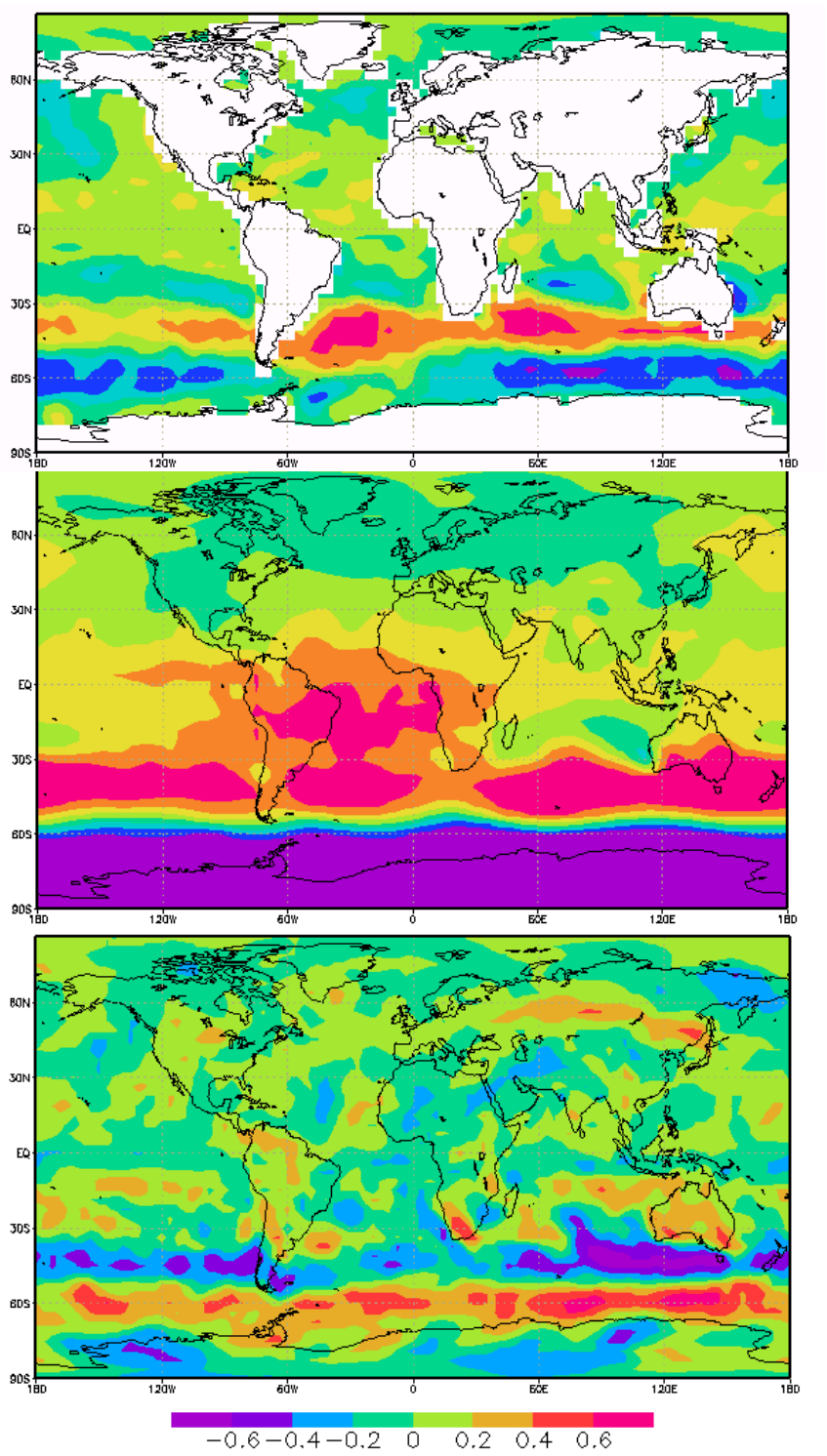

Figure 5.28: Correlation between the timeseries of ECHO-G ENAT-simulated Southern Annular Mode and global fields, filtered using a 7-50 year band pass filter. Top: global SST, middle; global SLP, bottom: global rainfall.

Second, the modulating influence of the SAM presents a convincing argument for a strong relationship in ECHO-G between the SAM and South Atlantic (r=0.588, 34% of variance explained) and the subtropical SWIO (r=0.662, 49% of variance explained). The strength of this relationship helps to explain the co-variance of the South Atlantic and SWIO subtropical regions relative to the ENAT rainfall and associated variability in circulation, and is presented as a convincing explanation for the 'atmospheric driven variability' that Hermes and Reason (2005) described as uniting the two ocean regions. It seems likely that – as with ENSO – the primary influence is not by direct action but through the modulation of locally important teleconnections.

SAM variability has previously been established at the interannual scale in reanalysis data (Gillett et al., 2006) and climate models (Gupta & England, 2006), showing precipitation changes during the positive phase of the SAM along the eastern coast of southern Africa. This is likely to be linked to anomalous easterly winds and the advection of moisture (Reason & Rouault, 2005), but is also associated with increased geopotential height, decreased cloudiness (Gupta & England, 2006) and a southward shift in the storm track away from the mid-latitudes (Karoly, 2003; Gupta & England, 2006). It is not clear from Gillett et al. (2006)'s analysis what seasons are involved: it is suggested that although both Antarctic mainland cooling and the Peninsula warming are largest in austral winter, the correlation with the SAM mode in austral summer provided the strongest link (Marshall, 2007).

Although limited in scope, these studies show that the SAM is a viable mechanism for the modulation of southern latitude climates, and therefore can be considered a plausible

explanation for the variability observed in ECHO-G's simulation. Work on the longer term variability of this index region has been previously hampered by latitude-related problems in reanalysis data, together with an abbreviated record from which to derive meaningful spectral analysis. The interested reader is referred to Gillett et al. (2006)'s discussion of the problems faced by generating SAM data for more detail.

The importance of the SAM is likely to be inversely proportional to the influence of ENSO in coupled simulations – the significant absence of correlation in the mid-latitude regions with the NINO 3.4 SST index happens to coincide with the key latitudes for the SAM. It is therefore not clear how these large-scale patterns interact, and whether the "weaker" quasi-decadal simulation of ENSO artificially enhances the perceived role of the SAM in ECHO-G, or if the SAM is simply a more robust signal in ECHO-G. This hypothesis remains to be tested. Some evidence may be provided using HadCM3's simulations, but it would require further investigation in multiple climate models to draw more reliable conclusions.

5. 2. 4 ECHO-G Simulation Summary

Several regions have been identified as demonstrating a correlation-based relationship with southern African rainfall at quasi-decadal timescales. It should be noted that this analysis is based on the ENAT simulation – the naturally forced ECHO-G simulation, with no control run available. It is unclear to what extent this behaviour is driven by the natural forcings or symptomatic of the underlying intrinsic ocean-atmosphere variability generated by the model: this can be tested with the CTR/NAT simulations of HadCM3. The suggested regions differ slightly from the results presented in the observed data, and therefore present a series of questions to be answered in the investigation of HadCM3.

First, the tropical Atlantic Ocean was identified as a region of correlation, but showed no obvious mechanisms of influencing southern African rainfall, and little evidence of quasi-decadal variability. It seems likely that the relationship between the tropical Atlantic Ocean and more influential regions is the most plausible explanation for this region's apparent correlation.

One of these relationships is thought to link the tropical Atlantic with the tropical Indian Ocean. As in the previous observed data section, there is justification for splitting the SW Indian Ocean "dipole" in to separate tropical and sub-tropical regions for analysis, and the tropical Indian Ocean shows strong links to ENSO-like variability and other tropical ocean regions.

Exploration of the NINO 3.4 SST index – representing ENSO's influence – showed little quasi-decadal variability, and is proposed as one hypothesis to explain the relative

weakness of ENSO-forced regions in influencing southern African rainfall in ECHO-G. Since the ECHO-G simulation is forced by "natural" variability, it is not clear if this simulation of ENSO is a model-specific (or simulation-specific) result, and this will be tested further in examination of HadCM3 and the anthropogenically-forced simulations.

Unlike the correlation-based relationship identified in the observed data, the sub-tropical mode of SW Indian Ocean SST variability was shown to be more important to southern African decadal rainfall than the tropical mode in ENAT. Variability in the subtropical circulation – similar to the interannual mechanisms of rainfall variability – provides a link to rainfall, and this was linked to co-varying signals in both South Atlantic and SW Indian Ocean. Analysis suggests that these regions are driven by a similar atmospheric forcing (Hermes & Reason, 2005). This forcing mechanism was suggested to relate to the Southern Annular Mode, giving new scope to the work of Hermes & Reason (2005) at decadal scales in ECHO-G.

Spectral examination of the SAM showed significant quasi-decadal variability which plausibly explained similar spectral peaks in the South Atlantic and subtropical SWIO. Analysis of the 500 hPa winds showed anomalous flow in the mid-latitude winds, thought to influence the development of anomalous SLP patterns in the oceans and over the subcontinent in a rain-bearing pattern.

Unlike the observed data, ECHO-G's decadal scale rainfall appears to be dominated by this SAM-driven variability and shows less inclination to respond to ENSO forcing. It is not clear whether this is a model-specific association, a result of natural forcing or a

response to a modelled ENSO which is notable for absence of any low-frequency variability (Guilyardi et al., 2004; Guilyardi, 2006).

Further investigation could test the model's response to idealised NINO forcing, with quantified decadal variability, to establish whether the weakness lies within the nature of the model response, or in the simulation of quasi-decadal ENSO-like behaviour under natural forcing. Comparison with HadCM3's NINO index will be made to establish whether climate models are capable of generated decadal-scale ENSO-like signals, and how this influences the regional forcing of rainfall variability. The addition of the CTR simulation in HadCM3 will help to identify whether the reversed SWIO SST influence, and links to ENSO and SAM are intrinsic to the model, or as a result of natural forcing.

Much like the observed data, the quasi-decadal variability operates in a manner consistent with interannual variability – using similar mechanisms and locations of potential influence. This supports the integration theory (Vimont, 2007), suggesting that the decadal variance reflects the interannual and multi-annual variability, identified in the observed data. This reduces the probability that this is a data-specific result, and provides an interesting point of reference from which to examine simulated decadal rainfall variability in HadCM3.

5.3 Simulated Variability in HadCM3

Examination of HadCM3 allows the extension of the available record beyond the 220 yrs of ECHO-G, and offers the addition of 850hPa wind data to the investigation. This section aims to develop the results obtained using ECHO-G, and test some of the hypotheses posed in analysis of the results to better understand simulated rainfall variability at decadal time scales.

To begin, correlation analysis is carried out between the southern African sub-continental rainfall and coupled atmosphere-ocean variables using filtered data from HadCM3. The unfiltered correlation analysis (not shown) agrees with both the degree and key locations of correlations identified in the observations, and confirms that the surrounding ocean regions are a logical starting point to examine potential mechanisms (Mason, 1995; Jury et al., 2004).

The decadal correlation is obtained using a 7-50 year band pass Kaiser filter, described previously. All data described here should be interpreted as filtered using this method, unless specifically described otherwise. There is evidence of influence in two regions of the Atlantic; with a tropical Atlantic dipole, and a further region of correlation in the South Atlantic at approximately 40°S (Figure 5.29). There are also areas of correlation with the South Pacific and Tasman Sea regions, suggesting a potential southern hemisphere relationship.

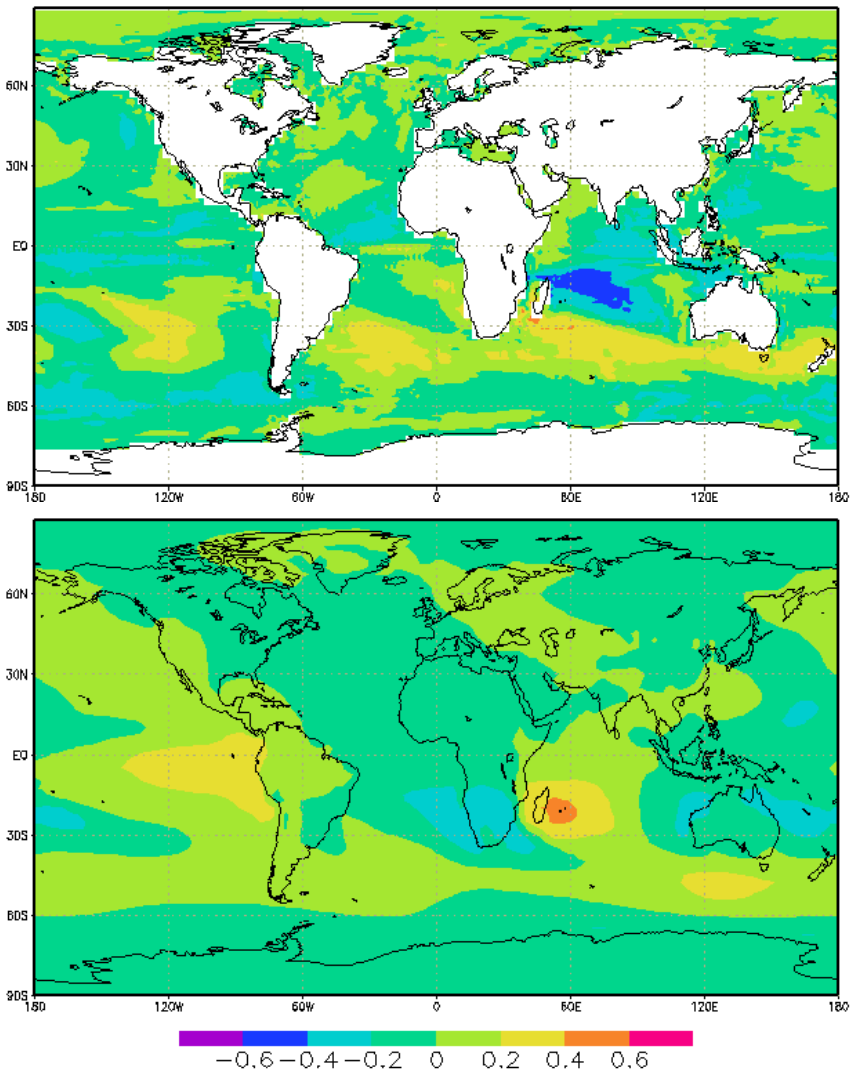

Figure 5.29: Correlation between the timeseries of HadCM3 CTR-simulated sub-continental (15-35ºS, 15-35ºE) southern African precipitation and global fields, filtered using a 7-50 year band pass filter. Top: global SST; bottom: global SLP

Correlation between rainfall and SLP at decadal timescales also shows a positive relationship with the Mascarene high pressure region (centred at about 55°E, 20°S), together with a negative loading over the subcontinent in the NW-SE orientation of previous chapters, extending west out in to the South Atlantic, and limited by the Equator to the north. There is further evidence of large-scale patterns in variability, including El Nino-like patterns in the Pacific Ocean, and agreement with the SST-based suggestion of hemisphere scale patterns in the Southern Oceans.

Many of these regions of correlation correspond with the regions identified in the observations and previous model studies as influencing southern African precipitation, and will form the basis of the investigation of mechanisms in HadCM3's simulation of decadal variability.

It should be noted at the outset that the analysis presented in this chapter is predominantly taken from the control simulation of HadCM3. Despite the slightly damped spectral response shown in the previous chapter, there is broad agreement between some regions of the CTR and NAT simulations. These areas are described in this chapter, and may be taken to represent potential mechanisms of model variability under control and natural forcing conditions: suggesting that although the spectral nature of the variability in these regions may be changed by the addition of natural forcing, the underlying mechanisms remain similar. However, there are other SST regions where the CTR and NAT simulations differ considerably. Since the NAT response is qualitatively aligned with the ALL simulated variability, these regions are described in the next chapter which covers the impact of forcing in more detail.

5. 3. 1 Tropical Atlantic Dipole

The relationship between southern African rainfall and the tropical Atlantic dipole is one of the key differences between unfiltered and decadally-filtered correlation maps (not shown) in both CTR and NAT simulations. The area was not identified as linked to southern African rainfall in the observed data, and the ECHO-G data reflected a monopole structure over the domain. The correlation between southern African rainfall and global rainfall and SST in HadCM3 (Figure 5.30) show a coherent dipole likely to reflect shifts in the ITCZ, with a narrower band pass filter (7-25 years) removing the potential low frequency influences of the Atlantic Multidecadal Oscillation (Knight et al., 2005; 2006) and isolating the quasi-decadal spectral band.

EOF analysis is performed over the domain 20°S-20°N, 60°W-20°E following Knight et al. (2005) methods. The leading EOF modes are similar to the work of Knight et al., and are consistent through filtering at decadal frequencies (7-50 yr band pass). Precipitation EOF 1 describes a lateral dipole which bears strong resemblance to the structure of the ITCZ (Figure 5.31), while the leading SST EOF describes a cross-equatorial dipole with basin-wide coverage. MTM analysis (not shown) of both leading modes shows decadal scale influences, with a significant ~35 year peak occurring in both spectra.

Correlation between the leading EOF of precipitation and global SST (Figure 5.32) shows an SST dipole in the tropical Atlantic that strongly resembles the leading EOF of SST. Correlation analysis using the leading mode of SST suggests a localised relationship that extends to NE Brazil rainfall, and influences over the western coast of southern Africa.

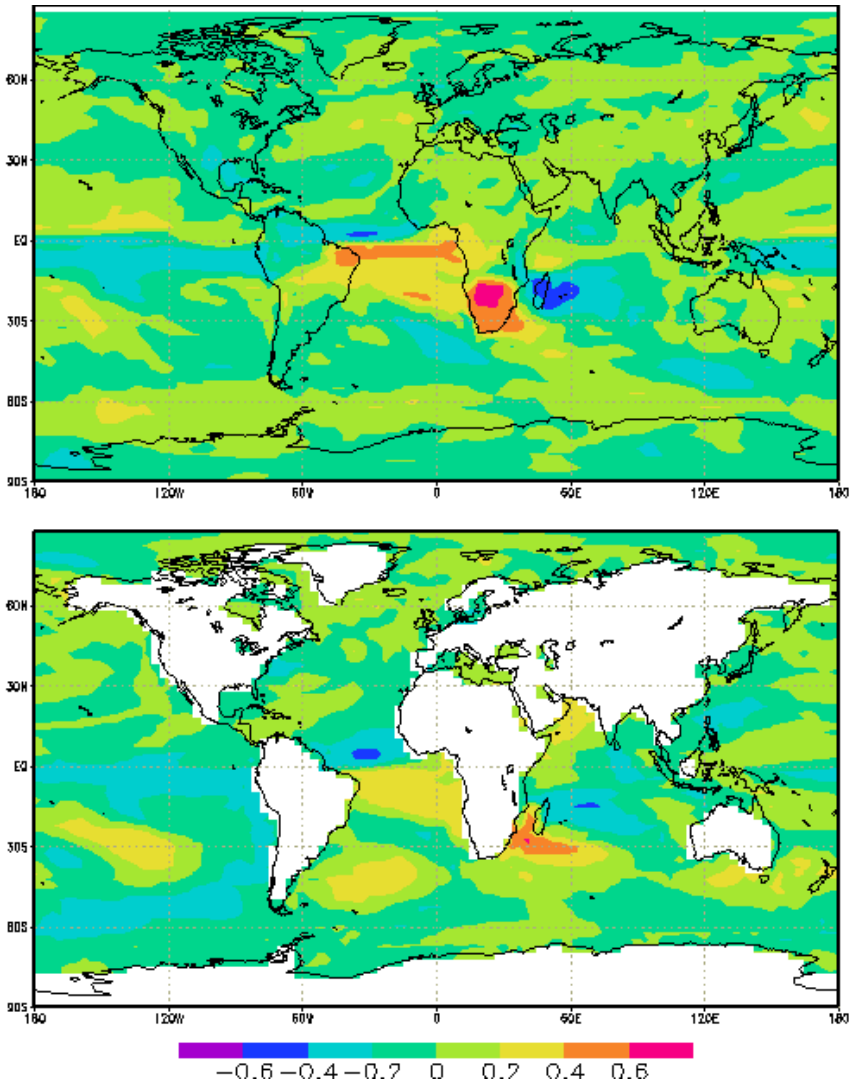

Figure 5.30: Correlation between the timeseries of HadCM3 CTR-simulated southern African sub-continental (15-35ºS, 15-35ºE) precipitation and global precipitation (top) and global SST (bottom). All fields are filtered at a narrower (7-25) band pass to remove potential influence from 60-120 yr variability of the Atlantic Multidecadal Oscillation.

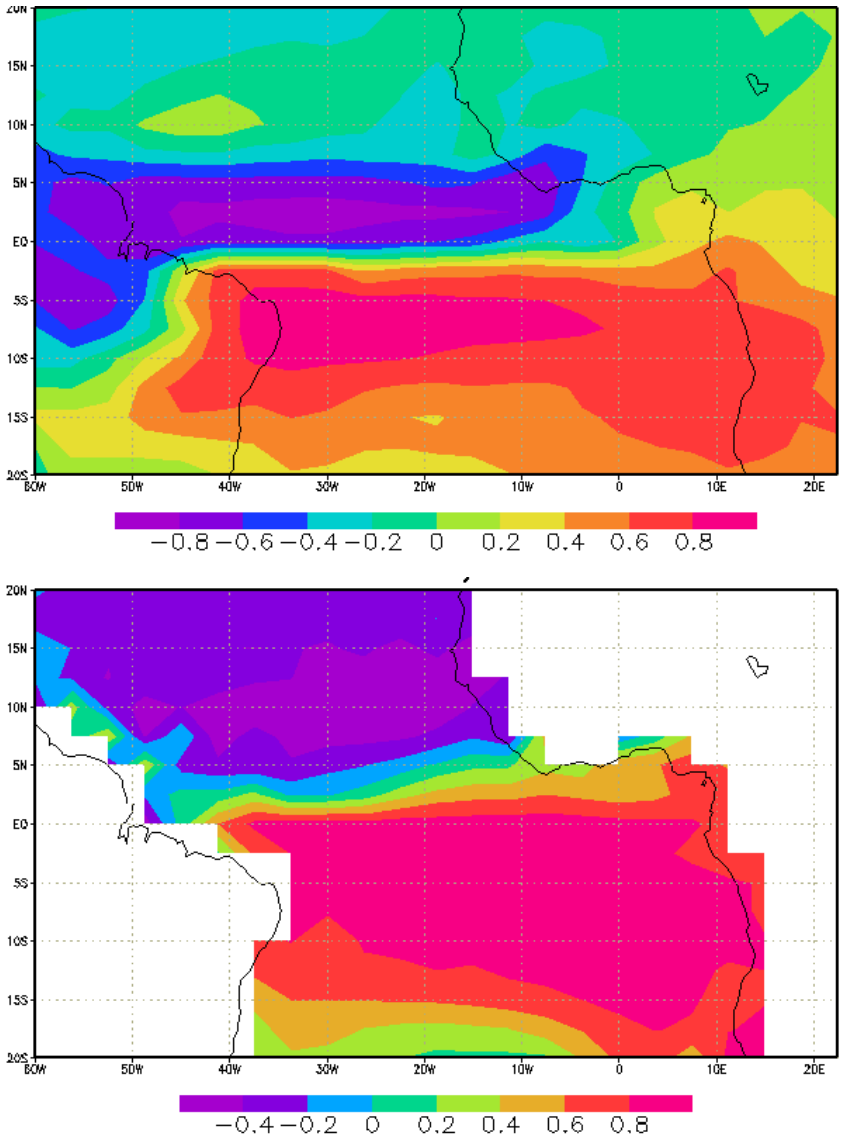

Figure 5.31: Leading EOF structures from analysis conducted on decadally filtered (7-25 yr) HadCM3 CTR precipitation (top) and SST (bottom) data over the tropical Atlantic region (defined as 20ºS-20ºN, 60ºW-20ºE). Note the different EOF scales compared to other figures.

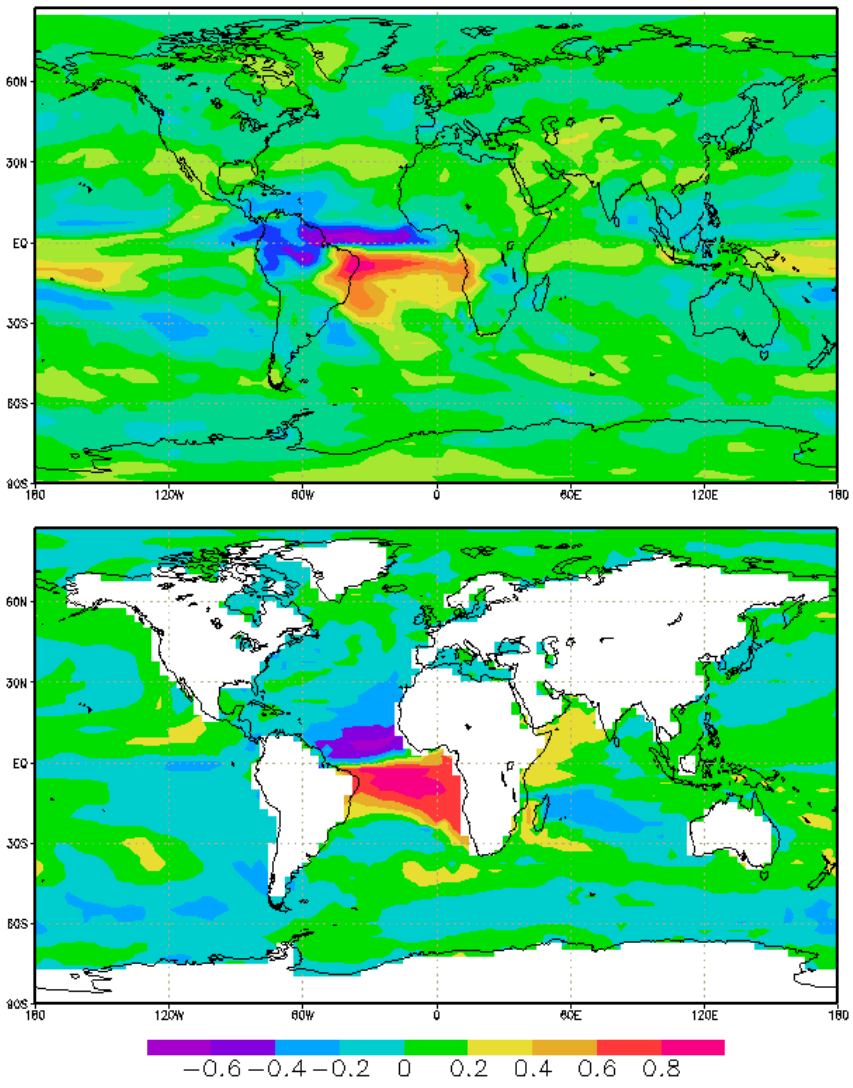

Figure 5.32: Correlation between the timeseries of the leading EOF over the tropical Atlantic region identified in the previous figure, and global fields, filtered using a 7-25 year band pass filter. Top: leading mode of SST correlated with global precipitation, bottom: leading mode of precipitation correlated with global SST.

This area has previously been linked to the Atlantic Meridional Mode, the leading statistical mode of tropical Atlantic variability (Chiang & Vimont, 2004; Vimont, 2005; Vimont & Kossin, 2007) and may also have links to the Atlantic Multidecadal Oscillation (AMO; Knight et al., 2005a, 2005b; Knight et al., 2006; Dima & Lohmann, 2007). These phenomena are dominated by an anomalous meridional SST gradient across the mean ITCZ latitude, and a cross-gradient atmospheric boundary layer flow toward the warmer hemisphere (Nobre & Shukla, 1996; Chang et al., 1997). The mode has been identified in observational and modelling studies (Chang et al., 2000; Ruiz-Barradas et al., 2000; Chang et al., 2001; Chiang et al., 2002), and is well encompassed by the leading EOFs of precipitation and SST shown here.

Chiang & Vimont (2004) have suggested that there is not an intrinsic timescale associated with the meridional mode. In their mechanism, the ocean surface mixed-layer thermodynamics and the adjustment time of the atmosphere are coupled at all timescales, and therefore any forcing will be echoed in the behaviour of the coupled mode (e.g. a 5 yr oceanic forcing will result in a coupled mode at 5 yrs). Chiang & Vimont link the Atlantic to a Pacific meridional mode, and suggest that both modes of variability are potentially excited by the Arctic Oscillation and North Atlantic Oscillation in their respective basins. This mid latitude link to ENSO and Atlantic Nino events has been proposed and explored (Servain et al., 1999; Vimont et al., 2003), with potential implications for the spectral power of the Atlantic modes. MTM analysis of the leading EOF of SST in HadCM3 (not shown) shows 3-4 year spectral peaks at both 99% and 95% confidence, which may support the hypothesis of an Atlantic-ENSO link.

The Atlantic meridional mode is linked to a range of impacts on rainfall and climate variability in the surrounding continents, including hurricane activity (Goldenberg & Shapiro, 1996; Goldenberg et al., 2001; Vimont & Kossin, 2007), NE Brazilian rainfall variability (Folland et al., 2001; Nobre et al., 2006), US rainfall variability (McCabe et al., 2004; McCabe et al., 2007) and the Sahel and West African coastal rainfall (Folland et al., 1986; Rowell, 2003; Vigaud et al., 2006). Similar impacts have been described at decadal-centennial timescales as a result of the Atlantic Multidecadal Oscillation (Knight et al., 2006 and references therein), and in basin-scale analysis of the South Atlantic in observed and modelled studies (Colberg & Reason, 2007). It is not yet clear what links, if any, exist between the different timescales, although it is believed that the meridional mode may play a role in exciting the decadal variability of the AMO (Knight, 2007, pers. comm).

The correlation between the leading SST mode and precipitation over southern Africa is weaker and shows little spatial coherence by comparison. There is very limited previous evidence linking the tropical Atlantic to southern Africa, so why should the correlation appear in the initial rainfall-based method?

First, a running correlation between SAFR rainfall and the tropical SST dipole is constructed to examine the long term variability of the relationship. The range (and sign) of the correlation are sensitive to the choice of correlation window (therefore it is not shown here, as a non-robust result) but both 30 and 60 year windows show variability about the long term average correlations observed in the correlation mapping.

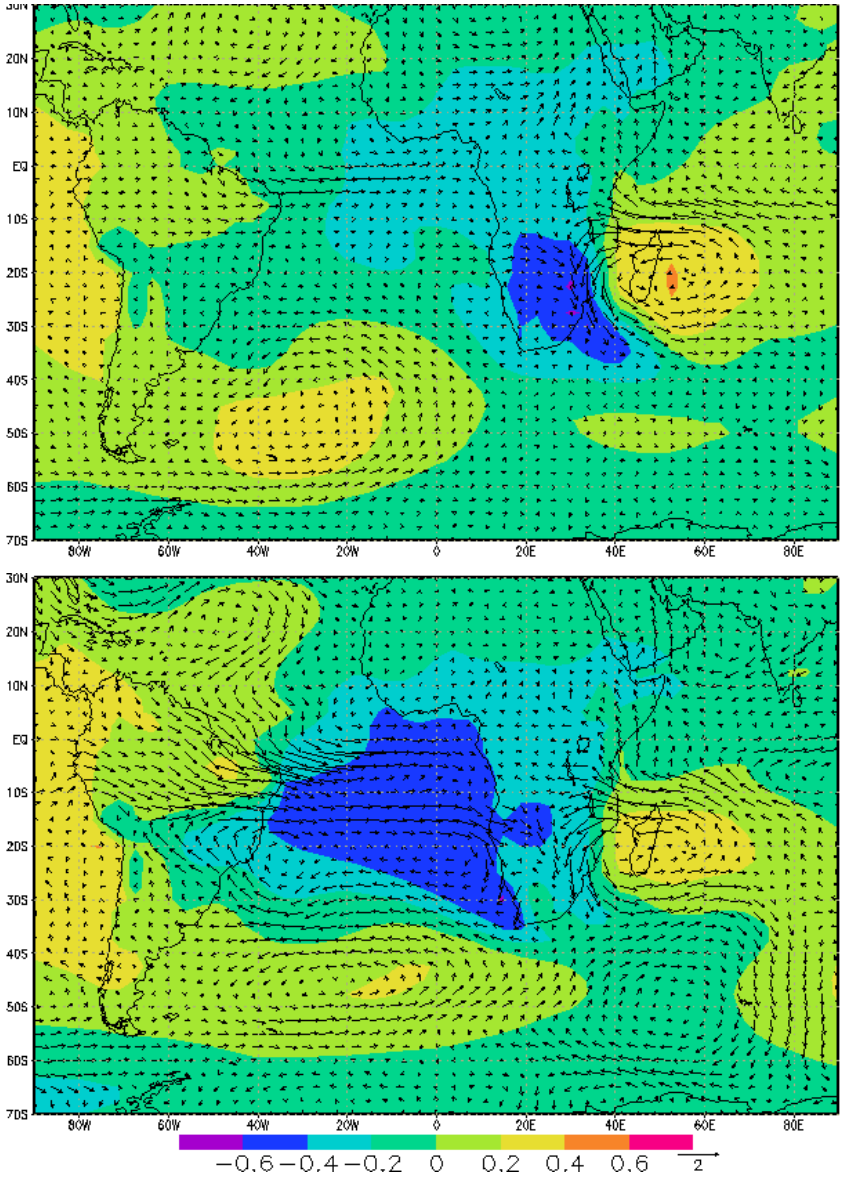

Figure 5.33: Correlation between the timeseries of regional rainfall extracted from the HadCM3 CTR-simulated rainfall data and global SLP, with an overlay of wind anomalies generated by a 2σ regression analysis. Top: east (25-35°E) rainfall; bottom: west (15-25°E) rainfall. Note that the wind scale bar for the top (east) wind vector is equivalent to 4m/s, compared to the 2m/s shown for the bottom (west) vector scale.

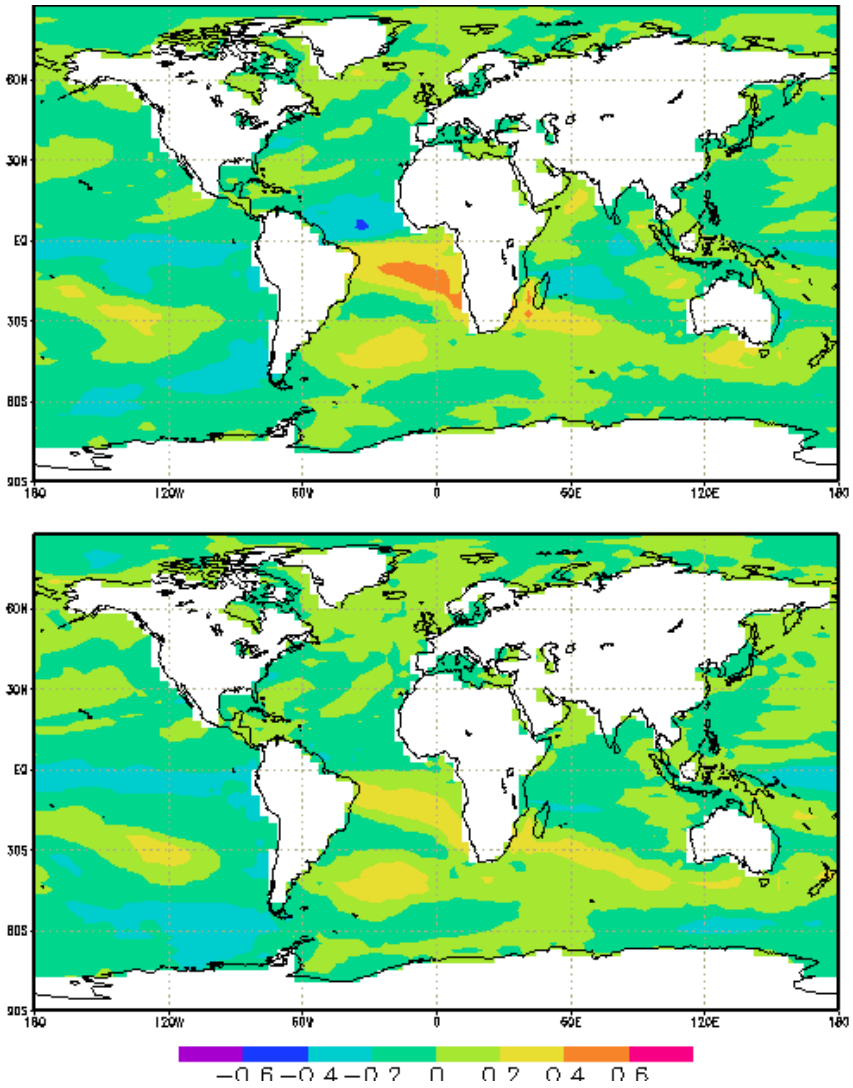

Figure 5.34: Correlation between the timeseries of regional rainfall extracted from the HadCM3 CTR-simulated rainfall data and global SST, filtered with a 7-50 year band pass. Top: north-west (15-25°S, 15-25°E) rainfall, bottom: south-west (25-35°S, 15-25°E) rainfall.

Second, since the tropical Atlantic is not known to have significant impact over southern Africa as a sub-continental region (Rajagopalan et al., 1998), the initial correlation analysis is repeated for the east (25-35°E) and west (15-25°E) of the subcontinent respectively. Figure 5.33 shows that eastern southern African sub-continent is dominated by the SW Indian Ocean dipole in SSTs, and SW Indian Ocean (Mascarene) high circulation pattern observed in the wind regression. These features are retained in the analysis of the western subcontinent, but other influences become apparent. The correlation with SST shows the South and Tropical Atlantic regions identified earlier, with an influx of moisture from the tropics feeding into the SW Indian Ocean high.

Further investigation shows that the western subcontinent is dominated by the north west (15-25°E, 15-25°S), which shows strong correlation with the Tropical Atlantic region compared to the south west region of the subcontinent (Figure 5.35). This result is consistent with both the NW-SE alignment of the EOF analysis described in Section 4.3 and previous observations of SW southern African winter rainfall dominance (Reason et al., 2001; Reason et al., 2002; Reason & Rouault, 2005).

The influence over coastal rainfall identified in the correlation analysis of local scale correlation and the orientation of the rainfall EOFs suggests that there may be local influences which are incorporated in to the sub-continental analysis, and this is presented as the most plausible explanation for the correlation with the Tropical Atlantic described here.

5. 3. 2 South Atlantic Ocean

Unlike the tropical Atlantic Ocean, the South Atlantic region has previously been identified as playing a role in southern African rainfall variability at a range of timescales (Reason et al., 2006; Colberg & Reason, 2007) and in both observed and ECHO-G results. It has been shown that Hadley Centre models are sensitive to representations of SST anomalies in the subtropical and mid-latitude South Atlantic during austral winter (Reason & Jagadheesha, 2005) and it is possible that this sensitivity extends to summer rainfall too. As shown in the previous section, comparison studies using reanalysis data (Sterl & Hazeleger, 2003) and other observed data sets (Venegas et al., 1996; 1997) show that different methods (rotated EOFs, detrended data) have substantial impacts on how EOF techniques behave over the South Atlantic (Colberg & Reason, 2007). This region is therefore examined primarily via an SST index constructed over the initial region of identified correlation for the CTR run (25-35°W, 40-45°S) filtered at 7-100 year band pass scales.

The SST index shows evidence of variability at low frequency timescales. MTM analysis (Figure 5.35) shows spectral power at ~10 and ~12 years with 99% confidence, but there is a notable absence of quasi-decadal spectral power. Correlation analysis (Figure 5.36) with global SST shows a strong positive relationship with the South Atlantic area centred on ~42°S, validating the index region as a suitable proxy choice for the quasi-decadal variability, and in agreement with the correlation based on southern African sub-continental rainfall.

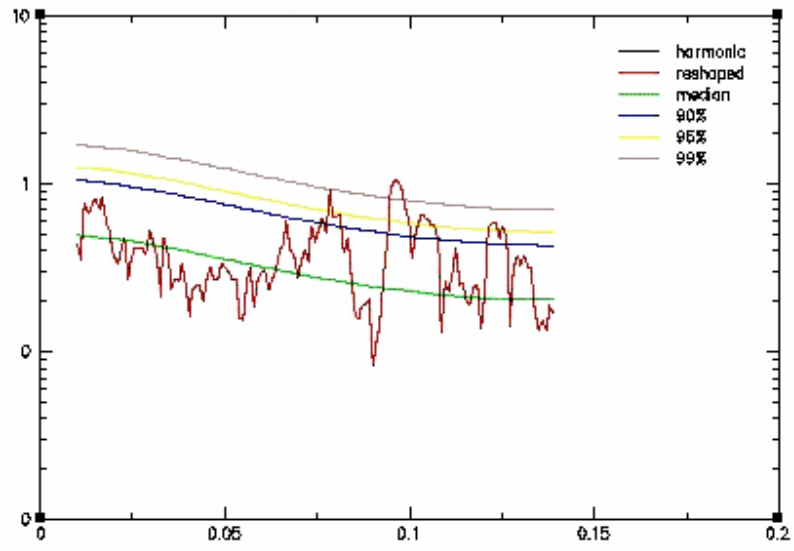

Figure 5.35: Spectral analysis (MTM, 7-100 year band pass filtered), HadCM3 CTR-simulated South Atlantic SST index.

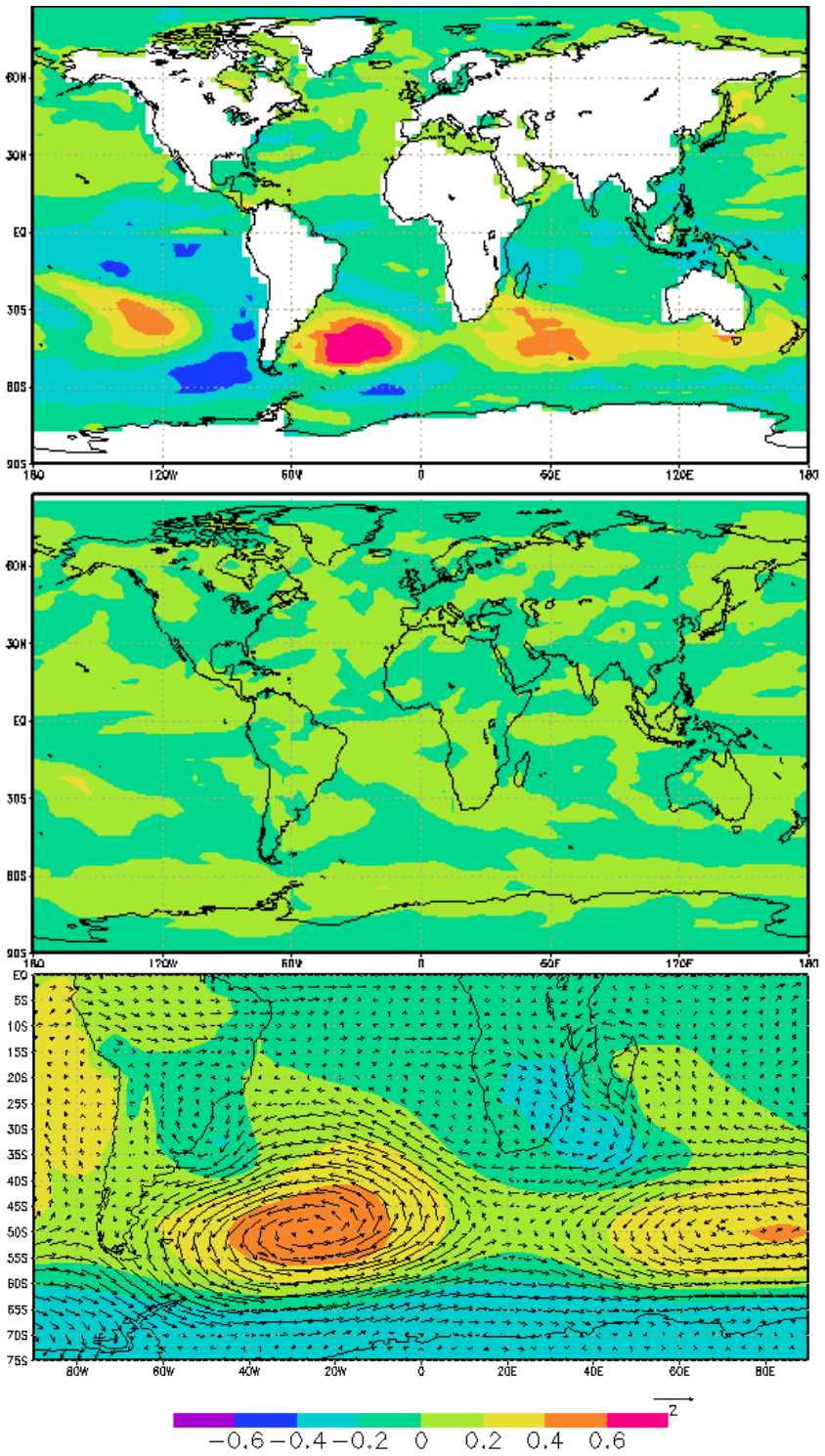

Figure 5.36: Correlation of the timeseries of HadCM3 CTR-simulated South Atlantic SST index (band pass filtered, 7-100 yr) with global fields. Top: Global SST; middle: global rainfall; and bottom: global SLP. The SLP correlation has an overlay of 850 hPa wind anomalies generated by regression on a 2σ rainfall anomaly. Note the scale of the wind vector (m/s).

The structure of variability described here qualitatively agrees with that described by the third (fourth) EOF of unfiltered SST analysis of the ORCA2 ocean model (NCEP-NCAR reanalysis data) centred in the mid-latitudes (Colberg & Reason, 2007). Spectral analysis of the unfiltered ORCA2 EOF shows interdecadal (10-40 yr) power, so the presence of a similar structure in the decadally filtered HadCM3 data is not unexpected. Colberg & Reason (2007)'s lagged correlation analysis of the wind stress agree with the 850hPa wind anomalies shown, and confirm that the strongest correlations occur in the mid-latitudes at zero lag.

The 850hPa wind analysis describes an anomalous anti-cyclone-like pattern in the mid-latitudes, reducing the westerly wind strength at the centre of the SST anomaly (42°S) consistent with a reduction in latent heat flux, and joining up with an enhanced westerly flow at approximately 60°S. A similar anomaly is observed in the mid-latitude South Indian Ocean, suggesting that this variability is not confined to the South Atlantic.

By contrast, negative correlation over the sub-continent in a NW-SE orientation displays a pattern consistent with an anomalous rainfall response, and is linked to enhanced moisture flow from the South West Indian Ocean. The extension of the low pressure trough in to the Agulhas region is a likely explanation for the return wind flow at 40°E, 35°S.

This mode is examined in ORCA2 using horizontal advection and mixing/heat flux terms, and this explanation therefore draws heavily on the oceanographic analysis of Colberg & Reason (2007). It is shown that the underlying geostrophic variability in the east is dominated by southward Ekman flow, consistent with reduced westerly wind stress anomalies, and a secondary mechanism involving changes in the Falklands and Brazil

Currents may be important in driving upper-ocean temperatures in the west of the basin. Positive correlation with the first mixing term over areas of observed upper-ocean warming suggests that weakened westerlies lead to reduced vertical mixing processes, and favour the evolution of a warm SST anomaly. It would be expected that this would relate to a shallower mixed layer, but analysis shows a deepened layer, suggesting that the mechanisms for altering the mixed layer depth are not related to the apparent wind stress anomalies. This explanation is supported by the correlation sequence for the mixed layer depth, which reveals a strong oscillation on interdecadal timescales similar to the geostrophic velocities.

Spectral analysis of the mean geostrophic flow peaks at 10-20 yr variability, with additional ~5 yr peaks showing a link to ENSO. This result agrees with Colberg et al. (2004) who showed that significant temperature changes in the South Atlantic SST originate in changes to the subtropical high pressure system exerting an influence on anomalous Ekman transport. The timing, region and baroclinic nature of this mode agree in principle with that described by Reason (2000) and Wainer & Venegas (2001).

This variability shows a positive relationship with southern African sub-continental rainfall, but the correlation is not particularly strong (r=0.285) and the South Atlantic SST index only explains 11% of the rainfall variability. This response is in agreement with Washington & Preston (2006)'s interannual analysis whereby the circulation and 'ingredients for enhanced rainfall' are well simulated, but the rainfall itself does not respond, probably because of convective parameterisation in HadCM3 (Washington & Preston, 2006: 9).

It is not clear what drives this mode of variability in either ORCA2 or HadCM3. Links have been suggested between the South Atlantic Ocean and ENSO (Venegas et al., 1996; Colberg et al., 2004; Hermes & Reason, 2005), and have previously been argued to initiate the subtropical changes that result in changes to the mid-latitude geostrophic flow. It is possible that decadal ENSO-like structures (Mantua et al., 1997) may force similar evolutions at decadal timescales.

Similarly, the coherent southern hemisphere response strongly resembles the modification of standing wave patterns associated with the Southern Annular Mode (Antarctic Oscillation) (Thompson & Wallace, 2000; Dima et al., 2002; Thompson & Solomon, 2002), and it may be possible that some form of interdecadal mechanism operates to link the mid-latitudes in this manner. Phase relationships of this nature have been found in other studies (Reason, 2000; Reason et al., 2001; Reason et al., 2002; Fauchereau et al., 2003b; Reason et al., 2006a), in both austral summer and winter rainfall variability, with the co-evolution typically determined by the magnitude of atmospheric variability (Hermes & Reason, 2005).

It has been shown that there is a correlation between southern African rainfall and South Atlantic SST variability. An index constructed over the region of strongest correlation revealed correlation patterns and wind anomaly distribution consistent with a physical mechanism identified by Colberg & Reason (2007) whereby geostrophic variability and an Ekman response lead to reduced (enhanced) westerly flow and anomalous warming (cooling) of the mid-latitude ocean north (south) of approximately 50°S. This anti-cyclone-like response is also observed in the South Indian Ocean, and negatively

correlated with an enhanced moisture flux from the SW Indian Ocean associated with a low pressure trough over the subcontinent. Although significant responses in the rainfall were not found, conditions which favour increased rainfall were generated, and this has previously been interpreted as a feature of HadCM3's parameterisation schemes (Washington & Preston, 2006).

5. 3. 3 South West Indian Ocean

The South West Indian Ocean (SWIO) is thought to be the dominant region of forcing for southern African rainfall, and has been identified in observed and modelled studies at the interannual scale as well as in the observed and ECHO-G data at decadal scales. Correlation analysis in HadCM3 CTR simulation at decadal timescales agrees with the location and approximate strength of the relationship identified at the interannual scale, as well as at the decadal scale in the observed analysis presented in the previous section. Like the South Atlantic Ocean, the SWIO region is thought to be influenced by a range of structures which complicate the regional variability, including SST variability linked to ENSO (Tyson & Preston-Whyte, 2000; Reason & Rouault, 2002; Swann et al., 2003).

It is thought that this region is the most critical in understanding the simulated differences between CTR and other HadCM3 simulations, and the analysis presented in this section is therefore based entirely on the CTR simulation. The results from NAT and ALL simulations are described in the next chapter on forcing of decadal variability.

Although identified in the observed SST data by unrotated EOF analysis, it is only rotated EOF analysis (Kay, 2007, pers. comm.) which identifies a subtropical dipole centred on

55°E, 32°S, and a tropical dipole centred on 65°E, 12°S with influence over the sub-continent in HadCM3. SST indexes are constructed averaging over these grid points.

Since the correlation between the two dipole regions at filtered timescales (r=-0.404) is less than previously identified at interannual timescales (r=-0.6), this study examines the index regions separately, rather than as a combined SWIO dipole 'mode'. MTM analysis of both indexes shows quasi-decadal spectral power with 99% confidence; the subtropical dipole shows spectral power at 9.5 and 15 years (Figure 5.37), with 8.5, 10.4 and 20.4 year power displayed by the tropical pole. The slight difference in spectral power is also displayed in filtered correlation analysis. Both nodes show a southern hemisphere-linked SST response, with correlation reaching ±0.4 in the South Atlantic and South Pacific regions. The subtropical (Figure 5.38) node shows a coherent link to the South Atlantic mid-latitude circulation whereas the tropical (Figure 5.39) SWIO node shows a stronger response in the immediate Mascarene/SW Indian Ocean circulation (note the difference in 850hPa wind scale). Both SWIO indexes generate a NW-SE aligned rainfall response over the sub-continent, albeit with some minor differences in the locations of maximum correlation (±0.4).

This correlation analysis is consistent with the mechanisms identified at interannual timescales driving the rainfall variability over southern Africa, suggesting that the SWIO operates in a similar way at decadal scales. Like the annual variability, the strengthened (weakened) Mascarene high pressure leads to enhanced (reduced) westerly moisture flow over the sub-continent at decadal scales.

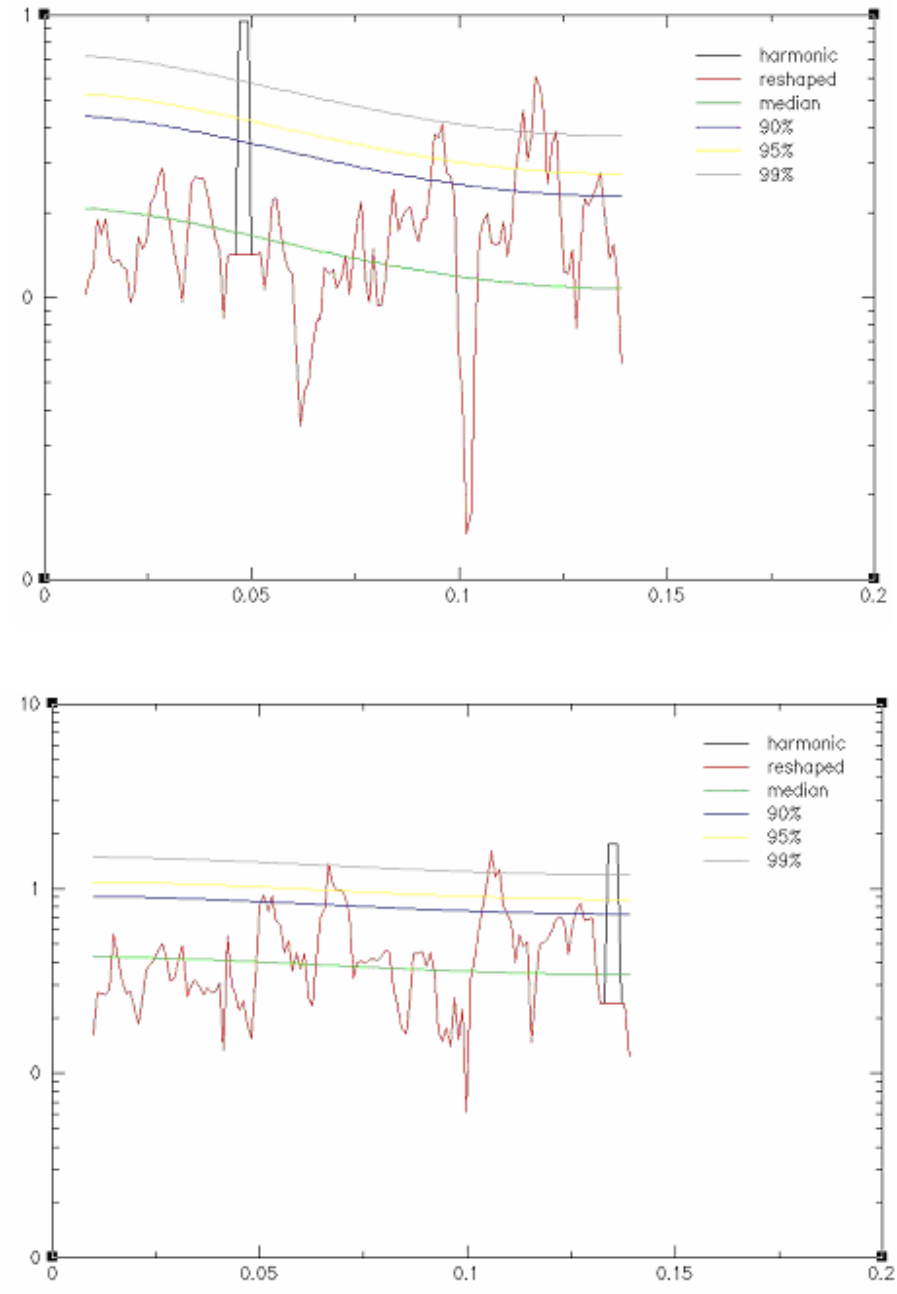

Figure 5.37: Spectral analysis (MTM, filtered) of HadCM3 CTR-simulated SWIO SST index regions, showing elements of quasi-decadal spectral power. Top: tropical node (5-10ºS, 60-80ºE); bottom: subtropical node (30-35ºS, 40-60ºE).

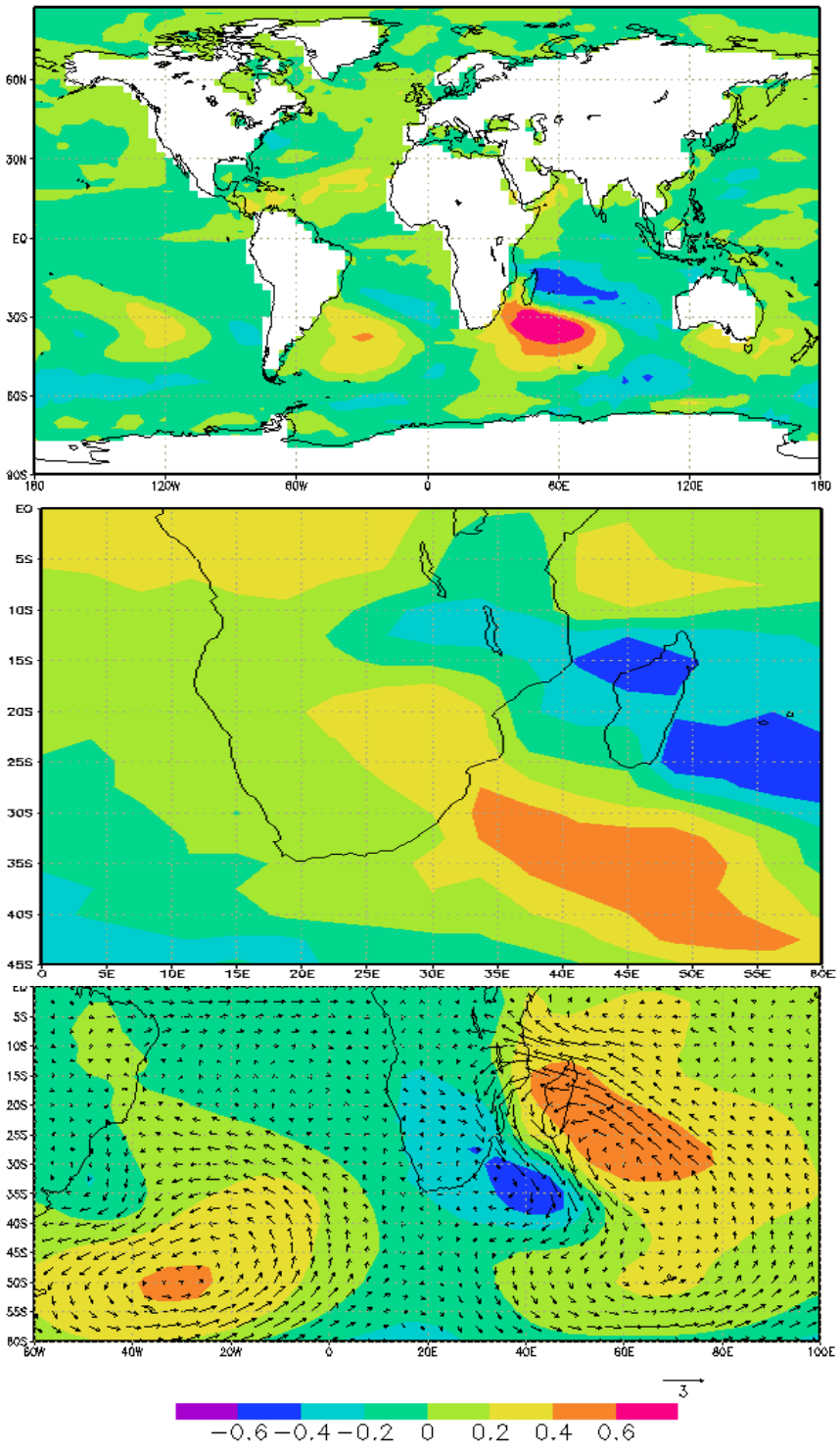

Figure 5.38: Correlation between the timeseries of HadCM3 CTR-simulated SWIO sub-tropical SST and global fields, filtered using a 7-50 year band pass filter. Top: global SST; middle: regional precipitation, and bottom: regional SLP anomalies with a wind anomaly generated by a 2σ regression of 850 hPa winds on rainfall over southern Africa.

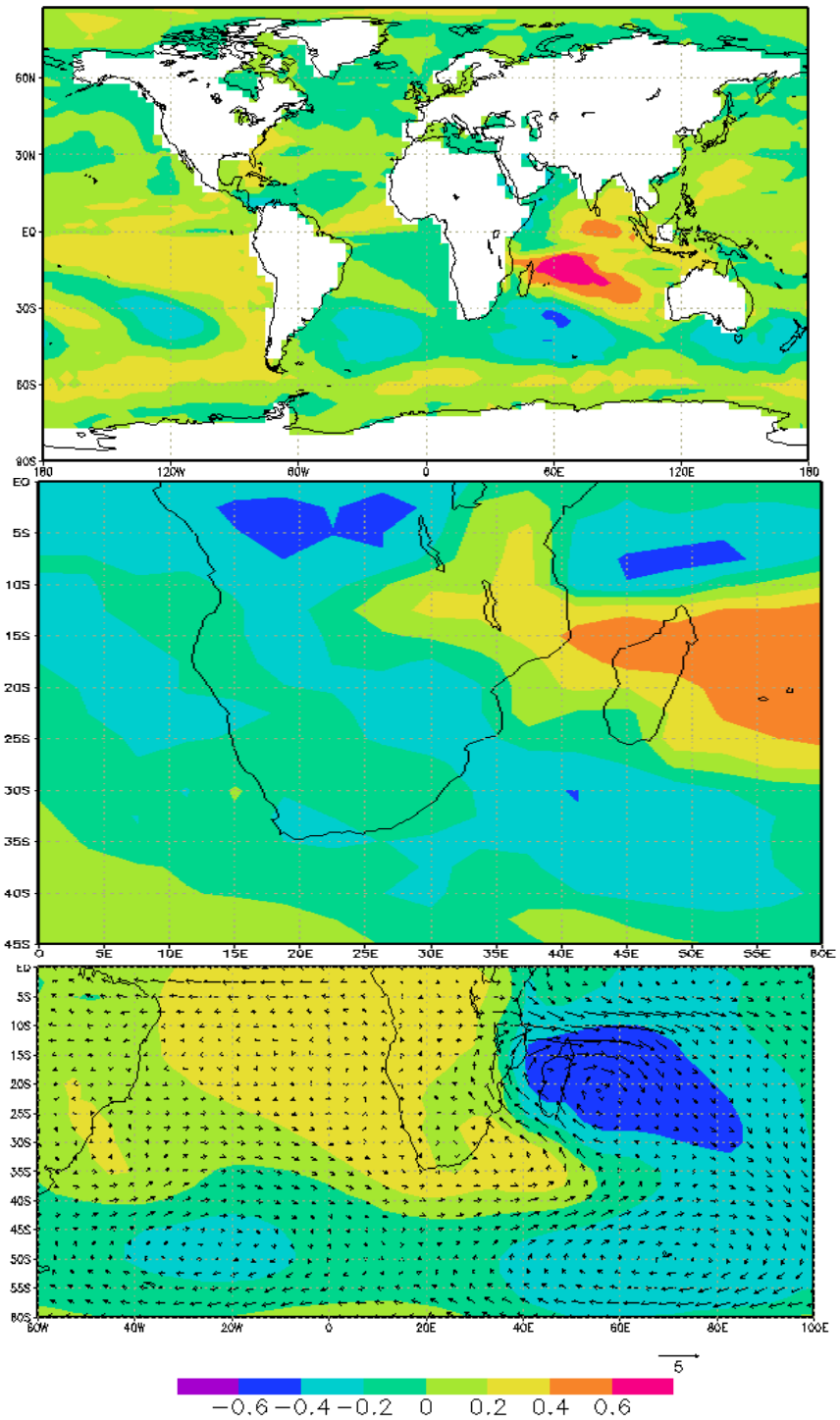

Figure 5.39: Correlation between the timeseries of HadCM3 CTR-simulated SWIO tropical SST and global fields, filtered using a 7-50 year band pass filter. Top: global SST; middle: regional precipitation, and bottom: regional SLP anomalies with a wind anomaly generated by a 2σ regression of 850 hPa winds on rainfall over southern Africa. Note the different wind vector scale to the previous figure.

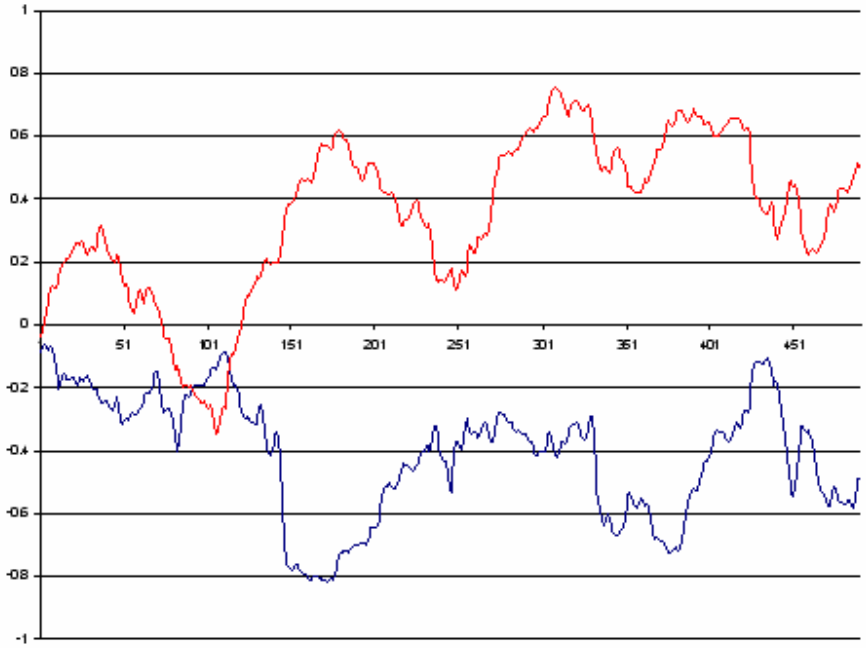

Figure 5.40: Running correlations (constructed using a 60 year correlation window) between HadCM3 CTR-simulated southern African rainfall and the indices of the SWIO nodes. The subtropical SST index is shown in red, and the tropical SST index shown in blue. The rainfall data and SST index are filtered using a 7-50 yr band pass filter.

The response is also coherent across the southern hemisphere, with links to the South Atlantic maintained at decadal timescales, in agreement with the relationship identified in the previous section. As in the observed data, an apparently stronger circulation response is related to the tropical node of the dipole, with a marginally higher correlation with SAFR rainfall (r=-0.402) than the subtropical node (r=0.376). This agrees with the different contribution of the two nodes described by Washington & Preston (2006) at the interannual scale. Using idealized model experiments of HadAM3 interannual variability with a linear detrending of the ENSO signal, they note that 'significant circulation changes resulting from tropical SWIO cooling are greater in magnitude and spatial extent than the more localised responses resulting from the sub-tropical SWIO warming' (Washington & Preston, 2006:12), and suggest that this result is also found in reanalysis data which emulates the experiments (Jury, 1997; Jury et al., 1999) as well as modelling studies (Goddard & Graham, 1999).

The work presented here suggests that the differential relationship between nodes of SWIO variability is also present at decadal timescales, and since this relationship appears in both observed and model studies without anthropogenic forcing, is unlikely to be a data-specific result.

Running correlation with a 60yr window (Figure 5.40) shows that the relationship between SWIO indexes and the southern African rainfall is variable. The tropical index shows particularly high periods of correlation ($r \geq -0.6$) with rainfall, and there is some agreement in the timing of correlation variability between the positive and negative indexes. Although there are periods where the decadal rainfall variability is strongly linked to the

SWIO nodes, it appears that there are also times where other forcing becomes more important, and the correlation with the SWIO is minimised. This appears to be in agreement with variability at the interannual scale, where the various forcing mechanisms are identified as waxing and waning in importance through the record (Reason et al., 2004), and is echoed by long term analysis of the relationship between ENSO and southern African rainfall, which often manifests itself in SWIO variability (Pfeiffer et al., 2004; Zinke et al., 2004; Grottoli & Eakin, 2007).

The relationship between the SW Indian Ocean and the rainfall variability over southern Africa has been established in observed and model data. This study has shown that it is equally important at decadally filtered timescales, and although varies in strength and relative importance, plays an established role in CTR-simulated southern African rainfall variability. The pattern of circulation response links to strengthening of the sub-tropical high pressure system, and an increased moisture flux in to the east of the sub-continent, and appears to operate in the same manner as the interannual variability. Washington & Preston (2006) have shown that the model often reproduces the patterns of circulation change accurately, even if the rainfall distribution is not always quite so well simulated.

5. 3. 4 Global Teleconnections

Although the tropical Atlantic, South Atlantic and SW Indian Ocean regions have been identified as important regions for influencing decadal rainfall variability over southern Africa, the analysis of each region has supported the concept of hemispheric interconnected variability, particularly in the global oceans. The presence of this large scale response agrees with the coherent influences between and within ocean basins described by coupled atmosphere-modes of variability. In order to test the hypotheses proposed in explanation of ECHO-G's simulation of global teleconnections, this section considers both ENSO-like variability and the influence of the Southern Annular Mode.

El Nino-Southern Oscillation (ENSO)

Potentially the most important of these is the ENSO signal, typically characterised by a 3-5 yr peak in spectral analysis. Clearly, the "classic" ENSO signal is removed by the decadal filtering applied during this study, but this does not account for potential decadal influences of ENSO and/or the Pacific Decadal Oscillation (Mantua et al., 1997). ENSO is known to be a significant contributor to interannual variability in southern African rainfall, and any decadal variability of ENSO is likely to retain influence at these time scales. However, the long-term correlation between the NINO 3.4 index and SAFR rainfall (r=-0.27744) is substantially weaker than the interannual correlation (r=-0.5; Tyson & Preston-Whyte, 2000), which suggests a reduced influence of ENSO at decadal timescales.

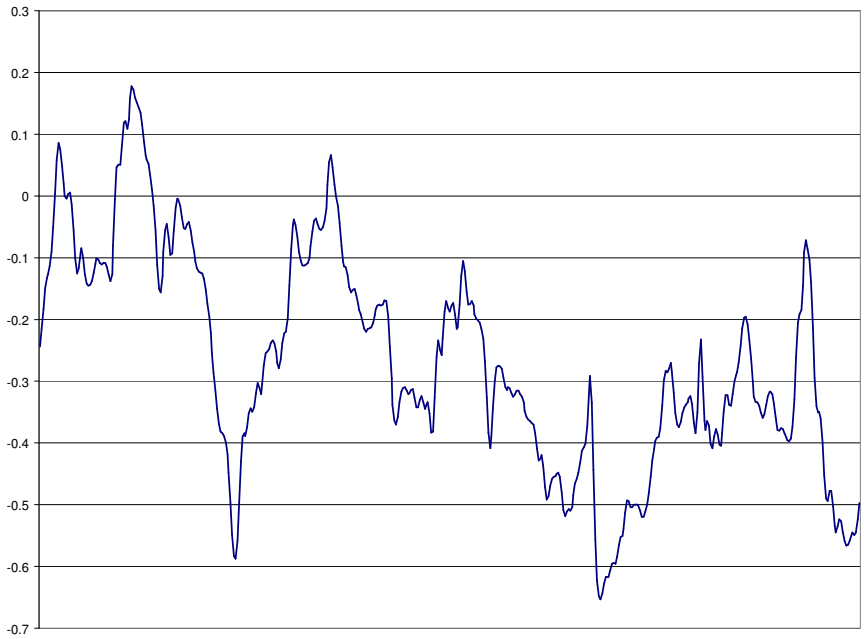

Figure 5.41: Running correlations (constructed using a 60 year correlation window) between HadCM3 CTR-simulated southern African rainfall and the NINO 3.4 SST index. The rainfall data and SST index are filtered using a 7-50 yr band pass filter.

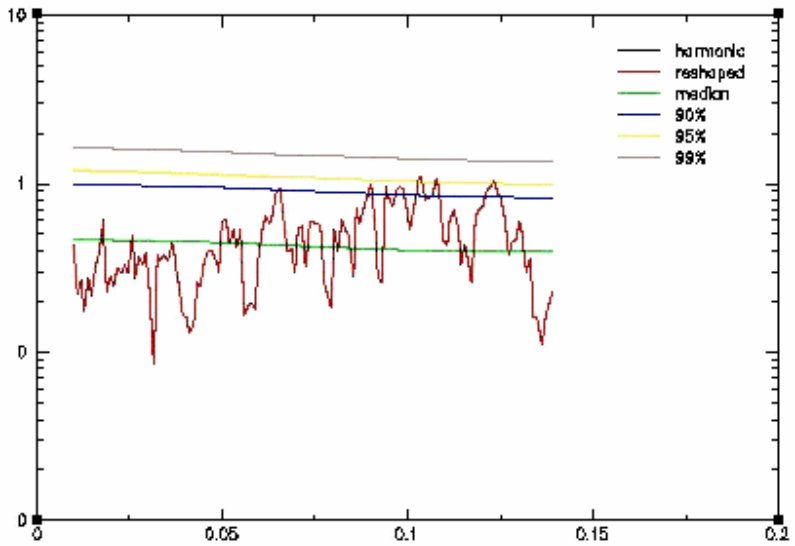

Figure 5.42: Spectral analysis (MTM, filtered) of HadCM3 CTR-simulated NINO 3.4 SST index (filtered)

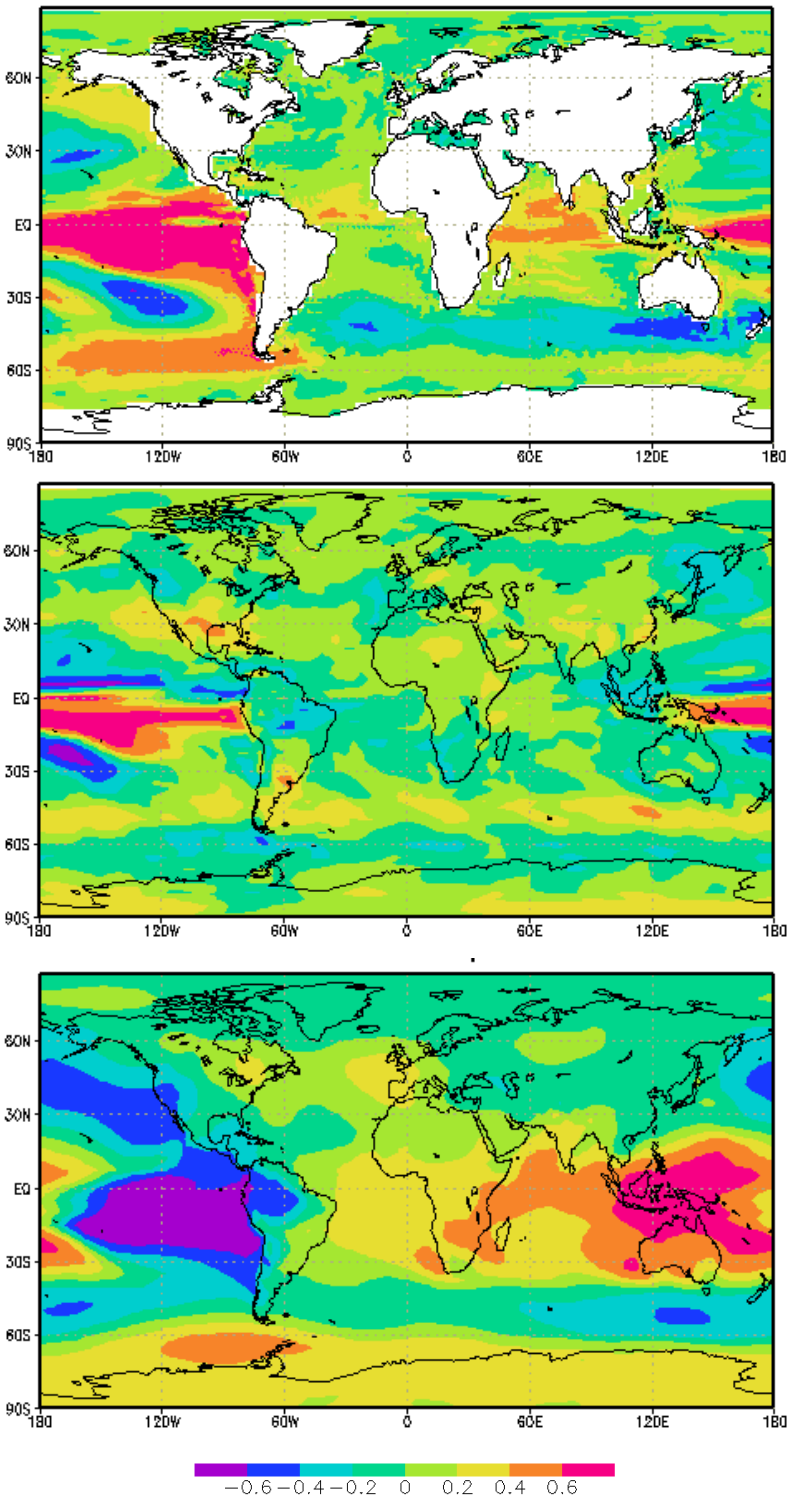

Figure 5.43: Correlation between the timeseries of HadCM3 CTR-simulated NINO 3.4 SST index and global fields, filtered using a 7-50 year band pass filter. Top: global SST; middle: global precipitation, and bottom: global SLP.

Running correlation constructed using a 60 year window shows a significant variability in the strength of ENSO's influence over the sub-continent (Figure 5.41), which may explain the relative importance of ENSO (Richard et al., 2000) and the weaker decadal correlation strength. Spatial correlation based on the NINO 3.4 SST index (Figure 5.43) shows a coherent response in SST and SLP patterns. The North Pacific dominance of the Pacific Decadal Oscillation-type pattern (Mantua et al., 1997) is notably absent – the decadal correlation is consistent with interannual ENSO patterns.

Although the average El Nino (La Nina)-driven condition is for a drying (wetter) southern Africa, with strong correlations observed ($r>0.6$), there are also areas of weak correlation and indications that southern Africa may have previously been wetter under these conditions during the first part of the CTR simulation. Tyson & Preston-Whyte (2000) suggest that this influence on southern African rainfall (at interannual scales) may be modulated at higher frequencies by the Quasi-Biennial Oscillation (QBO), with a higher proportion of rainfall variability explained by ENSO under the westerly QBO phase (36% of variance) compared to the easterly QBO phase (16% of variance; statistically insignificant), but this theory has not received significant support in recent literature.

The link is confirmed by spectral analysis of the NINO 3.4 index, with the unfiltered index (not shown) demonstrating characteristic ENSO timescales and a spectral peak at 3.5 timescales known to be associated with interannual southern African rainfall variability (Mason & Jury, 1997). Clearly, the interaction between the 2-3 yr QBO and the 3.5 yr preferred ENSO-led variability is muted by decadal filtering, which may explain the reduced correlation observed at quasi-decadal timescales. The ~10 yr spectral peak in the

filtered NINO3.4 analysis (Figure 5.42) may agree with the 10-12 yr spectral power in the SAFR rainfall spectrum, as well as ~10 yr spectral power in both SWIO SST indexes.

This spectral power at quasi-decadal scales – although weak by comparison to the initial rainfall signal – contrasts sharply with the behaviour of ECHO-G's ENSO-like signal. The decadal variability in ENSO agrees with that observed in the tropical and subtropical nodes of the SWIO SST, and provides further support for the hypothesis linking the tropical SWIO and ENSO-like variability. It is suggested that although the direct relationship between ENSO and SAFR rainfall may be weakened, there are modulating links to regions of importance to the rainfall variability at decadal timescales (Reason et al., 2000; Reason, 2001b; Reason & Rouault, 2002; Swann et al., 2003).

The interannual effects of ENSO are well studied over the southern African region. Any decadal variability in the strength or sign of the ENSO teleconnection would have significant impacts on rainfall variability, in particular, and it has been suggested here that some evidence for this can be observed in HadCM3 model data. It is again worth noting that the use of CTR simulation precludes this change in ENSO from being driven by anthropogenic forcing, and therefore we may consider ENSO to have variability at low frequency timescales as well as the 'classic' spectral peaks. It is beyond the scope of this study to identify the mechanism by which ENSO may operate at decadal timescales.

Southern Annular Mode (SAM)

In order to explain the relationships observed in the ECHO-G simulation, it was hypothesised that the relationship between South Atlantic and sub-tropical SW Indian Ocean SST was controlled at quasi-decadal scales by the Southern Annular Mode (SAM). It was further suggested that the reduced influence of ENSO at quasi-decadal scales in ECHO-G augmented the role of the SAM, but without testing, this could not be confirmed as a valid explanation. This section tests the relationship between SAFR rainfall, ENSO and the SAM in HadCM3, and explores the CTR-simulated relationship to establish whether the ECHO-G hypothesis is model or forcing-specific.

The SAM index is constructed using the same method outlined previously, employing the mean SLP at 45°S and 65°S as a proxy (Gong & Wang, 1999). Although HadCM3 has 850hPa geopotential fields available and the more traditional method of SAM index construction could be utilised (Thompson & Wallace, 2000; Thompson & Solomon, 2002), employing the same method removes the potential for the generation of index-specific results.

Spectral analysis of the SAM index (Figure 5.44) shows a substantially different result to the ECHO-G SAM index. There is a peak at ~42 yrs (90% confidence), but then an absence of further quasi-decadal power in the index. The index-based correlation analysis also shows considerable differences to ECHO-G. The expected relationship with South Atlantic SST (r=0.179) and sub-tropical SWIO (r=0.313) are much weaker than those observed in the ECHO-G simulation (r=0.589 and r=0.683, respectively).

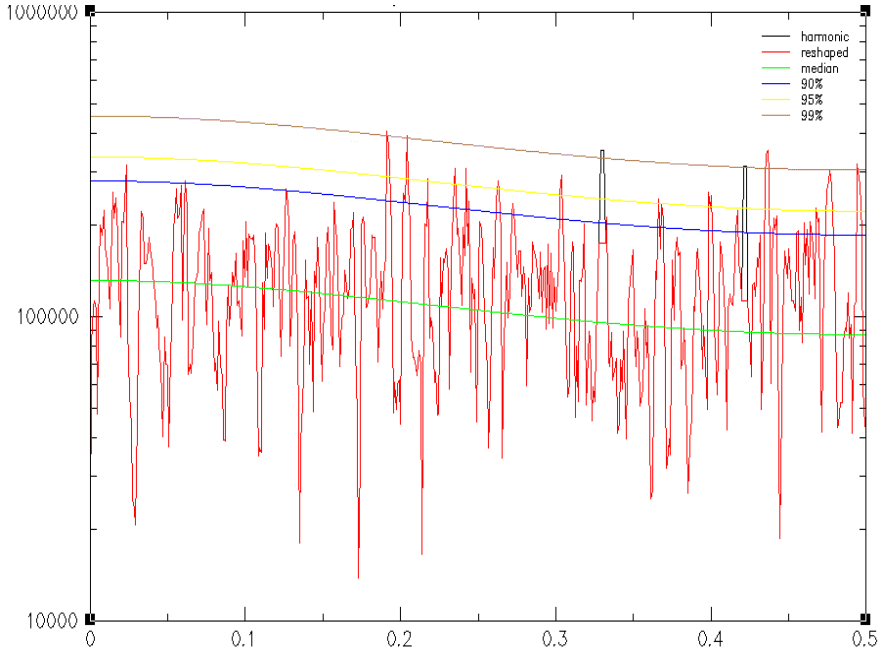

Figure 5.44: Spectral analysis (MTM, unfiltered) of HadCM3 CTR-simulated Southern Annular Mode index.

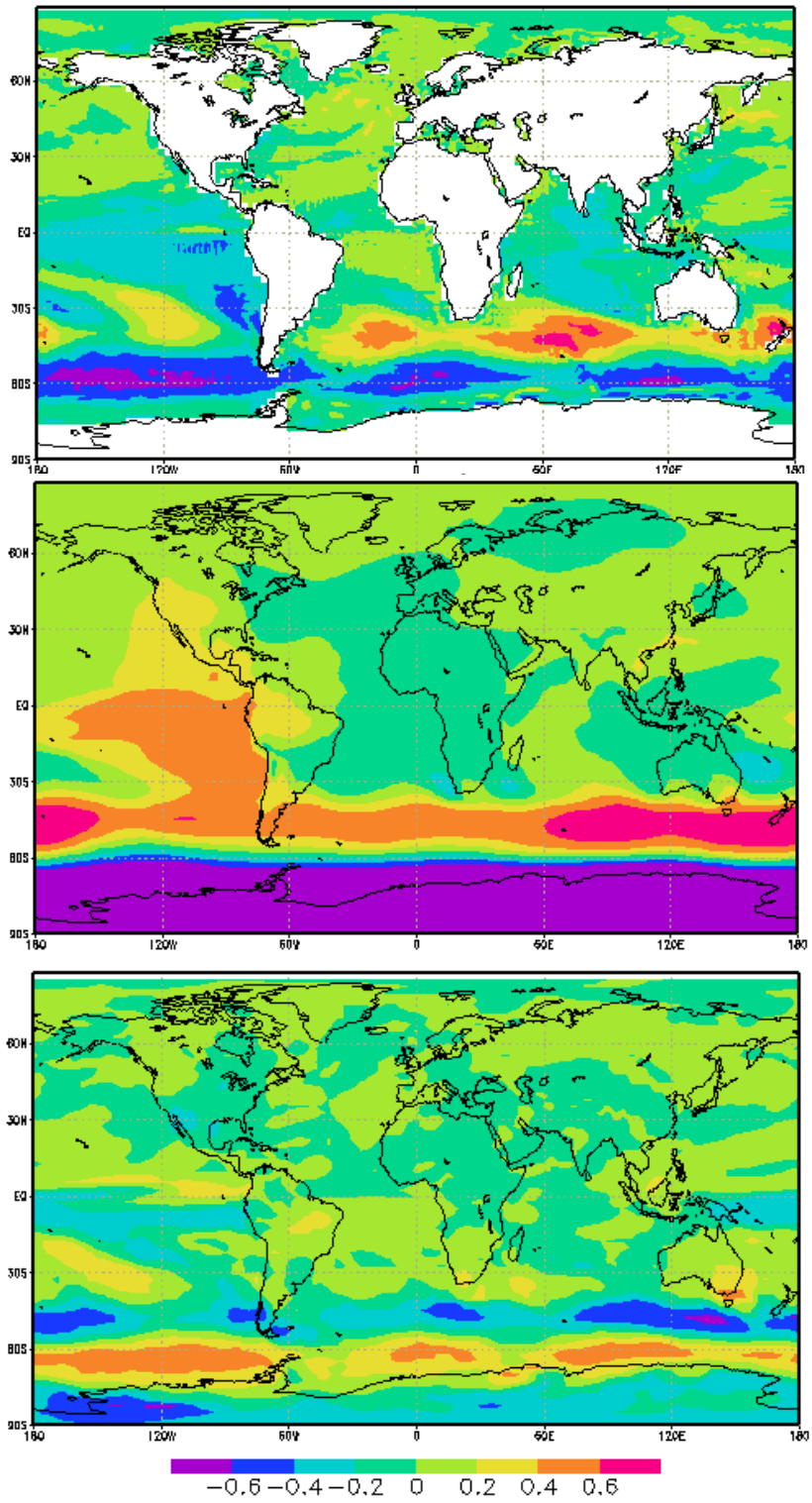

Figure 5.45: Correlation between the timeseries of HadCM3 CTR-simulated Southern Annular Mode and global fields, filtered using a 7-50 year band pass filter. Top: global SST, middle; global SLP, bottom: global rainfall.

However, HadCM3's SAM index has stronger relationships with the NINO 3.4 SST index (r=-0.354) and through the tropical teleconnection, the tropical SWIO node (r=-0.329) which results in a correlation with SAFR rainfall (r=0.292) similar in strength to that observed in ECHO-G's simulation (r=0.325). This initial analysis suggests that the simulations of SAM differ substantially in HadCM3 and ECHO-G.

Correlation mapping provides some insight in to where the main differences lie (Figure 5.45). First, the weaker correlations with the South Atlantic and sub-tropical SWIO are linked to a much weaker SLP correlation with the Atlantic basin in HadCM3. The dominance of this region in ECHO-G is suggested through index and mapped correlation. Second, HadCM3 shows strengthened relationships with both SST and SLP in the Pacific Ocean compared to ECHO-G. This may explain the stronger anti-correlation with the NINO index, and link to the tropical SWIO through the atmospheric bridge teleconnection proposed earlier.

The combined relationships with ENSO-like variability and the mid-latitude ocean variability result in a similar rainfall distribution in HadCM3 and ECHO-G. The mapped correlation over SE Australia, for example, is remarkably consistent across model simulations, and links to this region's decadal influences on rainfall (Power ref). The rainfall correlation over southern Africa is less clearly defined over southern Africa – potentially reflecting the hypothesis of Washington & Preston (2006) that rainfall generating regional circulation in the model does not always result in the appropriate rainfall response – but shows similar overall strength to that defined in ECHO-G.

The analysis presented here suggests that ENSO has an influence over southern Africa at decadally filtered time scales, the strength and sign of which may vary considerably through the record. It seems that ENSO modulates the strength of locally important variables (e.g. the SWIO SST) which has a subsequent effect on rainfall. The examination of regression of SWIO SST on ENSO suggests that this modulation – previously thought to be important at interannual scales (Swann et al., 2003) – is likely to operate at quasi-decadal scales also. The CTR SAM index in HadCM3 appears to be simulated as a more integrated element of the climate system. The lack of quasi-decadal power prevents it being a strong influence at these timescales, and the strength of HadCM3's simulated ENSO does not generate a mid-latitude demarcation in the same way that ECHO-G appears to.

Although the large difference in model simulations of this index might be used as evidence that the dominance of the SAM index in ECHO-G is a model-specific result, related to a weaker ENSO simulation, it should be remembered that the global teleconnections presented are from the CTR simulation only. Although the simulated NAT ENSO and SAM indexes (not shown) are not substantially different from their CTR counterparts, their relationship with southern African rainfall variability at decadal timescales is altered by the different behaviour of the SWIO region identified in Section 5. 3. 3. This global relationship is explored in the next chapter, and further examination with different climate models at quasi-decadal timescales should provide additional non-model specific information about how these large-scale oscillations may interact to generate regional variability.

5. 3. 5 HadCM3 Simulation Summary

Through correlation analysis, ocean-atmosphere variability associated with southern African rainfall at decadal timescales has been identified in three regions in the CTR simulation of HadCM3. It is worth noting *a priori* that some of these quasi-decadal relationships with rainfall variability must be intrinsic to HadCM3's simulation of the climate system, since they are identified in the CTR and NAT simulations alike.

First, a coupled mode of variability with quasi-decadal spectral power was identified in the tropical Atlantic in both CTR and NAT simulations. This mode is thought to have links to the Atlantic Meridional Mode (Chiang & Vimont, 2004), and possibly the Atlantic Multidecadal Oscillation (Knight et al., 2005). Although not causally linked to the wider sub-continental rainfall, the influence of this region on the west coast rainfall was incorporated in to the sub-continent average, and shown to be the primary link to the decadal rainfall variability. The mode is relatively unchanged under different forcing scenarios, with modulation of relative importance described in the later chapter on anthropogenic forcing.

Second, quasi-decadal variability was identified in the South Atlantic. An index constructed over the area of strongest correlation showed links to coupled variability in the South Atlantic and South West Indian Ocean. Colberg & Reason (2007) proposed a similar mechanism of variability, reliant on changes in the Ekman circulation to reduce (enhance) mid-latitude westerly wind flow and create anomalously high (low) SST patterns linked to anticyclonic circulation. This circulation was also identified in the South Indian Ocean, together with an anomalous NW-SE aligned low pressure over the sub-

continent, linked to enhanced (reduced) moisture flux from the SWIO region. Despite this low pressure structure and the associated circulation response, an immediate correlation was not identified in the rainfall analysis. This is hypothesised to be a result of model-specific parameterisation, and has previously been observed in HadCM3 (Washington & Preston, 2006) at interannual timescales. Correlation with the South Atlantic was also observed in NAT simulated variability, but thought to be slightly weaker.

Third, the SW Indian Ocean was examined through construction of SST indexes in regions of high correlation at decadal scales. These areas were known to influence southern African rainfall at interannual scales (Mason & Jury, 1997; Reason, 2001), and have now been shown as important at decadal scales for rainfall variability. Analysis showed that this was a key region of change under forcing conditions, and the CTR simulation results are described here. The NAT simulated variability is described in the next chapter, since it agrees with the variability simulated under anthropogenic forcing. In the control run, it was shown that the separate tropical and sub-tropical SWIO SST index regions contributed to an increased (reduced) westerly moisture flux from the Indian Ocean as a result of a strengthened (weakened) Mascarene high, influencing rainfall in the NW-SE orientation described in the nature of variability. It was further demonstrated that there is a subtle difference in the response to each index, and that like Washington & Preston (2006)'s work with reanalysis and HadAM3 idealized experiments, the tropical node was associated with a stronger circulation response than the subtropical node at decadal timescales.

Finally, the relationship of southern African rainfall variability to external teleconnections was examined. The direct influence of ENSO at decadal timescales appears to be weaker than at interannual timescales. However, the nature of the circulation response to the changes in SWIO SST resemble those driven by ENSO and the cross-spectral analysis combine to support the hypothesis of Swann et al. (2003) that the SWIO is modulated at decadal timescales by ENSO teleconnections. The spatial structure of ENSO – identified through NINO 3.4 SST-based correlation analysis – strongly resembles the classic ENSO structure. It is likely that the use of the tropical Pacific NINO 3.4 SST index has generated a biased analysis in this respect, but it was the most suitable method for understanding the relationship to southern African rainfall. The decadal ENSO paradigm is not fully understood (Vimont, 2007), and it remains unclear whether there is an inherent difference between the Pacific Decadal Oscillation (Mantua et al., 1997) and the decadal ENSO-like structures in the tropical Pacific observed here.

Examination of the SAM index suggests that HadCM3 effectively integrates the southern hemisphere variability with ENSO, linking the variability in the South Atlantic, South (West) Indian Ocean and southern African rainfall. Comparison to the naturally-forced ECHO-G simulation was inconclusive; suggesting that the weak ENSO and reversed SWIO dipole influence in ECHO-G could be a result of the natural forcing or a model-specific simulation result. Although links to the decadal ENSO like variability were thought to influence the SW Indian Ocean, a substantial portion of variance remains unexplained by this relationship. Washington & Preston (2006)'s work at interannual scales may suggest a role for intrinsic decadal variability of the "SWIO dipole" region, but

such analysis has not been conducted here. The interaction of global teleconnections must not, therefore, rule out the possibility of intrinsic variability playing a role at decadal timescales.

5.4 Summary of Associated Variability

The previous chapter showed evidence of quasi-decadal variability in southern African rainfall in observed, proxy and simulated climate records. In this chapter, the variability in atmosphere and ocean fields associated with the rainfall variability has been presented. This section reviews the potential associations identified, and outlines the principal conclusions derived from these results.

First, some general comments about the nature and associations of decadal rainfall variability can be made. The evidence presented here, employing a range of correlation and regression techniques strongly suggests that the observed decadal variability is not simply an artifice of spectral techniques applied to rainfall. The identification of features with similar spectral powers in other ocean-atmosphere fields suggests that there is some basis for this variability in the (simulation of) climate.

In addition, the influence of anthropogenic forcing can be ruled out as the primary cause of this decadal variability. Although an anthropogenic signal has not been removed from the observed data presented here, a similar signal has been found in simulations driven by internal (HadCM3 control) and natural (ECHO-G ENAT, as well as corroboration from HadCM3 NAT) variability. This decadal rainfall variability has been observed in non-anthropogenic simulations, but there is some difference found in the associated variability across the different forcing scenarios. Further discussion of the influence of anthropogenic forcing is presented in the next chapter.

Finally, it is worth noting that none of the regions identified in the analysis presented here possess variability at the 18 year period identified by Tyson (1971). In the previous chapter, it was suggested that the integration of grid-scale resolution rainfall data produced a broader spectral peak (16-20 years), and that resolution issue may be carried over in to the analysis of associated variability. Some regions showed evidence of variability within this spectral band (or near it), but no single region possessed substantial cross-spectral agreement.

There is therefore thought to be general agreement in the way in which driving mechanisms operate, and there are two key findings which underpin all of the observed and simulated data. First, all results show a complex driving relationship linked to multiple regions, which 'wax and wane through the record' (Reason et al., 2004) and which are integrated with global (ENSO) and hemispheric-scale (SAM) mechanisms of variability at decadal scales. Second, the decadal variability appears to modulate the mechanisms of variability which operate at interannual scales, and the results indicate that the teleconnections identified in this study are consistent in scale and influence with those operating at seasonal to interannual time scales.

These two strands support the hypothesis of Vimont (2007), and suggests that the decadal variance identified is an extension of the interannual mechanisms, integrated by the coupled ocean-atmosphere system to produce quasi-decadal variability. The spectral analysis shows this to be significant relative to red-noise, suggesting that the interaction of the interannual mechanisms creates some coherence, rather than just reddening the spectrum in a random pattern. This may go some way to explaining why the 18 year

rainfall oscillation identified by Tyson (1971) and the broader decadal variability over southern Africa (Tyson & Preston-Whyte, 2000; Tyson et al., 2002) has never been precisely attributed to an individual mechanism. The analysis presented here strongly suggests that there is no "decadal" mechanism which influences rainfall over southern Africa, but that instead, the interannual mechanisms combine (with varying degrees of influence) to generate decadal variance in a consistent manner.

These mechanisms operate from commonly identified driving regions of oceanic influence. Of these, the tropical Atlantic is the least consistent across observed and model data results, and may remain model-specific as a result. In the observed data, there is little evidence of any relationship with the tropical Atlantic, while correlation is identified in the climate models. ECHO-G shows links to a narrow tropical region, but no consistent forcing mechanism is identified. By contrast, the HadCM3 simulations link to a tropical Atlantic dipole known to operate at all timescales, but this is thought to reflect likely loading patterns in sub-continental rainfall structures.

The South Atlantic Ocean – not typically associated with summer rainfall variability – was identified in some results, and thought to link to variability the SW Indian Ocean. Hermes & Reason (2005) proposed that this relationship could occur under a common atmospheric driver, and analysis of ECHO-G suggest the importance of the Southern Annular Mode in this teleconnection. However, the role of the SAM was not clear in either observed or HadCM3 simulated data, and remains a model-specific result at this stage.

All data sources identified a "dipole"-like feature in the South West Indian Ocean at decadal timescales, echoing the dominance of this region at interannual timescales. It was

shown to be substantially less coherent as a dipole at decadal scales, and therefore was examined separately as "tropical" and "subtropical" nodes (Washington & Preston, 2006). Although there is evidence for links between the tropical node and ENSO-like behaviour in all sources, the subtropical node appears to have a more ENSO-independent role. Given the work by Washington & Preston (2006) which identified the role of intrinsic (specifically, non-ENSO) variability in this region at interannual timescales, it is not clear whether similar intrinsic variability may operate at quasi-decadal scales.

The two nodes were shown to link to circulation features in the Mascarene region, with warmer (cooler) tropical (subtropical) SSTs driving enhanced high pressure and increasing the moisture flux in to a low-pressure dominated sub-continent. Washington & Preston (2006) identified this as "moisture-bearing circulation", and showed that although it did not always generate the expected rainfall response, this was likely to be a deficiency of the model's simulation of precipitation. This ocean-based forcing was therefore considered to be the most plausible mechanism by which southern African rainfall was influenced at decadal scales, and was demonstrated to be consistent through all results presented.

The SW Indian Ocean nodes were shown to agree with Washington & Preston (2006)'s findings (under non-ENSO conditions at interannual timescales) by having different relationships with southern African rainfall variability. The tropical node was shown to dominate the observed data and HadCM3's CTR simulation, while the ECHO-G 'ENAT' simulation was dominated by the subtropical node. This result is tested further in the next chapter, and hypothesised to be related to the role of natural forcing in the simulations.

This differing response also forms part of a wider hypothesis linking variability in the forcing regions to wider global teleconnections. The results suggest that the tropical Indian Ocean node has strong links to ENSO-type variability, whereas the sub-tropical node is related to covariance in the mid-latitudes and South Atlantic. The relative importance of these teleconnections is supported by evidence from the results.

In the observed data and HadCM3 CTR simulation, the quasi-decadal nature of the ENSO-like variability (represented by the NINO 3.4 SST index for analysis) is associated with a similar spectral response in the tropical SWIO node. The weaker subtropical node links to the South Atlantic, and although this node has evidence of ENSO-independent variability, it is dominated by the tropical ENSO signal at decadal timescales. The decadal ENSO-like behaviour, simulated by HadCM3, has not been evaluated in detail in this study, but it does appear to show similar teleconnections to the 'classic' ENSO spatial pattern.

This contrasts with the behaviour of ECHO-G, which exhibits little low-frequency variability in the NINO region and is known for weak ENSO simulation. Consequently, although the relationship with the tropical SWIO is retained, the region shows little influence over southern African rainfall at quasi-decadal timescales. This strengthens the relative importance of the subtropical node and the associated mid-latitude variability in the South Atlantic. Both regions are thought to be driven by variability in the Southern Annular Mode, with considerable cross-spectral agreement and strong relationships exhibited in the results. Under a weakened ENSO, this SAM variability is suggested as the likely common atmospheric driver proposed by Hermes & Reason (2005).

Although the global teleconnections have varying direct influence on southern African rainfall, the results presented here suggest they play a substantial role in modulating the variability of locally significant regions at decadal timescales.

At the interannual scale, Washington & Preston (2006) showed that the SWIO possessed intrinsic variability that operated independently of ENSO-like teleconnections. A similar analysis was not undertaken in this study, principally because of the difficulty of filtering specific signals from an already filtered dataset. The work presented here suggests that no individual teleconnection fully explains the variability in either southern African rainfall or individual "forcing" regions. This leaves the possibility of intrinsic variability as important at decadal scales also. Further work on understanding how the SW Indian Ocean operates, and what timescales are associated with its' internal variability would enhance our knowledge of this critical region for southern African rainfall. It seems likely that the relative strength of the teleconnections combines with intrinsic regional variability to provide ample decadal variation, and hence generate rainfall at these scales.

The model specific nature of this result cannot be avoided at this time. Although the observed data agrees with HadCM3, the inherent anthropogenic signal in the real-world data may render it an unsuitable comparator. Previous inter-comparisons of ENSO-simulation in climate models have presented the results of spectral analysis (Achuta-Rao & Sperber, 2002, 2006), but have been limited to variability at timescales less than ten years. Achuta-Rao & Sperber (2006) show that, despite improvements over the CMIP2 models, approximately 25% of IPCC models still fail to simulate a 2-7 yr spectral peak in NINO regions, and these models are also notable for their weak tropical SST variability.

This link between tropical SST and ENSO simulation ability gives credence to the hypothesis, but since the decadal behaviour of ENSO remains less well understood than the classic ENSO events, it should be examined in other climate models to better assess the likelihood of this being a specific result.

The poor understanding of decadal ENSO is not substantially advanced by this study. Use of the NINO 3.4 SST index is justified for the examination of relationships with southern African rainfall, but makes *a priori* assumptions that are not suitable for an investigation of the nature of decadal ENSO-like behaviour. It is not clear how the competing theories of tropical ENSO-like behaviour and the Pacific Decadal Oscillation are resolved in to understanding the variability in the Pacific, and more work will undoubtedly be done in this area in future.

We do not yet understand whether the variability of this region arises from integrations of high-frequency variance by the oceans to produce lower-frequency variability (Vimont, 2007), or if there are mechanisms which operate at quasi-decadal scales to generate independent variability. The analysis presented here shows that the global teleconnections associated with this variability remain similar in scope and influence to the classic ENSO forcing, and this may have implications for how decadal ENSO-like variability is perceived, and lend support to the integration hypothesis presented earlier.

It is also clear that comparisons between a model's control simulation and natural simulation will generate different results. Unfortunately, the absence of ECHO-G's control simulation means that direct comparisons are not possible in this study. However, the NAT simulation of HadCM3 displays a different response in certain areas of influence

over southern Africa. In particular, the nature of the forcing and response in the South West Indian Ocean is considerably altered compared to the CTR simulation, and it is thought that much of the modelled differences can be explained by the introduction of natural forcing in this region.

The implications for prediction or detection/attribution studies are therefore unclear. The nature of the associations identified, and their potential response to modulation of interannual forcing mechanisms holds a double-edged implication for rainfall predictability. The interaction of global teleconnections and local variability does not appear to have an underlying spectrum, and it is therefore difficult to assess the relative contribution of any particular region at a given or future time step. However, the quantification of seasonal-interannual prediction methods can be applied once forcing events (e.g. El Nino event) are identified, and this should mean reduced prediction uncertainty associated with low-frequency variability.

In order to better understand how knowledge of this variability can be used in detection/attribution studies, the response of southern African rainfall variability to different forcing conditions need to be considered. Results from an investigation using suitable simulations of HadCM3 and ECHO-G are presented in the next chapter.

(6) Is decadal variability altered by anthropogenic forcing?

If detection and attribution of anthropogenic forcing is to be performed on observations of southern African rainfall variability, then understanding the natural decadal variability identified in the previous chapter is the first step (Hegerl et al., 2007). In addition, the fingerprint of the anthropogenic signal needs to be accurately identified (Hegerl et al., 1996; Allen & Stott, 2003). This chapter aims to explore the effects of anthropogenic forcing on decadal variability of rainfall over southern Africa in order to increase our knowledge of the impacts of anthropogenic change on decadal variability.

This variability is first explored in coral reef proxy data, which is thought to represent SST variability in the South West Indian Ocean and its likely influence over southern African rainfall. Damassa et al. (2006) present analysis which suggests that the secular warming trend of the twentieth century reduces the spectral signal of decadal variability, and this hypothesis is investigated in proxy data and state of the art anthropogenically forced climate model simulations (Gonzalez-Rouco et al., 2003; Tett et al., 2007).

Having ascertained the likely spectral response to anthropogenic forcing, this chapter then examines what is likely to change in decadal rainfall variability – in terms of spatial distribution or spectral power, and potential alterations to the associated ocean-atmosphere interaction. Given the differences in model simulation of teleconnections in the previous chapter, the experiments from ECHO-G and HadCM3 are considered separately.

6.1 Evidence from Proxy Data

The limitations of the observed record in examining variability in the tropical/subtropical climate have created interest in proxy records. The use of these records allows comparisons between "natural" (pre-industrial) and "anthropogenic" conditions in 'real world' data: a major advantage over the observed record. In the Indian Ocean, previous work has indicated the importance of (intrinsic) SST anomalies in the south west of the basin for southern African rainfall (Reason & Godfred-Spenning, 1998; Reason, 2000; Reason et al., 2000; Zinke et al., 2004; Washington & Preston, 2006), and proxy records from this region are critical to understanding the long-term variability of the Indian Ocean's influence on southern African climate.

Although dendrochronology contains useful information about the state of the climate over the sub-continent, it is coral reef data which provides insight in to the variability of the oceans (Bradley, 1999; Grottoli & Eakin, 2007). Studies in the western Indian Ocean have largely concentrated on the relationship with ENSO. A 150 year coral core from the Seychelles (Charles et al., 1997), 160 year core from La Reunion (Pfeiffer et al., 2004) and a 194 year core from Kenya (Cole et al., 2000) provided the technique validation studies, and longer cores have subsequently been extracted from Madagascar (Zinke et al., 2004), Kenya (Kayanne et al., 2006) and Tanzania (Damassa et al., 2006).

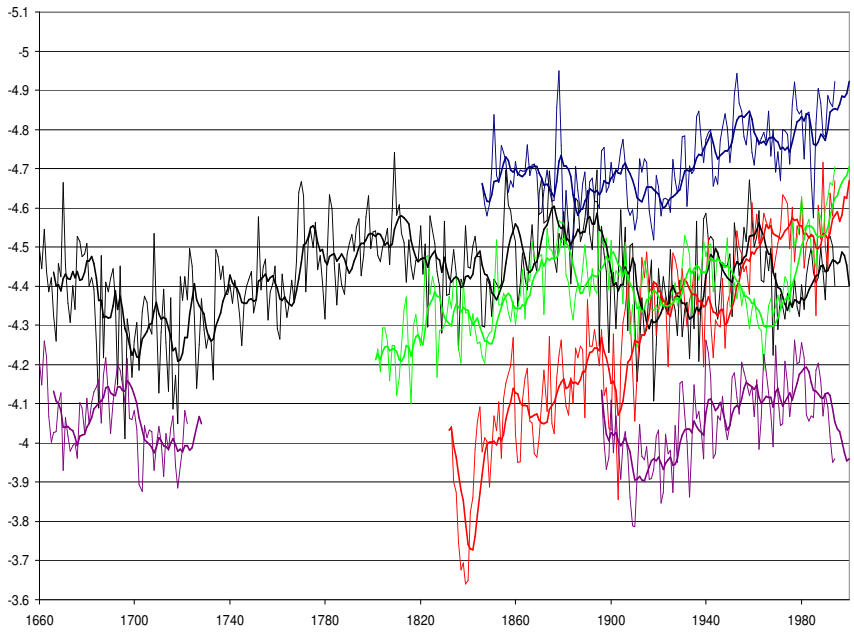

Figure 6.1: Plot of mean (JFM) $\delta^{18}O$ reconstructions using coral-based proxy records in the South West Indian Ocean region. Source regions: Seychelles (blue line), Ifaty (black line), La Reunion (red line), Malindi (green) and Mafia (purple). The smoothed line is the running mean (7 yr period). Note that the y-axis is reversed.

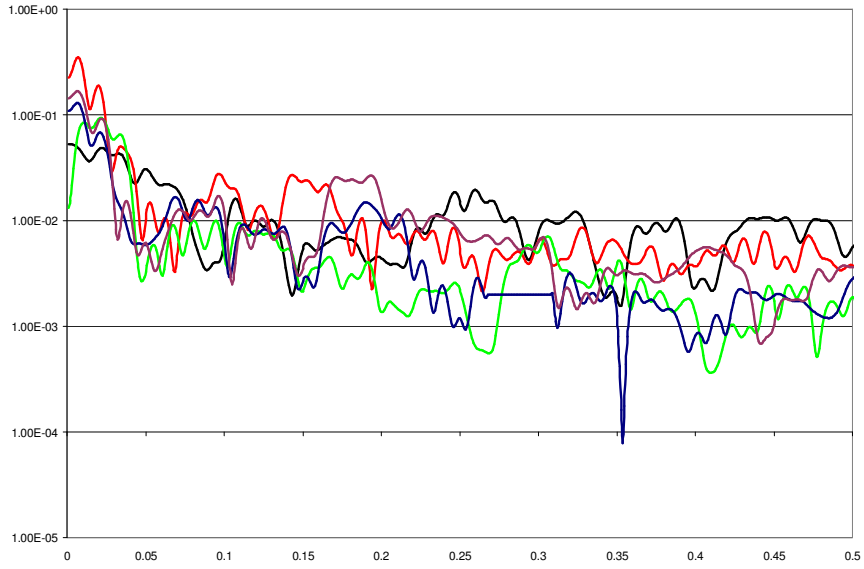

Figure 6.2: Spectral analysis (MTM; unfiltered) of mean JFM $\delta^{18}O$ reconstruction using coral-based proxy records for the twentieth century only. Source regions are defined as for the previous figure.

These studies have typically regarded the $\delta^{18}O$ of the coral reef records as a proxy for SST, and carried out cross spectral analysis with indices for ENSO, East African rainfall or the Indian monsoon regions (Kayanne et al., 2006). They have found correlations with ENSO, and interannual variance similar to ENSO periodicities and longer inter-decadal periodicity during the 17th century.

Figure 6.1 shows a summary of the data from these cited studies. Annual laminations are used for some proxy sources; otherwise the JFM mean is calculated from the monthly resolution data. Full details of the extraction and calibration techniques can be found in the papers describing the individual datasets. The influence of anthropogenic forcing on the trend of the data is apparent from ~1820 onwards, and the 7yr running mean shows evidence of variability throughout the records. Figure 6.2 shows a combined plot of spectral analysis of the proxy records using data from the 1890s onwards, since all records cover this period.

This analysis supports the ability of proxy records to capture a range of timescales of variability. Quasi decadal variability is evident in all coral records, and is particularly important in the La Reunion and Malindi sites. Both have spectral peaks at ~37 years, and La Reunion also shows spectral power at 25.6 years. The cores from Ifaty and the Seychelles show spectral peaks between 11-13 years, with Ifaty showing harmonic power at 15.6 yrs. The majority of the records incorporate some sort of 'classic' ENSO signal (3-7 year spectral power), in keeping with the focus of the coral studies.

Damassa et al. (2006) use *Diploastrea heliopora* coral cores from the Mafia archipelago off the Tanzanian coast to compare the strength of interannual variability in the Indian

ocean between the seventeenth and twentieth centuries, and to explore potential links with change in ENSO strength. They demonstrate that the major difference between records lies in the low-frequency variability structure, where the twentieth century record is shown to be dominated by a secular trend (probably anthropogenic forcing).

Figure 6.3 shows the spectral analysis of both 17th (black line) and 20th century (red line) records. Peaks at 18.5 and 26.3 years in the 17th century spectrum are part of a wider dominant period between 15-35 years by comparison to the 20th century spectrum. The analysis shows that the 20th century record is not without spectral power of its' own – there are peaks between 5.1-5.8 years and 10.3-13.89 years, together with some peaks in the 2-3 year range – but the quasi-decadal frequency band is substantially reduced by comparison to the seventeenth century. This low frequency variability is identified as the principal SSA-reconstructed component in Damassa et al. (2006)'s analysis, explaining 32% of the $\delta^{18}O$ variance. Other published records – including reconstructions of the Nino 3.4 SST index (Mann et al., 2000; D'Arrigo et al., 2005), Northern Hemisphere temperatures (Mann et al., 1998), and the PDO (Gedalof & Smith, 2001) – display prominent interdecadal (15-35 yrs) oscillations that agree well with the Mafia record (Cobb et al., 2003; Damassa et al., 2006).

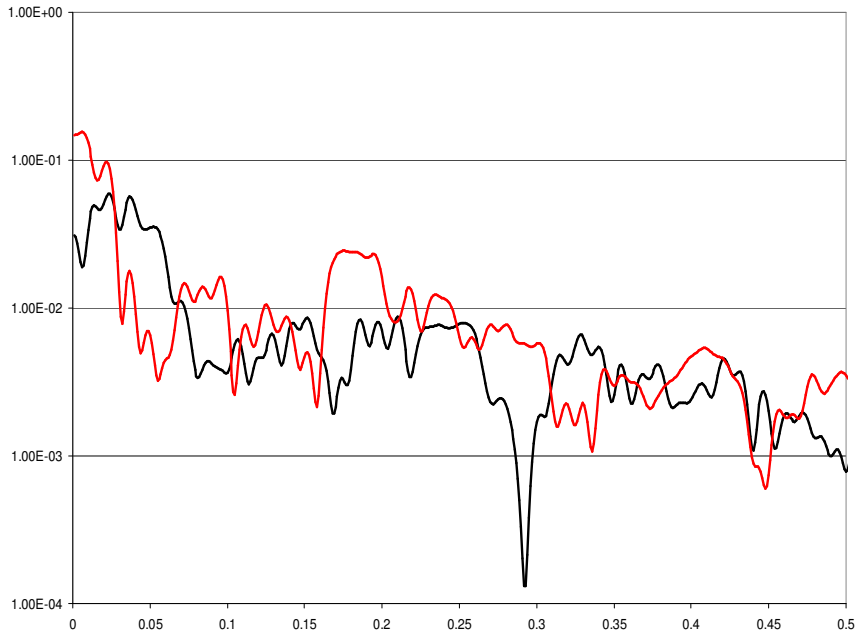

Figure 6.3: Spectral analysis (MTM; unfiltered) of Mafia coral records from the 17th century (black line) and 20th century (red line), following Damassa et al. (2006).

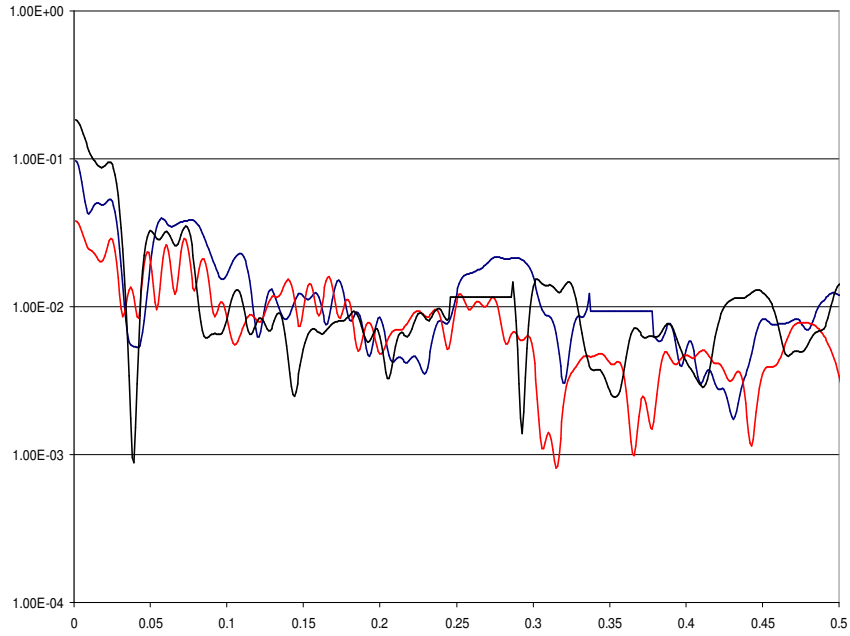

Figure 6.4: Spectral analysis (MTM; unfiltered) of Ifaty coral record segments. Blue line: 17th century variability (as for Mafia records); Red line: transition period (1723-1896); Black line: twentieth century variability (as before).

Further comparison is made to the coral record of Zinke et al. (2004) from the Ifaty lagoon (SW Madagascar) which extends back to 1660 and can be analysed in a similar method. Figure 6.4 shows the spectral analysis of three 100 year segments of the Ifaty core, dating from 1660-1760 (blue line), 1761-1860 (red line) and 1861-1960 (black line). Like the Mafia coral record, there is a period of substantially higher power in the 1660-1760 segment, showing peaks at 9.0 yrs and enhanced power at 12.5-17.24 yrs. The 1860-1960 record is dominated by the secular trend, registering as enhanced power above ~35 years in the spectral analysis. The quasi-decadal timescale is marked by a notable drop (around ~25.6 yrs), suggesting an agreement with the key finding of Damassa et al. (2006). The 19th century (1761-1860) record is included for comparison, and shows little evidence of power at almost all periods. This may be indicative of a 'transition' period as the anthropogenic forcing begins to become important, but further speculation would be imprudent.

These results suggest a common pattern of low-frequency variability in the seventeenth century that involves tropical and extra tropical regions. Damassa et al. (2006) suggest that the interdecadal variations of climate in this region (potentially analogous to Mantua et al. (1997)'s twentieth century PDO) had a relatively strong effect in the seventeenth century compared to the twentieth, where the interannual variability and secular warming trend dominate the record.

It is clear from spectral analysis and visual inspection of the record in Figure 6.1 that quasi-decadal variability exists in the twentieth century, but that the substantial anthropogenic forcing damps the response considerably by comparison (Damassa et al.,

2006) and may change the 'spatial signature' of ENSO (Zinke et al., 2004). The lack of such forcing in the seventeenth century is thought to enable the emergence of a different low-frequency structure of variability (Damassa et al., 2006).

Unlike the observed data, which is intrinsically entwined with the anthropogenic climate signal, the proxy data presented here has demonstrated the potential to separate "natural" and "anthropogenic" forcing in real world measurements of climate variables. Based on the work of Damassa et al. (2006), it has been shown that the "naturally forced" records show considerably more quasi-decadal variability than is found in the twentieth century records. This damping is thought to be the result of a dominant secular warming trend imposed upon the post-industrial climate, and the twentieth century record subsequently reflects the interaction between natural and anthropogenic forcing mechanisms.

Although this provides an interesting basis for detection and attribution questions, the nature of coral proxy records minimises the potential for hypothesis testing. However, the climate model simulations made available for use in this study (ALL250 and ERIK) are ideally suited for the investigation of quasi-decadal variability in southern African rainfall, and their response to anthropogenic forcing. In examining the model simulations, the aim is to understand the nature and mechanisms of climate variability more completely, and to establish if anthropogenic forcing generates different results to those presented in the previous chapters. The results of this investigation are presented in the next section.

6.2 Evidence from Climate Simulations

The climate model simulations offer the potential to study the behaviour of the climate system under anthropogenic forcing, and comparison with the control and naturally forced simulations presented earlier in the study provide some insight in to how the nature and mechanisms of variability may be influenced. To begin, the simple spectral nature of variability is examined under the forcing simulations, and differences are compared to the control and natural simulations. Next, the potential mechanisms of variability under anthropogenic forcing are compared to the previous results, in order to explore the way in which the additional forcing alters the relationship between southern African rainfall and wider ocean-atmospheric variability. The modelled mechanisms are examined separately, since it has already been shown that their simulations of quasi-decadal variability differ.

First, simple spectral analysis is carried out on the simulated sub-continental rainfall index from HadCM3 (ALL250) and ECHO-G (ERIK). ALL250 shows classic ENSO-like spectral features (3-7 years), but little quasi-decadal variability (Figure 6.5). The centennial variability (99% confidence) is thought to be a reflection of the anthropogenic trend, or possibly a spectral artifice given the relatively short record length. By contrast, the ERIK spectrum shows quasi-decadal power with peaks at 12.6 (95% confidence), 40 yrs (harmonic power), and the centennial peak of 160 yrs (99% confidence) is thought to be a more robust result because of the record length (Figure 6.6).

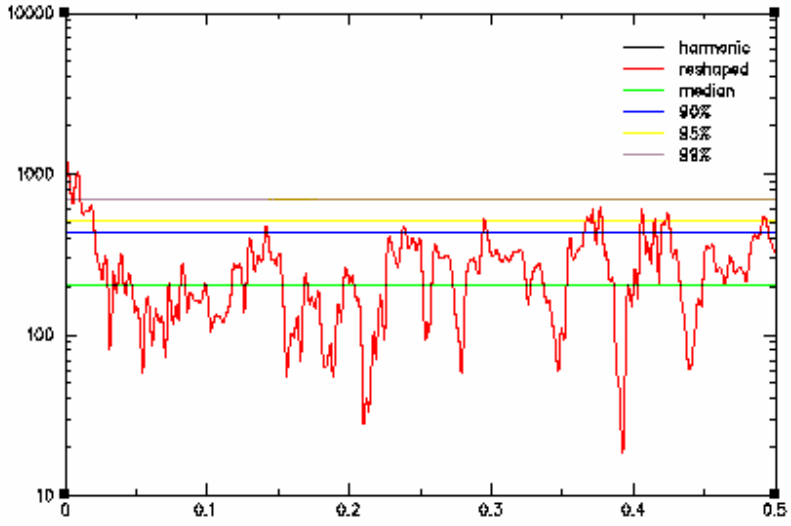

Figure 6.5: Spectral analysis (MTM, unfiltered), HadCM3 ALL250 simulation of sub-continental rainfall (15-35ºS, 15-35ºE)

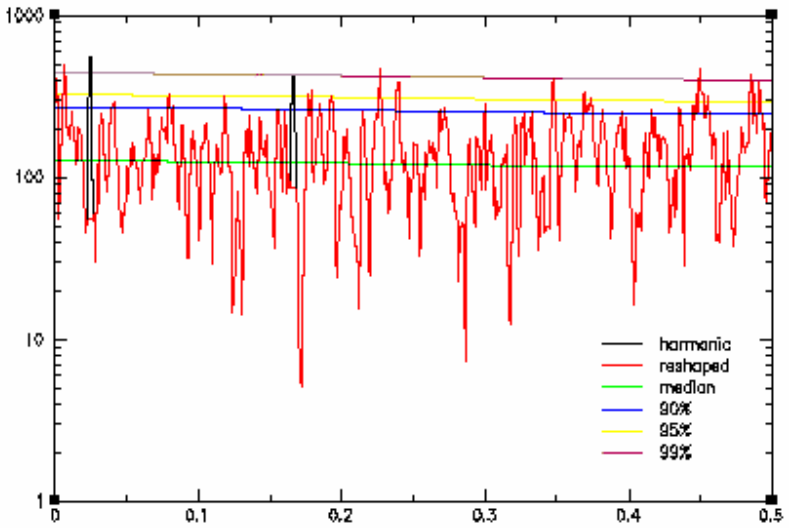

Figure 6.6: Spectral analysis (MTM, unfiltered), ECHO-G ERIK simulation of sub-continental rainfall (15-35ºS, 15-35ºE)

For HadCM3 in particular, the relative record length makes it possible that the absence of quasi-decadal variability in the anthropogenic simulation is a result of a naturally induced period of low decadal variability in the model. Comparison is therefore made to 20 samples of 250 yrs which have been estimated from different points within the CTR simulation, with the sample start years determined using "Monte Carlo" techniques (Allen & Smith, 1996). The MTM analysis of the ALL simulation (red line) is within the ensemble range for most periods lower than 8 yrs, but considerably reduces in spectral power compared to the ensemble between 8 and 20 years (Figure 6.7). At certain frequencies of interest – e.g. the 16-20 year band of power, the ALL simulation is outside the ensemble range by a clear margin, while at others (e.g. the 10-12 yr spectral band), the ALL simulation falls towards the lower range of the CTR ensemble. This analysis is repeated for the NAT simulation. The ALL simulation also falls outside the envelope of NAT variability between 12-25 years. There is generally greater agreement in the spectral variation of the NAT-simulated samples, but this may be explained by the shorter duration of the model run and reduced range of potential ensemble components.

Similar comparisons using the ECHO-G model data prove to be more complicated. The anthropogenic simulation (ERIK) is the longer (990 yr) of the runs available, with the naturally forced ENAT simulation only providing 220 years of data. However, the 990 year ERIK data set encompasses a range of forcing conditions, and can be split in to three distinct sections which possess slightly different spectral characteristics (Figure 6.8). A relatively unforced period (1000-1250) shows similar spectral power to the anthropogenic period (ANTH; 1750-1990).

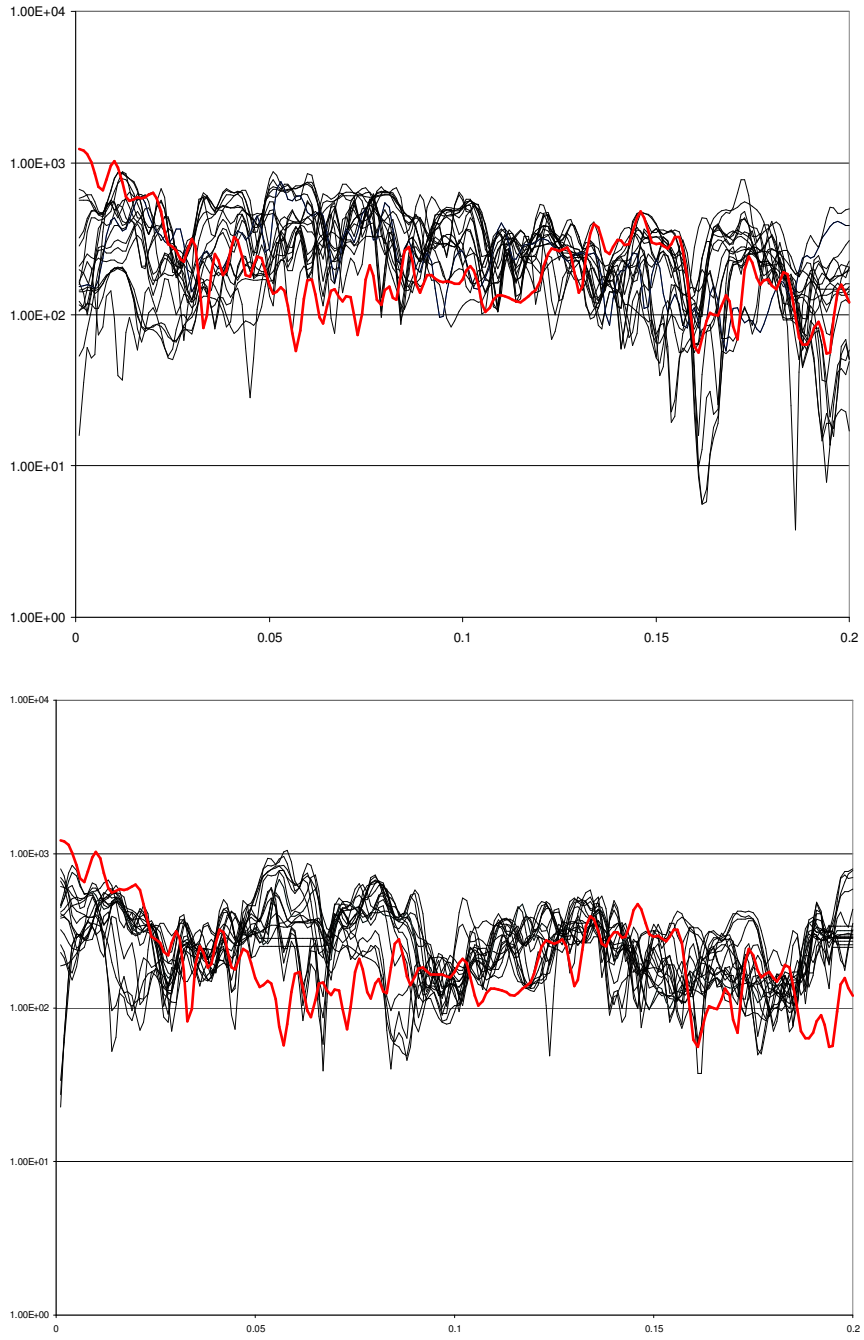

Figure 6.7: Spectral analysis (MTM, filtered) of ALL250 simulated sub-continental (15-35ºS, 15-35ºE) rainfall (red line), and twenty samples of non-anthropogenically forced sub-continental rainfall (black lines), filtered using a 7-50 year band pass filter. Start points for the control/natural simulations were chosen by random number generation. Top: CTR simulation samples, bottom: NAT simulation samples.

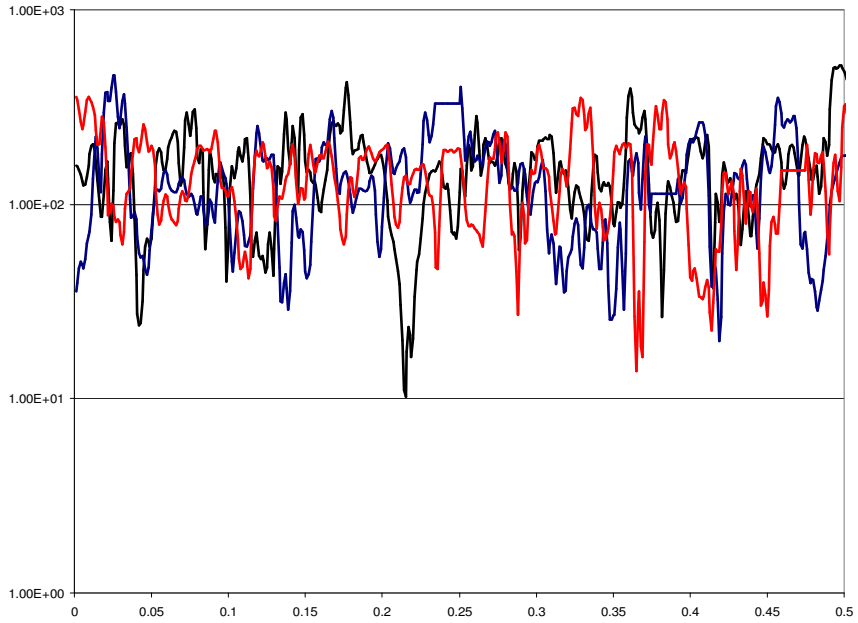

Figure 6.8: Spectral analysis (MTM, unfiltered) of rainfall as simulated by three sample periods from the ERIK simulation. Black line: 1000-1250; blue line: 1500-1730 (equivalent to ENAT simulation period), and red line: 1750-1990 (equivalent to HadCM3 ALL250 and described as "anthropogenic" throughout this chapter).

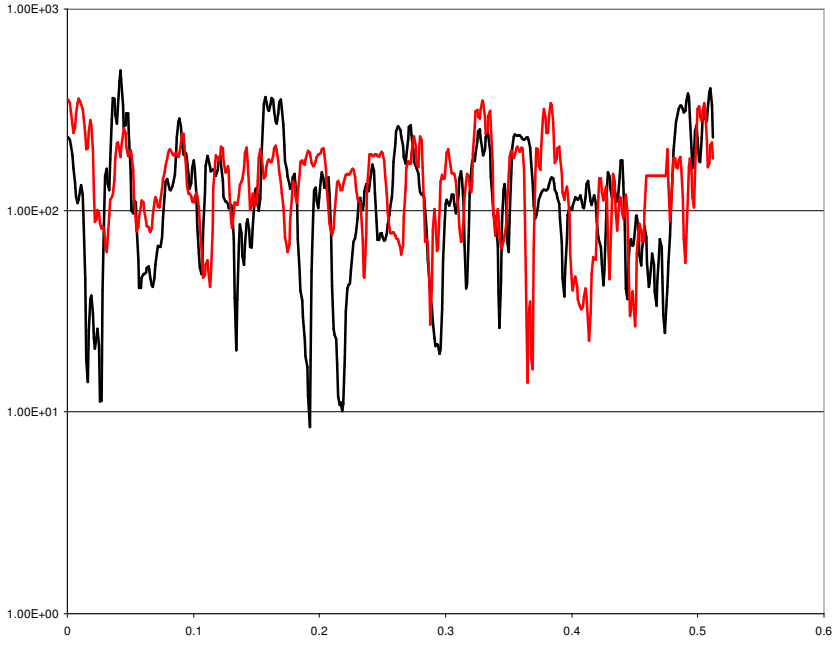

Figure 6.9: Spectral analysis (MTM; unfiltered) of the sub-continental (15-35ºS, 15-35ºE) rainfall index under ENAT simulation (black line) and the anthropogenic (1750-1990) section of the ERIK simulation (red line).

The ‘transition’ period – a similar time period to the ENAT simulation, and thought to have similar forcing characteristics – appears to have different spectral power, particularly in the simulation of quasi-decadal variability between 20-30 years. The ANTH (1750-1990) range of variability has the strongest anthropogenic signals, and this period is therefore utilised through the rest of the chapter as a focus for anthropogenic changes in ECHO-G. Specific comparison between the ANTH (1750-1990) spectrum and ENAT simulated spectrum is presented in Figure 6.9, and shows that ENAT’s variability differs subtly to the ‘unforced’ ERIK time periods (1000-1250, 1500-1730). ANTH (red line) agrees broadly with the ENAT simulated peaks (black line), showing enhanced power in the ‘classic’ ENSO timescales, and in the quasi-decadal range between 20-30 years.

In HadCM3, the behaviour of the anthropogenic (ALL) simulation appears to be substantially different from the range of spectral power taken from CTR and NAT simulations, with the clear separation increasing the confidence in this result. This suggests that anthropogenic forcing has an important role to play in HadCM3.

The variability in ECHO-G is less clearly identified. It appears that a shift in ENSO-like variability takes place under anthropogenic forcing, and low-frequency variability is also affected. It is possible that the enhanced low-frequency (quasi) centennial variability in both anthropogenic simulations is a reflection of the secular warming trend described by Damassa et al. (2006), but this is difficult to isolate and does not seem consistent with the nature of the digital filter applied. The reduced quasi-decadal variability in ECHO-G is likely to be further influenced by anthropogenic trends, but it is difficult to determine the precise nature of variance at this time.

Both models are therefore investigated to explore how the anthropogenic forcing may influence the modification of southern African rainfall at decadal timescales. Having shown in the previous chapter that the models show substantial differences in their simulation of decadal variability, they are investigated separately.

6. 2. 1 Anthropogenic Simulation under ECHO-G

This section aims to explore what changes under forcing scenarios in ECHO-G, beginning with an examination of the spatial nature of rainfall through EOF analysis. As in Section 4. 3. 1, the leading EOFs of decadally filtered (7-50 year band pass) rainfall data are presented in Figure 6.10. There are only minor differences to the EOFs simulated by ENAT, although the order of EOFs 2 and 3 are reversed. EOF 1 explains 11.9% of variance (ENAT EOF 1: 14.0%), while EOF 2 and 3 explain approximately 9.0% and 7.6% of variance respectively (ENAT EOF 3: 8.1% and EOF 2: 10.3% as equivalent spatial patterns). This suggests that the spatial pattern of rainfall is not the main change under anthropogenic forcing, and this means that the sub-continental rainfall index can continued to be used as the basis for analysis. Analysis of the potential mechanisms influencing southern African rainfall starts with the consideration of the variability associated with decadal sub-continental rainfall. Figure 6.11 shows the range of spatial correlation maps generated by different sections of the ERIK simulation. Although there are broad similarities in the correlation regions, the strength in individual areas varies subtly, and is weakest in the analysis based on the full 990 year record.

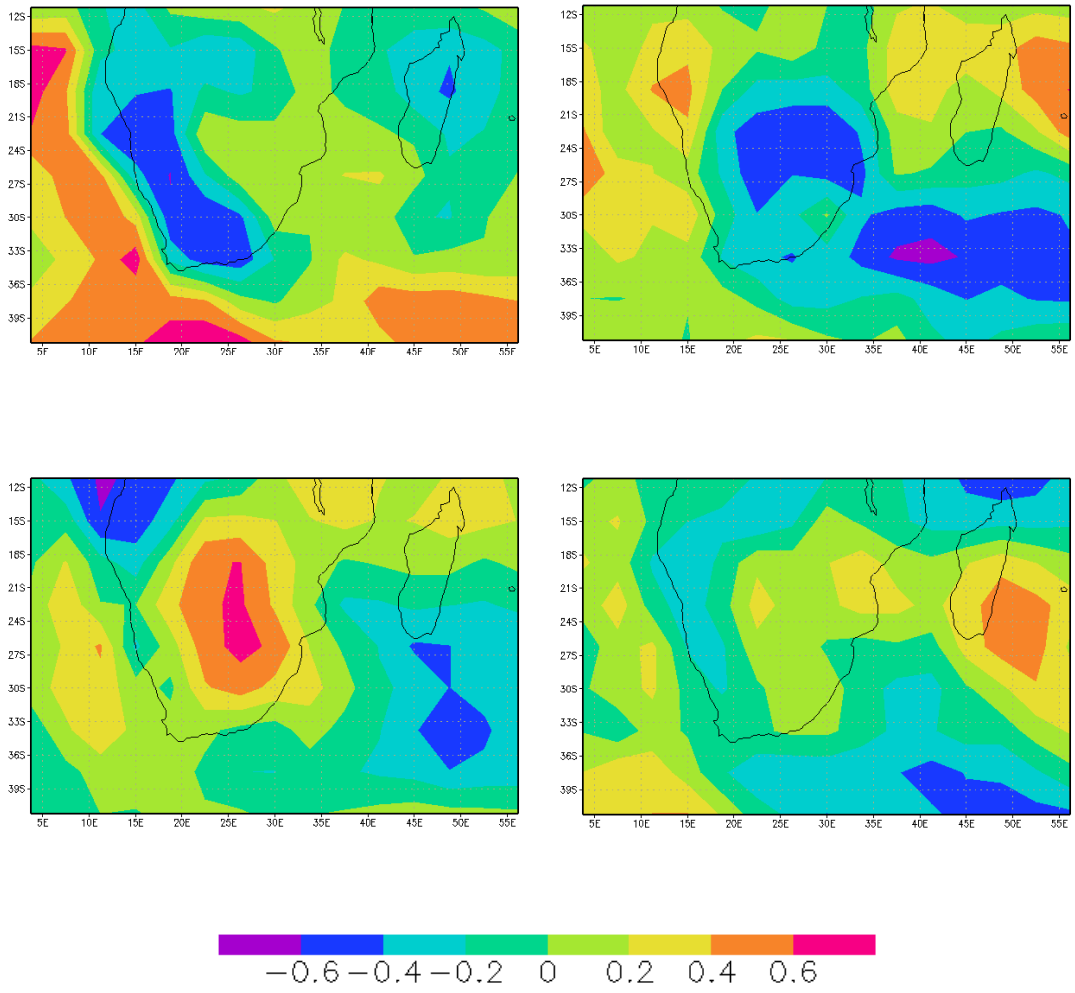

Figure 6.10: EOF analysis of filtered (7-50 yr BP) rainfall over southern Africa simulated by ECHO-G ERIK under anthropogenic years 1750-1990. Top left, EOF 1; top right, EOF 2; bottom left, EOF 3; bottom right, EOF 4.

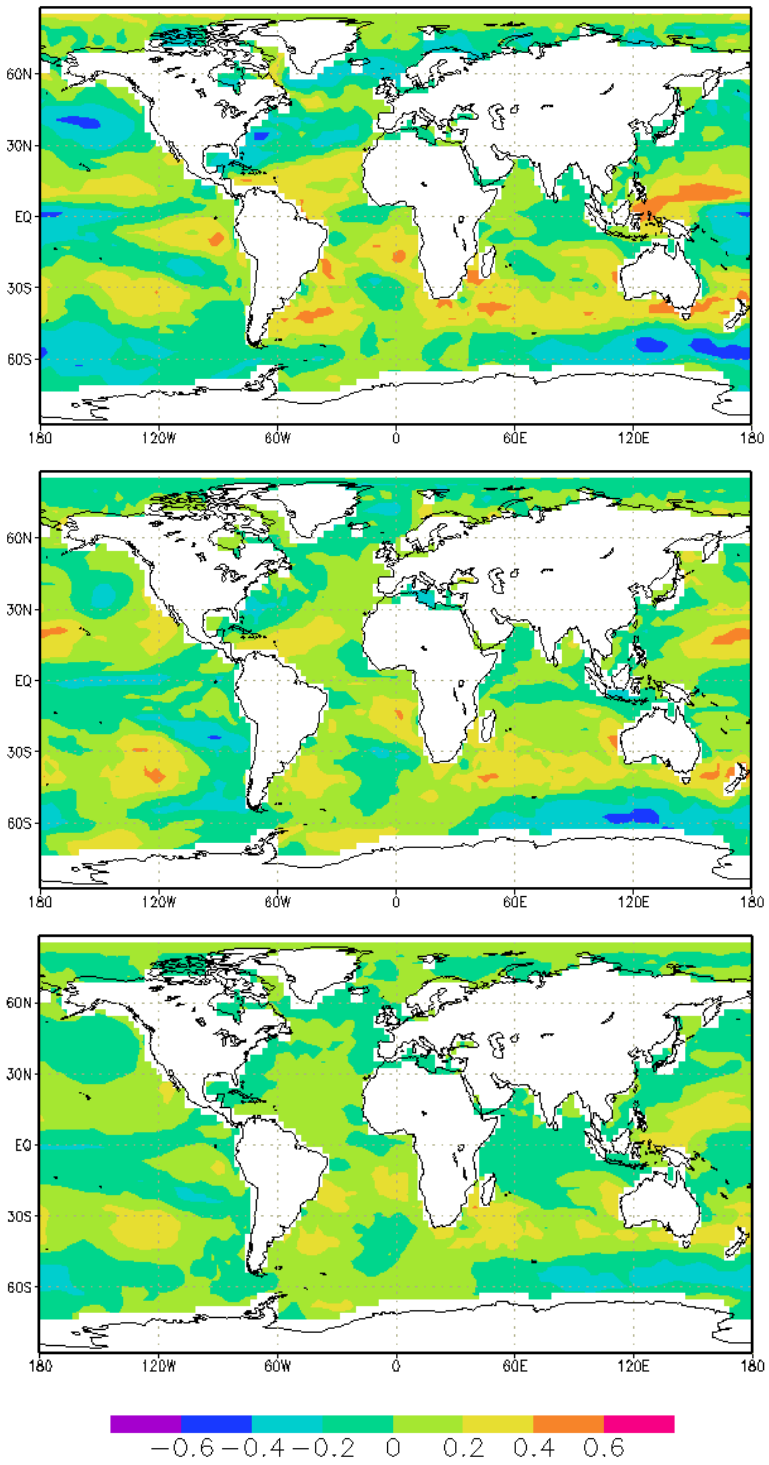

Figure 6.11: Correlation between the time series of ERIK simulated-rainfall (15-35ºS, 15-35ºE) and global SST for sample time periods within the ERIK simulation. Top: 1000-1250, middle: 1750-1990, and bottom: full 990 year simulation.

Focusing on the ANTH section of the ERIK run (1750-1990), the main areas of correlation are not dissimilar to previous analysis. The "dipole" in the SWIO appears slightly different, and may be more centrally located in the Indian Ocean than in other simulations and models. Studies show that the relationship with southern African rainfall may be controlled by the proximity of the dipole to the coast (Behera & Yamagata, 2001; Reason, 2002; Hansingo & Reason, 2006), and the increased distance observed here may well explain the reduced influence of this region over the continental rainfall.

The decadal rainfall variability in the ANTH (240 years) shows a strong relationship with Southern Annular Mode (SAM)-type variability, and associated variability in the South Atlantic (r=0.317) and subtropical SWIO (r=0.298). Both SST regions show strong correlation with the SAM index (SATL: r=0.604; subtropical SWIO: r=0.495) and with each other (r=0.515) echoing the possibility of a common atmospheric forcing mechanism suggested in the previous chapter (Hermes & Reason, 2005). By comparison to ENAT, this SAM-based relationship is slightly enhanced, but the largest difference is in the augmented role of ENSO and influence over the tropical SWIO. Although still relatively weak (NINO r=-0.174; tropical SWIO r=0.145), the relationship shows a substantial strengthening compared to the same regions in ENAT (NINO 3.4 r=-0.048; tropical SWIO r=-0.0679). The correlation sign in tropical SWIO has reversed by comparison, with a positive relationship in ERIK ANTH compared to ENAT's negative relationship.

Although the initial spectral analysis of decadal variability was relatively inconclusive, the correlation shown in Figure 6.11 suggests that there are substantial changes in the

behaviour of the ERIK ANTH section compared to ENAT. The regions are considered separately, as in Chapter (5).

The South Atlantic region is briefly examined first. Defined by the region of maximum correlation as 35-45°S, 60-30°W, this region shows enhanced power across the spectrum in the ANTH segment (Figure 6.12). As well as the addition of unexplained power at centennial scales, the power is enhanced at ~10 years (95% confidence) and ~3 years by comparison to the ENAT spectrum, but this increased power is not immediately evident in spatial correlation patterns. The correlation maps appear very similar to those identified in ENAT, and are therefore not presented here. A slightly increased influence spreading up to the Tropical Atlantic is a minor change, but the strong correlation with of South Atlantic SST index with the subtropical SWIO region suggests that this remains the most likely link to southern African rainfall at decadal scales.

Like the South Atlantic, the subtropical SWIO (defined for this analysis as 30-40°S, 40-60°E) has broadly enhanced power across the spectrum, with particular peaks at ~10 years (95% confidence) and 6 years (95% confidence) which appear likely to be connected to similar power in the global teleconnections of ENSO and SAM (Figure 6.13). The spatial correlation pattern reflects a slightly more central maximum correlation location (Figure 6.14), and the shift of the peak correlation region away from the sub-continent may explain the reduced influence of this region (Behera & Yamagata, 2001) compared to the relationship observed in ENAT.

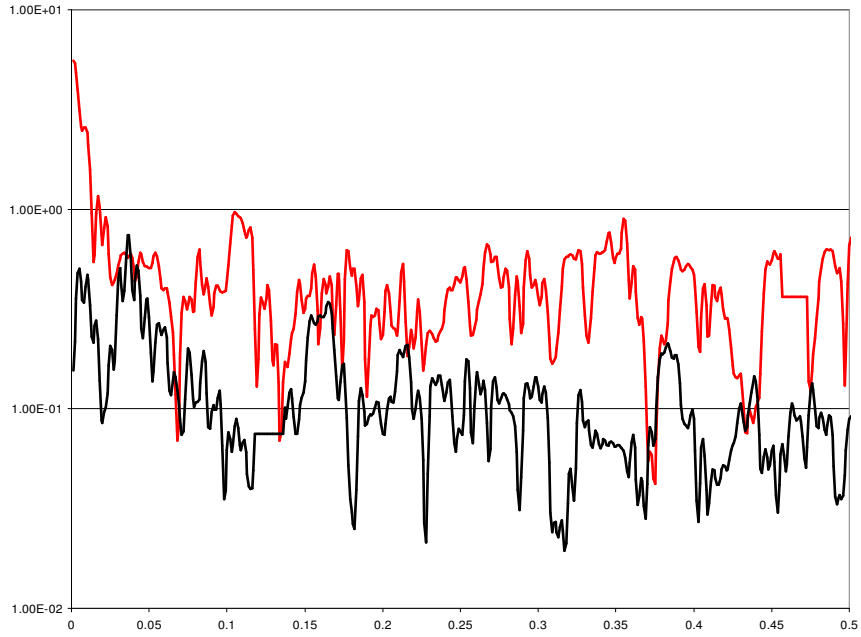

Figure 6.12: Spectral analysis (MTM; unfiltered) of the ECHO-G South Atlantic SST index region under ENAT simulation (black line) and the anthropogenic (1750-1990) section of the ERIK simulation (red line).

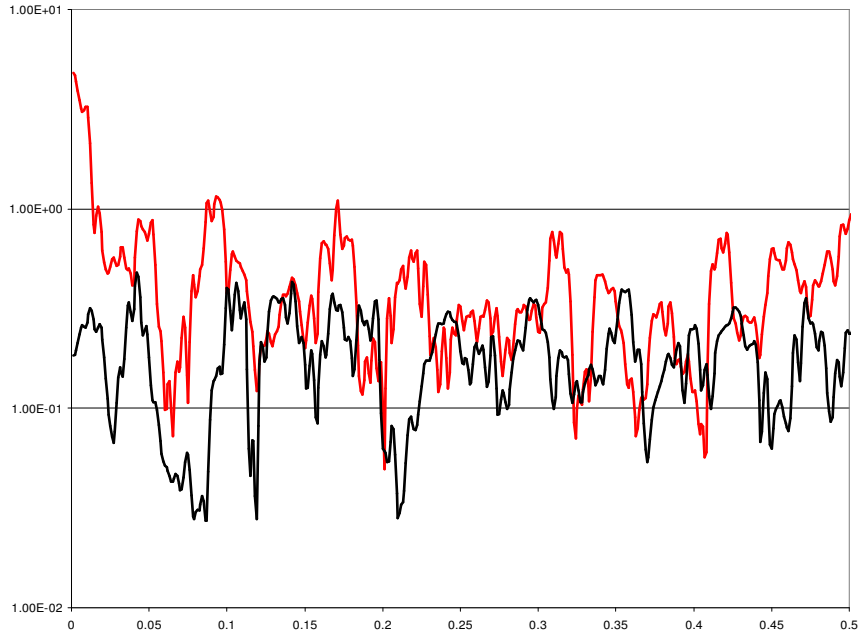

Figure 6.13: Spectral analysis (MTM; unfiltered) of the ECHO-G subtropical SWIO SST index region under ENAT simulation (black line) and the anthropogenic (1750-1990) section of the ERIK simulation (red line).

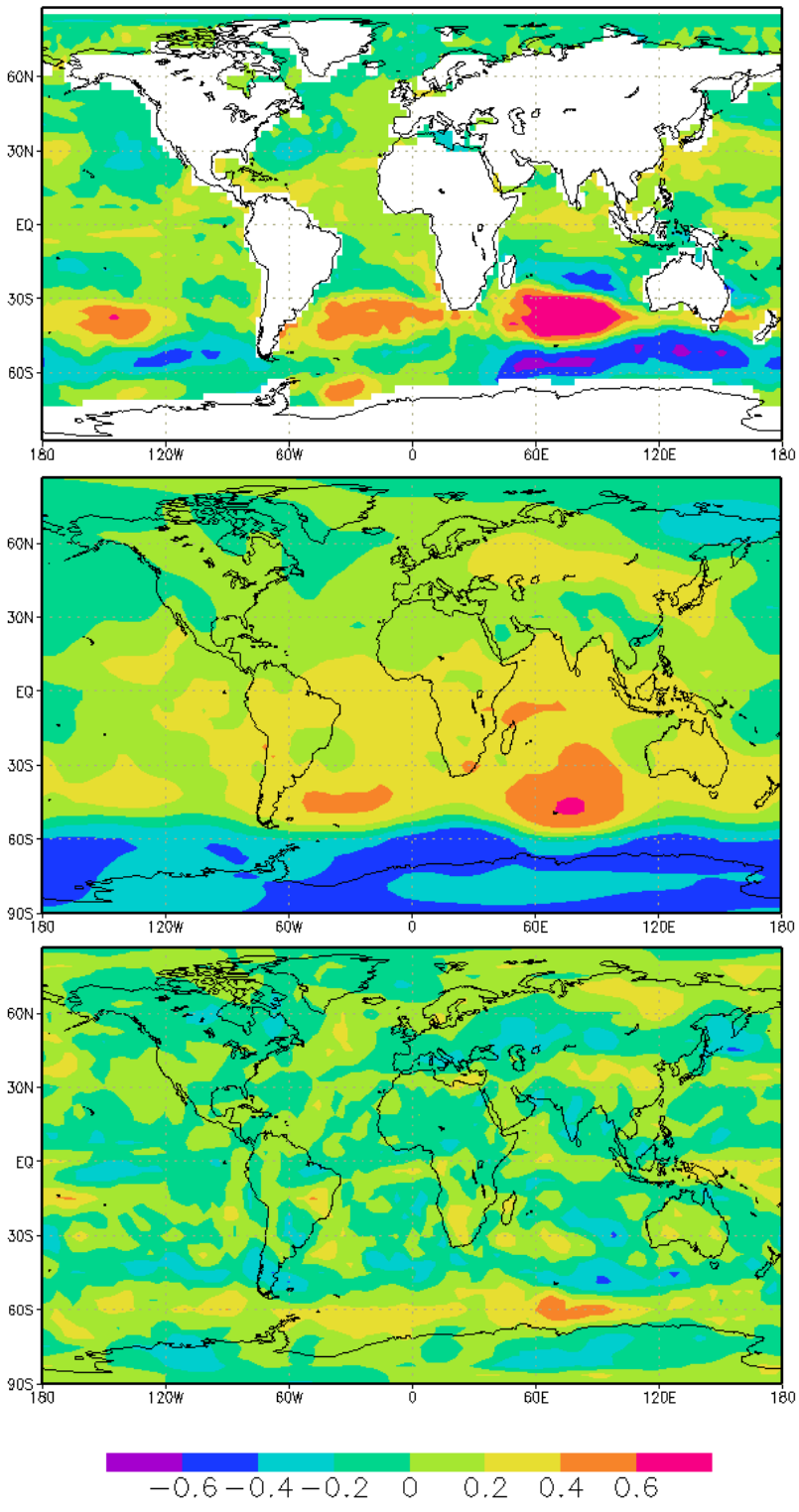

Figure 6.14: Correlation between the timeseries of ECHO-G ERIK (1750-1990) subtropical SWIO SST index and global fields. Top: global SST, middle: global SLP, bottom: global rainfall.

Similarly, the tropical SWIO correlation region has shifted 10-15° south and 10° east, in to a more central position in the Indian Ocean (15-30°S, 70-90°E). This may explain the reversed SLP patterns (Figure 6.15) compared to ENAT, and the increased rainfall correlation under anthropogenic forcing. Unlike the majority of regions in the analysis of ECHO-G ERIK, however, the tropical SWIO does not have especially enhanced spectral power (Figure 6.16).

There are some regions of power which are raised above the ENAT spectrum (e.g. at ~10 years, ~7 years and ~6 years), but these do not reach levels of significance (90% confidence) in the MTM analysis (not shown). The weakened link between SWIO SST and ENSO (r=0.186 compared to r=0.695 in ENAT) may explain the southward shift in the SST region, but it is not clear why this would occur.

This change is particularly difficult to attribute, since the spatial structure of correlation between ENSO and global SST is relatively unchanged (Figure 6.18). It seems possible that enhanced quasi decadal power in the simulation of ENSO itself (Figure 6.17) could be responsible for the increased influence on rainfall (r=-0.17 compared to ENAT r=-0.04).

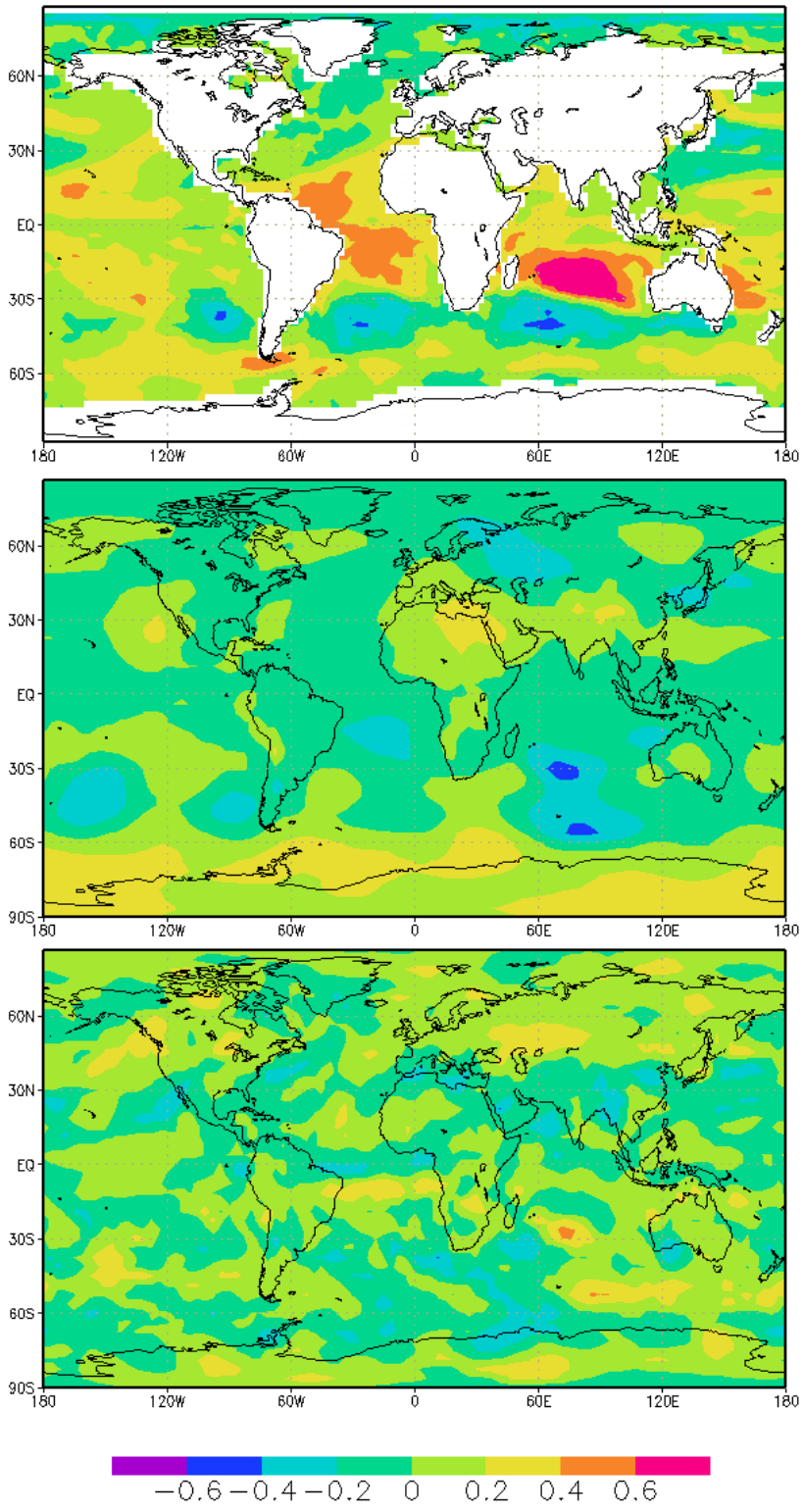

Figure 6.15: Correlation between the timeseries of ECHO-G ERIK (1750-1990) tropical SWIO SST index and global fields. Top: global SST, middle: global SLP, bottom: global rainfall.

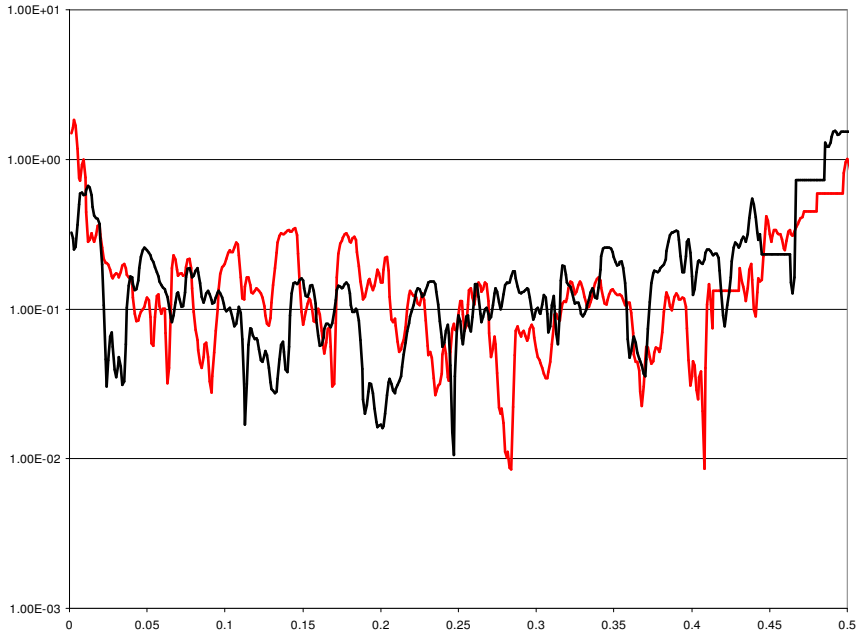

Figure 6.16: Spectral analysis (MTM; unfiltered) of the ECHO-G tropical SWIO SST index region under ENAT simulation (black line) and the anthropogenic (1750-1990) section of the ERIK simulation (red line).

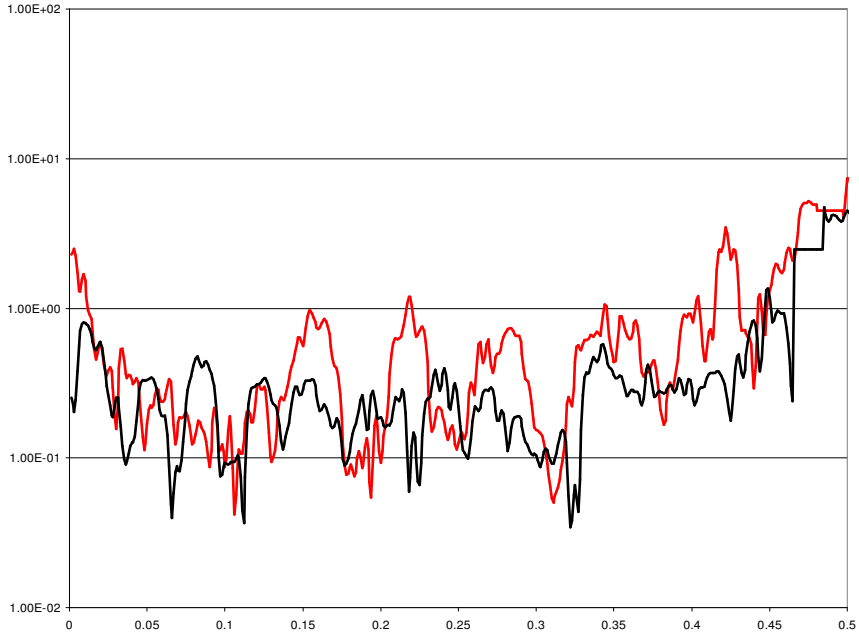

Figure 6.17: Spectral analysis (MTM; unfiltered) of the ECHO-G NINO 3.4 SST index region under ENAT simulation (black line) and the anthropogenic (1750-1990) section of the ERIK simulation (red line).

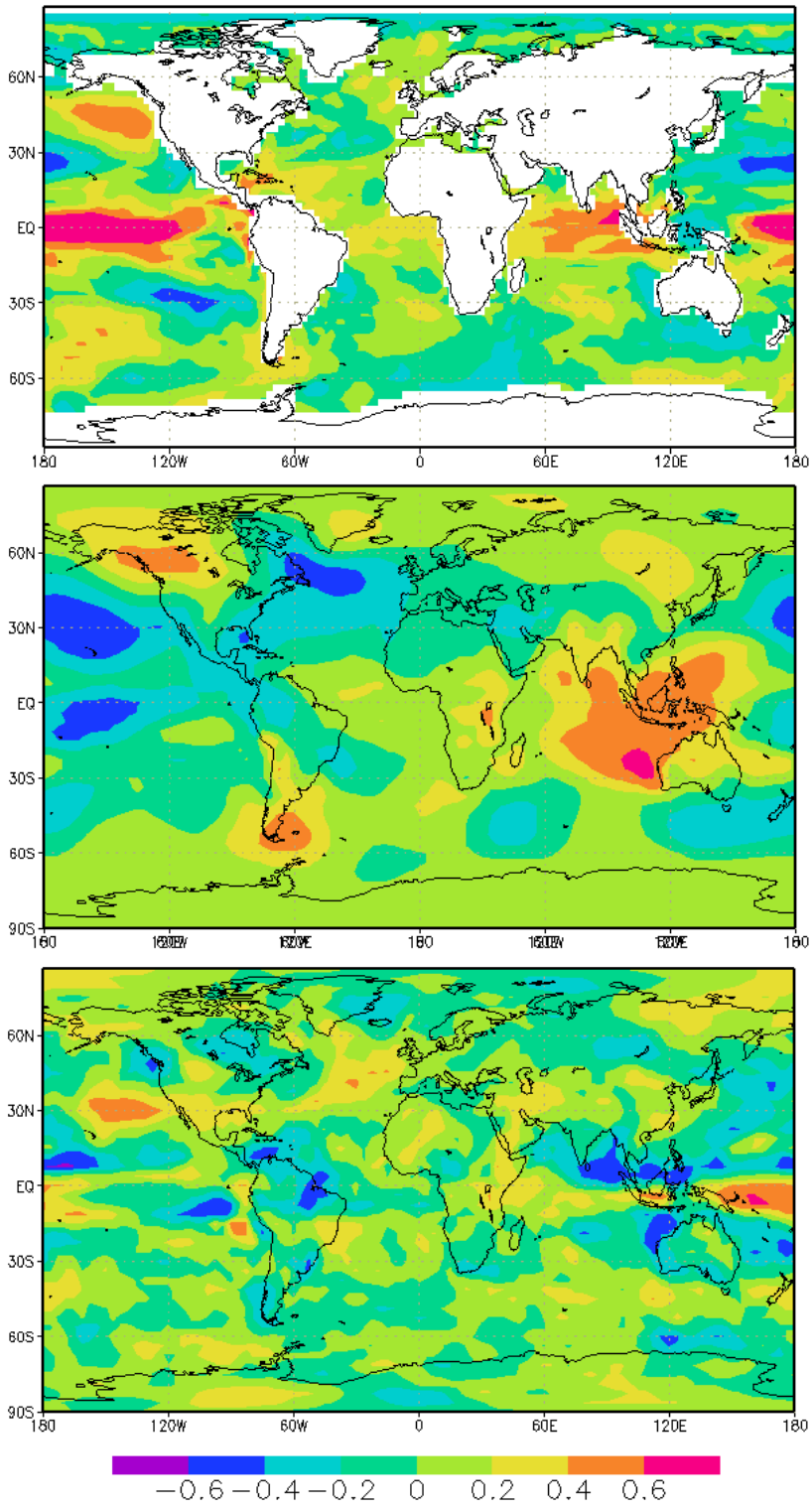

Figure 6.18: Correlation between the timeseries of ECHO-G ERIK (1750-1990) NINO 3.4 SST index and global fields. Top: global SST, middle: global SLP, bottom: global rainfall.

This enhanced decadal power of NINO 3.4 SST and strengthened correlation with southern African rainfall could be attributed to anthropogenic forcing. However, comparisons across the other segments of the ERIK simulation (1000-1250 and 1500-1730) show a consistent correlation between southern African rainfall and the NINO 3.4 SST index (r is within ±0.01 across all segments). This casts some doubt on anthropogenic forcing as a root cause of the change in the decadal ENSO-like behaviour.

An alternative explanation may arise from the slightly reduced influence of the SAM under anthropogenic forcing. The SAM variability shows an enhanced correlation with rainfall (ERIK r=0.40, ENAT r=0.32), similar influence over the South Atlantic (ERIK r=0.60, ENAT r=0.589), but reduced influence over the subtropical SWIO. The location of both SWIO nodes agrees with the spatial structure generated by correlation between the SAM and global SST (Figure 6.19). It is possible that this influence has forced the southward shift in regions of highest correlation with southern African rainfall. It is unclear how this shift may operate, and although it is possible that the interaction of the Indian Ocean with ENSO is at least partially responsible for the reduced coherence under anthropogenic forcing, the intrinsic variability of the SW Indian Ocean cannot be discounted in explanation. Spectrally, the SAM is broadly similar to its ENAT counterpart, but shows more significant variability throughout (Figure 6.20), with notably enhanced regions compared to ENAT including spectral power at ~22 years, ~12 years, ~6 years and ~3-4 years. Despite the apparent increase, MTM analysis (not shown) shows that only the ~6 year variability reaches significant levels (95%) against a red noise background.

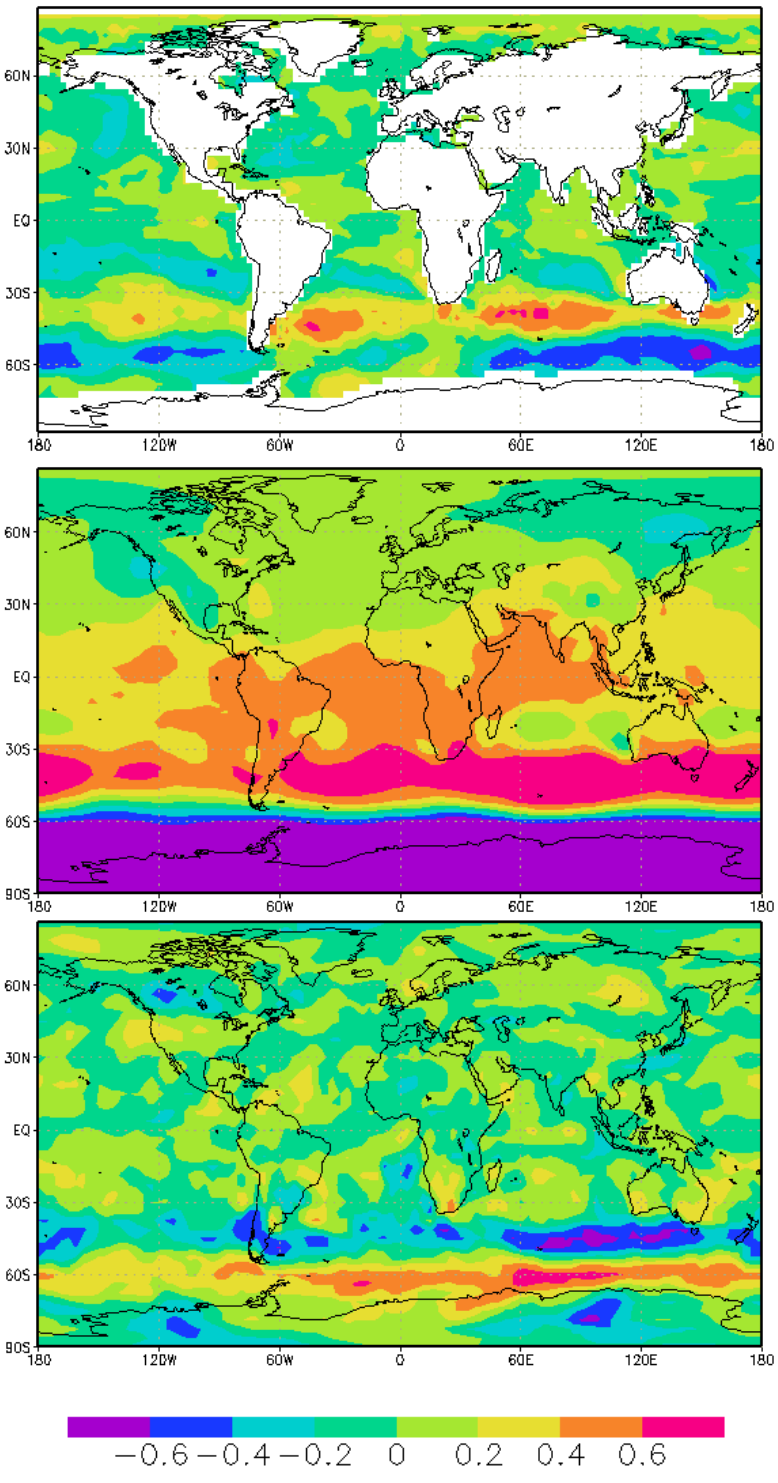

Figure 6.19: Correlation between the timeseries of ECHO-G ERIK (1750-1990) Southern Annular Mode index and global model fields. Top: global SST, middle: global SLP, bottom: global rainfall

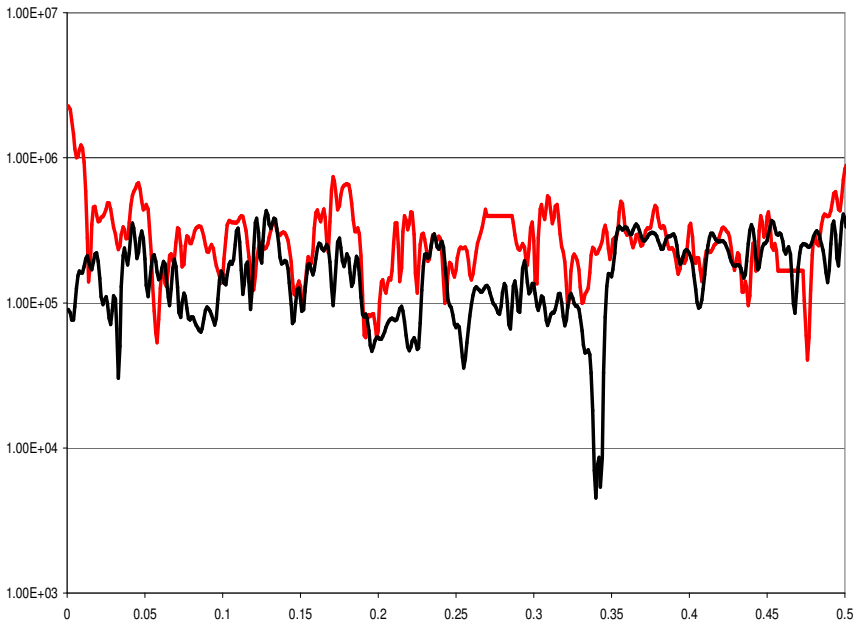

Figure 6.20: Spectral analysis (MTM; unfiltered) of the SAM index region under ECHO-G ENAT simulation (black line) and the anthropogenic (1750-1990) section of the ECHO-G ERIK simulation (red line).

Unlike the cross-spectral power identified in the analysis of ENAT-simulated southern African rainfall and Southern Annular Mode variability in the previous chapter, the ~22 year peak in ERIK-simulated Southern Annular mode does not match the ~40 year (harmonic) peak in southern African rainfall. It is not clear if (how) the SAM interacts with ENSO-type variability, despite the appearance of 'classic' ENSO spectral power in this analysis, or whether the observed change in SAM behaviour is a direct result of anthropogenic forcing.

The analysis here has shown that all of the SST regions have slightly different spectral and spatial relationships to those observed in ENAT, and no region has a distinctive "fingerprint" on to which southern African rainfall can be clearly attributed.

Perhaps one of the most significant changes is in the Indian Ocean: the 10-15° southward shift of tropical and subtropical nodes in to effectively sub-tropical and mid-latitude positions in the central ocean should be significant in impacting rainfall-generating mechanisms over southern Africa. Previously reviewed model studies have shown that the distance from the SST anomaly to the continent is critical in generating rainfall (Behera & Yamagata, 2001; Reason, 2002; Hansingo & Reason, 2006), and increasing the separation is likely to result in reduced rainfall signal.

The location of both 'subtropical' and 'tropical' SWIO nodes appears to be closely linked to the SAM in ECHO-G, but it is not clear whether the southward shift can be attributed solely to this, nor have any explanations for this spatial variability been identified. This SAM relationship has not been identified in observed data, and remains a potentially model-specific result. It is not understood why ECHO-G appears to prefer this region.

Decadal variability in southern African rainfall in ECHO-G appears to be related strongly to the relative strength and spectral power of two global teleconnections – the Southern Annular Mode and ENSO – and how they interact. The Southern Annular Mode is closely linked to South Atlantic and subtropical SWIO SST variability, and appears to have a controlling influence on the position of anomalies in the southern oceans. ENSO appears to have a stronger influence on tropical variability, and is typically linked to tropical SSTs including the Indian Ocean.

Under anthropogenic forcing – simulated by the period between 1750 and 1990 in ERIK – this relationship is subtly different to that observed in ENAT. The resulting spectrum of rainfall shows altered quasi-decadal variability, and analysis of the contributing SST region spectra shows slight changes in the simulation of variability. There is little evidence of the reduced quasi-decadal power presented by Damassa et al. (2006) in proxy data, and comparison with ENAT suggests that the combined oceanic and atmospheric regions explain more decadal variance under anthropogenic forcing than under natural forcing alone. The influence of these two modes appears to be symbiotic: a strengthened ENSO response in ERIK ANTH coincides with a slightly weaker SAM response. The stronger ENSO in this part of the ERIK simulation (with a more clearly defined decadal spectral pattern) may be of interest to model comparison studies, which typically do not regard ECHO-G's ENSO as particularly well-simulated across different ocean configurations (Guilyardi et al., 2004; Guilyardi, 2006).

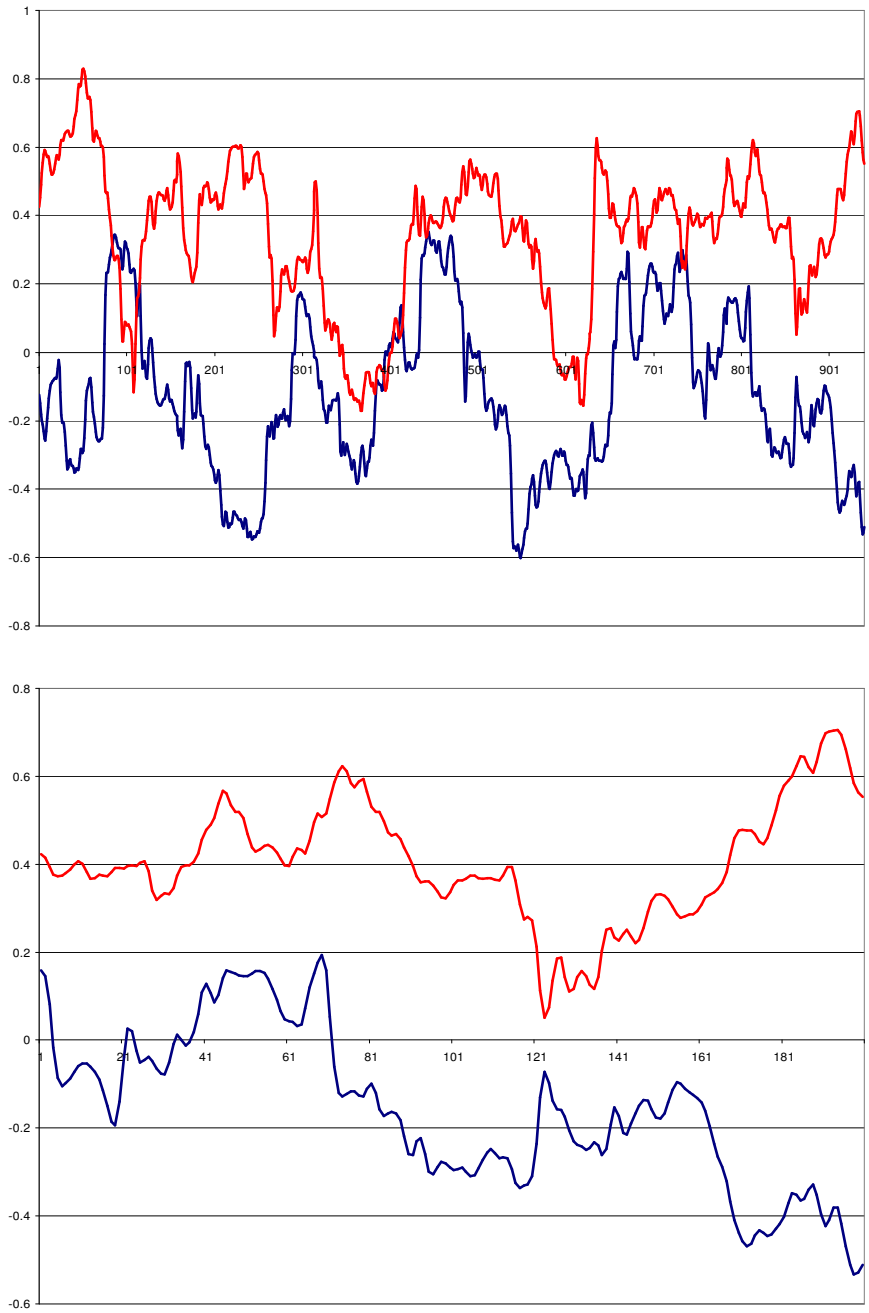

Figure 6.21: Running correlations (constructed using a 50 year correlation window) between ECHO-G ERIK-simulated southern African rainfall and indices of NINO 3.4 SST (blue line) and the Southern Annular Mode (red line), respectively. Correlations are shown for the full 990 year record (top) and the anthropogenic period (1750-1990, bottom). The rainfall data and both indexes are filtered using a 7-50 yr band pass filter.

It is not clear whether the SAM and ENSO have any interaction, or whether their co-existence is modulated by other factors: the clear demarcation between SAM-driven SSTs and ENSO-driven SSTs in ENAT is less obviously defined in ERIK. Running correlations between rainfall and NINO and SAM indexes (using a 50 year window) on filtered data (7-50 year band pass) shows the dynamics of the respective relationships to southern African rainfall variability in the ERIK simulation (Figure 6.21). The relationship is examined under the full 990 year record (despite acknowledged forcing shifts), as well as in the anthropogenic section (1750-1990) section of the simulation.

The correlations appear to oscillate between approximate phase relationships (e.g. correlation years 350-600 in the full record, years 0-115 in the ANTH record) and out of phase relationships (e.g. correlation years 0-115 in the full record, years 150-200 in the ANTH record) with no evident periodicity. The centennial power in the spectral analysis has previously been proposed as representative of the underlying secular warming trend, but this may instead be evidence of inherent multi-decadal variability in the global-scale climate oscillations. Examination of the individual indexes (not shown) does not identify obvious underlying spectral power, or an apparent trend in either SAM or NINO indexes.

Part of the reason for this lack of clarity is the remaining uncertainty associated with comparison studies using ECHO-G ERIK. First, the model SSTs in ERIK and ENAT are not the same: ENAT outputs a T30 resolution 'skin temperature' SST, compared to ERIK's T42 resolution ocean surface layer temperature, with enhanced resolution in the tropics. A different ocean simulation, with different resolution, reduces the possibility of identifying and attributing changes to forcing levels, rather than model differences.

This problem is further compounded by the lack of control simulation available for use in this study. Corroboration of attribution hypotheses – provided by comparisons between CTR, NAT and ALL in HadCM3 – are not possible with ECHO-G, and the study is hampered by being unable to correctly identify model-specific simulation features versus naturally or anthropogenically forced changes. Although it is possible to utilise the early part of the ERIK record (e.g. 1000-1250) as a pseudo-control simulation, the inherent problems associated with the parametrisation and forcing schemes employed (Osborn et al., 2006) are not thought to accurately generate a 'control' type simulation environment.

6. 2. 2 Anthropogenic Simulation under HadCM3

Having shown that quasi-decadal rainfall variability is reduced under anthropogenic simulations in HadCM3, this section aims to explore what may be associated with this change. First, the spatial nature of rainfall variability is examined through EOF analysis to ascertain whether anthropogenic forcing has altered rainfall distribution. Using the same techniques outlined in Section 4.3, the leading EOFs of decadally filtered rainfall data are calculated. Figure 6.22 shows the four leading EOF modes, and shows no substantive changes to the CTR simulated EOFs, although the order of modes 3 and 4 is reversed by comparison. EOF 1 explains 17.6% of variance (CTR EOF 1: 17.5%), with EOF 2 and 3 explaining ~9% of variance each like their CTR counterparts. This suggests that anthropogenic forcing does not change the spatial pattern of rainfall at decadal scales, and allows the continued use of the sub-continental rainfall index as the basis for analysis.

Next, the role of decadal teleconnections identified in the previous chapter are investigated, and considered in terms of their spectral and spatial relationships with southern African sub-continental rainfall. The correlation techniques are applied to filtered (7-50 year band pass) data from the ALL simulation in the same way as the previous CTR examination, in order to ensure that the only differences observed are the result of changed model simulation. Multiple regression analysis on the ALL simulation (using the regions outlined in the CTR discussion) explains only 15% of the variance, compared to ~30% of variance under CTR. It is not immediately apparent whether this is a result of weaker relationships, or a change in locations of importance to the ALL simulated rainfall.

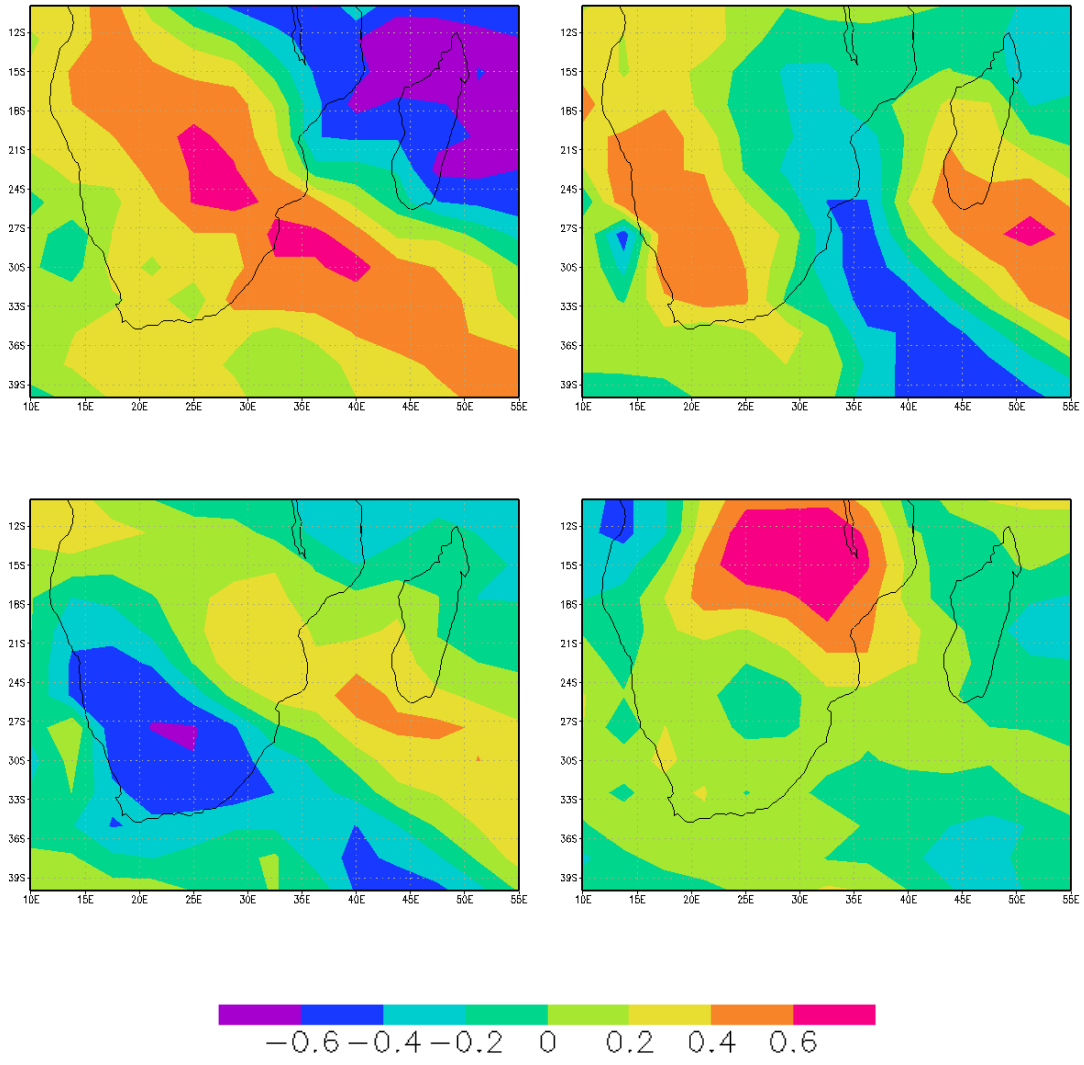

Figure 6.22: EOF analysis of filtered (7-50 yr BP) rainfall over southern Africa simulated by HadCM3 ALL250. Top left, EOF 1; top right, EOF 2; bottom left, EOF 3; bottom right, EOF 4.

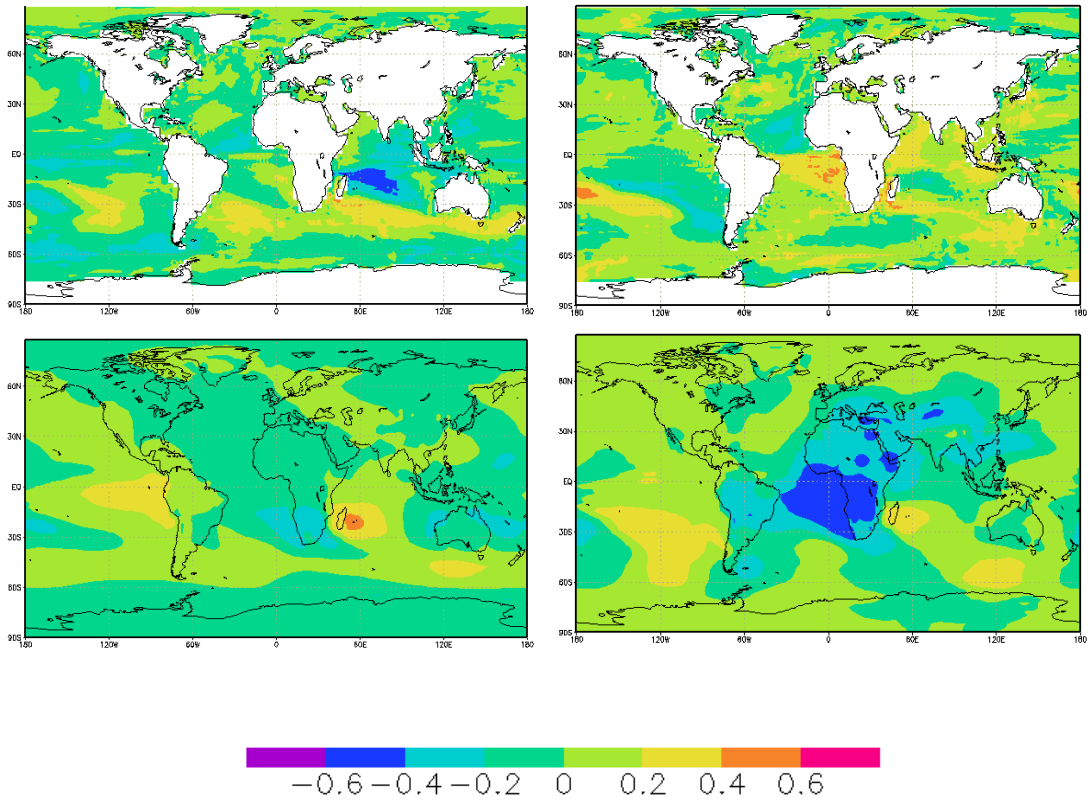

Figure 6.23: Comparison of the correlation between the timeseries of sub-continental (15-35ºS, 15-35ºE) southern African rainfall index and global fields. Top: global SST, bottom; global SLP, as simulated by HadCM3 CTR (left) and ALL250 (right).

This can be established through spatial correlation (Figure 6.23), which shows some elements of resemblance to the CTR-simulated correlation map. Many of the regions identified in the CTR simulation are represented, but there are substantial differences in how they appear to relate to southern African rainfall.

The reduced influence of South Atlantic SST correlation in the ALL simulation (r=0.195) contrasts with the apparent increase in strength of relationship with the tropical Atlantic region in both SST and SLP correlation. However, the tropical Atlantic correlation in CTR (r=0.2847) is marginally stronger than the same correlation in ALL (r=0.2726), and this suggests that the apparent increase is relative by comparison to weaker correlations elsewhere.

One of the notably weaker correlation relationships concerns the SW Indian Ocean region. Although the "dipole-like" structure is apparent, the correlation with the individual nodes in the ALL simulation (tropical SWIO r=0.09; subtropical SWIO r=0.2837) is considerably weaker than the same relationship in the CTR simulation (tropical SWIO r=-0.402; subtropical SWIO r=0.376).

As in the previous chapter, these regions are now examined to assess how they may be associated with southern African rainfall in comparison to the CTR-simulated teleconnections proposed. Spectral analysis will also be employed in investigating whether the damped decadal response extends to – or is potentially explained by – the forcing regions of southern African rainfall.

The regional analysis begins with the Tropical Atlantic SST index, which is relatively prominent in the rainfall based-correlation index. The SST correlation in the Atlantic basin (not shown) agrees with the mapping of the CTR simulation, perhaps explaining the characteristic agreement of the global rainfall field in the tropical dipole and extending in to the coastal regions of Africa and South America as before. Spectral analysis of the regional index shows evidence of the secular anthropogenic trend (50 yr variability at 99% confidence), but little quasi-decadal power otherwise. Comparison to the spectrum of the CTR region shows a broadly similar response (Figure 6.24), with some differences to be expected through intrinsic noise in the spectrum.

The consistent response, coupled with lack of spectral variability, suggests that the tropical Atlantic mechanism does not change under anthropogenic forcing. It is likely that it remains a peripheral region for southern African rainfall variability, and that the relative importance in the initial rainfall-based correlation (Figure 6.23) is artificially enhanced by weak correlations elsewhere.

The South Atlantic region is one of the weaker correlations. Spectral analysis of the SST region (45-60°S, 60-30°W) shows enhanced spectral power at 15 yrs (95% confidence) compared to a ~10 yr peak in the CTR simulation (Figure 6.25), and the spatial correlation shows an altered pattern of associated variability (Figure 6.26).

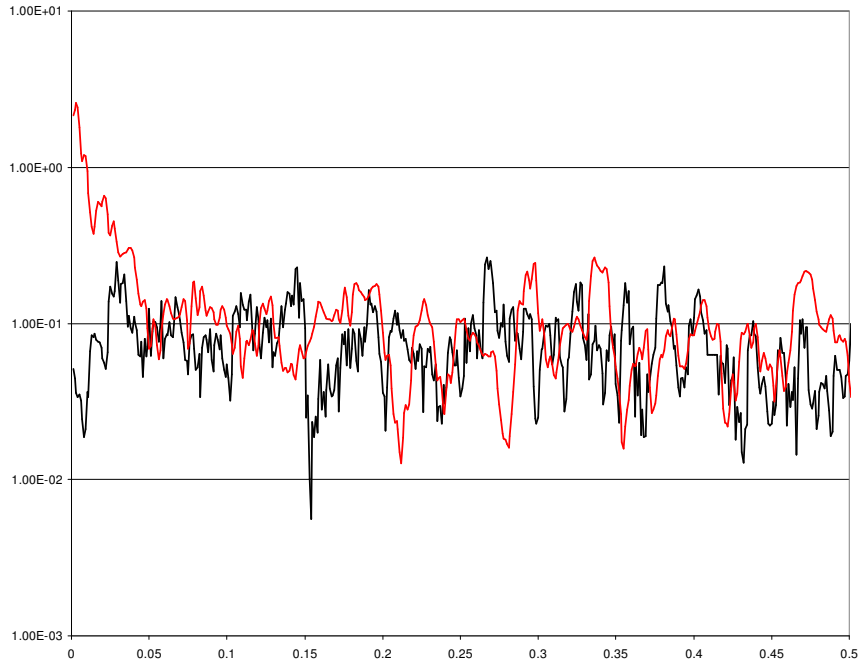

Figure 6.24: Spectral analysis (MTM; unfiltered) of the HadCM3 Tropical Atlantic SST index region under CTR simulation (black line) and the anthropogenic ALL simulation (red line).

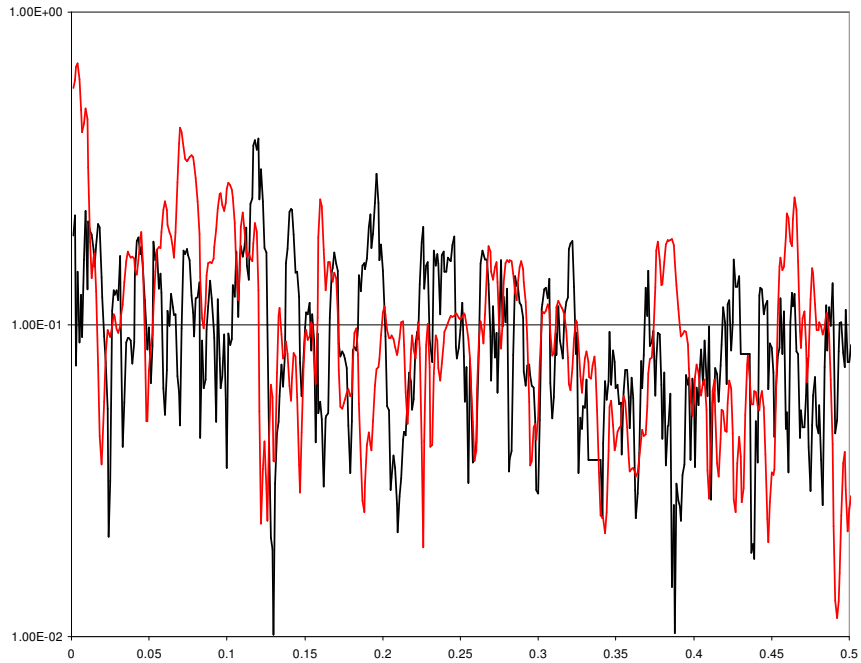

Figure 6.25: Spectral analysis (MTM; unfiltered) of the HadCM3 South Atlantic SST index region under CTR simulation (black line) and the anthropogenic ALL simulation (red line).

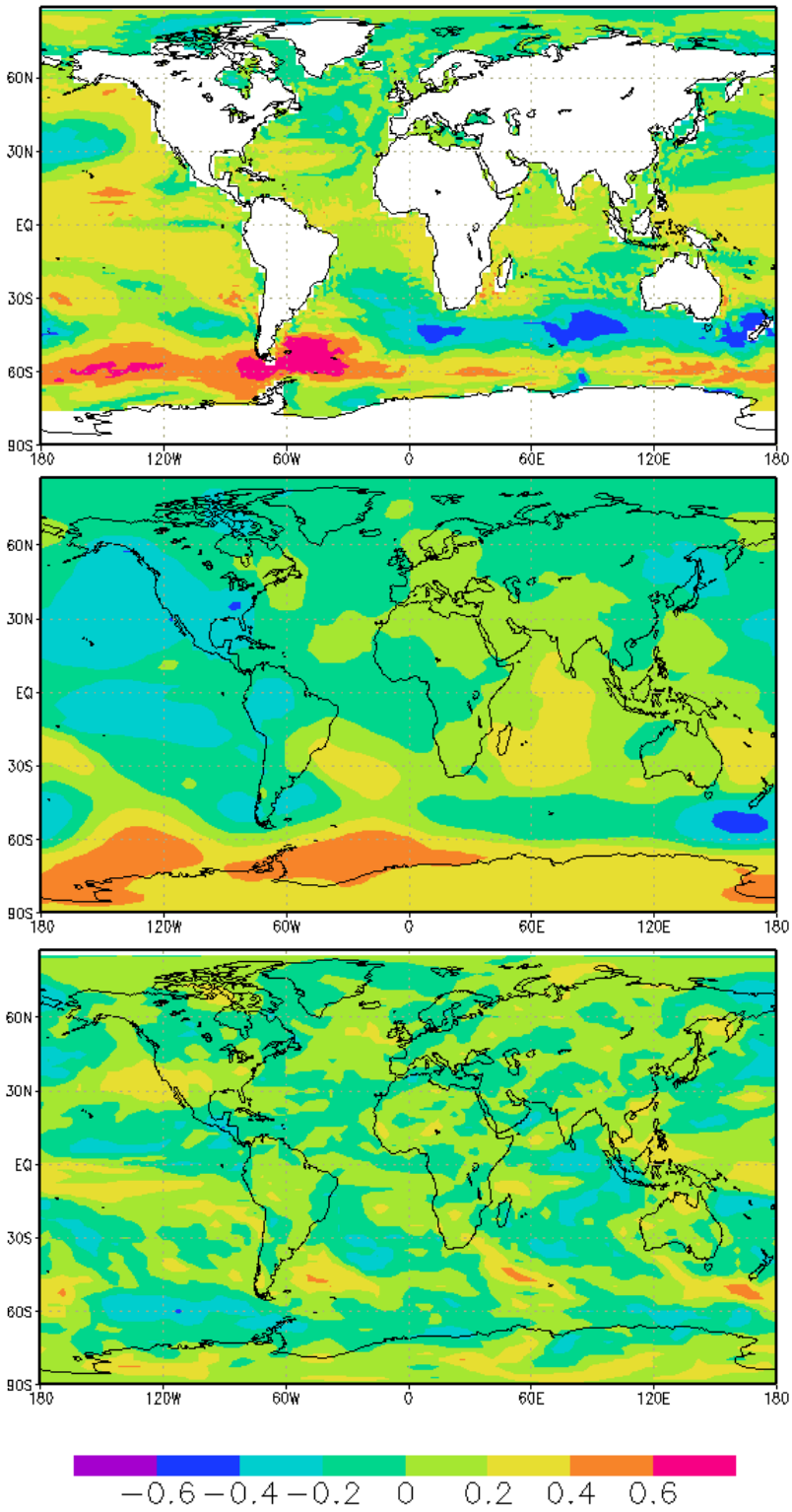

Figure 6.26: Correlation between the timeseries of HadCM3 ALL South Atlantic SST index and global fields. Top: global SST, middle: global SLP, bottom: global rainfall.

The latitudinal bands of the CTR correlation appear to be shifted south from ~45° to ~60°, and the relationship with other ocean basins appears to be altered too. This is particularly evident in the SW Indian Ocean – there is now a negative correlation with the Agulhas region (35-45°S, 0-40°E) and the South Indian Ocean (35-45°S, 60-100°E).

The SLP correlation agrees, with evidence of high pressure anomalies more usually associated with Southern Annular Mode-type locations, and a subtropical anomaly in the Atlantic (centred on 30°S) and Indian Ocean basins. By contrast, the relationship with the Pacific Ocean has weakened compared to the CTR simulation, despite some SST correlation strength in the Drake Passage and South Pacific. The rainfall response is broadly similar to the CTR simulated rainfall, although the locations of strongest correlation appear to be shifted towards higher latitudes in agreement with other fields.

It has previously been suggested that the South Atlantic's influence on southern African decadal rainfall was unclear, and thought to be primarily linked via the SW Indian Ocean by probable atmospheric variability as proposed by Hermes & Reason (2005). This association appears to be weakened under anthropogenic forcing, and the shift towards higher latitudes observed in the correlations is likely to explain the reduced correlation with the South Atlantic region in the ALL simulation. Without detailed analysis, it is left unclear where the driving force for this shift originates: in the South Atlantic, the South West Indian Ocean, or in a global-scale forcing mechanism change? Although the global impacts of ENSO and the Southern Annular Mode are explored later in this section, work remains to be done in testing this result further.

The South West Indian Ocean was shown in the previous chapter to be most closely linked with southern African rainfall variability, both at interannual and quasi-decadal scales. It is therefore likely that changes in this region under anthropogenic forcing – as suggested by the proxy analysis presented earlier in this chapter – will prove to be the most significant for rainfall variability.

The analysis of teleconnections in the previous chapter presented the case for exploring the subtropical and tropical 'nodes' of the SW Indian Ocean separately, and demonstrated that the "dipole" concept did not retain coherence at decadal timescales. Both nodes showed a consistent link to the subtropical high pressure, and variability of the moisture flux driven by circulation associated with this feature. The decadally filtered CTR simulation agreed with interannual CTR simulations (Washington & Preston, 2006) and decadal observations, and suggested that the tropical node played a more substantial role in southern African rainfall variability than the subtropical node.

First, the behaviour and role of the subtropical node (30-35°S, 40-60°E) relative to southern African rainfall is considered in the ALL simulation. Figure 6.27 shows the subtropical SST-based correlation analysis. The SST relationship in ALL (r=0.284) is consistent with the CTR simulation (r=0.376), and the SLP response is consistent with the proposed mechanism of rainfall variability. As in the CTR simulation, the rainfall response is not as strong as the circulation features would suggest, but this is thought to be a model-based feature (Washington & Preston, 2006).

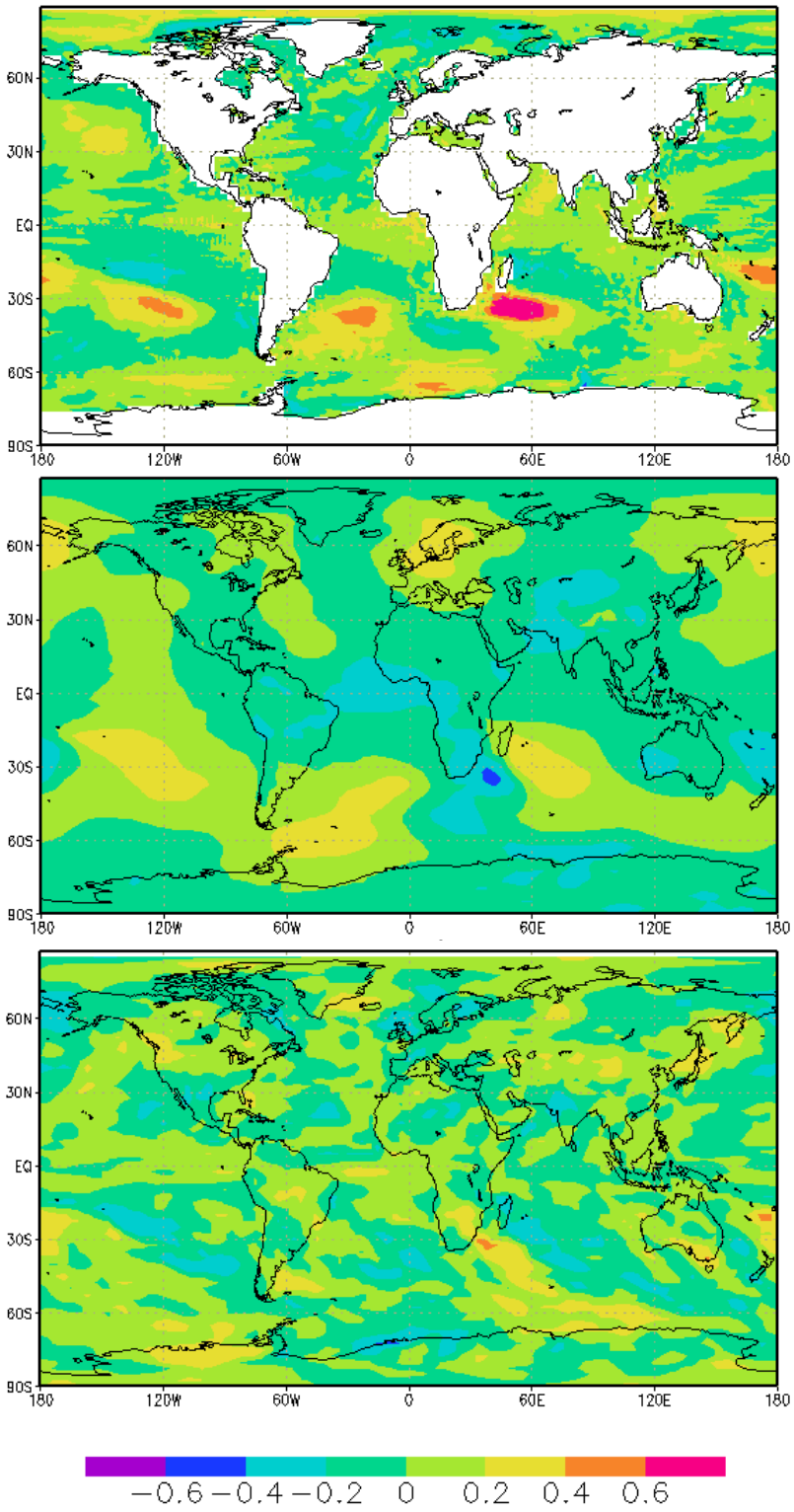

Figure 6.27: Correlation between the timeseries of HadCM3 ALL sub-tropical SWIO SST index and global fields. Top: global SST, middle: global SLP, bottom: global rainfall.

Spectral analysis of the ALL simulation shows a very similar response to the previously described CTR analysis, as described in Figure 6.28: peaks in the ENSO-frequencies (99% confidence) support quasi-decadal power at ~10 yrs (95% confidence) and ~18 yrs (90% confidence). It is thought the consistent nature of this correlation is indicative of a stable subtropical node under anthropogenic forcing, operating at similar timescales and employing similar mechanisms to influence southern African rainfall to those described in the previous chapter.

The major change in the South West Indian Ocean under ALL simulation appears to be in the relationship with the tropical node. The correlation between subtropical and tropical nodes in the ALL simulation (r=0.0446) is substantially weaker and of different sign to that found in the CTR simulation (r=-0.404). The stability of the subtropical node strongly suggests that it is changes to the tropical SST node itself that has driven these changes.

First, the spectral analysis of the index of tropical SWIO SST shows some substantive changes to under ALL simulation conditions (Figure 6.29). Reduced power in ENSO-frequencies contrasts with augmented power at ~30 years (99% confidence).

Next, the correlation between the tropical SW Indian Ocean node and southern African rainfall shows a considerable difference between CTR (r=0.2837) and ALL (r=0.094) simulations. Correlation between the tropical SW Indian Ocean SST index and global model fields reveal a substantial change in the spatial patterns associated with the region (Figure 6.30).

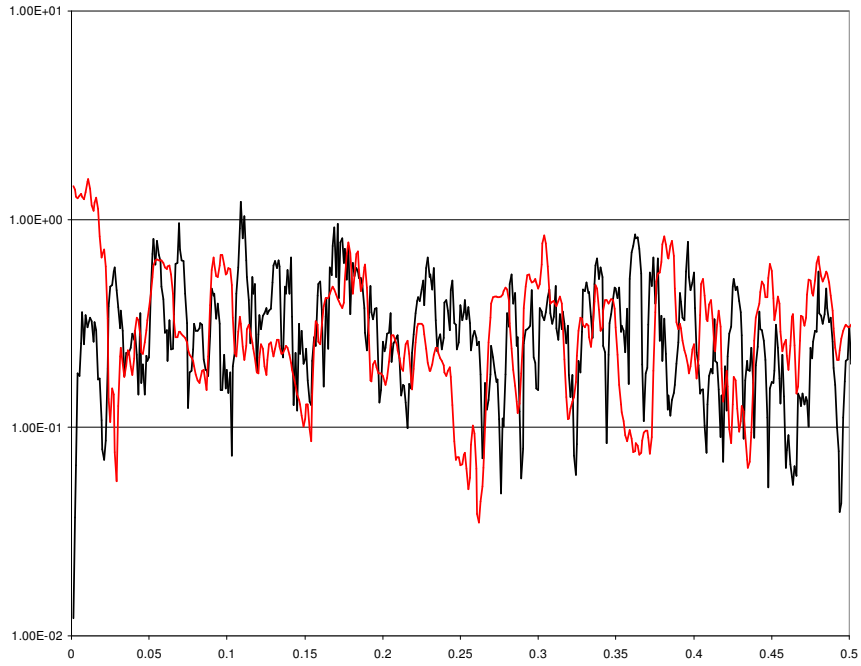

Figure 6.28: Spectral analysis (MTM; unfiltered) of the HadCM3 sub-tropical SWIO SST index region under CTR simulation (black line) and the anthropogenic ALL simulation (red line).

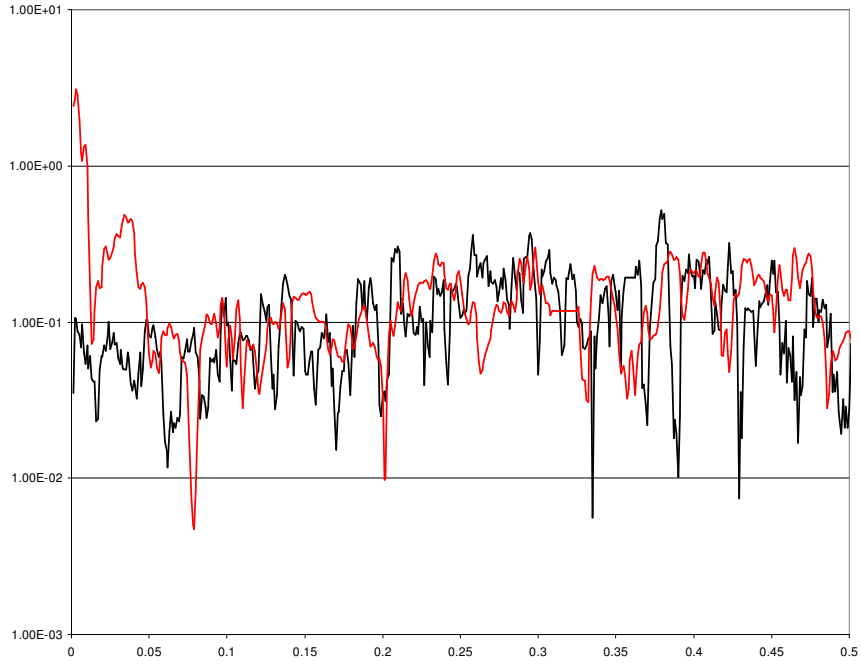

Figure 6.29: Spectral analysis (MTM; unfiltered) of the HadCM3 tropical SWIO SST index region under CTR simulation (black line) and the anthropogenic ALL simulation (red line).

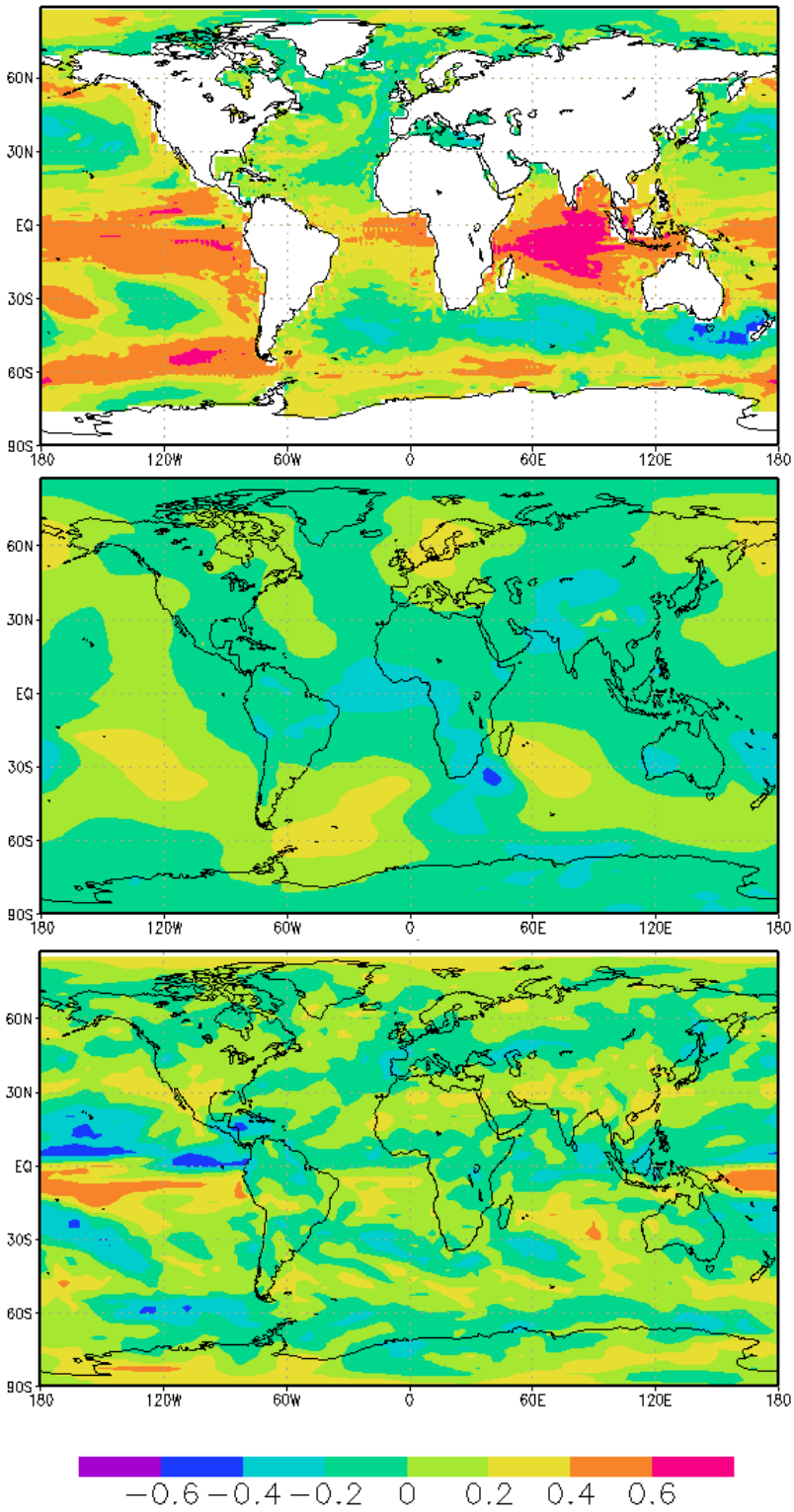

Figure 6.30: Correlation between the timeseries of the HadCM3 ALL tropical SWIO SST index and global fields. Top: global SST, middle: global SLP, bottom: global rainfall.

The global rainfall response is weak, despite bearing some resemblance to the NW-SE orientation described in previous chapters. Much of the rainfall response can be explained by apparent changes in the relationship with the subtropical circulation. SLP correlation indicates that the pressure anomalies are reversed by comparison to those simulated in the CTR experiment, and the subsequent moisture flux is considerably reduced. As a result, the shape and scale of rainfall correlation is altered, to the extent of potentially neutralising the teleconnection of the tropical SWIO region to southern African rainfall.

As suggested in the previous chapter, this result is not experiment-specific, and occurs in the NAT-simulated variability. Without extensive multi-model examination – which is beyond the immediate scope of this work – it is not clear how this circulation response is altered, or how model specific this result is. Washington & Preston (2006) identified this region as possessing intrinsic variability at interannual scales, and a similar possibility cannot be discounted at this stage. Two additional explanations are offered here.

First, a series of modelling studies have suggested that drying over Africa is consistent with sensitivity to global SST trends (Paeth & Hense, 2004) A trend towards increased aridity since 1950 has emerged over southern Africa (Hulme, 1996), with an observed 20% reduction in the summer rainfall (compared with a 35% reduction in the Sahel; Hoerling et al., 2006). Using a range of AR4-based model simulations (including HadCM3 and ECHO-G), Hoerling et al. (2006) show the sign and magnitude of 50 yr sample rainfall trends over southern Africa appears to have been determined by global SSTs (79 of 80 realisations yield a drying trend over southern Africa). The possibility that the observed rainfall trends are not the sole consequence of natural variation is supported

by the fact that no single 50-yr trend in unforced coupled models yields such drying rates (Hoerling et al., 2006), and nearly half the AGCM simulated trends fall outside the envelope of coupled model simulations. This result must be carefully considered, as the current generation of coupled models does not offer a completely accurate picture of natural low-frequency variability, with well known mean SST biases and problems in adequately simulating ENSO (Achuta-Rao & Sperber, 2002, 2006).

Hoerling et al. (2006) further suggest that the models may have insufficient oceanic low frequency variations, with evidence obtained by comparing atmospheric-GCMs with coupled models. Since a comparable distribution of rainfall trends is shown to occur in both model types, the intrinsic oceanic noise is implied to be either small and/or not contributing to multidecadal African rainfall change. Hoerling et al. (2006) propose that this is more likely to reflect model deficiencies than the true measure of the ocean's role (e.g. Barnett, 1999).

The speculated mechanism for drying is a large scale subsidence within a descending branch of an anomalous Walker circulation, whose ascending branch is located over the Indian Ocean, where both observed and modelled evidence for localised SST warming leading to rainfall change has been demonstrated (Goddard & Graham, 1999; Hurrell et al., 2004; Lu & Delworth, 2005). Additional support for the role of the Indian Ocean has been provided by experiments on coupled models (Bader & Latif, 2003; Bader et al., 2003; Collins et al., 2004).

A range of mechanisms have been suggested, including the southward migration of the ITCZ (Biasutti et al., 2004), and the stabilisation of the atmosphere for deep convection

through tropical SST-forced tropospheric temperatures (Chiang et al., 2002; Herceg et al., 2007). Statistical links have also been proposed to the Indian Ocean SST variability, and it has been suggested that the late twentieth century oceanic warming trend may be linked to Sahelian drying (Giannini et al., 2003).

In order to explore this potential Indian Ocean warming, the mean temperature of the SST region (5-10°S, 60-80°E) from the ALL simulations is plotted for comparison against samples of CTR-simulated SST. The CTR samples (black lines) show the unforced variability of SST, with no inherent trend, and give an indication of the typical modelled temperatures of the region. The NAT simulation (not shown) reflects a small (0.025ºC/100 years) cooling trend, while the ALL simulated SST (28.89°) reflecting a cooler initial period, with a warming trend (Figure 6.31).

However, it has previously been shown that the NAT and ALL simulations respond in a similar way, despite their apparent cooling/warming trend differences. Application of a 7-50 yr band pass filter to the ALL simulated SST, for example, may help to explain how the two model simulations appear to respond in the same way. Figure 6.32 shows the filtered SST index (red line) compared to the unfiltered SST (black line), which has removed the long term trend from the data.

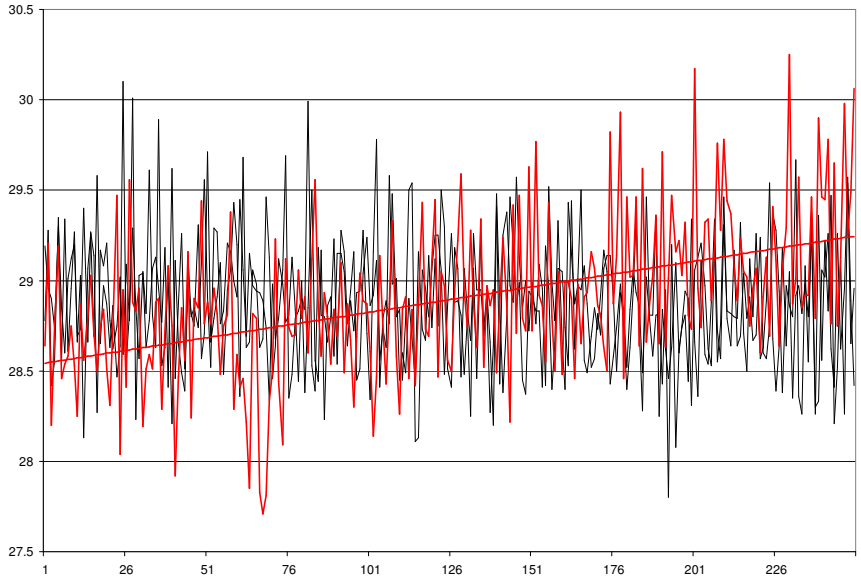

Figure 6.31: Comparison of the mean tropical Indian Ocean SST (5-10°S, 60-80°E) simulated by HadCM3 ALL250 (red line) and two 250 year samples taken from the HadCM3 CTR simulation (black lines). Note that the indexes are unfiltered.

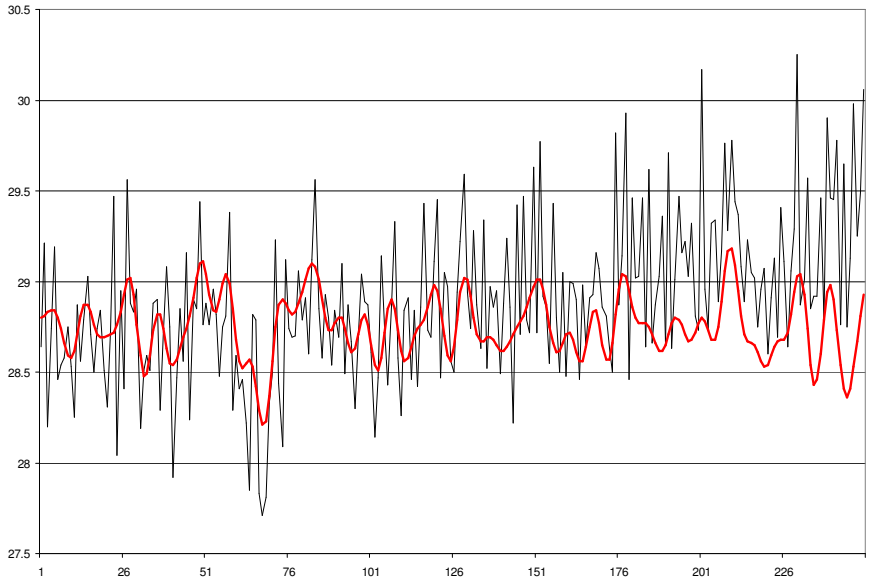

Figure 6.32: Timeseries plot of mean tropical Indian Ocean SST (5-10°S, 60-80°E) simulated by HadCM3 ALL 250. The data shows the SST index before filtering (black line), and after a 7-50 yr band pass filter has been applied (red line).

The role of the warmer (cooler) ocean in the ALL (NAT) simulation, therefore, cannot be the cause of the neutralised tropical SWIO; which is present in decadally filtered SST data. Hoerling et al. (2006) take this result further, and perform detection and attribution analysis using rainfall from 1950-2049 over 15-35°S, 15-35°E in all eighteen AR4 model simulations. Though there is considerable spread in the models, the majority project a decline in rainfall over southern Africa, with the ensemble average showing a ~5% decline during 2000-2049. Phase space analysis shows that southern African observations exhibit no projection upon the GHG fingerprint pattern, nor does the fingerprint pattern explain the observed change in amplitude. Since the phase space of the GHG fingerprints is virtually independent of that associated with the global SST fingerprint, Hoerling et al. (2006) suggest that the observed SST forcing – which played a critical role in southern African drying – is not itself a consequence of GHG forcing.

This interpretation contradicts the finding that observed Indian Ocean warming is the immediate cause for the drying simulated in the atmosphere GCMs and that such warming was attributable to twentieth century GHG changes (Hurrell et al, 2004). Hoerling et al. (2006) note that although the amplitude and timing of the observed twentieth-century Indian Ocean warming is well simulated, the ensemble average of AR4 simulations does not yield a southern African drying trend during 1950-99, and suggest that additional work is required to confirm the immediate physical impacts of a warmer Indian Ocean as related to southern African rainfall variability.

Second, another potential explanation may result from the stronger relationship with the tropical oceans found in SST correlation. An enhanced link to the tropical Atlantic

(r=0.574), strong response in the whole tropical Indian Ocean, and clear links to the tropical Pacific Ocean suggest an enhanced role for decadal ENSO-like variability. The correlation between NINO 3.4 SST and tropical SWIO (r=0.5644) in the ALL simulation is approximately double the equivalent relationship in CTR (r=0.26), and regression analysis suggests that ENSO-like variability explains 32% of the variance in the SWIO.

The proxy-based evidence suggested that the major difference in seventeenth and twentieth century models was the role played by decadal ENSO variability – could an 'altered structure' of ENSO-like behaviour (Zinke et al., 2004) explain the regional circulation changes observed here? Comparative spectral analysis of ALL's NINO 3.4 SST index (Figure 6.33) shows that although the characteristic ENSO time scales (3-5 years) are reduced in observed power compared to the CTR simulation, harmonic power (individual MTM analysis not shown) represents this range adequately. A quasi-decadal peak in ALL (11.95 yrs, 90% confidence) is above that of the CTR simulation, and although the spectral peaks do not reach significant levels in the MTM analysis, there is generally more low frequency power in the ALL simulation than in CTR.

However, this enhanced decadal power under anthropogenic forcing is unlikely to cause a net reduction in rainfall variability at similar timescales. Spatial correlation based on the NINO 3.4 index is also inconclusive (Figure 6.35). The SST and SLP fields agree broadly with the CTR simulations of ENSO, and are concentrated on the tropics.

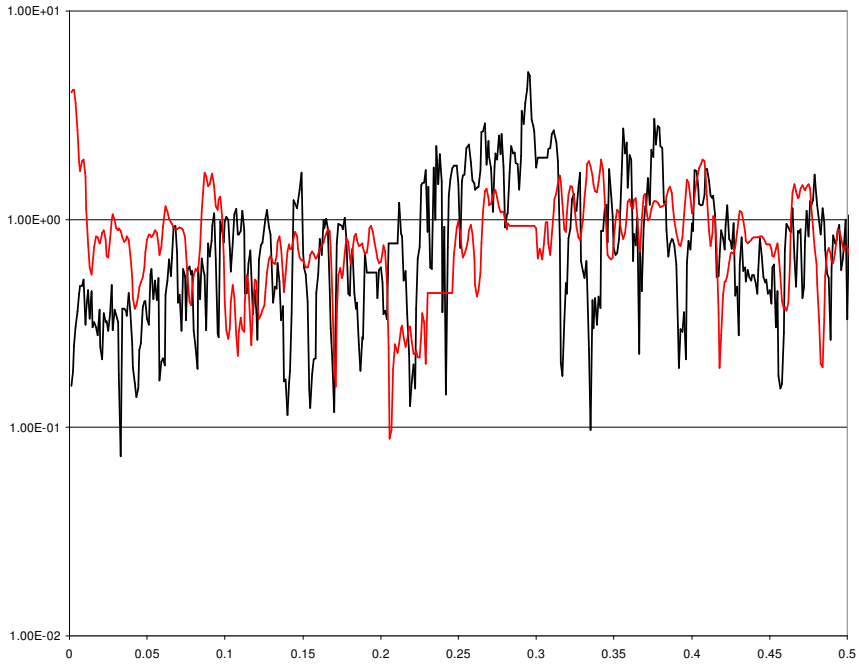

Figure 6.33: Spectral analysis (MTM; unfiltered) of the HadCM3 ENSO NINO 3.4 SST index region under CTR simulation (black line) and the anthropogenic ALL simulation (red line).

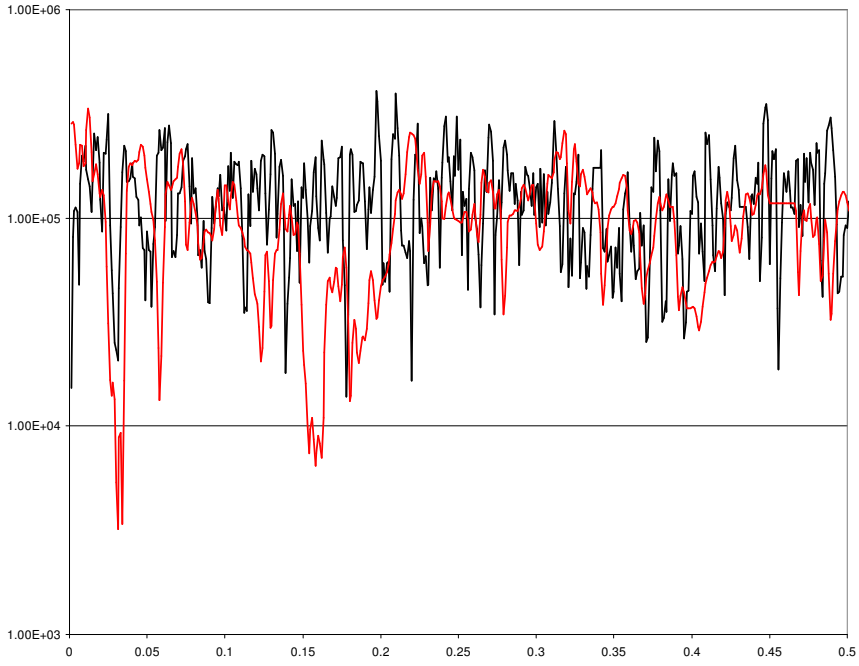

Figure 6.34: Spectral analysis (MTM; unfiltered) of the HadCM3 Southern Annular Mode index under CTR simulation (black line) and the anthropogenic ALL simulation (red line).

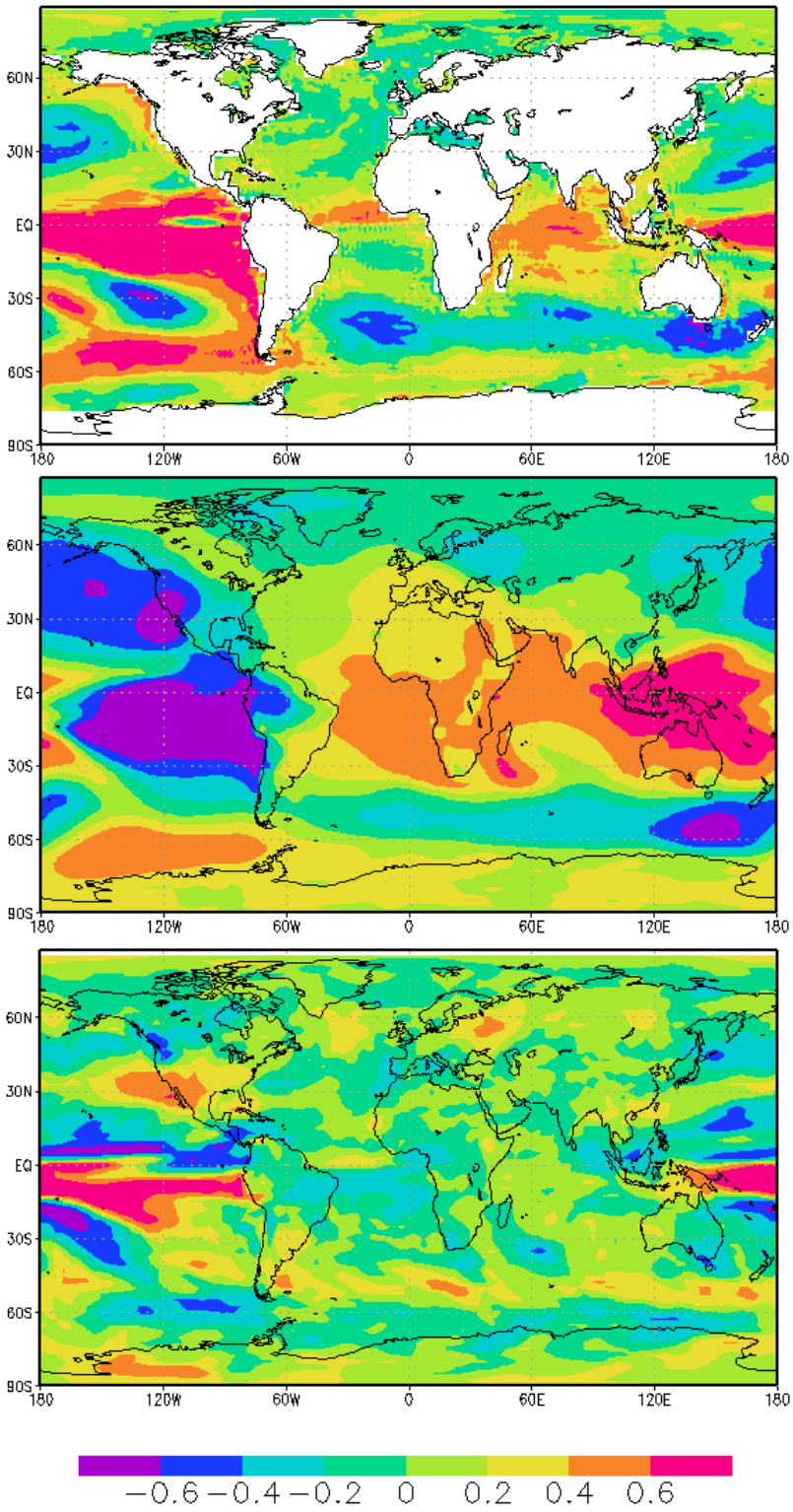

Figure 6.35: Correlation between the timeseries of the HadCM3 ALL NINO 3.4 SST index and global fields. Top: global SST, middle: global SLP, bottom: global rainfall.

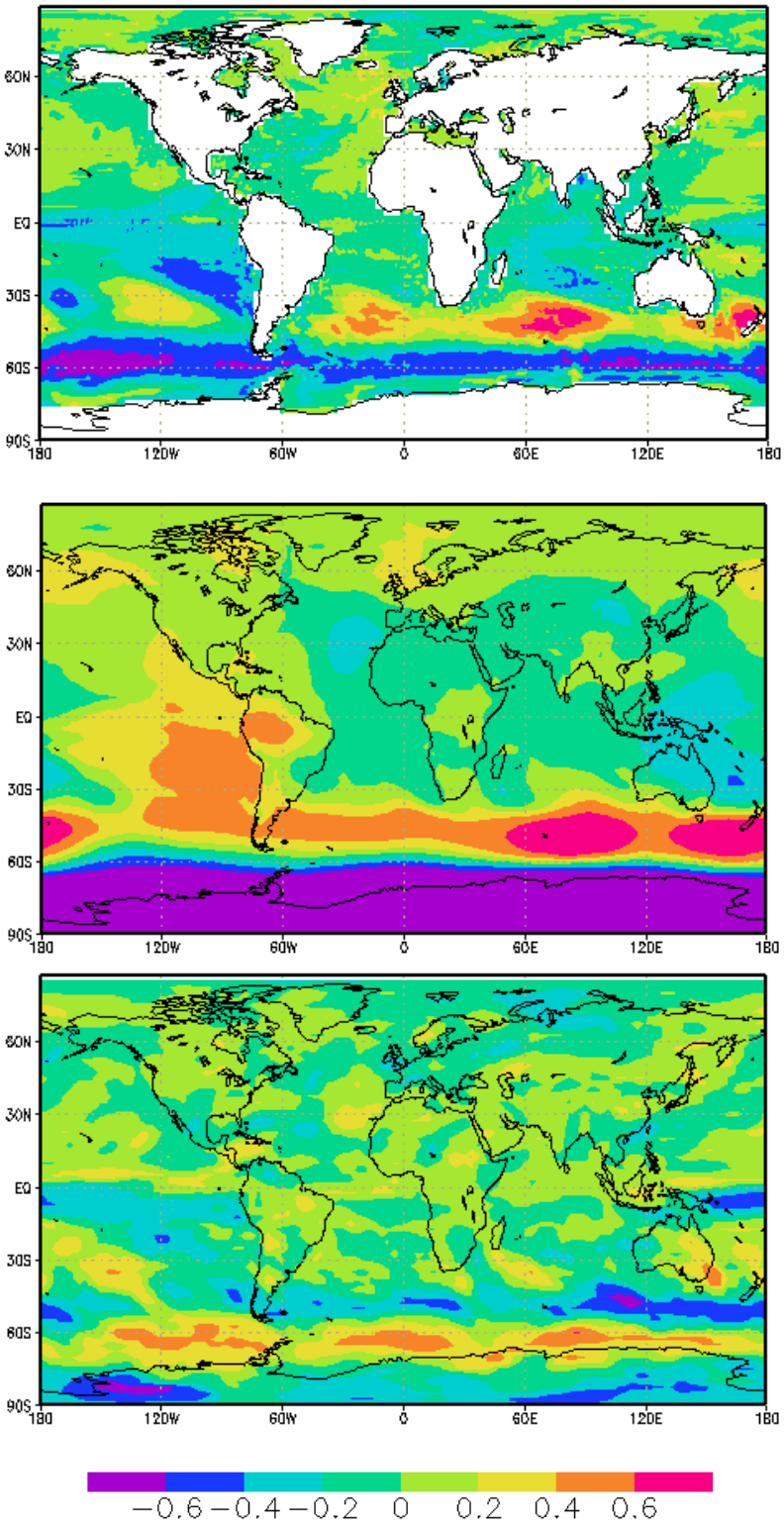

Figure 6.36: Correlation between the timeseries of the HadCM3 ALL Southern Annular Mode index and global fields. Top: global SST, middle: global SLP, bottom: global rainfall.

There is some evidence for a reduced impact over the tropical Atlantic – also thought to relate to drying trends in the Sahel (Hoerling et al., 2006) – but there is no evidence which would explain the changes to the tropical Indian Ocean or the reduction in correlation with southern African rainfall shown here.

Similar analysis of the Southern Annular Mode – shown to be more influential in the naturally forced ECHO-G ENAT simulation – also proves to be relatively unchanged under anthropogenic forcing in HadCM3. Spectral analysis shows a substantially weaker power spectrum between 5-10 years (Figure 6.34), but the other spectral power appears to closely match that simulated by the control run. Spatial correlation (Figure 6.36) shows slightly more SAM-based influence over the Indian Ocean in ALL than CTR, perhaps explaining the stronger relationship with tropical SWIO (r=-0.334) than subtropical SWIO (r=0.09), but this is unlikely to generate the substantial changes observed in the SLP-based relationship. There is evidence of the expected relationship with South Atlantic variability (r=-0.4067) but weak influence over the SAFR rainfall region itself (r=-0.02454) compared to the same relationship in CTR (r=0.2918).

Global teleconnections therefore appear unlikely to be the driving force behind the changes observed in NAT and ALL-simulated tropical SWIO. Despite the increased covariance between tropical SWIO and NINO 3.4 SST indexes, there is no intrinsic spectral or spatial variability which exhibits a substantial change, and this leads to the conclusion that the observed change is unlikely to be driven by decadal ENSO-like behaviour.

6.3 Summary

Analysis of long Indian Ocean coral proxy SST records by Damassa et al. (2006) suggested that quasi-decadal variability was reduced under anthropogenic forcing scenarios. Their data, together with a similar record from the Ifaty lagoon (Zinke et al.) were examined using spectral techniques. Although there were regions of under-simulated variability at decadal scales in the anthropogenic samples, it was not substantially different across all spectral power. The hypothesised reduction in quasi-decadal power was then tested in two anthropogenic climate model simulations.

In ECHO-G, comparisons with naturally forced spectra showed agreement with the proxy data result and showed evidence of altered quasi-decadal power under anthropogenic forcing. Evaluation of segments from the 990 year ERIK simulation showed separate phases of forcing, correlation and associated spectral power, and the 1750-1990 ("ANTH") period was utilised as representative of anthropogenic forcing under ECHO-G. As in the previous mechanisms chapter, regional analysis of forcing factors showed that the interaction between ENSO-forced tropical/subtropical regions and Southern Annular Mode (SAM)-driven mid-latitude regions was the most likely candidate for variability at quasi-decadal scales. Southward shifts in the location of the key SW Indian Ocean region were examined, and suggested to relate to the SAM correlation patterns, but no firm conclusions about the mechanism behind the change were put forward. Centennial scale variability in the spectral analysis, previously thought to represent the secular anthropogenic trend, was proposed as a potential source of long term variability in the relationship between global teleconnections and southern African rainfall.

By contrast, HadCM3 provided evidence of suppressed quasi-decadal variability, which reflected generally weaker power across the spectral range. Analysis of both natural and anthropogenic simulations showed that the principal change in variability lay in the Indian Ocean, and the substantial change in behaviour of the tropical SW Indian Ocean node related to southern African rainfall. Previously identified as the dominant node in the SWIO 'dipole', and strongly related to ENSO through the tropical oceans, the tropical node was thought to enhance Walker-type circulation over the sub-continent, and act in concert with the subtropical node. In both natural and anthropogenic forcing simulations, the node was shown to reverse in sign, and displayed substantially weaker relationships with southern African rainfall. Exploring the hypothesis of Giannini et al. (2003), potential warming trends in the Indian Ocean and their impacts were investigated, but shown to be predominantly filtered out by the decadal methods utilised. Like the ECHO-G changes, the mechanisms driving the change in Indian Ocean behaviour remain unclear. Given Washington & Preston (2006)'s previous work at interannual timescales, the role of intrinsic variability at decadal timescales cannot be ruled out.

Although this study does not intend to make an extended discussion on the nature and change to decadal ENSO-like behaviour, some conclusions may be drawn from the analysis presented in this chapter. Despite the variation in how the models simulate ENSO, there is consistency between the control, natural, and anthropogenic simulations in their spatial representations of the NINO 3.4 SST index. Both models show similar patterns in the major atmosphere and ocean fields associated with decadal ENSO-like

behaviour, suggesting that the influence of large scale anthropogenic forcing is limited with respect to decadal ENSO structure.

Both models also show decadal ENSO's spectral response to the anthropogenic forcing experiments, but the model-specific problems identified in the previous chapter remain important. HadCM3 shows enhanced quasi-decadal power, balanced by some reduction in classic ENSO power. By contrast, ECHO-G shows muted quasi-decadal power under ERIK ANTH (1750-1990) forcing, with a broad enhancement of spectral power under 5 years.

Clearly, further work needs to be carried out to identify the best approach to evaluate decadal ENSO-like behaviour in climate models, and this will need to take account of model-specific results like those presented here. Neither model appears to support the hypothesis of Zinke et al. (2004), and propose a spatially altered ENSO structure as the principal difference between pre-industrial and anthropogenically forced climates in the SW Indian Ocean region.

Attributing the changes described in this chapter to anthropogenic forcing appears very difficult at this stage, and the implications for decadal predictability remain unclear. Further work is needed in understanding the ocean behaviour in these models, and employing other coupled anthropogenic simulations to assess how extensively the Indian Ocean response, in particular, is generated. Until a more coherent examination of the model-specific nature of this result is obtained, the decadal predictability remains limited. The initial results presented here suggest that the majority of potential forcing regions and relationships (in both models) remain broadly consistent under the anthropogenic, natural

(and control) simulations, which generate similar distribution of rainfall identified in the EOF analysis.

Although both models contribute to the proxy-based evidence of an anthropogenic signal in decadal rainfall variability over southern Africa, they provide slightly different mechanisms and changes in oceanic variables. It is therefore difficult to assess the degree to which this result is model specific. The existence of the control simulation, and subsequent mechanistic corroboration with the NAT simulation increases the confidence in the result presented by HadCM3, but the lack of explanation for the origins of the change in Indian Ocean SST behaviour in both models leaves some room for doubt.

Despite Damassa et al. (2006)'s confidence, the changing nature of quasi-decadal variability under anthropogenic forcing remains uncertain. Evidence from both climate models suggests that large-scale changes in ocean patterns and associated circulation anomalies result in less substantial modifications to rainfall distribution and spectral power over southern Africa. Further work is clearly needed before decadal rainfall attribution can be made with confidence over this complex region.

(7) Discussion & Conclusions

Southern Africa is a region of substantial climate variability on a range of timescales (Reason et al., 2004; Boko et al., 2007) which generates human (Washington et al., 2006; Osbahr & Roberts, 2007) and financial costs (Ravallion & Chen, 2004). Despite this, decadal variability in the region is one of the least well understood features of established circulation (Tyson, 1971; Handorf et al., 1999; Tyson et al., 2002).

This study has presented the first coherent analysis of decadal rainfall variability over southern Africa using a range of proxy, observed and state of the art climate model simulations (Gonzalez-Rouco et al., 2006; Tett et al., 2007). This chapter aims to bring together the principal results, and to consolidate the contribution of this study to the understanding of real world and climate model simulated decadal rainfall variability over southern Africa. In Chapter (1), the current state of our research knowledge was outlined, and four questions were posed in response to the gaps identified in the literature.

In the first section of this chapter, these research questions are restated in light of the study progress, and it is shown where the results presented here can help to understand some of the issues faced by southern African climate research. Next, the questions and challenges remaining are explored, together with suggestions for how future work could reduce the uncertainty in our knowledge of areas of decadal rainfall variability. Finally, the implications of this work for forecasting and detection/attribution studies are examined.

7.1 Principal Findings

The four research questions identified key issues that would help in understanding the decadal variability of southern African rainfall, and how this knowledge could contribute to a greater understanding of this region in decadal forecasting and climate change detection and attribution studies. In this section, the questions are re-examined, and the principal findings of the study explored in response.

(1) To what extent do General Circulation Models reproduce the southern African decadal variability?

Underpinning the rest of the study, the evaluation of the modelled climate over southern Africa showed that both HadCM3 and ECHO-G could be used with appropriate consideration to examine climate variability. This caution was exercised in the light of a brief model evaluation, which considered only mean state climates rather than repeat the intercomparison studies of variability and reproduction of major climate features (e.g. ENSO).

Drawing on work by Hudson & Jones (2002a,b) which investigated the behaviour of GCMs compared to nested Regional Models, it was shown that larger scale models were prone to precipitation estimation problems as they struggled to capture local topographic or oceanographic gradients. Hewitson & Crane (2006) showed this was particularly common over southern Africa, with specific orography creating problems for model simulation. Washington & Preston (2006) also noted that the general circulation structure was well represented in HadCM3, but that precipitation events did not necessarily respond as expected.

Linking in to the second research question, the models showed spatial and spectral responses in rainfall variability consistent with the observed data despite the issues raised in the model evaluation. As with all large scale models, the problems of localised precipitation have been identified, but the regional focus of this study is likely to have averaged out these issues to present a reasonable sub-continental scale picture. The salient details of the circulation were well captured, and the distribution of JFM mean rainfall (and other fields) adequately captured variability beyond synoptic scales. Although the global climate models would be not be the first choice of data for examining short term or localised variability, the use of the JFM seasonal average to evaluate decadal scale rainfall variability at the sub-continental scale was thought to be a reasonable representation of the real world climate behaviour.

The state of the art climate models climate models are an essential component of understanding decadal variability, and their potential for exploring extended fields and long samples make them a strong tool for investigating any long-term climate phenomenon. However, this does not mean they are without flaws. Both models showed substantial weaknesses in capturing elements of the regional circulation, and inconsistency with each other relative to the observed data. The combined evidence from model evaluation and subsequent analysis suggests that the climate models used here are adequate at reproducing the decadal climate of southern Africa, and the associated variability in the surrounding oceans and atmosphere, but that large improvements still remain possible.

(2) What is the nature of decadal variability in southern African rainfall?

Chapter (4) presented the first comprehensive analysis of the nature of decadal variability in southern African rainfall across a range of proxy, observed and model data sources. Sample decadal rainfall events, chosen from periods of high decadal variability in wavelet analysis, showed broad agreement with the suggested wet bias of HadCM3 compared to both observed and ECHO-G mean rainfall.

Spectral analysis of all sources showed elements of consistency, and typically agreed with previously described analysis (e.g. Tyson, 1971; Allan, 2000; Tyson et al., 2002). The ENSO signal, for example, was reasonably well captured by most data, although the known problems of ENSO simulation in ECHO-G (Achuta-Rao & Sperber, 2002; Guilyardi et al., 2004; Achuta-Rao & Sperber, 2006; Guilyardi, 2006) resulted in a slightly higher-frequency range of variability in this area. In the climate models, spectral power was highest in the control simulation, and became somewhat subdued under the addition of natural and anthropogenic forcing scenarios.

At a quasi-decadal scale, there was broad agreement on the appearance of 10-12 year spectral power with varying degrees of confidence. There was also reasonable agreement over spectral power at 16-20 years in observed, proxy and HadCM3-simulated rainfall. ECHO-G's simulations showed differences relating to their forcing; ENAT showed evidence of power at ~25 years compared to ~32 years under ERIK's anthropogenic forcing conditions.

Chapter (4) also showed that the precise 18 year oscillation period initially identified by Tyson (1971; 1980) that has been the focus of previous decadal rainfall studies over

southern Africa is not found in any of the data presented here. It was suggested that this could be a result of the spectral techniques employed to examine the wider issue of decadal variability, rather than attempting to explore a precise oscillatory frequency (Chandler, 2007). It was also hypothesised that the wider resolution datasets (compared to Tyson's station data or point source proxy techniques) are thought to broaden the resulting power spectrum, and that the 16-20 year spectral power identified in several data sources was a good approximation of the "18 year cycle" described in the literature.

Wavelet analysis on all spectral records showed that the periods of enhanced spectral power at particular frequencies were not consistent throughout the record, and became intermittent periods of power. Comparative analysis between observed and proxy records showed uncertainty in the timing of spectral power, for example, and SSA techniques were employed to show the variability possessed broad spectral power rather than precise oscillatory frequencies. This supported the expected nature of decadal variability in climate systems (Chandler, 2007; Tozuka et al., 2007).

Empirical orthogonal function analysis was employed to ascertain the spatial nature of decadal variability. The point-source proxy data was discarded, and domain-specific results generated by land-based observed precipitation concentrated the analysis on model data. There was broad agreement in the spatial simulation of rainfall between model experiments, and both models showed characteristics which qualitatively resembled interannual variability over southern Africa. In particular, the models were dominated by a NW-SE orientation which was thought to link to the synoptic scale tropical temperate trough formation (Todd & Washington, 1999; Washington & Todd, 1999).

The decadal rainfall variability presented in this chapter was thought to agree broadly with the previous work over southern Africa. HadCM3 matched the observed spectral power more closely, with some differences noted in ECHO-G's simulation of the regional rainfall. The spatial analysis was consistent with structures identified at synoptic and interannual scales in observations. This result led to an investigation of the structures of variability associated with decadal rainfall over southern Africa.

(3) What ocean-atmosphere variability is associated with decadal rainfall variability over southern Africa?

Having identified real and simulated variability in rainfall at decadal scales over southern Africa, the associated variability was examined in Chapter (5). Common regions of oceanic influence were identified in the observed and modelled data, and found to be in agreement with previously identified regions for interannual variability. This discussion concentrated on control simulations (ENAT simulation in ECHO-G, in the absence of a control run), rather than the forced simulations of ERIK and ALL described in Chapter (6).

Although HadCM3 showed evidence of links to the tropical Atlantic Meridional variability (Knight et al., 2005a, 2005b; Knight et al., 2006), the South Atlantic is typically regarded as a secondary moisture source for southern African JFM rainfall and most often linked to winter storm tracks or the SW Cape region. In this study, weak links were identified in all three datasets. Although possible explanations have been identified elsewhere (e.g. Venegas et al., 1996, 1997; Colberg & Reason, 2007), it was thought that links to the decadal variability of southern African rainfall were probably driven by common atmospheric variability (Hermes & Reason, 2005) with the SW Indian Ocean

region and this could explain the observed correlation. In the model data, the role of the Southern Annular Mode was explored as a potential source for this atmospheric variability, and was thought to be a more substantial influence in ECHO-G than HadCM3.

In agreement with the analysis of regions associated with interannual variability, the Indian Ocean provided stronger teleconnections with southern African rainfall at decadal scales. The classic "dipole" pattern in the SW Indian Ocean was observed, but shown to be a less coherent entity at decadal scales than interannual, and the 'tropical' and 'subtropical' nodes of the dipole considered as separate index regions. The nodes of the SWIO region were found to have different relationships with southern African rainfall at decadal timescales. In HadCM3, the tropical node was linked more coherently to southern African rainfall, compared to the stronger subtropical node of ECHO-G ENAT.

This differential relationship was thought to reflect the model's simulation and teleconnections with ENSO, and linked to the role and behaviour of the Southern Annular Mode in ECHO-G. Known to have a weak ENSO simulation, the lack of teleconnections in the tropical oceans in ECHO-G augmented the apparent role of the SAM in driving South Atlantic and SW Indian Ocean variability and enhanced the relative strength of the subtropical node. The more realistic ENSO simulation in HadCM3 reflected a stronger teleconnection with the tropical Indian Ocean, and the stronger tropical node relative to southern African rainfall was thought to be more closely aligned with observed and reanalysis data results.

The role of decadal ENSO-like behaviour was considered in all data sources. Notable differences were observed between the model simulations. This was linked to known

problems with ECHO-G's simulation of ENSO like behaviour, and suggested that the model also struggles to adequately capture the variability of the tropical Pacific at decadal timescales. In the observations and HadCM3 simulation, the decadal ENSO-like variability was shown to possess similar characteristics and teleconnections to the classic ENSO variability. Links were demonstrated between the tropical Pacific and tropical Indian Ocean regions, and thought to represent the decadal extension of the atmospheric bridge relationship observed at interannual timescales.

Finally, the analysis presented here does not rule out possibility of intrinsic variability in the identified regions at decadal timescales. Although Washington & Preston (2006) present a method for removing the influence of classic ENSO variability in order to examine the intrinsic variability of the SW Indian Ocean, it is difficult to see how a similar analysis could be performed at decadal timescales. Although the associated variability described here is shown to have substantial influence over southern African rainfall, a considerable portion of the variance remains unexplained. It is suggested that the intrinsic variability proposed by Washington & Preston (2006) could well be expected to operate at decadal scales, and should be included in future analysis of this region.

The similarity between the nature of interannual and decadal rainfall variability was clearly demonstrated in the examination of the mechanisms identified in the observed and modelled data. Similar forcing regions were considered, and shown to be in agreement with mechanisms and ocean-atmosphere links identified in seasonal and interannual studies.

This result – found in all data sources – strongly suggests that the decadal variability observed over southern Africa is the result of the integration of interannual and multi-annual variability by the coupled ocean-atmosphere system to produce a decadal variance signal. The peaks at quasi-decadal scales, identified as significant relative to a red noise background, are consistent across a range of data sources, and this suggests that there is a more coherent relationship between the multi-annual variability than just random reddening of the power spectrum. Although the nature of this variability is not clear, there is evidence to suggest that key forcing regions vary in influence over southern Africa through time, and that this interaction happens consistently to generate the appearance of decadal variability in the rainfall records evaluated here. This result makes a considerable contribution in support of the integrative hypothesis (Vimont, 2007), and may have implications for the wider study of decadal variability as a phenomenon in other regions of the ocean-atmosphere system.

The principal difference is suggested to result from a reduced coherence in Indian Ocean dipole, and consequently, the need to consider both correlation regions as separate 'nodes' is thought to be important at decadal scales. The associated variability was then examined in anthropogenic forcing scenarios, in order to assess the potential implications for decadal predictability and detection and attribution studies.

(4) Is decadal variability altered by anthropogenic forcing?

Analysis of coral reef proxy data from 1660 onwards, thought to represent SSTs in the SW Indian Ocean (Cole et al., 2000), allowed comparisons to be made between natural and anthropogenic forced records. Damassa et al. (2006) suggested that the quasi-decadal variability observed in the seventeenth century was substantially damped by secular anthropogenic-induced warming trends, and it was also thought that the reduced variability was link to changing spatial structures of ENSO-like variability (Zinke et al., 2004).

Spectral analysis was conducted to ascertain how decadal scale rainfall was influenced by anthropogenic trends in model simulations, and to test this damping hypothesis. Comparisons of spectral power in ECHO-G ENAT (natural) and ERIK (anthropogenic) simulations showed some minor differences in the timing of quasi-decadal variability, but there was considerable noise in the distribution of spectral samples which made detection difficult. Similar comparisons based on HadCM3 control simulation with NAT (natural) and ALL (anthropogenic) experiments showed substantially reduced spectral power across all frequencies under anthropogenic forcing. Spatial analysis (using EOF techniques as previously described) showed that the rainfall distribution was not substantially altered in either model's anthropogenic simulation, suggesting that the change in decadal variability was a result of altered forcing.

Spatial correlation techniques were employed in the same way as in Chapter (5), and explored the principal regions of influence in both anthropogenic model simulations. In ECHO-G, the role of the South (Tropical) Atlantic was found to be consistent with

unforced simulations, and the Southern Annular Mode did not exhibit major changes in intrinsic characteristics. For both simulations, however, the role of the Indian Ocean variability showed substantial changes.

In HadCM3, the locations of principal correlation were approximately similar, but the relationship with the previously stronger tropical node of the SWIO was substantially reduced. Although the subtropical node remained consistent, the tropical node showed minimal correlations with southern African rainfall and ENSO teleconnections, and was thought to reverse the relationship observed in section 5.3, creating a different circulation response in the Walker-type circulation. Correlations based on global teleconnections (ENSO and SAM) did not show evidence of substantial change, and these oscillations were thought unlikely to drive the changes shown. Similarly, the Indian Ocean warming hypothesis proposed by Giannini et al. (2003) was evaluated in the context of driving the tropical SST change, and found to be inadequate to explain the observed differences. Similar behaviour was observed in the NAT simulation, potentially ruling out anthropogenic forcing as the cause of oceanic change.

In ECHO-G, the Indian Ocean was also the main region of change under anthropogenic forcing. A subdued relationship between South Atlantic and subtropical SW Indian Ocean contrasted with an enhanced ENSO influence in the tropical oceans. The subtropical and tropical nodes identified in the SW Indian Ocean were moved substantially southwards, taking up new positions in a more subtropical/mid-latitude location in the central Indian Ocean. This 10-15° shift moved the rainfall based correlation index regions in to agreement with SST correlations identified by the Southern Annular Mode, but there was

minimal evidence of intrinsic change in the SAM to support this as a forcing mechanism. As in the natural simulation, the interaction between ENSO and SAM forcing appeared to be a major influence over southern Africa, but the mechanisms driving the change observed here remain unclear.

In addressing these four research questions, this study has contributed to our understanding the decadal variability of real and simulated rainfall over southern Africa. The nature and associated variability have been explored, and the similarity to interannual variability demonstrated using two climate models. The results of the study support the concept of decadal variance as the integration of interannual and multi-annual variability by the ocean-atmosphere system, and suggest that there are no "decadal" mechanisms to identify in relation to southern African rainfall variability. The study has also investigated the changes to quasi-decadal rainfall variability under simulated anthropogenic forcing scenarios, and shown how the spatial and spectral distribution may alter under different forcing conditions. There remains a series of unanswered questions which have arisen during the previous chapters. In the next section, these are explored in greater detail.

7.2 Questions remaining:

This section discusses the principal remaining questions, and identifies some of the issues which have prevented this study fully answering them. Some thoughts on further work to build on this study are offered, and suggestions are made to reduce the uncertainty associated with the questions presented where possible.

How model specific are these results?

The question of model specificity is unavoidable in a study employing a small number of models. Comparison of SRES-based model simulations of precipitation (not described here), and model intercomparison studies suggest that precipitation is the most difficult of variables to accurately simulate, and consequently a range of simulated amounts and structures of precipitation are to be expected.

This uncertainty is evident in the results presented here – with both models differing from each other and the observed data. Of the two, perhaps HadCM3 – despite the known wet bias – performs slightly better in capturing the spatial structure and variability of the observed data. Both models typically agree on the mechanisms which influence the southern African region, and this agreement gives greater confidence in the continued use of these forcing regions as decadal predictors. Subtle differences in the strength of relationships are thought to relate to ECHO-G's known ENSO simulation issues and the interaction between ENSO and Southern Annular Mode.

Increased confidence in these results can be obtained by repeating this study on a range of models, but the paucity of full range experiments (control, natural and anthropogenic forcing) means that only a small number of models may be analysed in this way.

Why does the observed data agree more closely with the control simulation, not the anthropogenic simulations?

The proposed stronger tropical SWIO node in HadCM3 CTR simulated variability agrees with the observed decadal relationship described earlier. Although it also agrees with work by Washington & Preston (2006) at the interannual scale, it is important to note that their work was specifically detrending the potential influence of 'classic' ENSO, and it is not clear how robust their results may be in interpreting this particular relationship. Since the ALL and ERIK simulations are designed to be the close approximations of the real climate of the last 250 years (Gonzalez-Rouco et al., 2003; Tett et al., 2007), the disparity between observed and simulated rainfall mechanisms therefore leads to one of three conclusions.

First, perhaps the models do not simulate the relationship between rainfall variability over southern African sub-continent and the presence of anthropogenic forcing accurately. Although Tett et al. (2007) have extensively tested their simulations of the recent Holocene; the focus has been on simulation of temperature and global scale trends, rather than that of localised variability. Key elements for southern Africa may have been parameterised in order to reproduce the global trends more accurately.

Alternatively, the models may replicate the relationship between forcing and natural variability adequately, but underestimate the overall level of natural decadal variability, therefore leading all models to be 'damped' in comparison to the observations. The simulation of decadal-scale variability is difficult for models to reproduce and verify, particularly with respect to rainfall (Ansell et al., 1998; Barnett et al., 2005; Douville, 2006) as it is an inherently noisy variable (Hegerl & Allen, 2002; Meinke et al., 2005; Hegerl et al., 2006; Hannachi, 2006b). This is a difficult concept to test, especially after

discussion of the limitations and uncertainty associated with the deployment of proxy reconstruction techniques, and the spread of simulated decadal variance across both models and their experiments.

Third, there may be an unidentified influence which causes the significantly damped tropical SWIO response, and substantially alters the mechanistic relationship between this region and southern African rainfall. This could be related to the altered SST response in the tropical SWIO under anthropogenic forcing, and may well explain why the models and observed data do not fully agree.

What is driving the different response of the tropical SWIO in the NAT & ALL simulations?

The key change under anthropogenic forcing conditions appeared to be the substantial shifts in the response of the tropical SWIO, but the mechanisms underlying this change were not made clear from preliminary analysis.

Using HadCM3's experiment range as a guide, the role of anthropogenic forcing itself can be challenged, since a similar result appears under natural forcing. Analysis of the trend data also showed that long term secular warming trends were considered unlikely to influence the position of the correlation node, as they were effectively removed by the application of the digital band pass filter. Comparisons with ECHO-G simulations are inconclusive – the weak relationship with ENSO seems to rule out a coherent response in the tropical SWIO in both ENAT and ERIK simulations.

Shifts in the Southern Annular Mode – particularly in ECHO-G – appeared to control the spatial position of the subtropical and tropical SWIO nodes, but analysis of the behaviour

of both the SAM index and ENSO suggested that little had changed under anthropogenic forcing. It is possible that enhanced spectral power in the quasi-decadal band of these indexes could excite poorly understood elements of the Indian Ocean or thermohaline circulation, but there is no evidence for this in the results shown here.

Further work is therefore required to fully understand the changing role of the Indian Ocean under anthropogenic forcing, and to investigate the initial conditions of the naturally forced simulations which may generate this observed pattern. This may have important consequences for the predictability of rainfall over southern Africa, as well as potentially improving our understanding of the implications of the warming trends proposed by Giannini et al. (2003) over regions like the Sahel.

To what extent does decadal ENSO-like behaviour dominate decadal rainfall variability over southern Africa?

The role of decadal ENSO-like behaviour was notably inconsistent through this study. The limitations of ECHO-G's simulation of ENSO were identified in explaining the poor teleconnections with the tropical oceans and southern African rainfall. In HadCM3, ENSO simulation matched the observations more closely. Correlations with southern African rainfall at the decadal scale were weaker than the relationship observed at the interannual scale. This reflects the general pattern of interannual/decadal teleconnections, but may have additional implications for the relative importance of decadal ENSO over southern Africa. The difficulties with attaching confidence and significance levels to the filtered data described in Chapter (2) make attribution of the reduced correlation uncertain.

Further examination showed that both observed and HadCM3 datasets had strong similarities in structure and teleconnections between classic and decadal ENSO variability. However, the choice of NINO 3.4 SST index as a measure of ENSO variability was identified as a potential mechanistic bias in the analysis presented in this study, and is thought to explain the absence of Pacific Decadal Oscillation-type variability in the results. The NINO 3.4 index was argued to be a valid choice for exploring the variability associated with the southern African rainfall at decadal scales, but does not provide an appropriate platform from which to examine the nature and behaviour of decadal ENSO, because of the inherent assumptions made by this choice of index region. Further investigation is required to define this phenomenon, and explore the mechanisms by which it operates at a decadal scale.

Decadal ENSO remains one of the key areas of uncertainty in the examination of rainfall variability over southern Africa at decadal timescales. There is no clear understanding of the spatial or spectral structure of this phenomenon, and approaches to studying it are faced with considerable challenge. It is not clear whether the decadal variability and predictability of this region can (or should) be addressed with the phenomenon/mechanism approach, but scientists have not yet identified a more suitable methodology (Vimont, 2007).

What are the implications for decadal predictability?

There are three key implications for decadal predictability as a result of this study. First, in identifying the spatial and structural similarity between interannual and decadal rainfall variability in the region, this study has shown that future analysis of decadal predictability

should look to these regions initially. The results have shown that decadal variability arises – as a spectral peak with real significance relative to a red noise background – as a result of interaction between interannual and multi-annual variability, and the subsequent integration of this variability by the coupled ocean-atmosphere system. As a consequence, there is not thought to be an underlying "decadal" mechanism of variability associated with southern African rainfall, and existing predictors may continue to be used. The downside to this result is the lack of intrinsic regularity – the interaction of factors does not appear to be controlled by any particular mechanism, and therefore identifying which will take the dominant role in future climate variability is a difficult task.

Second, although the majority of forcing regions identified in the study showed a consistent influence between interannual and decadal timescales, some changes to their coherence were observed under anthropogenic forcing experiments. The key result for prediction of rainfall at decadal scales is to note the less integrated response of the SW Indian Ocean "dipole" at lower frequencies, and to identify both nodes of correlation as separate entities for prediction purposes at long range.

Third, the anthropogenic changes remain unclear. No distinct shifts in spatial distribution (or major changes in the timing of spectral power) were observed, but it is worth noting that the control simulation of HadCM3 was the closest match to the observed data. The uncertainty associated with natural and anthropogenic forcing, particularly in the critical Indian Ocean variability, does not improve confidence in their use as predictive tools. Further work is needed to assess their potential impact on predictability studies, and their reliability as indicators of climate variability that corresponds to the observed data.

Fourth, the state of the art in model simulation over the region is still notably weak in reproducing southern African circulation. Key weaknesses – e.g. the simulation of the Angolan heat low – are resolved with the introduction of nested high-resolution regional models, but there remains work to be done in improving the performance of general circulation models in reproducing the basic circulation features of southern Africa. Although they offer a substantial contribution to studies involving decadal variability, the models have some way to go before they are consistently reliable for this region.

7.3 Conclusions:

In the first chapter, the implications of rainfall variability on the vulnerable population of southern Africa were explored. It was shown that seasonal forecasting efforts – linked predominantly to the Quasi-Biennial Oscillation and ENSO phase (Cane et al., 1994; Goddard et al., 2001) – typically showed reasonable skill in predicting the rainfall (Landman et al., 2001).

No major changes to the methods of seasonal forecasting are proposed as a result of this study. Quasi-decadal variability possesses similar spatial structures and associated variability to those identified at synoptic to interannual scales (Mason & Jury, 1997; Mason, 2001; Reason, 2001b), thought to result from the integration of this variability with multi-annual variability by the coupled ocean-atmosphere system to generate decadal variance. Forecasts which are aiming to understand multi-decadal variability may wish to take notice of the reduced coherence of the "dipole" pattern in the SW Indian Ocean at decadal scales, particularly compared to the interannual relationship, but other mechanisms and forcing regions seem consistent. It is therefore considered likely that the current methods of forecast account for the decadal variability adequately.

A similar outlook is proposed for detection and attribution of anthropogenic change over southern Africa. The prevalence of synoptic scale features at all timescales appear to render the identification of interannual, multi-annual or quasi-decadal 'fingerprints' unlikely, and the broad spectral nature of rainfall variability over the region does not lend itself well to trend-based detection methods.

The complex forcing of southern African rainfall remains uncertain at the decadal scale. Warming and changing Indian Ocean SSTs need to be clearly understood, and the effects of anthropogenic forcing identified through further detection and attribution studies. We cannot be sure whether the predicted drying trends will further impact the decadal variability of this region, but it seems likely that increasing pressure on the hydrology of the region will create enhanced vulnerability in the next century (Boko et al., 2007; Christensen et al., 2007). The consistency in the nature and mechanisms of rainfall variability across timescales may well contribute to understanding and forecasting the rainfall, and so will be more important than ever as the effects of anthropogenic climate change continue.

Appendix 1: Data Sources

The datasets used in this study were obtained from the following sources, acknowledged with gratitude.

Proxy data:

The precipitation reconstruction from Zimbabwe (Therrell et al., 2006) was obtained using World Data Centre for Paleoclimatology (http://www.ncdc.noaa.gov/paleo/recons.html) online datasets. The coral reef data employed was obtained through the 'Coral & Sclerosponge' data page of the same website, with the exception of the Mafia coral record (Damassa et al., 2006) which was personally supplied by Professor Julia Cole (University of Arizona).

Observed data:

The majority of observed datasets (HadISST, HadSLP2, CRUTEM3, HadCRUT3) were obtained through the UK Met Office Hadley Centre observation dataset page (http://hadobs.metoffice.com/index.html). The CRU global gridded precipitation data set is constructed and supplied by Professor Mike Hulme at the Climate Research Unit, University of East Anglia, UK.

Climate model data:

HadCM3 control run data was supplied through the British Atmospheric Data Centre (BADC). The NATURAL and ALL forcing experiments were designed by Professor Simon Tett, and obtained through Dr. Philip Brohan and the Simulations, Observations & Palaeoclimate (SO&P) data project, led by Dr. Tim Osborn at the Climate Research Unit, University of East Anglia, UK. This work was supported by the European Commission (EVK2-CT-2002-00160 SOAP).

The majority of ECHO-G data was supplied by the SO&P website described above. The ERIK SST data set was supplied by Dr. Jesus-Fidel Gonzalez-Rouco (Universidad Complutense de Madrid, http://chubasco.fis.ucm.es/~fi/), and gratefully acknowledged.

References:

(1) Abarca-del-Rio and Mestre (2006). "Decadal to secular time scales variability in temperature measurements over France." Geophysical Research Letters **33**(13): L13705.

(2) Achuta-Rao and Sperber (2002). "Simulation of the El Nino Southern Oscillation: Results from the coupled model intercomparison project." Climate Dynamics **19**(3-4): 191-209.

(3) Achuta-Rao and Sperber (2006). "ENSO simulation in coupled ocean-atmosphere models: are the current models better?" Climate Dynamics **27**: 1-15.

(4) Adler, et al. (2003). "The Version 2 Global Precipitation Climatology Project (GPCP) monthly precipitation analysis (1979-present)." Journal of Hydrometeorology **4**(6): 1147-1167.

(5) Aldrian, et al. (2007). "Seasonal variability of Indonesian rainfall in ECHAM4 simulations and in the reanalyses: The role of ENSO." Theoretical and Applied Climatology **87**: 41-59.

(6) Alexander, et al. (2002). "The atmospheric bridge: the influence of ENSO teleconnections on air-sea interaction over the global oceans." Journal of Climate **15**(16): 2205-2231.

(7) Allan (2000). ENSO and climate variability in the last 150 years. El Nino and the Southern Oscillation: Multiscale Variability, Global and Regional Impacts. Diaz and Markgraf. Cambridge, Cambridge University Press**:** 496.

(8) Allan and Ansell (2006). "A new globally complete monthly historical gridded mean sea level pressure dataset (HadSLP2): 1850-2004." Journal of Climate **19**(22): 5816-5842.

(9) Allan, et al. (1995). "Multidecadal variability in the climate system over the Indian ocean region during the austral summer." Journal of Climate **8**: 1853-1873.

(10) Allan, et al. (2003). "Protracted ENSO episodes over the Indian Ocean region." Deep Sea Research - Part II **50**: 2331-2347.

(11) Allen and Robertson (1996). "Distinguishing modulated oscillations from coloured noise in multivariate datasets." Climate Dynamics **12**: 775-784.

(12) Allen and Smith (1996). "Monte Carlo SSA: detecting oscillations in the presence of coloured noise." Journal of Climate **9**: 3373-.

(13) Allen and Smith (1997). "Optimal filtering in singular spectrum analysis." Physics Letters **234**: 419-428.

(14) Allen and Stott (2003). "Estimating signal amplitudes in optimal fingerprinting, part 1: theory." Climate Dynamics **21**(5-6): 477-91.

(15) Allen and Tett (1999). "Checking for model consistency in optimal fingerprinting." Climate Dynamics **15**(6): 419-434.

(16) Alverson, et al. (2001). "Improving climate predictability and understanding decadal variability using proxy climate data." CLIVAR-Exchanges **19**.

(17) Ammann, et al. (2003). "A monthly and latitudinally varying volcanic forcing dataset in simulations of 20th century climate." Geophysical Research Letters **30**(12): 1657.

(18) An, et al. (2007). "The influence of ENSO on the generation of decadal variability in the North Pacific." Journal of Climate **20**: 667-680.

(19) Annamalai, et al. (2006). "Southwest Indian Ocean SST variability: its local effect and remote influence on Asian monsoons." Journal of Climate **in press**.

(20) Ansell, et al. (2000). "Variability in the tropical southeast Indian Ocean and links with southeast Australian winter rainfall." Geophysical Research Letters **27**: 3977-3980.

(21) Ansell, et al. (1998). "Evidence for decadal variability in southern Australian rainfall and relationships with regional pressure and SST." International Journal of Climatology **20**(10): 1113-1129.

(22) Ashok, et al. (2004a). "Decadal variability of the Indian Ocean dipole." Geophysical Research Letters **31**: L24207.

(23) Ashok, et al. (2004b). "Individual and combined influences of ENSO and the Indian Ocean dipole on the Indian summer monsoon." Journal of Climate **17**(16): 3141-3155.

(24) Ashok, et al. (2003a). "Influence of the Indian Ocean dipole on the Australian winter rainfall." Geophysical Research Letters **30**(15): L017926.

(25) Auad (2003). "Interdecadal dynamics of the North Pacific Ocean." Journal of Physical Oceanography **33**: 2483-2503.

(26) Bader and Latif (2003). "The impact of decadal-scale Indian Ocean sea surface temperature anomalies on Sahelian rainfall and the North Atlantic Oscillation." Geophysical Research Letters **30**(22): 2169.

(27) Bader, et al. (2003). "The role of tropical SSTs in forcing Sahelian rainfall variations." CLIVAR-Exchanges **27**.

(28) Balachandran, et al. (1999). "Effects of solar cycle variability on the lower stratosphere and troposphere." Journal of Geophysical Research **104**: 27 321-27 339.

(29) Barnett (1999). "Comparison of near surface air temperature variability in 11 coupled global climate models." Journal of Climate **12**(2): 511-518.

(30) Barnett, et al. (1999). "Detection and attribution of climate change: a status report." Bulletin of the American Meteorological Society **80**(12): 2631-2659.

(31) Barnett, et al. (1999). "Origins of the midlatitude Pacific decadal variability." Geophysical Research Letters **26**: 1453-1456.

(32) Barnett, et al. (2005). "Detecting and attributing external influences on the climate system: a review of recent advances." Journal of Climate **18**: 1291-1314.

(33) Basnett and Parker (1997). Development of the global mean sea level pressure data set GMSLP2, Hadley Centre Climate Research Technical Note.

(34) Behera, et al. (2003). "Comments on 'A cautionary note on the interpretations of EOFs'." Journal of Climate **16**: 1087-1093.

(35) Behera and Yamagata (2001). "Subtropical SST dipole events in the southern Indian Ocean." Geophysical Research Letters **28**(2): 327-330.

(36) Berger (1978). "Long term variations of caloric insolation resulting from the Earth's orbital elements." Quaternary Research **9**(2): 139-167.

(37) Bharwani, et al. (2005). "Multi-agent modelling of climate outlooks and food security on a community garden scheme in Limpopo, South Africa." Philosophical Transactions of the Royal Society B **360**: 2183-2194.

(38) Biasutti, et al. (2004). "Mechanisms controlling the annual cycle of precipitation in the tropical Atlantic sector in an atmospheric general circulation model." Journal of Climate **17**(24): 4708-4723.

(39) Blunier, et al. (1995). "Variation in atmospheric methane concentration during the Holocene epoch." Nature **374**: 46-49.

(40) Boer, et al. (2000). "A transient climate change simulation with greenhouse and aerosol forcing: experimental design and comparison with the instrumental record for the 20th century." Climate Dynamics **16**(6): 405-425.

(41) Boer, et al. (2007). "Inferring climate sensitivity from volcanic events." Climate Dynamics **28**: 481-502.

(42) Boko, et al. (2007). Africa. Climate Change 2007: Impacts, Adaptation and Vulnerability. Contribution of Working Group II to the Fourth Assessment Report of the Intergovernmental Panel on Climate Change. Parry, Canziani, Palutikof and van-der-Linden. Cambridge, Cambridge University Press.

(43) Bradley (1999). Palaeoclimatology: Reconstructing Climates of the Quaternary, Harcourt Academic Press.

(44) Bratcher and Giese (2002). "Tropical Pacific decadal variability and global warming." Geophysical Research Letters **20**(19): L015191.

(45) Brohan, et al. (2006). "Uncertainty estimates in regional and global observed temperature changes: a new dataset from 1850." Journal of Geophysical Research **111**(D12): D12106.

(46) Bullard, et al. (1997). "Dunefield activity and interactions with climatic variability in the southwest Kalahari Desert." Earth Surface Processes and Landforms **22**: 165-174.

(47) Burger and Cubasch (2005). "Are multiproxy climate reconstructions robust?" Geophysical Research Letters **32**: L23711.

(48) Cane, et al. (2006). "Progress in palaeoclimate modelling." Journal of Climate **19**(20): 5031-5057.

(49) Cane, et al. (1994). "Forecasting Zimbabwean maize yield using eastern equatorial Pacific SSTs." Nature **370**(204-205).

(50) Carleton (1999). "Methodology in climatology." Annals of the American Association of Geographers **89**(4): 713-735.

(51) Chandler (2007). Statistical methods for trend detection and analysis in the environmental sciences. in press, Wiley.

(52) Chang, et al. (1997). "A decadal climate variation in the tropical Atlantic Ocean from thermodynamic air-sea interaction." Nature **385**: 516-518.

(53) Chang, et al. (2000). "The effect of local sea surface temperatures on atmospheric circulation over the tropical Atlantic." Journal of Climate **13**: 2195-2216.

(54) Chang, et al. (2001). "A hybrid coupled model study of tropical Atlantic variability." Journal of Climate **14**: 361-390.

(55) Charles, et al. (1997). "Interaction between the ENSO and the Asian Monsoon in a coral record of tropical climate." Science **277**: 925-928.

(56) Chelliah and Bell (2004). "Tropical multidecadal and interannual climate variability in the NCEP-NCAR reanalysis." Journal of Climate **17**(9): 1777-1803.

(57) Chiang, et al. (2002). "Deconstructing Atlantic ITCZ variability: influence of the local cross equatorial SST gradient and remote forcing from the eastern equatorial Pacific." Journal of Geophysical Research **107**: 4004.

(58) Chiang and Vimont (2004). "Analagous Pacific and Atlantic meridional modes of tropical atmosphere-ocean variability." Journal of Climate **17**(21): 4143-4158.

(59) Christensen, et al. (2007). Regional Climate Projections. Climate Change 2007: The Physical Science Basis. Contribution of Working Group 1 to the Fourth Assessment Report of the Intergovernmental Panel on Climate Change. Solomon, Qin, Manninget al. Cambridge, Cambridge University Press.

(60) Chung and Ramanathan (2006). "Weakening of North Indian SST gradients and the monsoon rainfall in India and the Sahel." Journal of Climate **19**: 2036-2045.

(61) Clark, et al. (2000). "Indian Ocean SST and Indian summer rainfall: predictive relationships and their decadal variability." Journal of Climate **13**: 2503-2519.

(62) Clay, et al. (2003). "Malawi and southern Africa: Climatic variability and economic performance." World Bank Disaster Risk Management Working Paper Series **7**: 92pp.

(63) Cobb, et al. (2003). "El Nino/Southern Oscillation and tropical Pacific climate change during the last millennium." Nature **424**: 271-276.

(64) Cockcroft, et al. (1987). "The application of a present day climatic model to the late Quaternary in southern Africa." Climatic Change **10**: 161-181.

(65) Cohen and Tyson (1995). "Sea surface temperature fluctuations during the Holocene off the coast of South Africa - implications for terrestrial climate and rainfall." The Holocene **5**(3): 304-312.

(66) Colberg and Reason (2007). "Ocean model diagnosis of low-frequency climate variability in the South Atlantic region." Journal of Climate **20**: 1016-1034.

(67) Colberg, et al. (2004). "South Atlantic response to ENSO induced climate variability in an OGCM." Journal of Geophysical Research **109**.

(68) Cole, et al. (2000). "Tropical Pacific forcing of decadal SST variability in the western Indian Ocean over the past two centuries." Science **260**: 1790-1793.

(69) Collins (2002). "Climate predictability of interannual to decadal timescales: the initial value problem." Climate Dynamics **19**(671-692).

(70) Collins, et al. (2004). "Predictability of Indian Ocean SSTs using canonical correlation analysis." Climate Dynamics **22**(5): 481-497.

(71) Collins and Sinha (2003). "Predictability of decadal variations in the thermohaline circulation and climate." Geophysical Research Letters **30**(6): 1306.

(72) Collins, et al. (2005). "El Nino or La Nina like climate change?" Climate Dynamics **24**: 89-104.

(73) Coughlin and Tung (2004). "11-year solar cycle in the stratosphere extracted by the empirical mode decomposition method." Advances in Space Research **34**: 323-329.

(74) Cox, et al. (1999). "The impact of new land surface physics on the GCM simulation of climate and climate sensitivity." Climate Dynamics **15**: 183-203.

(75) Crimp, et al. (1998). "Sensitivity of a tropical-temperate trough to sea surface temperature anomalies in the Agulhas retroflection region." Water SA **24**(2): 93-100.

(76) Crooks and Gray (2005). "Characterisation of the 11-year solar signal using a multiple regression analysis of the ERA40 dataset." Journal of Climate **18**(7): 996-1015.

(77) Crowley (2000). "Causes of climate change over the past 1000 years." Science **289**: 270-277.

(78) Crucifix, et al. (2002). "Climate evolution during the Holocene: a study with an Earth System model of intermediate complexity." Climate Dynamics **19**(1): 43-60.

(79) Cubasch, et al. (2005). "The direct solar influence on climate: modeling the lower atmosphere." Memorie della Societa Astronomica Italiana **76**: 810-818.

(80) Cubasch, et al. (2006). "Simulation of the role of solar and orbital forcing on climate." Advances in Space Research **37**(8): 1629-1634.

(81) Currie (1993). "Luni-solar 18.6- and 10-11 year solar cycle signals in South African rainfall." International Journal of Climatology **13**: 237-256.

(82) Currie (1993). "Luni-solar and solar cycle signals in the USA temperature records." International Journal of Climatology **13**(1): 31-50.

(83) Curry (1972). "Spectral spectra?" Annals of the American Association of Geographers **62**(3): 558.

(84) Cusack, et al. (1998). "The radiative impact of a simple aerosol climatology on the Hadley Centre Atmospheric GCM." Quarterly Journal of the Royal Meteorological Society **124**: 2517-2526.

(85) D'Abreton and Lindesay (1993). "Water vapour over Southern Africa during wet & dry early & late summer months." International Journal of Climatology **13**: 151-170.

(86) Dai, et al. (2004). "The recent Sahel drought is real." International Journal of Climatology **24**: 1323-1331.

(87) Damassa, et al. (2006). "Enhanced multidecadal climate variability in the seventeenth century from coral isotope records in the western Indian Ocean." Palaeoceanography **21**: PA2016.

(88) D'Arrigo, et al. (2005). "On the variability of ENSO over the past six centuries." Geophysical Research Letters **32**(3): L03711.

(89) Daubechies (1990). "The wavelet transform time-frequency localisation and signal analysis." IEEE Transformation Theory **36**: 961-1004.

(90) Daubechies (1992). Ten Lectures on Wavelets, Society for Industrial and Applied Mathematics.

(91) Davies, et al. (2006). "A new dynamical core for the Met Office's global and regional modelling of the atmosphere." Quarterly Journal of the Royal Meteorological Society **131B**(608): 1759-1782.

(92) Delworth and Greatbatch (2000). "Multidecadal thermohaline circulation variability driven by atmospheric surface flux forcing." Journal of Climate **13**: 1073-1097.

(93) Delworth, et al. (1993). "Interdecadal variations in the thermohaline circulation in a coupled ocean-atmosphere model." Journal of Climate **6**: 1993-2011.

(94) Delworth and Mann (2000). "Observed and simulated multidecadal variability in the Northern Hemisphere." Climate Dynamics **16**(9): 661 - 676.

(95) DeMott, et al. (2007). "Convective precipitation variability as a tool for GCM analysis." Journal of Climate **20**: 91-112.

(96) de-Ruijter, et al. (1999). "Indian-Atlantic inter-ocean exchange: dynamics, estimation and impact." Journal of Geophysical Research **104**: 20,885-20,910.

(97) Dery and Wood (2005). "Observed twentieth century land surface air temperature and precipitation covariability." Geophysical Research Letters **32**: L21414.

(98) Desanker and Magadza (2001). Africa. Climate Change 2001: Impacts, Adaptation and Vulnerability. McCarthy, Canziani, Leary and Dokken, Cambridge University Press**:** 487-531.

(99) Diab, et al. (1991). "Distribution of rainfall by synoptic type over Natal, South Africa." International Journal of Climatology **11**: 877-888.

(100) Diedhiou, et al. (2003). "Multiscale view of the Sahelian rainfall regimes." CLIVAR-Exchanges **27**.

(101) Dima and Lohmann (2007). "A hemispheric mechanism for the Atlantic multidecadal oscillation." Journal of Climate **20**: 2706-2719.

(102) Dima, et al. (2005). "Solar induced and internal climate variability at decadal time scales." International Journal of Climatology **25**: 719-733.

(103) Dima, et al. (2002). "Arctic oscillation variability generated through inter-ocean interactions." Geophysical Research Letters **29**(14): L014717.

(104) Domingues, et al. (2005). "On wavelet techniques in atmospheric sciences." Advances in Space Research **35**(5): 831-842.

(105) Dommenget (2006). "Evaluating EOF modes against a stochastic null hypothesis." Journal of Climate: in press.

(106) Dommenget and Latif (2002). "A cautionary note on the interpretation of EOFs." Journal of Climate **15**: 216-225.

(107) Dommenget and Latif (2003). "Reply to comments of Behera et al." Journal of Climate **16**: 1094-1097.

(108) Dong and Sutton (2005). "Mechanism of interdecadal thermohaline circulation variability in a coupled ocean-atmosphere GCM." Journal of Climate **18**(8): 1117-1135.

(109) Douville (2006). "Detection-attribution of global warming at the regional scale: how to deal with precipitation variability?" Geophysical Research Letters **33**: L02701.

(110) Drosdowsky and Chambers (2001). "Near-global sea surface temperature anomalies as predictors of Australian seasonal rainfall." Journal of Climate **14**: 1677-1687.

(111) Dufresne, et al. (2005). "Contrasts in the effects on climate of anthropogenic sulphate aerosols between the 20th and 21st century." Geophysical Research Letters **32**: L21703.

(112) Dunwiddie and Lamarche (1980). "A climatologically responsive tree ring record from W. cedarbergensis, Cape Province, SA." Nature **286**: 796-797.

(113) Edwards and Slingo (1996). "Studies with a flexible new radiation code. 1. Choosing a configuration for a large scale model." Quarterly Journal of the Royal Meteorological Society **122**: 689-720.

(114) Eischeid, et al. (1991). A comprehensive precipitation data set for global land areas. Washington DC, US Department of Energy Report No. DOE/ER-69017T-H1**:** 81.

(115) Enfield and Mestas-Nunez (1999). "Multiscale variabilities in global sea surface temperatures and their relationship with tropospheric climate patterns." Journal of Climate **12**: 2719-2733.

(116) England, et al. (2006). "Interannual rainfall extremes over southwest Western Australia linked to Indian Ocean climate variability." Journal of Climate **19**: 1948-1969.

(117) Etheridge, et al. (1996). "Natural and anthropogenic changes in atmospheric CO2 over the last 1000 years from air in Antarctic ice and firn." Journal of Geophysical Research **101**: 4115-4128.

(118) Farge (1992). "Wavelet transforms and their applications to turbulence." Annual Review of Fluid Mechanics **24**: 394-457.

(119) Fauchereau, et al. (2003b). "Sea-surface temperature co-variability in the southern Atlantic and Indian oceans and its connections with the atmospheric circulation in the Southern Hemisphere." International Journal of Climatology **23**: 663-677.

(120) Fauchereau, et al. (2003a). "Rainfall variability and changes in Southern Africa during the 20th century in the global warming context." Natural Hazards **29**(2): 139-154.

(121) February and Stock (1998). "An assessment of the dendrochronological potential of two Podocarpus species." Holocene **8**(6): 747-750.

(122) Fichtler, et al. (2004). "Climatic signals in tree rings of Burkea africana and Pterocarpus angolensis from semi arid forests in Namibia." Trees **18**: 442-451.

(123) Fischer, et al. (2005). "Socio-economic and climate change impacts on agriculture: An integrated assessment, 1990-2080." Philosophical Transactions of the Royal Society **360B**: 2067-2083.

(124) Florenchie, et al. (2003). "The source of Benguela Ninos in the South Atlantic Ocean." Geophysical Research Letters **30**: 12-1 - 12-4.

(125) Florenchie, et al. (2004). "Evolution of interannual warm and cold events in the southeast Atlantic Ocean." Journal of Climate **17**(12): 2318-2334.

(126) Folland, et al. (2001). Observed climate variability and change. Climate Change 2001: The Scientific Basis. Houghton, Ding, Griggset al. Cambridge, New York, Cambridge University Press**:** 99-181.

(127) Folland, et al. (1986). "Sahel rainfall and worldwide sea temperatures, 1901-85." Nature **320**: 602-607.

(128) Foufoula-Georgiou and Kumar (1995). Wavelets in Geophysics. New York, Academic.

(129) Frankignoul, et al. (1997). "A simple model of the decadal response of the ocean to stochastic wind forcing." Journal of Physical Oceanography **27**: 1533-1546.

(130) Friedlingstein, et al. (2006). "Climate-carbon cycle feedback analysis: results from the C^4MIP model inter-comparison." Journal of Climate **19**: 3337-3353.

(131) Gedalof and Smith (2001). "Interdecadal climate variability and regime-scale shifts in Pacific North America." Geophysical Research Letters **28**: 1515-1518.

(132) Gedney, et al. (2006). "Detection of a direct carbon dioxide effect in continental river runoff records." Nature **439**: 835-838.

(133) Geerts and Dejene (2005). "Regional and diurnal variability of the vertical structure of precipitation systems in Africa based on space-borne radar data." Journal of Climate **18**(7): 893-916.

(134) Gent and McWilliams (1990). "Isopycnal mixing in ocean circulation models." Journal of Physical Oceanography **20**: 150-155.

(135) Gershunov and Barnett (1998). "Interdecadal modulations of ENSO teleconnection." Bulletin of the American Meteorological Society **79**: 2715-2725.

(136) Ghil, et al. (2002). "Advanced spectral methods for climatic time series." Reviews of Geophysics **40**(1): 1003.

(137) Giannini, et al. (2003). "Oceanic forcing of Sahel Rainfall on Interannual to Interdecadal Time Scales." Science **302**(5647): 1027-1030.

(138) Giles (2007). "How to survive a warming world." Nature **446**: 716-717.

(139) Gillett, et al. (2006). "Regional climate impacts of the Southern Annular Mode." Geophysical Research Letters **33**: L23704.

(140) Gillett, et al. (2004). "Detection of volcanic influence on global precipitation." Geophysical Research Letters **31**: L12217.

(141) Gilman, et al. (1963). "On the power spectrum of 'red noise'." Journal of Atmospheric Science **20**: 182-184.

(142) Giorgetta, et al. (2006). "Preface to special section on climate models at Max Planck Institute for Meteorology." Journal of Climate **19**: 3769-3770.

(143) Giorgi (2005). "Interdecadal variability of regional climate change: implications for the development of regional climate change scenarios." Meteorology and Atmospheric Physics **89**: 1-15.

(144) Giorgi and Francisco (2000). "Evaluating uncertainties in the prediction of regional climate change." Geophysical Research Letters **27**: 1295-1298.

(145) Gissila, et al. (2004). "Seasonal forecasting of the Ethiopian summer rains." International Journal of Climatology **24**(11): 1345-1358.

(146) Gladstone, et al. (2005). "Mid Holocene NAO: A PMIP2 model intercomparison." Geophysical Research Letters **32**(16): L16707.

(147) Goddard and Graham (1999). "Importance of the Indian Ocean for simulating rainfall anomalies over eastern and southern Africa." Journal of Geophysical Research **104**(D16): 19099-19116.

(148) Goddard, et al. (2001). "Current approaches to seasonal to interannual climate predictions." International Journal of Climatology **21**(9): 1111-1152.

(149) Goldenberg, et al. (2001). "The recent increase in Atlantic hurricane activity: causes and implications." Science **293**: 474-479.

(150) Goldenberg and Shapiro (1996). "Physical mechanisms for the association of El Nino and west African rainfall with Atlantic major hurricane activity." Journal of Climate **9**(6): 1169-1187.

(151) Gong and Wang (1999). "Definition of Antarctic Oscillation index." Geophysical Research Letters **26**: 439-462.

(152) Gonzalez-Rouco, et al. (2006). "Simulation and inversion of borehole temperature profiles in surrogate climates: spatial distributions and surface coupling." Geophysical Research Letters **33**: L01703.

(153) Gonzalez-Rouco, et al. (2003). "Deep soil temperature as proxy for surface air-temperature in a coupled model simulation of the last thousand years." Geophysical Research Letters **30**(21): 2116.

(154) Goosse, et al. (2005a). "Modelling the climate of the last millennium: What causes the difference between simulations?" Geophysical Research Letters **32**: L06710.

(155) Goosse, et al. (2005b). "Internal and forced climate variability during the last millennium: a model data comparison using ensemble simulations." Quaternary Science Reviews **24**(12-13): 1345-1360.

(156) Goosse, et al. (2006). "Using palaeoclimate proxy-data to select optimal realisations in an ensemble of simulations of the climate of the past millennium." Climate Dynamics **27**: 165-184.

(157) Gordon, et al. (2000). "The simulation of SST, sea ice extents and ocean heat transport in a version of the Hadley Centre coupled model without flux adjustments." Climate Dynamics **16**: 147-168.

(158) Graf, et al. (1993). "Pinatubo eruption winter climate effects: model versus observations." Climate Dynamics **9**: 81-93.

(159) Gray, et al. (2005). Review of the influence of solar changes on the Earth's climate. Exeter, UK, Hadley Centre, Met Office.

(160) Gregory, et al. (2004b). "A new method for diagnosing radiative forcing and climate sensitivity." Geophysical Research Letters **31**: L03205.

(161) Gregory, et al. (1997). "Parametrization of momentum transport by convection. 2: Tests in single column and general circulation models." Quarterly Journal of the Royal Meteorological Society **123**(541): 1153-1183.

(162) Gregory, et al. (1998). "A new gravity-wave-drag scheme incorporating anisotropic orography and low-level wave breaking: Impact upon the climate of the UK Meteorological Office Unified Model." Quarterly Journal of the Royal Meteorological Society **124**(546): 463-493.

(163) Grist and Nicholson (2001). "A study of the dynamic factors influencing the rainfall variability in the West African Sahel." Journal of Climate **14**: 1337-1359.

(164) Groisman, et al. (2005). "Trends in intense precipitation in the climate record." Journal of Climate **18**: 1326-1350.

(165) Grottoli and Eakin (2007). "A review of modern coral delta-18-O and delta-14-C proxy records." Earth-Science Reviews **81**: 67-91.

(166) Gu and Adler (2003). "Seasonal rainfall variability within the West African Monsoon system." CLIVAR-Exchanges **27**.

(167) Guilyardi (2006). "El Nino mean state-seasonal cycle interactions in a multi-model ensemble." Climate Dynamics **26**(4): 329-348.

(168) Guilyardi, et al. (2004). "Representing El Nino in coupled atmosphere-ocean GCMs: the dominant role of the atmospheric component." Journal of Climate **17**(24): 4623-4629.

(169) Gupta and England (2006). "Coupled ocean-atmosphere-ice response to variations in the Southern Annular Mode." Journal of Climate **19**: 4457-4486.

(170) Hagemann, et al. (2006). "Evaluation of the hydrological cycle in the ECHAM5 model." Journal of Climate **19**: 3828-3843.

(171) Hagos and Cook (2005). "Influence of surface processes over Africa on the Atlantic marine ITCZ and South American precipitation." Journal of Climate **18**: 4993-5010.

(172) Handorf, et al. (1999). "Climate variability at decadal and interdecadal time scales." CLIVAR-Exchanges **14**.

(173) Hannachi (2006b). "Pattern hunting in climate: a new method for finding trends in gridded climate data." International Journal of Climatology: in press.

(174) Hannachi and Allen (2001). "Identifying signals from intermittent low-frequency behaving systems." Tellus **53A**: 469-480.

(175) Hannachi, et al. (2007). "Empirical orthogonal functions and related techniques in atmospheric science: a review." International Journal of Climatology **in press**.

(176) Hannachi, et al. (2006). "In search of simple structures in climate: simplifying EOFs." International Journal of Climatology **27**: 7-28.

(177) Hansen, et al. (2006). "Translating climate forecasts in to agricultural terms: advances and challenges." Climate Research **33**(1): 27-41.

(178) Hansen-Bauer, et al. (2003). "Temperature and precipitation scenarios for Norway: comparison of results from dynamical and empirical downscaling." Climate Research **25**: 15-27.

(179) Hansingo and Reason (2006). "Sensitivity of the atmospheric response to sea surface temperature forcing in the South West Indian Ocean: a regional climate modelling study." South African Journal of Science **102**(3-4): 137-143.

(180) Harrison (1984). "A generalised classification of South African summer rain bearing synoptic systems." Journal of Climatology **4**: 547-560.

(181) Hasegawa and Hanawa (2006). "Impact of quasi decadal variability in the Tropical Pacific on ENSO modulations." Journal of Oceanography **62**: 227-234.

(182) Hasselman (1988). "PIPs and POPs: the reduction of complex dynamical systems using principal interaction and oscillation patterns." Journal of Geophysical Research **93**: 11 015-11 021.

(183) Hasselman (1993). "Optimal fingerprints for the detection of time dependent climate change." Journal of Climate **6**: 1957-1971.

(184) Hasselman (1997). "Multi-pattern fingerprint method for detection and attribution of climate change." Climate Dynamics **13**: 601-611.

(185) Hastenrath (2000). "Zonal circulations over the equatorial Indian Ocean." Journal of Climate **13**: 2746-2756.

(186) Hastenrath, et al. (1995). "Prediction of the summer rainfall over South Africa." Journal of Climate **8**: 1511-1518.

(187) Hegerl and Allen (2002). "Origins of model-data discrepancies in optimal fingerprinting." Journal of Climate **15**(11): 1348-1356.

(188) Hegerl, et al. (2003). "Detection of volcanic, solar and greenhous gas signals in palaeo-reconstructions of Northern-Hemisphere temperature." Geophysical Research Letters **30**(5): L016635.

(189) Hegerl, et al. (1997). "Multi-fingerprint detection and attribution analysis of greenhouse gas, greenhouse gas plus aerosol and solar forced climate change." Climate Dynamics **13**(9): 613-634.

(190) Hegerl, et al. (2006). "Climate change detection and attribution: beyond mean temperature signals." Journal of Climate **19**: 5058-5077.

(191) Hegerl, et al. (1996). "Detecting greenhouse gas induced climate change with an optimal fingerprint method." Journal of Climate **9**(10): 2281-2306.

(192) Hegerl, et al. (2007). Understanding and Attributing Climate Change. Climate Change 2007: The Physical Science Basis. Contribution of Working Group 1 to the Fourth Assessment Report of the Intergovernmental Panel on Climate Change. Solomon, Qin, Manninget al. Cambridge, Cambridge University Press.

(193) Helama, et al. (2005). "Extracting long-period climate fluctuations from tree-ring chronologies over timescales of centuries to millennia." International Journal of Climatology **25**: 1767-1779.

(194) Hellstrom, et al. (2001). "A comparison of climate change scenarios for Sweden based on statistical and dynamical downscaling of monthly precipitation." Climate Research **19**: 45-55.

(195) Hendrix and Glaser (2007). "Trends and triggers: climate, cliamte change and civil conflict in sub-Saharan Africa." Political Geography **26**(6): 695-715.

(196) Hennessy, et al. (2007). Australia and New Zealand. Climate Change 2007: Impacts, Adaptation and Vulnerability. Contribution of Working Group II to the Fourth Assessment Report of the Intergovernmental Panel on Climate Change. Parry, Canziani, Palutikof and van-der-Linden. Cambridge, Cambridge University Press**:** 507-540.

(197) Herceg, et al. (2007). "Regional modelling of decadal rainfall variability over the Sahel." Climate Dynamics **29**: 89-99.

(198) Hermes and Reason (2005). "Ocean model diagnostics of interannual co-evolving SST variability in the South Indian and South Atlantic Oceans." Journal of Climate **18**(15): 2864-2882.

(199) Hewitson and Crane (2006). "Consensus between GCM climate change projections with empirical downscaling: precipitation downscaling over South Africa." International Journal of Climatology **26**(10): 1315-1337.

(200) Hickler, et al. (2005). "Precipitation controls Sahel greening trend." Geophysical Research Letters **32**: L21415.

(201) Hoerling, et al. (2006). "Detection and attribution of 20th century northern and southern African rainfall change." Journal of Climate **19**: 3989-4008.

(202) Holland, et al. (2006). "Propagating decadal sea surface temperature signal identified in modern proxy records of the tropical Pacific." Climate Dynamics **in press**.

(203) Holmgren, et al. (1999). "A 3000 year high-resolution stalagmite based record of palaeoclimate for northeastern South Africa." The Holocene **9**: 295-309.

(204) Holmgren, et al. (2003). "Persistent millennial scale climatic variability over the past 25 000 years in Southern Africa." Quaternary Science Reviews **22**(21-22): 2311-2326.

(205) Huck, et al. (2001). "On the robustness of the interdecadal modes of the thermohaline circulation." Journal of Climate **14**: 940-963.

(206) Hudson and Jones (2002a). Simulation of present day and future climate over southern Africa using HadAM3H, Hadley Centre, UKMO**:** 37.

(207) Hudson and Jones (2002b). Regional Climate Model simulations of present-day and future climates of southern Africa, Hadley Centre, UKMO.

(208) Hulme (1992). "A 1951-80 global land precipitation climatology for the evaluation of general circulation models." Climate Dynamics **7**(2): 57-72.

(209) Hulme (1992). "Rainfall changes in Africa, 1931-1960 to 1961-1990." International Journal of Climatology **12**: 685-699.

(210) Hulme (1994). Validation of large scale precipitation fields in General Circulation models. Global precipitation and climate change. Desalmand. Berlin, Springer-Verlag**:** 466.

(211) Hulme (1996). "Recent climatic change in the world's drylands." Geophysical Research Letters **23**: 61-64.

(212) Hulme (1999). Gridded precipitation data 'g55wld098.dat', version 1.0, Climate Research Unit, UEA.

(213) Hulme, et al. (1999). "Relative impacts of human-induced climate change and natural climate variability." Nature **397**(6721): 688-691.

(214) Hulme, et al. (1998). "Precipitation sensitivity to global warming: comparison of observations with HadCM2 simulations." Geophysical Research Letters **25**: 3379-3382.

(215) Hurrell, et al. (2004). "Twentieth century North Atlantic climate change. Part 1: Assessing determinism." Climate Dynamics **23**: 375-390.

(216) Hutchinson (1995). "Stochastic space-time weather models from ground based data." Agricultural and Forest Meteorology **73**(3-4): 237-264.

(217) Hyden and Sekoli (2000). "Possibilities to forecast early summer rainfall in the Lesotho Lowlands from ENSO." Water SA **26**(1): 83-90.

(218) IPCC (2001). Climate Change 2001: The Scientific Basis. Contribution of WG1 to the Third Assessment Report. Johnson. New York, Cambridge University Press**:** 944.

(219) James (2006). "An assessment of European synoptic variability in Hadley Centre global environmental models based on an objective classification of weather regimes." Climate Dynamics **27**(2-3): 215-231.

(220) Janicot, et al. (1996). "Sahel droughts and ENSO dynamics." Geophysical Research Letters **23**: 515-18.

(221) Janicot, et al. (2001). "Summer Sahel-ENSO teleconnections and decadal timescale SST variations." Climate Dynamics **18**(3/4): 303 - 320.

(222) Jenkins, et al. (2005). "Late 20th century attribution of drying trends in the Sahel from the Regional Climate Model (RegCM3)." Geophysical Research Letters **32**: L22705.

(223) Jevrejeva, et al. (2005). "Influence of large-scale atmospheric circulation on European sea level: results based on the wavelet transform method." Tellus **57A**: 183-193.

(224) Jochum and Murtugudde (2004). "Internal variability of the tropical Pacific Ocean." Geophysical Research Letters **31**(14): L14309.

(225) Jochum and Murtugudde (2005). "Internal variability of Indian Ocean SST." Journal of Climate **18**(18): 3726-3738.

(226) Johns, et al. (1997). "The second Hadley Centre coupled ocean-atmosphere model GCM: model description, spin up and validation." Climate Dynamics(103-134).

(227) Johns, et al. (2006). "The new Hadley Centre coupled climate model (HadGEM1): Evaluation of coupled simulations." Journal of Climate **19**(7): 1327-1353.

(228) Johns, et al. (2003). "Anthropogenic climate change for 1860-2100 simulated with the HadCM3 model under updated emissions scenarios." Climate Dynamics **20**: 583-612.

(229) Johnson and Marshall (2002). "A theory for surface Atlantic response to thermohaline variability." Journal of Physical Oceanography **32**(4): 1121 -1132.

(230) Jolliffe (2003). "A cautionary note on artificial examples of EOFs." Journal of Climate **16**: 1084-1086.

(231) Joly, et al. (2007). "African monsoon teleconnections with tropical SSTs: validation and evolution in a set of IPCC4 simulations." Climate Dynamics **29**: 1-20.

(232) Jones (1994). "Hemispheric surface air temperature variations: a reanalysis and update to 1993." Journal of Climate **7**: 1794-1802.

(233) Jones and Briffa (1992). "Global surface air temperature variations during the 20th century. Part 1: spatial, temporal and seasonal details." The Holocene **2**(2): 165-179.

(234) Jones, et al. (1999c). "Monthly mean pressure reconstructions for Europe for the 1780-1995 period." International Journal of Climatology **19**(4): 347-364.

(235) Jones and Mann (2004). "Climate over past millennia." Reviews of Geophysics **42**: 10.1029/2003RG000143.

(236) Jones and Moberg (2003). "Hemispheric and large scale surface air temperature variations: an extensive revision and update to 2001." Journal of Climate **16**: 206-223.

(237) Jones, et al. (1999b). "Surface air temperature and its variations over the last 150 years." Reviews of Geophysics **37**: 173-199.

(238) Jones, et al. (1997). "Estimating sampling errors in large scale temperature averages." Journal of Climate **10**: 2348-2368.

(239) Jones, et al. (2001). "Adjusting for sampling density in grid box land and ocean surface temperature time series." Journal of Geophysical Research **16**(D4): 3371-3380.

(240) Jones, et al. (1999a). "Modelling climatic change in South Africa from perturbed borehole temperature profiles." Quaternary International **57-58**: 185-192.

(241) Joseph and Nigam (2006). "ENSO evolution and teleconnections in IPCC's twentieth century climate simulations: realistic representations?" Journal of Climate **19**: 4360-4377.

(242) Jungclaus, et al. (2006). "Ocean circulation ad tropical variability in the coupled model ECHAM5/MPI-OM." Journal of Climate **19**: 3932-3951.

(243) Jury (1997). "Regional teleconnection patterns associated with summer rainfall over South Africa, Namibia and Zimbabwe." International Journal of Climatology **16**: 135-153.

(244) Jury (2002). "Economic impacts of climate variability in South Africa and development of resource prediction models." Journal of Applied Meteorology **41**: 46-55.

(245) Jury, et al. (2002). "Tropical monsoons around Africa: stability of ENSO associations and links with continental climate." Journal of Geophysical Research **107**(C10): 3151.

(246) Jury and Engert (1999). "Teleconnections modulating inter-annual climate variability over Northern Namibia." International Journal of Climatology **19**: 1459-1475.

(247) Jury and Levey (1993). "The climatology and characteristics of drought in the eastern cape of South Africa." International Journal of Climatology **13**(6): 629-641.

(248) Jury, et al. (1993b). "Flood episodes in central South Africa from satellite and ECMWF data." South African Journal of Science **89**: 263-269.

(249) Jury, et al. (1999). "Exploratory long-range models to estimate summer climate variability over Southern Africa." Journal of Climate **12**(7): 1892-1899.

(250) Jury, et al. (1993a). "Influence of the Agulhas Current on summer rainfall along the south east coast of South Africa." Journal of Applied Meteorology **32**: 1282-1287.

(251) Jury, et al. (2004). "Modelling the dominant climate signals around Southern Africa." Climate Dynamics **23**(7-8): 717-726.

(252) Kaiser (1974). Nonrecursive digital filter design using the io-sinh window function. IEEE International Symposium on Circuit Theory.

(253) Kaiser and Reed (1977). "Data smoothing using low pass digital filters." Review of Scientific Instruments **48**(11): 1447-1457.

(254) Kaiser and Schafer (1980). "Use of the io-sinh window for spectrum analysis." IEEE Transactions on Acoustics, Speech and Signal Processing **28**(1): 105-107.

(255) Kalnay, et al. (1996). "The NCEP/NCAR 40-year reanalysis project." Bulletin of the American Meteorological Society **77**(3): 437-471.

(256) Kaplan, et al. (2000). "Reduced space optimal interpolation of historical marine sea level pressure, 1854-1992." Journal of Climate **13**: 2987-3002.

(257) Karoly (2003). "Ozone and climate change." Science **302**: 236-237.

(258) Karoly and Braganza (2005a). "Attribution of recent temperature changes in the Australian region." Journal of Climate **18**: 457-464.

(259) Karoly and Braganza (2005b). "A new approach to detection of anthropogenic temperature changes in the Australian region." Meteorology and Atmospheric Physics **89**: 57-67.

(260) Karoly and Wu (2005). "Detection of regional surface temperature trends." Journal of Climate **18**: 4337-4343.

(261) Katz (2002). "Techniques for estimating uncertainty in climate change scenarios and impact studies." Climate Research **20**: 167-185.

(262) Kay (2005). Southwest Indian Ocean SST patterns and southern African rains. Royal Meteorological Society Conference, University of Exeter, 12-16 Sept 2005.

(263) Kayanne, et al. (2006). "Indian Ocean Dipole index recorded in Kenyan coral annual density bands." Geophysical Research Letters **33**: L19709.

(264) Kerr (2003). "Warming Indian Ocean Wringing Moisture From the Sahel." Science **302**: 210-211.

(265) Kestin, et al. (1998). "Time frequency variability of ENSO and stochastic simulations." Journal of Climate **11**: 2258-2272.

(266) Kijazi and Reason (2005). "Relationships between intraseasonal rainfall variability of coastal Tanzania and ENSO." Theoretical and Applied Climatology **82**: 153-176.

(267) Kiktev, et al. (2003). "Comparison of modelled and observed trends in indices of daily climate extremes." Journal of Climate **16**: 3560-3571.

(268) Kirst, et al. (1999). "Late Quaternary temperature variability in the Benguela Current system derived from alkenones." Quaternary Research **52**: 92-103.

(269) Kirtman and Schopf (1998). "Decadal variability in ENSO predictability and prediction." Journal of Climate **11**: 2804-2822.

(270) Kistler, et al. (2001). "The NCEP-NCAR 50-year reanalysis." Bulletin of the American Meteorological Society **82**(2): 437-471.

(271) Kleeman and Power (2000). Modulation of ENSO variability on decadal and longer timescales. El Nino and the Southern Oscillation: Multiscale variability and global and regional impacts. Diaz and Markgraf, Cambridge University Press**:** 496.

(272) Klein, et al. (1999). "Remote SST variations during ENSO: evidence for a tropical atmosphere bridge." Journal of Climate **12**: 917-932.

(273) Knight, et al. (2005a). "A signature of persistent natural thermohaline circulation cycles in observed climate." Geophysical Research Letters **32**(20): L20708.

(274) Knight, et al. (2005b). The Atlantic multidecadal oscillation: a signature of thermohaline circulation cycles in observed climate. Royal Meteorological Society Conference, University of Exeter, 12-16 Sept 2005.

(275) Knight, et al. (2006). "Climate impacts of the Atlantic Multidecadal Oscillation." Geophysical Research Letters **33**: L17706.

(276) Knopf, et al. (2005). "Forced versus coupled dynamics in Earth system modelling and prediction." Nonlinear Processes in Geophysics **12**(2): 311-320.

(277) Kripalani and Kumar (2004). "Northeast monsoon rainfall variability over south peninsular India vis a vis the Indian Ocean dipole mode." International Journal of Climatology **24**: 1267-1282.

(278) Kruger (1999). "The influence of the decadal-scale variability of summer rainfall on the impact of El Nino and La Nina events in South Africa." International Journal of Climatology **19**: 59-68.

(279) Kruger (2006). "Observed trends in daily precipitation indices in South Africa, 1910-2004." International Journal of Climatology: in press.

(280) Kumar, et al. (1999). "On the weakening relationship between the Indian monsoon and ENSO." Science **284**: 2156-2159.

(281) Lamb and Peppler (1992). "Further case studies of tropical Atlantic surface atmospheric and oceanic patterns associated with sub-Saharan drought." Journal of Climate **5**: 476-488.

(282) Lambert and Boer (2001). "CMIP1 evaluation and intercomparison of coupled climate models." Climate Dynamics **17**(2-3): 83-106.

(283) Lambert, et al. (2005). "Attribution studies of observed land precipitation changes with nine coupled models." Geophysical Research Letters **32**: L18704.

(284) Lambert, et al. (2004). "Detection and attribution of changes in 20th century land precipitation." Geophysical Research Letters **31**: L10203.

(285) Landman and Goddard (2002). "Statistical recalibration of GCM forecasts over southern Africa using model output statistics." Journal of Climate **15**: 2038-2055.

(286) Landman, et al. (2001). "Retroactive skill of multi-tiered forecasts of summer rainfall over Southern Africa." International Journal of Climatology **21**(1): 1-19.

(287) Latif (1998). "Dynamics of interdecadal variability in coupled ocean-atmosphere models." Journal of Climate **11**: 602-624.

(288) Latif (2006). "On Northern Pacific multidecadal climate variability." Journal of Climate **19**: 2906-2915.

(289) Latif and Barnett (1994). "Causes of decadal climate variability over the North Pacific and North America." Science **266**: 634-637.

(290) Latif and Barnett (1996). "Decadal climate variability over the North Pacific and North America: dynamics and predictability." Journal of Climate **9**: 2407-2423.

(291) Lau and Nath (1994). "A modelling study of the relative roles of tropical and extra tropical SST anomalies in the variability of the global atmosphere-ocean system." Journal of Climate **7**(8): 1184-1207.

(292) Lau and Nath (1996). "The role of the atmospheric bridge linking tropical Pacific ENSO events to extra tropical SST anomalies." Journal of Climate **9**(9): 2036-2057.

(293) Lau and Nath (2003). "Atmosphere-ocean variation in the Indo-Pacific during ENSO episodes." Journal of Climate **16**(1): 3-20.

(294) Lau and Weng (1995). "Climate signal detection using wavelet transform: how to make a time series sing." Bulletin of the American Meteorological Society **76**: 2391-2402.

(295) Layberry, et al. (2006). "Daily precipitation over southern Africa: a new resource for climate studies." Journal of Hydrometeorology **7**: 149-159.

(296) Lean, et al. (1995). "Reconstructions of solar irradiance since 1610 - implications for climate change." Geophysical Research Letters **22**: 3195-3198.

(297) Lee, et al. (2005). "Evidence of decadal climate prediction skill resulting from changes in anthropogenic forcing." Journal of Climate **19**: 5305-5318.

(298) Legutke and Maier-Reimer (1999). Climatology of the HOPE-G global ocean general circulation model, German Climate Computer Centre (DKRZ) Technical Report 18**:** 62.

(299) Legutke and Voss (1999). The Hamburg Atmosphere-Ocean Coupled Circulation Model ECHO-G. Hamburg, German Climate Computer Centre (DKRZ).

(300) Leloup, et al. (2007). "20th century ENSO characteristics in the IPCC database." Climate Dynamics: in press.

(301) Levitus, et al. (1994). "Interannual variability of temperature at a depth of 125 metres in the North Atlantic Ocean." Science **266**(5182): 96-99.

(302) Li, et al. (2005). "Statistical modelling of extreme rainfall in SW Western Australia." Journal of Climate **18**: 852-863.

(303) Lindesay (1988). "South African rainfall, the Southern Oscillation and a southern hemisphere semi-annual cycle." Journal of Climatology **8**: 17-30.

(304) Liu (1999). "Forced planetary wave response in a thermocline gyre." Journal of Physical Oceanography **29**: 1036-1055.

(305) Liu and Alexander (2007). "Atmospheric bridge, oceanic tunnel and global climatic teleconnections." Reviews in Geophysics **45**(2): RG2005.

(306) Lohmann and Latif (2005). "Tropical Pacific decadal variability and the sub-tropical tropical cells." Journal of Climate **18**(23): 5163-5178.

(307) Lu and Delworth (2005). "Oceanic forcing of the late 20th century Sahel drought." Geophysical Research Letters **32**: L22706.

(308) Luo, et al. (2003). "South Pacific origin of the decadal ENSO-like variation as simulated by a coupled GCM." Geophysical Research Letters **30**(24): L018649.

(309) Lutjeharms and de-Ruijter (1996). "The influence of the Agulhas Current on the adjacent coastal ocean: possible impacts of climate change." Journal of Marine Systems **7**(2-4): 321-336.

(310) Lyon and Mason (2007). "The 1997-98 summer rainfall season in southern Africa. Part 1: Observations." Journal of Climate **20**(20): 5134-5148.

(311) Makarau and Jury (1997). "Predictability of Zimbabwe summer rainfall." International Journal of Climatology **17**(13): 1421-1432.

(312) Manabe and Stouffer (1996). "Low frequency variability of surface air temperature in a 1000-yr integration of a coupled atmosphere-ocean-land surface model." Journal of Climate **9**: 376-393.

(313) Manabe and Stouffer (1999). "The role of thermohaline circulation in climate." Tellus A **51**: 91-104.

(314) Mann, et al. (1998). "Global scale temperature patterns and climate forcing over the past six centuries." Nature **392**: 779-787.

(315) Mann, et al. (2000). Long term variability in the El Nino-Southern Oscillation and associated teleconnections. El Nino and the Southern Oscillation: Multiscale variability and its Impacts on Natural Ecosystems and Society. Diaz and Markgraf. Cambridge, Cambridge University Press**:** 357-412.

(316) Mann and Lees (1996). "Robust estimation of background noise and signal detection in climatic time series." Climatic Change **33**: 409-445.

(317) Mann and Park (1994). "Global-scale modes of surface temperature variability on interannual to century timescales." Journal of Geophysical Research **99**: 25 819-25 833.

(318) Mann and Park (1996). "Joint spatiotemporal modes of surface temperature and sea level pressure variability in the Northern Hemisphere during the last century." Journal of Climate **9**: 2137-2162.

(319) Mann and Park (1999). "Multivariate signal detection in climate studies." Advances in Geophysics **41**: 1-131.

(320) Mann, et al. (1995). "Global interdecadal and century scale climate oscillations during the past five centuries." Nature **378**: 266-270.

(321) Mantua, et al. (1997). "A Pacific interdecadal climate oscillation with impacts on salmon production." Bulletin of the American Meteorological Society **78**: 1069-1079.

(322) Mapande and Reason (2005). "Interannual rainfall variability over Western Tanzania." International Journal of Climatology **25**: 1355-1368.

(323) Marshall (2007). "Half-century seasonal relationships between the Southern Annular Mode and Antarctic temperatures." International Journal of Climatology **27**(3): 373-383.

(324) Martin, et al. (2006). "The physical properties of the atmosphere in the new Hadley Centre Global Environmental Model (HadGEM1). Part I: model description and global climatology." Journal of Climate **19**(7): 1274-1301.

(325) Mason (1995). "SST-South African rainfall associations, 1919-1989." International Journal of Climatology **15**: 119-135.

(326) Mason (1998). "Seasonal forecasting of South African rainfall using a non-linear discriminant model." International Journal of Climatology **18**: 147-164.

(327) Mason (2001). "El Nino, climate change and southern African climate." Environmetrics **12**(4): 327-345.

(328) Mason and Jury (1997). "Climatic variability and change over southern Africa: a reflection on underlying processes." Progress in Physical Geography **21**: 23-50.

(329) Mason and Lindesay (1993). "A note on the modulation of southern oscillation-southern African rainfall associations with the quasi-biennial oscillation." Journal of Geophysical Research **98**: 8847-8850.

(330) Mason and Mimmack (1992). "The use of bootstrap confidence intervals for the correlation coefficient in climatology." Theoretical and Applied Climatology **45**: 229-234.

(331) Mason and Tyson (1992). "The modulation of SST and rainfall associations over southern Africa with solar activity and the QBO." Journal of Geophysical Research **97**(D5): 5847-5856.

(332) Matano and Beier (2003). "A kinematic analysis of the Indian/Atlantic interocean exchange." Deep-Sea Research II **50**: 229-249.

(333) McAvaney, et al. (2001). Model evaluation. Climate Change 2001: The Scientific Basis. Houghton, Ding, Griggset al. Cambridge, New York, Cambridge University Press**:** 471-523.

(334) McCabe, et al. (2007). "Associations of decadal to multidecadal SST variability with Upper Colorado River flow." Journal of the American Water Research Association **43**(1): 183-192.

(335) McCabe, et al. (2004). "Pacific and Atlantic Ocean influences on multidecadal drought frequency in the United States." Proceedings of the National Academy of Sciences, USA **101**(4136-4141).

(336) Meehl, et al. (1998). "Global scale decadal climate variability." Geophysical Research Letters **25**(21): 3983-3986.

(337) Meinke, et al. (2005). "Rainfall variability at decadal or longer timescales: signal or noise?" Journal of Climate **18**(1): 89-96.

(338) Milton and Wilson (1996). "The impact of parameterized subgrid-scale orographic forcing on systematic errors in a global NWP model." Monthly Weather Review **124**(9): 2023-2045.

(339) Min, et al. (2005). "Regional scale climate change detection using a Bayesian decision method." Geophysical Research Letters **32**(3): L03706.

(340) Min, et al. (2005a). "Internal variability in a 1000-yr control simulation with the coupled climate model ECHO-G - I. Near surface temperature, precipitation and mean sea level pressure." Tellus **57A**: 605-621.

(341) Min, et al. (2005b). "Internal variability in a 1000-yr control simulation with the coupled climate model ECHO-G - II. El Nino Southern Oscillation and North Atlantic Oscillation." Tellus **57A**: 622-640.

(342) Mitchell and Jones (2005). "An improved method of constructing a database of monthly climate observations and associated high-resolution grids." International Journal of Climatology **25**(6): 693-712.

(343) Mokhov, et al. (2004). "Decadal and longer term changes in El Nino-Southern Oscillation characteristics." International Journal of Climatology **24**: 401-414.

(344) Moron (1997). "Trend, decadal and interannual variability in annual rainfall of subequatorial and tropical North Africa." International Journal of Climatology **17**: 785-805.

(345) Moron, et al. (2003). "Skill of Sahel rainfall variability in four atmospheric GCMs forced by prescribed SSTs." Geophysical Research Letters **30**(23): 4.

(346) Moy, et al. (2002). "Variability of ENSO activity at millennial timescales during the Holocene epoch." Nature **420**: 162-165.

(347) Mulenga, et al. (2003). "Dry summers over NE South Africa and associated circulation anomalies." Climate Research **25**(1): 29-41.

(348) Murphy, et al. (2004). "Quantifying uncertainties in climate change from a large ensemble of general circulation model predictions." Nature **430**: 768-772.

(349) Murphy and Timbal (2007). "A review of recent climate variability and climate change in southeastern Australia." International Journal of Climatology: in press.

(350) Murphy, et al. (2002). "Seasonal forecasting for climate hazards: prospects and responses." Natural Hazards **23**: 171-196.

(351) Mwale, et al. (2004). "A new analysis of variability and predictability of seasonal rainfall of central southern Africa for 1950-94." International Journal of Climatology **24**: 1509-1530.

(352) Nakamura, et al. (1997). "Decadal climate variability in the North Pacific during recent decades." Bulletin of the American Meteorological Society **78**: 2215-2225.

(353) Nelson, et al. (2002). "Infusing the use of seasonal climate forecasting into crop management practice in North East Australia using discussion support software." Agricultural Systems **74**(3): 393-414.

(354) New, et al. (1999). "Representing twentieth century space-time climate variability. Part 1: development of a 1961-90 mean monthly terrestrial climatology." Journal of Climate **12**: 829-856.

(355) Newman (2007). "Interannual to decadal predictability of tropical and North Pacific sea surface temperature." Journal of Climate **20**: 2333-2356.

(356) Newman, et al. (2003). "ENSO-forced variability of the Pacific decadal oscillation." Journal of Climate **16**(23): 3853-3857.

(357) Nicholls (2000). "The insignificance of significance testing." Bulletin of the American Meteorological Society **81**(5): 981-986.

(358) Nicholson (1997). "An analysis of the ENSO signal in the tropical Atlantic and western Indian oceans." International Journal of Climatology **17**: 345-375.

(359) Nicholson and Entekhabi (1987). "Rainfall variability in equatorial and southern Africa: relationships with SSTs along the south-western coast of Africa." Journal of Climatology and Applied Meteorology **26**: 561-578.

(360) Nicholson and Kim (1997). "The relationship of ENSO to African rainfall." International Journal of Climatology **17**: 117-135.

(361) Nicholson, et al. (2000). "An analysis of recent rainfall conditions in West Africa, including the rainy seasons of the 1997 El Nino and the 1998 La Nina years." Journal of Climate **13**: 2628-2640.

(362) Nitta and Yamada (1989). "Recent warming of tropical SST and its relationship to the Northern Hemisphere circulation." Journal of the Meteorological Society of Japan **67**(3): 375-383.

(363) Nobre, et al. (2006). "Seasonal to decadal predictability and prediction of South American climate." Journal of Climate **19**(23): 5988-6004.

(364) Nobre and Shukla (1996). "Variations of sea surface temperature, wind stress and rainfall over the tropical Atlantic and South America." Journal of Climate **9**: 2464-2479.

(365) Noh, et al. (2003). "Improvement of the K-profile model for the planetary boundary layer based on large eddy simulation data." Boundary Layer Meteorology **107**: 401-427.

(366) North, et al. (1982). "Sampling errors in the estimation of empirical orthogonal functions." Monthly Weather Review **110**(7): 699-706.

(367) O'Connor and Thomas (1999). "The timing and environmental significance of Late Quaternary linear dune development in western Zambia." Quaternary Research **52**: 44-55.

(368) O'Mahony, et al. (2005). SST forcings in the South Atlantic and their influences on atmospheric circulation. Royal Meteorological Society Conference, University of Exeter, 12-16 Sept 2005.

(369) Oppo, et al. (2003). "Deepwater variability in the Holocene epoch." Nature **422**: 277-278.

(370) Osbahr and Roberts (2007). Climate change and development in Africa: policy frameworks and development interventions for effective adaptation to climate change, University of Oxford**:** 23.

(371) Osborn, et al. (2006). "Simulated climate change during the last 1000 yrs: comparing the ECHO-G GCM with the MAGICC simple climate model." Climate Dynamics **27**: 185-197.

(372) Paeth and Hense (2004). "SST versus climate change signals in West African rainfall: 20th century variations and future projections." Climatic Change **65**(1-2): 179-208.

(373) Parker, et al. (1995a). "Marine surface temperature: observed variations and data requirements." Climate Change **31**: 559-600.

(374) Parker, et al. (1995b). The GISST2.2 sea surface temperature and sea ice climatology. Exeter, Climate Research Tech Note 63, Hadley Centre, Met Office**:** 35.

(375) Partridge, et al. (1997). "Orbital forcing of climate over South Africa: a 200,000 year rainfall record from the Pretoria Salt Pan." Quaternary Science Reviews **16**: 1125-1133.

(376) Pfeiffer, et al. (2004). "Oceanic forcing of interannual and multidecadal climate variability in the SW Indian Ocean: evidence from a 160 yr coral isotopic record." Palaeoceanography **19**: PA4006.

(377) Philip and van-Oldenborgh (2006). "Shifts in ENSO coupling processes under global warming." Geophysical Research Letters **33**: L11704.

(378) Phillips, et al. (2004). "Evaluating parameterisations in general circulation models: climate simulation meets weather prediction." Bulletin of the American Meteorological Society **85**: 1903-1915.

(379) Podesta, et al. (2002). "Use of ENSO-related climate information in agricultural decision making in Argentina: a pilot experience." Agricultural Systems **74**(3): 371-392.

(380) Pope, et al. (2000). "The impact of new physical parametrizations in the new Hadley Centre climate model: HadAM3." Climate Dynamics **16**(2-3): 123-146.

(381) Power, et al. (1999a). "Inter decadal modulation of the impact of ENSO on Australia." Climate Dynamics **15**: 319-323.

(382) Power, et al. (1999b). "Decadal climate variability in Australia during the twentieth century." International Journal of Climatology **19**: 169-184.

(383) Powers, et al. (2005). "Large temperature variability in the southern African tropics since the Last Glacial Maximum." Geophysical Research Letters **32**: L08706.

(384) Prospero and Lamb (2003). "African drought and dust transport to the Caribbean; climate change implications." Science **302**: 1024-1027.

(385) Qiu (2003). "Kuroshio extension variability and forcing of Pacific decadal oscillations: responses and potential feedback." Journal of Physical Oceanography **33**: 2465-2482.

(386) Raisanen (2001). "CO_2 induced climate change in CMIP2 experiments: quantification of agreement and role of internal variability." Journal of Climate **14**: 2088-2104.

(387) Raisanen (2007). "How reliable are climate models?" Tellus **59A**(1): 2-29.

(388) Raisanen, et al. (2004). "European climate in the late twenty-first century: regional simulations with two driving global models and two forcing scenarios." Climate Dynamics **22**(1): 13-31.

(389) Rajagopalan, et al. (1998). "Observed decadal mid-latitude and tropical Atlantic climate variability." Geophysical Research Letters **25**: 3967-3970.

(390) Ramaswamy, et al. (2001). Radiative forcing of climate change. Climate Change 2001: The Scientific Basis. Johnson. Cambridge, Cambridge University Press**:** 349-416.

(391) Rautenbach and Smith (2001). "Teleconnections between global SSTs and the interannual variability of observed and model simulated rainfall over southern Africa." Journal of Hydrology **254**: 1-15.

(392) Ravallion and Chen (2004). "How have the world's poorest fared since the early 1980s?" The World Bank Research Observer **19**(2): 141-169.

(393) Rayner, et al. (2006). "Improved analyses of changes and uncertainties in marine temperature measured in situ since the mid 19th century: the HadSST2 dataset." Journal of Climate **19**: 446-469.

(394) Rayner, et al. (2003). "Globally complete analyses of sea surface temperature, sea ice and night marine air temperature, 1871-2000." Journal of Geophysical Research **108**.

(395) Reason (1998). "Warm and cold events in the SE Atlantic/South West Indian Ocean region and potential impacts on circulation and rainfall over Southern Africa." Meteorology and Atmospheric Physics **69**(1-2): 49-65.

(396) Reason (2000). "Multidecadal climate variability in the subtropics/mid-latitudes of the Southern Hemisphere oceans." Tellus **52A**: 203-223.

(397) Reason (2000). "Multidecadal climate variability in the sub-tropics/mid-latitudes of the southern hemisphere oceans." Tellus A **52**(2): 203-223.

(398) Reason (2001a). "Evidence for the influence of the Agulhas Current on regional atmospheric circulation patterns." Journal of Climate **14**(12): 2767-2778.

(399) Reason (2001b). "Subtropical Indian Ocean SST dipole events and southern African rainfall." Geophysical Research Letters **28**(11): 2225-2227.

(400) Reason (2002). "Sensitivity of the southern African circulation to dipole SST patterns in the South Indian Ocean." International Journal of Climatology **22**(4): 377-393.

(401) Reason, et al. (1996a). "Evidence for the influence of remote forcing on interdecadal variability in the southern Indian Ocean." Journal of Geophysical Research **101**(C5): 11867-11882.

(402) Reason, et al. (1996b). "Dynamical response of the oceanic circulation and temperature to interdecadal variability in the surface winds over the Indian Ocean region." Journal of Climate **9**: 97-114.

(403) Reason, et al. (2000). "ENSO and climatic signals across the Indian Ocean basin in the global context: Part 1, interannual composite patterns." International Journal of Climatology **20**: 1285-1327.

(404) Reason and Godfred-Spenning (1998). "SST variability in the south Indian ocean and associated circulation and rainfall patterns over South Africa." Meteorology and Atmospheric Physics **66**(3-4): 243-258.

(405) Reason, et al. (2005). "Interannual variability in rainy season characteristics over the Limpopo region of Southern Africa." International Journal of Climatology **25**: 1835-1853.

(406) Reason and Jagadheesha (2005). "A model investigation of recent ENSO impacts over southern Africa." Meteorology and Atmospheric Physics **89**: 181-205.

(407) Reason, et al. (2004). Seasonal to decadal predictability and prediction of southern African climate. CLIVAR Workshop on Atlantic Climate Predictability, 19-22 April, 2004, Reading, UK, International CLIVAR Project Office.

(408) Reason, et al. (2006a). "Seasonal to decadal prediction of Southern African climate and its links with variability of the Atlantic Ocean." Bulletin of the American Meterological Society **87**(7): 941-955.

(409) Reason and Mulenga (1999). "Relationships between South African rainfall and SST anomalies in the South West Indian Ocean." International Journal of Climatology **19**: 1651-1673.

(410) Reason and Rouault (2002). "ENSO-like decadal variability and South African rainfall." Geophysical Research Letters **29**(13).

(411) Reason and Rouault (2005). "Links between the Antarctic Oscillation and winter rainfall over western South Africa." Geophysical Research Letters **32**: L07705.

(412) Reason, et al. (2001). "Interannual winter rainfall variability in SW South Africa and potential influence from the Southern Ocean region." CLIVAR-Exchanges **22**.

(413) Reason, et al. (2002). "Interannual winter rainfall variability in SW South Africa and large scale ocean-atmosphere interactions." Meteorology and Atmospheric Physics **80**(1-4): 19-29.

(414) Renssen, et al. (2004). Recent developments in Holocene climate modelling. Past climate variability through Europe and Africa. Battarbee, Gasse and Stickley, Kluwer Academic**:** 610.

(415) Renssen, et al. (2006). "On the importance of initial conditions for simulation of mid-Holocene climate." Climate of the Past **2**(2): 91-97.

(416) Renssen, et al. (2005). "Simulating the Holocene climate evolution at northern high latitudes using a coupled atmosphere-sea ice-ocean-vegetation model." Climate Dynamics **24**(1): 23-43.

(417) Richard, et al. (2000). "Modification of the southern African rainfall variability/ENSO relationship since the late 1960s." Climate Dynamics **16**: 883-895.

(418) Ringer, et al. (2006). "The physical properties of the atmosphere in the new Hadley Centre Global Environmental Model (HadGEM1). Part II: Aspects of variability and regional climate." Journal of Climate **19**: 1302-1326.

(419) Rocha, et al. (2007). "High frequency precipitation changes in southeastern Africa due to anthropogenic forcing." International Journal of Climatology: in press.

(420) Rocha and Simmonds (1997). "Interannual variability of SE African summer rainfall. Part 1: Relationships with air-sea interaction processes." International Journal of Climatology **17**: 235-265.

(421) Rocha and Simmonds (1997b). "Interannual variability of SE African summer rainfall. Part 2: Modelling the impact of SSTs on rainfall and circulation." International Journal of Climatology **17**(3): 267-290.

(422) Rodgers, et al. (2004). "Tropical Pacific decadal variability and its relation to decadal modulations of ENSO." Journal of Climate **17**(19): 3761-3774.

(423) Roeckner, et al. (1996). The atmospheric general circulation model ECHAM4: model description and simulation of present-day climate. Hamburg, Max-Planck Institut fur Meteorologie.

(424) Roeckner, et al. (2006). "Sensitivity of simulated climate to horizontal and vertical resolution in ECHAM-5 atmosphere model." Journal of Climate **19**: 3771-3791.

(425) Rouault, et al. (2003). "SE tropical Atlantic warm events and southern African rainfall." Geophysical Research Letters **30**(5): L014840.

(426) Rouault, et al. (2002). "Ocean-atmosphere interaction in the Agulhas Current and a South African extreme weather event." Weather and Forecasting **17**: 655-669.

(427) Rowell (2003). "The impact of Mediterranean SSTs on the Sahelian rainfall season." Journal of Climate **16**: 849-862.

(428) Rowell, et al. (1992). "Modelling the influence of global sea surface temperatures on the variability and predictability of seasonal Sahel rainfall." Geophysical Research Letters **19**(9): 905-908.

(429) Ruiz-Barradas, et al. (2000). "Structure of interannual to decadal climate variability in the tropical Atlantic sector." Journal of Climate **13**(8): 3288-3297.

(430) Saji, et al. (1999). "A dipole mode in the tropical Indian Ocean." Nature **401**(360-363).

(431) Saji, et al. (2006). "Tropical Indian Ocean variability in the IPCC twentieth-century climate simulations." Journal of Climate **19**: 4397-4417.

(432) Saji and Yamagata (2003). "Structure of SST and surface wind variability during Indian Ocean Dipole mode events: COADS observations." Journal of Climate **16**: 2735-2751.

(433) Santer, et al. (1996). "A search for human influences on the thermal structure in the atmosphere." Nature **382**: 39-45.

(434) Santer, et al. (1993). "Correlation methods in fingerprint detection studies." Climate Dynamics **8**(6): 265-276.

(435) Schneider and Cornuelle (2005). "The forcing of the Pacific Decadal Oscillation." Journal of Climate **18**(21): 4355-4373.

(436) Schnur and Hasselman (2005). "Optimal filtering for Bayesian detection and attribution of climate change." Climate Dynamics **24**(1): 45-55.

(437) Schouten, et al. (2002). "An oceanic teleconnection between the equatorial and southern Indian Ocean." Geophysical Research Letters **29**(16): 1812.

(438) Schouten, et al. (2003). "Eddies and variability in the Mozambique Channel." Deep Sea Research - Part II **50**: 1987-2003.

(439) Schwierz, et al. (2006). "Challenges posed by and approaches to the study of seasonal-to-decadal climate variability." Climatic Change **79**: 31-63.

(440) Servain, et al. (1999). "Relationship between the equatorial and meridional modes of climatic variability in the tropical Atlantic." Geophysical Research Letters **26**: 485-488.

(441) Shindell, et al. (1999). "Solar cycle variability, ozone and climate." Science **284**: 305.

(442) Shindell, et al. (2001). "Solar forcing of regional climate change during the Maunder minimum." Science **294**: 2149-2152.

(443) Shindell, et al. (2003). "Volcanic and solar forcing of climate change during the preindustrial era." Journal of Climate **16**: 4094-4107.

(444) Shongwe, et al. (2006). "Performance of recalibration systems for GCM forecasts for southern Africa." International Journal of Climatology **26**: 1567-1585.

(445) Shriver and Hurlburt (1997). "The contribution of global thermohaline circulation from the Pacific to the Indian Ocean via Indonesian throughflow." Journal of Geophysical Research **102**(C3): 5491-5512.

(446) Simmons, et al. (2004). "Comparison of trends and low-frequency variability in CRU, ERA-40 and NCEP/NCAR analyses of surface air temperature." Journal of Geophysical Research **109**(D24): 115.

(447) Singleton and Reason (2006). "Numerical simulations of a severe rainfall event over the Eastern Cape coast of South Africa: sensitivity to sea surface temperature and topography." Tellus **58A**: 355-367.

(448) Small and Islam (2007). "Decadal variability in the frequency of fall precipitation over the United States." Geophysical Research Letters **34**: L02404.

(449) Smith (1990). "A scheme for predicting layer clouds and their water content in a GCM." Quarterly Journal of the Royal Meteorological Society **116**(492): 435-460.

(450) Smith and Reynolds (2004). "Reconstruction of monthly mean oceanic sea level pressure based on COADS and station data (1854-1997)." Journal of Atmospheric and Oceanic Technology **21**: 1272-1282.

(451) Spagnoli, et al. (2002). "Detecting climate change at a regional scale: the case of France." Geophysical Research Letters **29**(10): 1450.

(452) Stahle, et al. (1999). "Management implications of annual growth rings in Pterocarpus angolensis from Zimbabwe." Forest Ecology Management **124**: 217-229.

(453) Sterl (2001). "Decadal variability in the South Atlantic Ocean." CLIVAR-Exchanges **19**.

(454) Sterl and Hazeleger (2003). "Coupled variability and air-sea interaction in the South Atlantic Ocean." Climate Dynamics **21**: 559-571.

(455) Sterl, et al. (2007). "On the robustness of ENSO teleconnections." Climate Dynamics **29**: 469-485.

(456) Stocker (2000). "Past and future reorganisations in the climate system." Quaternary Science Reviews **19**(1-5): 301-319.

(457) Stocker and Mysak (1992). "Climatic fluctuations on the century timescale: a review of high resolution proxy data and possible mechanisms." Climatic Change **20**: 227-250.

(458) Stone, et al. (2001). "Projection of climate change on to modes of atmospheric variability." Journal of Climate **14**: 3551-3565.

(459) Stott (2003). "Attribution of regional scale temperature changes to anthropogenic and natural causes." Geophysical Research Letters **30**(14): 1728.

(460) Stott, et al. (2006). "Transient climate simulation with the HadGEM1 climate model: causes of past warming and future climate change." Journal of Climate **19**(12): 2763-2782.

(461) Stott, et al. (2003). "Do models underestimate the solar contribution to recent climate change?" Journal of Climate **16**: 4079-4093.

(462) Stott and Tett (1998). "Scale dependent detection of climate change." Journal of Climate **11**(12): 3282-3294.

(463) Stouffer, et al. (2000). "A comparison of surface air temperature variability in three 1000-yr coupled ocean-atmosphere model integrations." Journal of Climate **13**: 513-537.

(464) Stouffer and Manabe (2003). "Equilibrium response of thermohaline circulation to large chanes in atmospheric CO_2 concentration." Climate Dynamics **20**: 759-773.

(465) Stratton (1999). "A high resolution AMIP integration using the Hadley Centre model HadAM2b." Climate Dynamics **15**(1): 9-28.

(466) Swann, et al. (2003). "Tropical oceans and the predictability of southern African rainfall in the HadCM3 coupled climate model." CLIVAR-Exchanges **8**(2/3 Supplementary Paper).

(467) Tadross, et al. (2005). "The interannual variability of the onset of the maize growing season over South Africa and Zimbabwe." Journal of Climate(3079-3093).

(468) Tarhule and Lamb (2003). "Climate research and seasonal forecasting for West Africans: perceptions, dissemination and use?" Bulletin of the American Meteorological Society **84**: 1741-1759.

(469) Tennant and Reason (2005). "Associations between the global energy cycle and regional rainfall in South Africa and Southwest Australia." Journal of Climate **18**: 3032-3047.

(470) Terray, et al. (2003). "Sea surface temperature associations with the late Indian summer monsoon." Climate Dynamics **21**: 593-618.

(471) Terray and Dominiak (2005). "Indian Ocean SSTs and ENSO: a new perspective." Journal of Climate **18**(9): 1351-1368.

(472) Terray, et al. (2005). "Role of the southern Indian Ocean in the transitions of the monsoon-ENSO system during recent decades." Climate Dynamics **24**: 169-195.

(473) Tett, et al. (2007). "The impact of natural and anthropogenic forcings on climate and hydrology since 1550." Climate Dynamics **28**(1): 3-34.

(474) Tett, et al. (2002). "Estimation of natural and anthropogenic contributions to twentieth century temperature change." Journal of Geophysical Research **107**(D16): 4306.

(475) Therrell, et al. (2006). "Tree-ring reconstructed rainfall variability in Zimbabwe." Climate Dynamics **26**: 677-685.

(476) Thiaw and Mo (2005). "Impacts of SST and soil moisture on seasonal rainfall prediction over the Sahel." Journal of Climate **18**: 5330-5343.

(477) Thomas and Shaw (2002). "Late Quaternary environmental change in central southern Africa - new data, synthesis, issues and prospects." Quaternary Science Reviews **21**: 783-797.

(478) Thompson and Solomon (2002). "Interpretation of recent Southern Hemisphere climate change." Science **296**: 895-899.

(479) Thompson and Wallace (2000). "Annular modes in the extratropical circulation. Part 1: Month to month variability." Journal of Climate **13**: 1000-1016.

(480) Timbal, et al. (2006). "Attribution of the late twentieth-century rainfall decline in southwest Australia." Journal of Climate **19**: 2046-2062.

(481) Timmerman and Jin (2002). "A nonlinear mechanism for decadal El Nino amplitude changes." Geophysical Research Letters **29**(1): L013369.

(482) Tippett and Giannini (2006). "Potentially predictable components of African summer rainfall in an SST-forced GCM simulation." Journal of Climate **19**: 3133-3144.

(483) Todd and Washington (1999). "Circulation anomalies associated with tropical-temperate troughs in southern Africa and the south west Indian Ocean." Climate Dynamics **15**: 937-951.

(484) Torrence and Compo (1998). "A practical guide to wavelet analysis." Bulletin of the American Meteorological Society **79**: 61-78.

(485) Torrence and Webster (1999). "Interdecadal changes in the ENSO-monsoon system." Journal of Climate **12**: 2679-2690.

(486) Tourre, et al. (1999). "Evolution of interdecadal variability in sea level pressure, sea surface temperature and upper ocean temperature over the Pacific Ocean." Journal of Physical Oceanography **9**: 1528-1541.

(487) Tozuka, et al. (2007). "Decadal modulations of the Indian Ocean Dipole in the SINTEX-F1 coupled GCM." Journal of Climate **20**: 2881-2894.

(488) Trenberth and Shea (2005). "Relationships between precipitation and surface temperature." Geophysical Research Letters **32**: L14703.

(489) Trouet, et al. (2006). "Annual growth rings patterns in Brachystegia spiciformis reveal influence of precipation on tree growth." Biotropica **38**(3): 375-382.

(490) Tucker, et al. (1991). "Expansion and contraction of the Sahara Desert from 1980-1990." Science **253**: 299-301.

(491) Tudhope, et al. (2001). "Variability in the El Nino-Southern Oscillation through a glacial-interglacial cycle." Science **291**: 1511-1517.

(492) Tyson (1971). "Spatial variation of rainfall spectra in South Africa." Annals of the Association of American Geographers **61**: 711-720.

(493) Tyson (1980). "Temporal and spatial variation of rainfall anomalies in Africa south of latitude 22 deg during the period of the meteorological record." Climatic Change **2**: 363-371.

(494) Tyson (1999). "Late Quaternary and Holocene palaeoclimates of southern Africa: a synthesis." South African Journal of Geology **102**(4): 335-349.

(495) Tyson, et al. (2002). "Millennial to multi-decadal variability in the climate of southern Africa." International Journal of Climatology **22**(9): 1105-1117.

(496) Tyson and Dyer (1980). "The likelihood of droughts in the eighties in South Africa." South African Journal of Science **76**: 340-341.

(497) Tyson and Lindesay (1992). "The climate of the last 2000 years in southern Africa." The Holocene **2**(3): 271-278.

(498) Tyson and Preston-Whyte (2000). Weather and Climate of Southern Africa. Cape Town, Oxford University Press.

(499) Uppala, et al. (2005). "The ERA-40 reanalysis." Quarterly Journal of the Royal Meteorological Society **131**: 2961-3012.

(500) Usman and Reason (2004). "Dry spell frequencies and their variability over southern Africa summer rainfall." Climate Research **26**(3): 199-211.

(501) van-Loon and Labitzke (2000). "The influence of the 11-year solar cycle on the stratosphere below 30km; a review." Space Science Reviews **94**: 259-278.

(502) van-Oldenborgh and Burgers (2005). "Searching for decadal variations in ENSO precipitation teleconnections." Geophysical Research Letters **32**: L15701.

(503) Venegas, et al. (1996). "Evidence for interannual and interdecadal climate variability in the South Atlantic." Geophysical Research Letters **23**: 2673-2676.

(504) Venegas, et al. (1997). "Atmosphere-ocean coupled variability in the South Atlantic." Journal of Climate **10**(11): 2904-2920.

(505) Vigaud (2007). Water vapour transport from the South Atlantic and Indian Oceans and summer rainfall in southern Africa. Department of Oceanography, University of Cape Town**:** 253.

(506) Vigaud, et al. (2006). "Water vapour transport from the tropical Atlantic and summer rainfall in tropical southern Africa." Climate Dynamics: in press.

(507) Vimont (2005). "The contribution of the interannual ENSO cycle to the spatial pattern of decadal ENSO-like variability." Journal of Climate **18**(12): 2123-2127.

(508) Vimont (2007). "Decadal variability and predictability." CLIVAR-Variations **5**(2): 1-4.

(509) Vimont and Kossin (2007). "The Atlantic Meridional Mode and hurricane activity." Geophysical Research Letters **34**(7): L07709.

(510) Vimont, et al. (2003). "The seasonal footprinting mechanism in the Pacific: implications for ENSO." Journal of Climate **16**: 2668-2675.

(511) Vinayachandran, et al. (2002). "Indian Ocean Dipole mode events in an ocean general circulation model." Deep Sea Research - Part II **49**: 1573-1596.

(512) Visbeck, et al. (1997). "On the specification of eddy transfer coefficients in coarse resolution ocean circulation models." Journal of Physical Oceanography **27**: 381-402.

(513) Von-Storch (2004). A discourse about quasi-realistic climate models and their application in palaeoclimatic studies. The climate in historical times: towards a synthesis of Holocene proxy data and climate models. Fischer, Kumke, Lohmannet al. Berlin, Springer-Verlag**:** 487.

(514) von-Storch, et al. (2004). "Reconstructing past climate from noisy data." Science **306**: 679-682.

(515) von-Storch and Zwiers (1999). Statistical Analysis in Climate Research, Cambridge University Press.

(516) Vuille, et al. (2005). "Stable isotopes in East African precipitation record Indian Ocean zonal mode." Geophysical Research Letters **32**: L21705.

(517) Walker (1990). "Links between south African summer rainfall and temperature variability of the Agulhas and Benguela Current regions." Journal of Geophysical Research **95**(C3): 3297-3319.

(518) Walker and Shillington (1990). "The effect of oceanographic variability on South African weather and climate." South African Journal of Science **86**(7-10): 382-386.

(519) Walland, et al. (2000). "Decadal climate variability simulated in a coupled GCM." Climate Dynamics **16**(2-3): 201-211.

(520) Wang (2005). "Two climatic states and feedbacks on the THC in an Earth System model of intermediate complexity." Climate Dynamics **25**(2-3): 299-314.

(521) Wang and An (2001). "Why the properties of El Nino changed during the late 1970s." Geophysical Research Letters **28**: 3709-3712.

(522) Wang, et al. (2004). "Decadal variability of rainfall in the Sahel; results from the coupled GENESIS-IBIS atmosphere-biosphere model." Climate Dynamics **22**: 625-637.

(523) Wang, et al. (2003a). "A tropical ocean recharge mechanism for climate variability. Part I: Equatorial heat changes induced by off-equatorial winds." Journal of Climate **16**: 3585-3598.

(524) Wang, et al. (2003b). "A tropical ocean recharge mechanism for climate variability. Part II: A unified theory for decadal and ENSO modes." Journal of Climate **16**: 3599-3616.

(525) Wang and Neelin (1998). "On the role of ocean-atmosphere interaction in midlatitude interdecadal variability." Geophysical Research Letters **25**: 167-170.

(526) Ward (1998). "Diagnosis and short-lead time prediction of summer rainfall in tropical North Africa at interannual and multi-decadal timescales." Journal of Climate **11**: 3167-3191.

(527) Washington, et al. (2006). "African climate change: taking the shorter route." Bulletin of the American Meteorological Society **87**(10): 1355-1366.

(528) Washington and Preston (2003). "Southern African rainfall - the role of the Indian and Pacific Oceans in HadAM3 idealised experiments." CLIVAR-Exchanges **27**.

(529) Washington and Preston (2006). "Extreme wet years over southern Africa: role of Indian Ocean sea surface temperatures." Journal of Geophysical Research **111**: D1504.

(530) Washington and Todd (1999). "Tropical-temperate links in South Africa and the Southwest Indian Ocean daily rainfall." International Journal of Climatology **19**: 1601-1616.

(531) Waylen and Henworth (1996). "A note on the timing of precipitation variability in Zimbabwe as related to the southern oscillation." International Journal of Climatology **16**: 1137-1148.

(532) Webster, et al. (1999). "Coupled ocean dynamics in the Indian Ocean during the 1997-1998 El Nino." Nature **401**: 356-360.

(533) Weng (2005). "The influence of the 11yr solar cycle on the interannual-centennial climate variability." Journal of Atmospheric and Solar-Terrestrial Physics **67**: 793-805.

(534) Wigley, et al. (2000). "Correlation approaches to detection." Geophysical Research Letters **27**(18): 2973-2976.

(535) Wild and Roeckner (2006). "Radiative fluxes in the ECHAM5 general circulation model." Journal of Climate **19**: 3792-3809.

(536) Wolff, et al. (1997). The Hamburg Ocean Primitive Equation Model, German Climate Computer Centre (DKRZ) Technical Report**:** 98.

(537) World-Bank (2001). Action Plan for the Reduction of Poverty (2001-2005) (PARPA). Strategy Document for the Reduction of Poverty and Promotion of Economic Growth**:** 18pp.

(538) Worley, et al. (2005). "ICOADS release 2.1 data and products." International Journal of Climatology **25**(7): 823-842.

(539) Wright (1997). "A new eddy mixing parametrisation and ocean general circulation model." WOCE Newsletter **29**: 27-29.

(540) Xie, et al. (2002). "Structure and mechanisms of South Indian Ocean climate variability." Journal of Climate **15**: 864-878.

(541) Xie and Arkin (1997). "Global precipitation: a 17 year monthly analysis based on gauge observations, satellite estimates and numerical model outputs." Bulletin of the American Meteorological Society **78**: 2539-2558.

(542) Xie, et al. (2003). "GPCP pentad precipitation analyses: an experimental dataset based on gauge observations and satellite estimates." Journal of Climate **16**(13): 2197-2214.

(543) Yadav, et al. (2007). "Role of Indian Ocean sea surface temperatures in modulating northwest Indian winter precipitation variability." Theoretical and Applied Climatology **87**: 73-83.

(544) Yamagata, et al. (2002). "The Indian Ocean dipole: a physical entity." CLIVAR-Exchanges **7**(2): 15-18.

(545) Yeh and Kirtman (2004). "Tropical Pacific decadal variability and ENSO amplitude modulation in a CGCM." Journal of Geophysical Research **109**(C11): C11009.

(546) Yeh and Kirtman (2005). "Pacific decadal variability and decadal ENSO amplitude modulation." Geophysical Research Letters **32**(5): L05703.

(547) Yonetani and Gordon (2001). "Abrupt changes as indicators of decadal climate variability." Climate Dynamics **17**(4): 249-258.

(548) Yu and Lau (2004). "Contrasting Indian Ocean SST variability with and without ENSO influence: a coupled atmosphere-ocean GCM study." Meteorology and Atmospheric Physics **90**(3-4): 179-191.

(549) Yu and Zwiers (2007). "The impact of combined ENSO and PDO on PNA climate: a 1000 yr climate modelling study." Climate Dynamics **29**: 837-851.

(550) Zhang and Busalacchi (2005). "Interdecadal change in properties of ENSO in an intermediate coupled model." Journal of Climate **18**: 1369-1380.

(551) Zhang, et al. (1997). "ENSO-like interdecadal variability, 1900-93." Journal of Climate **10**(5): 1004-1020.

(552) Zhang, et al. (2007). "Detection of human influence on 20th century precipitation trends." Nature **448**(461-465).

(553) Zhang, et al. (2006). "Multimodel multiscale climate change detection at regional scale." Journal of Climate **19**: 4294-4307.

(554) Zhao, et al. (2005). "A multimodel analysis of the role of the ocean on the African and Indian monsoon during the mid Holocene." Climate Dynamics **25**(7-8): 777-800.

(555) Ziegler, et al. (2003). "Detection of intensification in global and continental hydrological cycles: temporal scale of evaluation." Journal of Climate **16**: 535-547.

(556) Zinke, et al. (2004). "ENSO and Indian Ocean subtropical dipole variability is recorded in a coral record off southwest Madagascar for the period 1659 to 1995." Earth and Planetary Science Letters **228**: 177-194.

(557) Zorita, et al. (2003). "Testing the Mann et al (1998) approach to palaeoclimate reconstruction in the context of a 1000-yr control simulation with the ECHO-G coupled climate model." Journal of Climate **16**: 1368-1390.

(558) Zorita, et al. (2004). "Climate evolution in the last five centuries simulated by an atmosphere ocean model: global temperatures, the North Atlantic Oscillation, and the late Maunder Minimum." Meterologische Zeitschrift **13**(4): 271-289.

(559) Zorita, et al. (2005). "Natural and anthropogenic modes of surface temperature variations in the last 1000 years." Geophysical Research Letters **32**(8): L08707.

(560) Zwiers and von-Storch (2004). "On the role of statistics in climate research." International Journal of Climatology **24**: 665-680.

(561) Zwiers and Zhang (2003). "Towards regional scale climate detection." Journal of Climate **16**: 793-797.